technische universität
dortmund

Development of Synthesis Methodology for DNA-Encoded Libraries

Dissertation

for the academic degree of

Doctor of Sciences

from the Faculty of Chemistry and Chemical Biology
of Technical University of Dortmund
presented by

Mateja Klika Škopić

Dean: Prof. Dr. Roland Winter

1. Examiner: Prof. Dr. Daniel Rauh
2. Examiner: Prof. Dr. Herbert Waldmann

“The most beautiful thing we can experience is the mysterious. It is the source of all true art and science.”

Albert Einstein

The work presented in this thesis was performed in the time period from November 2013 to October 2017 under the scientific guidance of Dr. Andreas Brunschweiger and supervision of Prof. Dr. Daniel Rauh at the Faculty of Chemistry and Chemical Biology of the Technical University of Dortmund.

Part of this work has been published in the following papers:

1. **Chemical Biology Probes from Advanced DNA-encoded Libraries**
H. Salamon, M. Klika Škopić, K. Jung, O. Bugain, A. Brunschweiger, *ACS Chem Biol* **2016**, *11*, 296-307.

2. **Design and synthesis of DNA-encoded libraries based on a benzodiazepine and a pyrazolopyrimidine scaffold**
M. Klika Škopić, O. Bugain, K. Jung, S. Onstein, S. Brandherm, T. Kalliokoski, A. Brunschweiger, *MedChemComm* **2016**, *7*, 1957-1965.

3. **Acid- and Au(I)-mediated synthesis of hexathymidine-DNA-heterocycle chimeras, an efficient entry to DNA-encoded libraries inspired by drug structures**
M. Klika Škopić, H. Salamon, O. Bugain, K. Jung, A. Gohla, L. J. Doetsch, D. Dos Santos, A. Bhat, B. Wagner, A. Brunschweiger, *Chem Sci* **2017**, *8*, 3356-3361.

4. **Exploration of a Au(I)-mediated three-component reaction for the synthesis of DNA-tagged highly substituted spiroheterocycles**
M. Klika Škopić, S. Willems, B. Wagner, J. Schieven, N. Krause, A. Brunschweiger, *Org Biomol Chem* **2017**, *15*, 8648-8654.

Part of this work has been published in the following patent:

A. Brunschweiger, N. Krause, A. Antonchick, M. Klika Škopić, H. Salamon, O. Bugain, K. Jung, B. Wagner, WO 2017108741 A1, 2017.

To Bojan and Aleksandra,

and in memory of my father Slavko

Table of contents

Table of contents I

Kurzfassung V

Abstract VII

1. Introduction 1

1.1. Entries to DNA-Encoded Libraries 5

1.1.1. Different formats of DNA-Encoded Libraries 5

1.1.2. Screening DNA-Encoded Libraries by selection 8

1.1.3. Bioactive compounds identified from selection of DNA-Encoded Libraries 9

1.2. Synthesis methodology for DNA-Encoded Libraries 12

1.3. Privileged scaffolds in drug discovery 28

1.3.1. The pyrazolo[3,4-d]pyrimidine structure - a privileged scaffold for kinase inhibition 29

1.3.2. Pyrazoles and pyrazolines 35

2. DNA-Encoded Library based on the pyrazolopyrimidine scaffold 43

2.1. Design and synthesis of trifunctionalized pyrazolopyrimidine scaffold 46

2.2. Selection of building blocks for pyrazolopyrimidine DNA-Encoded Library 47

2.3. DNA-Encoded Library synthesis strategy development 50

2.4. Synthesis of the pyrazolopyrimidine DNA-Encoded Library 52

2.4.1. Synthesis of the pyrazolopyrimidine DNA-Encoded Library - amide coupling on solid phase 53

2.4.2. Evaluation of azide building blocks 56

2.4.3. Finalization of the pyrazolopyrimidine DNA-Encoded Library - solution phase synthesis 58

2.5. Summary 59

3. Expanding chemical space of DNA-Encoded Libraries by “hexT”-approach 61

3.1. The challenge: chemical instability of DNA 63

3.2. Development of the Thymidine-initiated DNA-Encoded Chemistry (TiDEC) concept 65

3.3. Approaches towards synthesis of pyrazoles and pyrazolines 68

3.3.1. Synthesis of pyrazolines by Au(I)-catalyzed annulation reaction 72

3.4. Synthesis of the hexathymidine-pyrazol(in)e conjugates by the Au(I)-mediated annulation reaction 76

3.4.1. Optimization of the Au(I)-mediated annulation reaction 76

3.4.2. Synthesis of reference molecules: pyrazoline, propargyl hydrazide, and pyrazole 87

3.4.3. Synthesis of hexathymidine-pyrazole conjugates by oxidative aromatization of hexathymidine-pyrazolines 89

3.4.4. Reaction conditions controlled access to hexathymidine-pyrazolines and hexathymidine-pyrazoles 91

3.4.5. Exploration of the scope of unsymmetrically substituted hydrazides for Au(I)-mediated pyrazol(in)e synthesis 92

3.5. Towards oligothymidine-initiated DNA-Encoded Library (tiDEL) based on the pyrazol(in)e scaffold 94

3.5.1. Exploration of aldehyde scope for the Au(I)-mediated pyrazol(in)e synthesis . 94

3.5.2. Evaluation of carboxylic acids reactivity for library synthesis 96

3.5.3. Enzymatic encoding of hexathymidine-pyrazol(in)e conjugates by T4-DNA ligase 98

3.5.4. Synthesis of the oligothymidine-initiated DNA-Encoded Library (tiDEL) 102

3.5.5. Quality control of the pyrazol(in)e library: PCR amplification and streptavidin pull-down experiment 104

3.6. Increasing structural complexity of hexathymidine-heterocycle conjugates 105

3.6.1. [N,O]-spiroacetals and their accessibility 106

3.6.2. Synthesis of the hexathymidine-6-oxa-1,2-diazaspiro[4.4]nonane conjugates 108

4. Conclusion 141

5. Experimental part 149

5.1. Reagents and instruments 151

5.2. Amide coupling on solid support 153

5.2.1. Amide coupling of carboxylic acids to 5'-amino-linker modified DNA 153

5.2.2. Synthesis of DNA-PEG linker conjugates 154

5.3. DNA-Encoded Library based on the pyrazolopyrimidine scaffold 155

5.3.1. Synthesis of the DNA-pyrazolopyrimidine conjugate 155

5.3.2. Synthesis of model DNA-alkyne conjugates for evaluation of azide building blocks 156

5.3.3. Coupling reactions of 94 carboxylic acids to the DNA-pyrazolopyrimidine conjugate 157

5.3.4. Evaluation of halides for library synthesis 166

5.3.5. Synthesis of the DNA-Encoded Library based on the pyrazolopyrimidine scaffold 175

5.3.6. Synthesis and characterization of the pyrazolopyrimidine scaffold 176

5.4. Synthesis of the oligothymidine-initiated DNA-Encoded Library based on the pyrazol(in)e scaffold 179

5.4.1. Synthesis of the hexathymidine-alkyne conjugate 179

5.4.2. Optimization of reaction conditions of the Au(I)-mediated annulation reaction 180

5.4.3. Au(I)-mediated annulation reaction to hexathymidine-pyrazol(in)e conjugates 181

5.4.4. HPLC chromatograms and MALDI-MS spectra of 20 representative library members 191

5.4.5. HPLC chromatograms and MALDI-MS spectra of hexathymidine-pyrazolines - hydrazide scope 197

5.4.6. Evaluation of carboxylic acids for library synthesis 200

5.4.7. Enzymatic encoding of hexathymidine conjugates: T4 ligation of duplex DNA sequences 213

5.4.8. Synthesis and analysis of the pyrazol(in)e based oligothymidine-initiated DNA-Encoded Library (tiDEL) 214

5.4.9. Synthesis of reference molecules and intermediates 217

5.5. Synthesis of hexathymidine-6-oxa-1,2-diazaspiro-[4.4]nona- ne conjugates by Au(I)-mediated [3+2]-cycloaddition 227

5.5.1. Synthesis of DNA-aldehyde, -hydrazide, and -alkynol conjugates 227

5.5.2. Optimization of reaction conditions of the Au(I)-mediated [3+2]-cycloaddition 232

5.5.3. Au(I)-mediated [3+2]-cycloaddition to DNA-6-oxa-1,2-diazaspiro[4.4]nonane conjugates 234

5.5.4. HPLC chromatograms and MALDI-MS spectra of hexathymidine-6-oxa-1,2-diazaspiro[4.4]nonane conjugates - reactant scope 235

5.5.5. MALDI-MS spectra of DNA-6-oxa-1,2-diazaspiro[4.4]nonane conjugates - sequence scope 237

5.5.6. Synthesis of hexapyrimidine-pyrazoline and -ß-carboline conjugates 238

5.5.7. Synthesis of small molecule intermediates 241

6. Literature 243

Abbreviations 261

Acknowledgements 265

Curriculum Vitae 267

Eidesstattliche Versicherung (Affidavit) 269

Kurzfassung

Eine grundlegende Herausforderung in der Medizinischen Chemie und Chemischen Biologie stellt die Identifizierung von niedermolekularen Molekülen dar, die an physiologisch relevante Zielproteine binden und deren Funktion modulieren. Solche bioaktiven Moleküle können zur Aufklärung komplexer biologischer Prozesse beitragen oder sogar Ausgangspunkte zur Entwicklung von Arzneimitteln darstellen. Daher ist die Entwicklung von Screening-Technologien, die einen großen chemischen Raum abdecken und eine effiziente Identifizierung von Proteinbindern ermöglichen, in den Lebenswissenschaften von großem Interesse. DNA-kodierte Substanzbibliotheken (DELs) sind eine validierte Technologie zur Identifizierung von Proteinbindern. Diese Bibliotheken bestehen aus einer Vielzahl von Molekülen, welche kovalent an DNA-Sequenzen gebunden sind. Die DNA-Sequenzen dienen dabei der Identifizierung der verknüpften Moleküle und ermöglichen eine effiziente Synthese und Handhabung von numerisch extrem großen Substanzbibliotheken. Im Vergleich zum *high-throughput-screening* (HTS) diskreter Substanzbibliotheken, das häufig in der forschenden Pharmaindustrie genutzt wird um bioaktive Verbindungen zu identifizieren, sind DELs wesentlich kostengünstiger, da sie das gleichzeitige Screenen von allen Bibliotheksverbindungen in einem Experiment ermöglichen. Diese Arbeit beschreibt die Synthese einer 8658 Moleküle umfassenden DNA-kodierten Substanzbibliothek auf Basis eines Pyrazolopyrimidin-Grundgerüsts und einer 6816 Moleküle umfassenden DNA-kodierten Substanzbibliothek auf Basis von Pyrazol- und Pyrazolin-Grundgerüsten. Zudem zeigt diese Arbeit einen Zugang zu DNA-Konjugaten vollständig gesättigter, hochsubstituierter 6-Oxa-1,2-diazaspiro-[4.4]nonanen.

Kapitel 1 gibt eine Einführung in die Technologie der DNA-kodierten Bibliotheken. Zusätzlich wird das Prinzip des DEL-Selektionsassays beschrieben, sowie bioaktive Verbindungen, die über DEL-Selektionen identifiziert wurden. Außerdem gibt es einen umfassenden Überblick über die chemischen Reaktionen, die derzeit für die Synthese von DELs zur Verfügung stehen. Zusätzlich wird in diesem Kapitel eine Einführung in das Konzept der sogenannten „privilegierten“ Strukturen gegeben. Da der Aufbau des Grundgerüsts für das Design einer DNA-kodierten Substanzbibliothek eine wichtige Rolle spielt, wurden die in dieser Arbeit synthetisierten Bibliotheken aus Grundgerüsten aufgebaut, die unter bioaktiven Verbindungen „privilegiert“ d.h. hochrepräsentiert sind, wie Pyrazolopyrimidin-, Pyrazol- und Pyrazolin-Grundgerüste. Um die Auswahl dieser Heterocyclen zu begründen, werden einige Beispiele für bioaktive Pyrazolopyrimidine, Pyrazole und Pyrazoline gegeben. Kapitel 2 und 3 beschreibt die Synthese der oben erwähnten Bibliotheken unter Verwendung von zwei verschiedenen Synthesestrategien. Die

Pyrazolopyrimidin DEL (Kapitel 2) wurde durch bekannte DNA-kompatible Reaktionen wie Amidkupplung und Cu(I)-katalysierte Azid-Alkin-Cycloaddition (CuAAC) synthetisiert. Um die strukturelle Diversität der Bibliothek zu maximieren, wurden die Synthesebausteine für die Bibliothek mit Hilfe cheminformatischer Methoden ausgewählt.

Die erfolgreiche Identifizierung von Proteinbindern durch das Screening von DELs hängt zum einen stark vom chemischen Raum ab, der von den DELs abgedeckt wird, zum anderen ist die Integrität der DNA, der genetischen Information entscheidend für die Funktionalität der kodierten Bibliothek. Die chemische Labilität der DNA setzt dabei dem Einsatz von Katalysatoren für chemische Reaktionen extrem enge Grenzen. Starke Säuren und viele Übergangsmetalle sind attraktive Katalysatoren, die die Synthese einer Vielzahl wirkstoffartiger Strukturen aus einfachen, leicht verfügbaren Ausgangsmaterialien ermöglichen. Allerdings wird durch solche Katalysatoren der genetische Code vor allem durch Depurinierung zerstört (Kapitel 3.1). Um dieses Hindernis für die Anwendung solcher Katalysatoren für die DEL-Synthese zu umgehen, entwickelten wir die TiDEC-Strategie (***T****hymidin-****i****nitiated* ***D****NA-****E****ncoded* ***C****hemistry*), eine neue Bibliothekssynthesestrategie, die ein Hexathymidin-Oligonukleotid, als “hexT“ bezeichnet, als Adapteroligonucletid nutzt. Es übersteht harsche Reaktionsbedingungen und läßt sich nach der erfolgten Synthese der Zielstrukturen an kodierende DNA-Sequenzen ligieren. Es ermöglicht so den Zugang zu einem breiten Spektrum von Strukturen für die kodierte Bibliothekssynthese. DNA-kodierte Bibliotheken (DELs), die mit einem Hexathymidin-Oligonukleotid-Adapter initiiert werden, werden tiDELs genannt (Kapitel 3.2). In dieser Arbeit untersuchte ich den Zugang zu hexT-Pyrazol(in)-Konjugaten durch eine Au(I)-vermittelte Annelierungsreaktion (Kapitel 3.4, 3.5). Die Optimierung der Reaktionsbedingungen ermöglichte den Zugang zu hochsubstituierten hexT-Pyrazolinen und hexT-Pyrazolen unter Verwendung der gleichen Ausgangsmaterialien. Es wurden insgesamt 71 hexT-Pyrazol(in)-Konjugate unter Verwendung eines hexT-Alkinkonjugats, einer Reihe von Aldehyd-Bausteinen, und einem aminofunktionalisierten Hydrazid zur weiteren Funktionalisierung der hexT-Pyrazol(in)-Konjugate durch Amidkupplung, synthetisiert. Alle hexT-Konjugate wurden durch präparative HPLC aufgereinigt und massenspektrometrisch charakterisiert. Anschließend wurden kodierende DNA-Sequenzen ligiert und die kodierte Bibliothek mit der Kopplung durch 96 validierte Carbonsäuren komplettiert. Die analoge Reaktion, die statt des Alkins ein Alkinol einsetzt, ergab DNA-konjugierte, hochsubstituierte, vollständig gesättigte 6-Oxa-1,2-diazaspiro[4.4]nonane. In diesem Projekt wurde der Einfluss der Konnektivität zwischen DNA und kleinem Molekül auf die Darstellbarkeit des letzteren untersucht (Kapitel 3.6).

Abstract

The identification of small drug-like molecules binding and modulating (patho-) physiologically relevant protein targets is a fundamental challenge in medicinal chemistry and chemical biology. Bioactive small molecules may serve to elucidate complex biological processes, they may even show potential for the development of drugs. Therefore, the development of screening technologies that allow for rapid identification of protein binders by interrogation of large chemical space is of high interest in life sciences. DNA-encoded compound libraries (DELs) are a validated technology for identification of protein binders. DELs are collections of small molecules covalently coupled to DNA sequences identifying the connected molecules. DNA-tagging allows for efficient synthesis and handling of numerically large compound libraries. In contrast to high-throughput screening (HTS) of discrete compound libraries which is regularly used by corporate research groups for identification of bioactive compounds, DELs are much more economical as they enable simultaneous interrogation of all library members in a screening experiment which is based on the principle of selection.

This thesis describes the synthesis of a 8568-membered DNA-encoded library based on pyrazolopyrimidine scaffold, the synthesis of a 6816-membered library based on pyrazole and pyrazoline scaffolds, and demonstrates the access to fully saturated, highly substituted 6-oxa-1,2-diazaspiro-[4.4]nonanes in a DNA-encodable manner.

Chapter 1 gives an introduction to DNA-encoded libraries, including an overview over existing formats of DELs, the principle of the DEL selection assay, bioactive compounds identified from DEL selections, and enumerates chemical transformations available for the synthesis of DELs. As the selection of scaffold represents an important parameter of DNA-encoded library design, we decided to base our libraries on scaffolds that are highly represented, i.e. “privileged”, among bioactive compounds: pyrazolopyrimidine, pyrazole, and pyrazoline scaffolds. The chapter also provides an introduction to the concept of “privileged” structures and an overview over a number of bioactive pyrazolopyrimidines, pyrazoles, and pyrazolines, giving a rationale for scaffold choice.

Chapters 2 and 3 describe the synthesis of the aforementioned libraries by using two different synthesis strategies. The pyrazolopyrimidine DEL (Chapter 2) was synthesized by well-known DNA-compatible reactions: amide coupling and Cu(I)-catalyzed azide–alkyne cycloaddition (CuAAC). The building blocks for library synthesis were selected with help of

chemoinformatics to filter out undesirable structural motifs and to maximize the structural diversity of the library.

Identification of protein binders in DEL screening campaigns is highly dependent on the chemical space covered by DELs. On the other hand, preservation of the DNA genetic information is crucial for functional DELs. The chemical reactivity of DNA sets tight limitations to the use of catalysts: acid organocatalysts and many transition metals are attractive catalysts furnishing diverse drug-like structures from simple readily available starting materials, yet they cause DNA degradation mainly by depurination (Chapter 3.1). To circumvent this obstacle we developed TiDEC (Thymidine-initiated DNA-Encoded Chemistry), a new library synthesis strategy which rests on hexathymidine oligonucleotide, called "hexT" which survives harsh reaction conditions and gives access to a potentially broad spectrum of structures in the initial step of library synthesis. DNA-encoded libraries (DELs) which are initiated with hexathymidine oligonucleotide adapter are called tiDELs (Chapter 3.2).

I investigated the access to hexT-pyrazoline conjugates by a Au(I)-mediated annulation reaction (Chapters 3.4, 3.5). Optimization of reaction conditions afforded access to densely substituted hexT-pyrazolines and hexT-pyrazoles using the same simple starting materials. Altogether, 71 hexT-pyrazol(in)e conjugates were synthesized using a hexT-alkyne conjugate, a set of aldehyde building blocks representing one diversification point, and a hydrazide displaying an amine functionality for further functionalization of hexT-pyrazol(in)e conjugates by amide coupling. All hexT conjugates were purified by preparative HPLC, and characterized by analytical HPLC and MALDI-TOF/TOF-MS analysis. Then, they were ligated to coding DNA sequences yielding encoded library which was concluded by introducing of a set of 96 validated carboxylic acids.

Using an analogous reaction system to the synthesis of hexT-pyrazolines, but exchanging the alkyne with an alkynol component, highly substituted, fully saturated spirocycles hexT-6-oxa-1,2-diazaspiro-[4.4]nonanes were accessed by a Au(I)-mediated [3+2]-cycloaddition. In this project, the impact of the connectivity between DNA and small molecule on reaction outcome was studied (Chapter 3.6).

1. Introduction

The discovery of small molecules that are able to modulate protein target function remains a major focus in life sciences research.[1] These molecules are extensively used as “probes” to illuminate the role of selected protein in biological systems.[2] Additionally, they can provide key information whether perturbation of the target protein activity might have therapeutic potential. Sequencing of the human genome was a revolutionary event in the life sciences as it revealed coding sequences of all proteins. It calls for the development of tools to probe the function of proteins in a methodical manner.[3] Finally, understanding of molecular mechanisms of diseases is the key for rational design of diagnostics and therapeutics.

To modulate protein target function, a small molecule first of all needs to bind to it. Discovery of small molecules protein binders, often depends on screening of number of molecules in suitable biochemical assays (high-throughput screening, HTS). HTS relies on large compound libraries, sophisticated bioassays, and complex infrastructure including robotic equipment, and logistics. In addition to the high cost, the whole process is often time consuming as library members are usually screened individually. Other possibilities for hit discovery involve fragment-based and computer-assisted methods. Faster and less expensive are display technologies including phage display,[4,5] yeast display,[6] mRNA display,[7] ribosome display,[8] and SELEX,[9,10] which have been used to generate large libraries of biomolecules (antibodies, peptides, proteins, and nucleic acids) in combinatorial manner. The combination of both technologies is embodied in DNA-encoded compound libraries (DELs). These are assemblies of small molecules encoded with PCR amplifiable DNA tags. DELs enable the interrogation of exceptionally large small molecule libraries by affinity-based selection assays against immobilized protein targets, requiring drastically reduced cost and time investment as compared to conventional HTS campaigns.[11] DNA is an excellent medium to store information. For example, a 20-mer oligonucleotide is able to encode billions of library members.[12] Additionally, the DNA-encoded library can be analyzed with very high sensitivity as only sub-fmol quantities of DNA are required for PCR amplification, massive parallel DNA-sequencing then enables deconvolution of a complex mixtures of DNA sequences.

In 1992 Brenner and Lerner presented their vision on combinatorial library synthesis encoded with DNA sequences.[13] Since then, great progress has been made from theory to practice. Initial efforts were mainly demonstrating the principle of DEL selection. Therefore, the molecular properties of hit compounds were not a major concern. In recent years the chemical space covered by DNA-encoded libraries gained a lot of attention.[14] Consequently, DEL screens are nowadays delivering protein binders that are more likely to fit into drug-like space

and undergo hit-to-lead stage in drug discovery process. However, we hypothesize that the expansion, and design of DEL chemical space is a key requirement for successful DEL screening campaigns. Thus, the development of chemical methodology for the synthesis of DELs represents an important challenge in the field.[15]

1.1. Entries to DNA-Encoded Libraries

DELs are collections of chimeric compounds that consist of small molecules covalently linked to single- (ss) or double-stranded (ds) DNA oligonucleotides (Fig. 1.1).

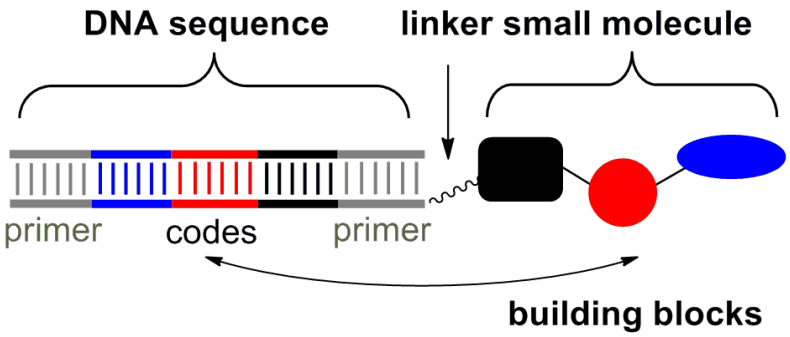

Figure 1.1. DNA-encoded compounds.

Each small molecule is linked to unique DNA sequence which contains terminal polymerase chain reaction (PCR)-primer regions and internal coding regions explicitly identifying small molecule (Fig. 1.1). Due to the amplifiable DNA tag, DELs can be pooled to extremely large number of conjugates, and then they can be screened by affinity-based selections.

1.1.1. Different formats of DNA-Encoded Libraries

An often used format for the synthesis of DELs is DNA-recorded combinatorial split-and-pool approach (Fig. 1.2).[15] Synthesis of these libraries involves cycles of iterative organic synthesis and encoding steps that record the synthesis. Library synthesis is initiated with the conjugation of bi- or trifunctionalized building blocks or scaffolds to short single- (ss) or double-stranded (ds) DNA sequences. The DNA contains a flexible linker moiety, very often with a primary amino group which allows for conjugation of small molecules by amide coupling. The linker also serves as spacer between the small molecule and the DNA barcode as interference between both, as well as interactions between the DNA and the protein target must be avoided during selection assays. Upon introduction, each building block is encoded by a specific DNA sequence. As they are encoded with DNA, the products of the first synthesis cycle can be pooled, and split for the next cycle (Fig. 1.2).

This iterative combinatorial procedure has been repeated up to four times. In one published case it gave rise to a library of four billion genetically tagged small molecules, a stunning number only in reach with DNA tagging.[16]

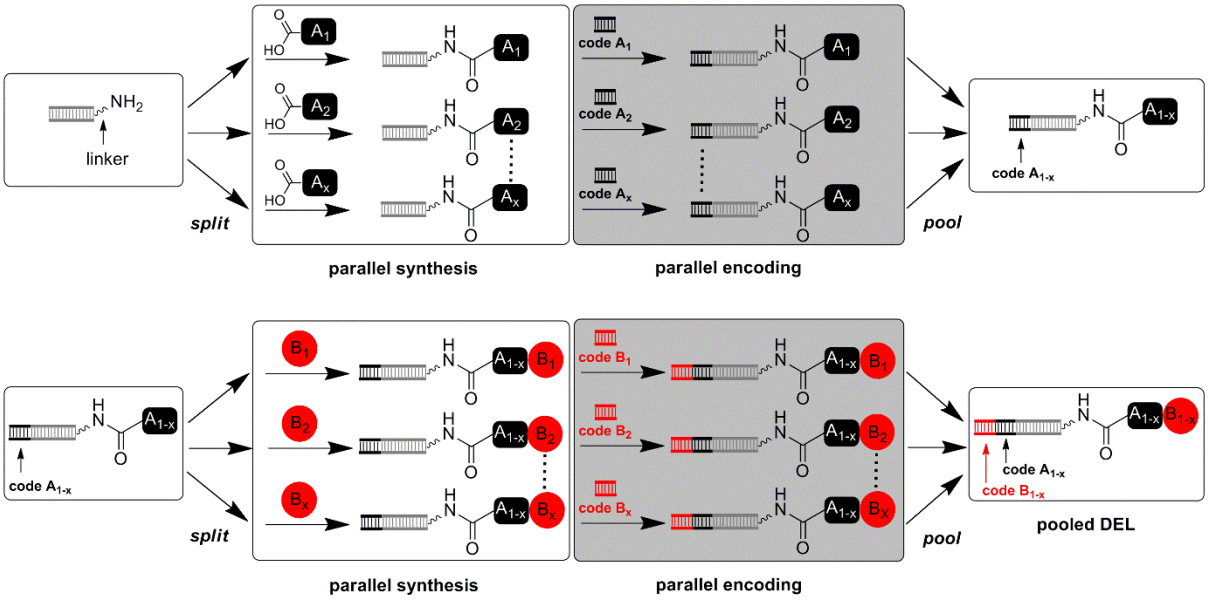

Figure 1.2. DNA-recorded mix-and-split combinatorial synthesis.

Methods to encode the building blocks include Klenow fill-in of two partially complementary DNA strands that each encode one building block,[17] T4-DNA ligation,[18] and chemical ligation of short alkyne- and azide-modified ssDNA by Cu(I)-catalyzed cycloaddition with a final Klenow fill-in step.[19,20] Libraries that undergo several cycles of synthesis and encoding are usually encoded with T4-DNA ligation. The scope of chemical reactions that are DNA-compatible, and therefore applicable for DEL synthesis is quite narrow and described in detail in Chapter 1.2.

Another DEL format is DNA-templated synthesis (DTS) where DNA encodes, and also directs the chemical reactions (Fig. 1.3A).[21] A template ssDNA-reactant conjugate is hybridized with a ssDNA bearing another reactant conjugated to the DNA via a cleavable linker. Both DNAs possess complementary regions that will be recruited by each other through Watson-Crick base-pairing. Upon DNA hybridization the two reactants are forced to close proximity to each other facilitating chemical reaction. In this strategy, a template DNA has to be synthesized for each final compound, and all building blocks must be conjugated to the anticodon DNAs via a cleavable linker. This synthesis methodology enabled synthesis of a 13.000-membered macrocycle library.[22] DTS can be simplified by use of a universal DNA

template which incorporates deoxyinosine capable of indiscriminate base-pairing, thus can hybridize with multiple DNA sequences instead of a specific one.[23]

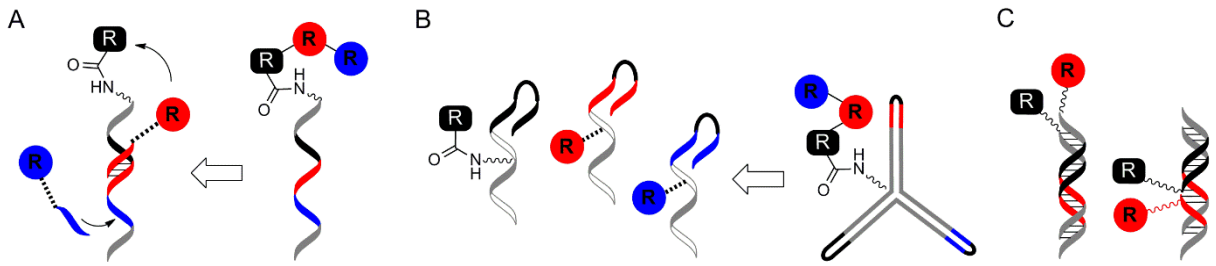

Figure 1.3. A) A DNA-templated chemistry; B) assembly of the "yoctoreactor"; C) assembly of DNA-small molecule fragment conjugates.

An example of the self-assembling DEL format is "yoctoreactor" approach (Fig. 1.3B), which relies on self-assembly of partially complementary DNA-reactant conjugates into three-dimensional three-, or four-way junctions.[24] Each DNA encodes the reactant which is conjugated to it via a cleavable linker, except of one reactant that is linked to the encoding DNA via a noncleavable linker. The junction forces the DNA-conjugated reactants into proximity, and increases their actual concentration facilitating the chemical reaction.[24] After each reaction, ligation of the coding DNA sequences is performed, and one reactant is released upon linker cleavage.

Finally, Encoded Self-Assembly Chemical libraries (ESAC, Fig. 1.3C) represent a DEL format which allows screening of small molecule fragments conjugated to the coding DNAs.[25] Libraries of fragments conjugated to the DNA at the 3'-end are hybridized with libraries of fragments conjugated to the DNA at the 5'-end.[25] The ESAC technology has potential to identify fragments which bind synergistically to two different binding sites of the protein target. However, chemistry for linking of the fragments upon their identification can be challenging.

1.1.2. Screening DNA-Encoded Libraries by selection

Pooled DELs are screened by affinity-based selection assays (Fig. 1.4).[26] The selection assay includes the immobilization of a purified protein target on the surface of a resin[27,17] or magnetic beads.[27,28] Proteins can be immobilized on reactive surfaces such as CNBr-activated sepharose,[29] or by directed immobilization using a His-tag,[27] biotin-tag,[28] or Flag-tag.[30]

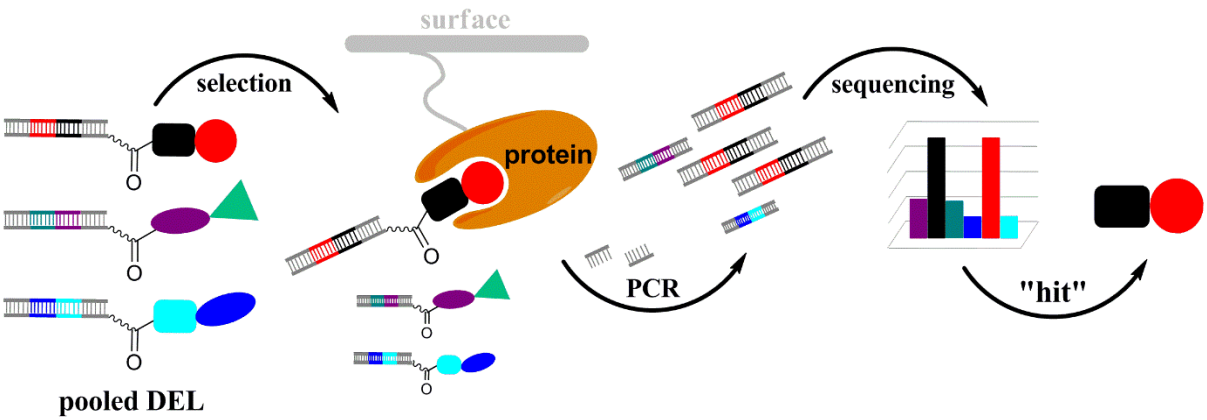

Figure 1.4. Selection against immobilized target protein. PCR: polymerase chain reaction.

Selection experiments typically involve incubation of pooled DEL in picomol amounts with the immobilized protein target. The amount of the protein required for the selection assay is usually in the microgram scale, thus in a huge excess to individual library members. Non-binding molecules are removed through extensive washing cycles leading to enrichment of protein binders. In the next step binders are eluted by heat denaturation of the protein. Elution of the binders can be followed by further selection rounds, i.e. the eluate is incubated with the fresh sample of the protein target. The final eluate is PCR-amplified, and the amplicon mixture is then submitted to DNA sequencing which provides quantitative information about enriched DNA sequences, and reveals the identity of small molecule binders.[27,17,31,32] Hits are identified by counting the sequences relative to control selection experiments. Once identified, hit molecules must be resynthesized without DNA tag, and validated for their activity in suitable biochemical assays.

DELs are usually synthesized on nanomole scale which is adequate for thousands of screens.[11] In contrast to HTS, DELs allow simultaneous screening of all library members, where invested time and effort are independent on library size.[12] Expensive robotics and

logistics that are required for HTS are omitted in DEL technology as DELs can be stored in a normal cooler as a compound pool in a single Eppendorf tube.[11]

1.1.3. Bioactive compounds identified from selection of DNA-Encoded Libraries

Screening of DNA-encoded libraries has delivered bioactive ligands for several proteins across the human proteome, and for target proteins from pathogenic organisms.

Many screening efforts have been directed to protein kinases. Screening of triaminotriazine-based DELs identified nanomolar ATP-competitive inhibitors of Aurora A kinase and p38 MAP kinase two kinases.[18] DELs also delivered the starting point for development of a selective and brain-penetrant GSK-3β-inhibitor **1** (Fig. 1.5).[33] A library of substituted biphenyls yielded **2** (Fig. 1.5), an equipotent single-digit nanomolar inhibitor of wild-type and H1047R-mutated phosphoinositide 3-kinase α (PI3Kα), a mutation frequently observed in cancer.[34] A 13.000-membered library of macrocycles led to micromolar inhibitors for the kinases Scr, Pim1, MK2, Akt3, and p38α MK2.[35] Macrocycles inhibiting Src were studied more in detail as they showed a high degree of selectivity within the Src family. An optimized compound **3** (Fig. 1.5) revealed a unique binding mode, with the macrocycle binding both to the ATP-binding site and the substrate peptide binding site.[36] Screening of an ethylenediamide- and an *N*-substituted carboxamide-based DEL which was designed according to the rule-of-five criteria,[37] yielded a new class of inhibitors of tankyrase 1 (TNKS1), a member of the family of poly(ADP-ribose)polymerases (PARPs).[28,38] The hits, among them **4** (Fig. 1.5) revealed *N*1-phenyl-substituted uracil as a novel PARP-binding motif for development of potent and selective inhibitors in the family of PARPs. A combination of several DELs numbering in total 14 billion of compounds was successfully screened against mitochondrial branched chain aminotransferase (BCATm), a potential target for treatment of metabolic diseases. The screening campaign led to the identification of compound **5** (Fig. 1.5) that could be used as a starting point for rational drug design.[39] Triaminotriazine libraries yielded nanomolar inhibitors for the Zn-metalloproteases ADAMTS-4 and -5 with good selectivity profile with respect to a panel of zinc-metalloproteases.[16,40] DEL synthesized by amide coupling of DNA-carboxylic acid conjugates with mono-protected diamines and followed by nucleophilic aromatic substitution

with reactive halide-substituted heterocycles revealed compound **6** (Fig. 1.5), as pan-SIRT1-3 inhibitor with nanomolar potency.[30]

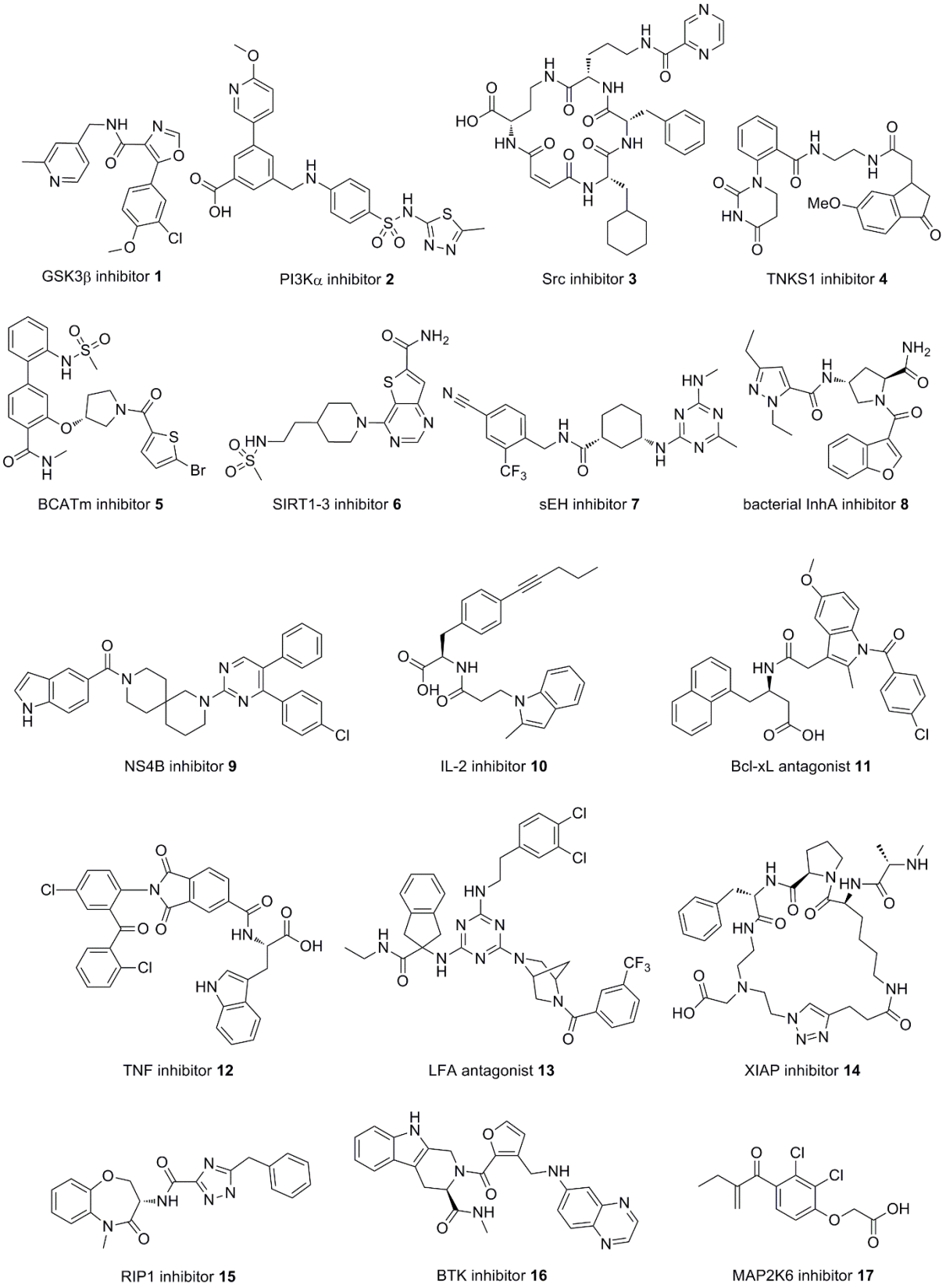

Figure 1.5. Bioactive compounds identified from selection of DELs.

The soluble epoxide hydrolase (sEH) inhibitor **7** (Fig. 1.5) is the first reported example of a clinical candidate that originates from a DEL-screen.[19,41,42] With the increasing appearance of drug-resistant pathogens, there is a need for anti-infective compounds with novel modes of action.[43] An effort was invested to develop enoyl-ACP reductase InhA inhibitors that will have different mode of action then antitubercular drug isoniazid which is likely targeting InhA, but suffers from development of drug resistant strain. Optimization of a DEL screening hit afforded the diacylated aminoproline **8** (Fig. 1.5) which inhibited InhA with an IC_{50} of 4 nM *in vitro*. The hepatitis C virus (HCV) non-structural 4B (NS4B) protein is required for viral replication. Thus, it represents a promising target for antiviral treatment. A DEL screen led to compound **9** (Fig. 1.5) with a different pharmacophore, and a partially different resistance profile *in vitro* when compared to previously identified NS4B inhibitors.[44]

Several screening efforts were directed at perturbation of protein-protein interactions. They delivered small molecule ligands for challenging protein targets such as IL-2 (**10**),[45] Bcl-xL (**11**),[29] and TNFα (**12**),[46] with low nanomolar to micromolar affinity (Fig. 1.5). Triaminotriazine **13** (Fig. 1.5) was identified as nanomolar inhibitor of the interaction of LFA lymphocyte function associated antigen 1 (LFA-1) with intercellular adhesion molecule-1 (ICAM-1).[47] A focused library of DNA-programmed pentapeptide macrocycles yielded compound **14** (Fig. 1.5) with micromolar *in vitro* activity against inhibitor of apoptosis proteins (XIAP, cIAPs).[48]

A three-cycle amino acid based DEL delivered a new series of benzoxazepinones with highly potent inhibitory activity against receptor interacting protein kinase 1 (RIP1) that has emerged as promising target for treatment of various inflammatory diseases. The optimization of the DEL hit yielded compound **15** (Fig. 1.5) which is currently in phase 2a of clinical trials for psoriasis, rheumatoid arthritis, and ulcerative colitis.[49,50] Screening of 110 million-membered DEL synthesized by two acylation and one reductive amination synthetic cycle against Bruton's tyrosin kinase (BTK) resulted in potent BTK inhibitor **16** (Fig. 1.5).[51] A co-cristal structure of BTK and compound **16** revealed a novel binding mode and a new binding pocket in BTK near the ATP binding site.

Screening of 136 DNA-linked molecules against 289 human kinases in a single experiment with interaction determination using unpurified proteins (IDUP) method revealed ethacrynic acid **17** (Fig. 1.5), an FDA approved diuretic, as partially covalent inhibitor of MAP2K6 kinase.[52] IDUP is method for *in vitro* identification of ligand-protein target pairs from a mixture of DNA-small molecule conjugates and DNA-tagged unpurified proteins in cell lysates.[53] DNA sequences linked to both, small molecules and proteins, contain barcode

region and hybridization region. Binding of a ligand to the protein target stabilizes the hybridization of complementary regions leading to duplex DNA that is subjected to primer extension, followed by PCR amplification. The matching ligand-protein target pairs are deconvoluted by high-throughput DNA sequencing.[52,53]

1.2. Synthesis methodology for DNA-Encoded Libraries

Design of DNA-encoded libraries influences the molecular properties of encoded compounds, thus of potentially identified hits as well. Important library design parameters include scaffold selection, number of diversity points, geometry of assembled compounds, selection of a building blocks, and chemical reactions used for library assembly.[14]
Set of chemical transformations available for the synthesis of DELs has the strong influence on library design and correlates with coverage of the concomitant chemical space.[54] Chemical reactions that are used for DEL synthesis must be robust, high yielding, cover broad reactant scope, and must preserve the integrity of the DNA code.[55] Oligonucleotides are polyfunctional biomolecules that limit the number of reactions that are DNA-compatible. For instance, acid-catalyzed and many transition metal-catalyzed transformations need to be avoided due to possible degradation of the DNA code, i.e. by depurination (see chapter 3.1). Thus, the set of chemical reactions that are applicable for synthesis of DELs is still relatively narrow. As a consequence, the chemical space of DNA-encoded libraries is restricted.

A list of reactions that were reported to be useful for DEL synthesis was collected, and these were compared with reactions that were actually used for synthesis of DNA-encoded libraries. For analysis were included only those reactions for which technical details were provided, and patent data were not involved. DNA-compatible reactions were clustered in four groups: protecting group chemistry (Table 1), functional group transformations (Table 2), appendage reactions (Table 3), and heterocyclic chemistry (Table 4). For references refer to Tables 1-4. Out of 41 reported reaction (Fig. 1.6, Tables 1-4), 13 reactions belong to the protecting group chemistry (Table 1), three reactions allow for functional group transformations (Table 2), appendage reactions compose the largest cluster numbering 20 reactions (Table 3), and heterocyclic chemistry afforded access to 14 different heterocyclic structures (Table 4).

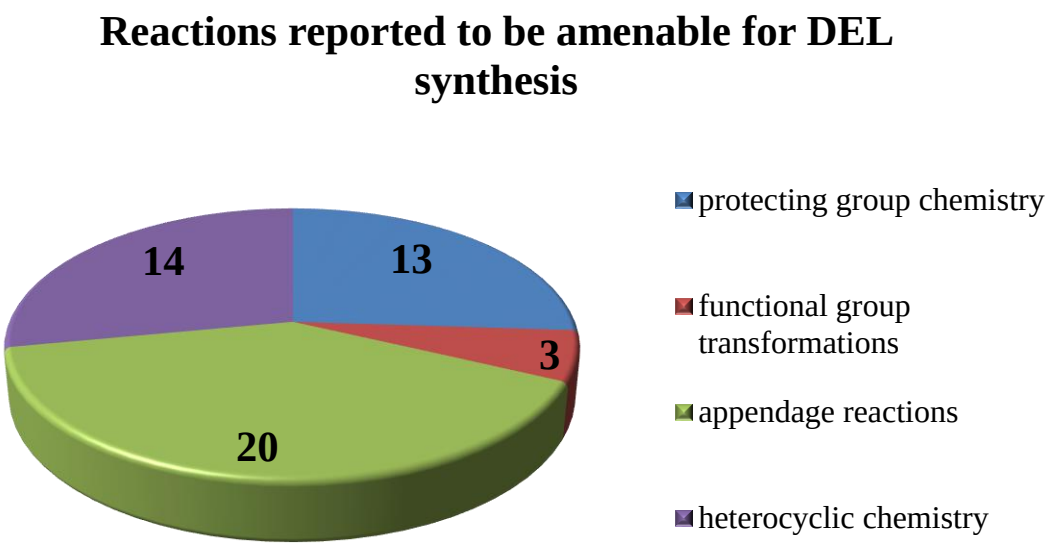

Figure 1.6. Statistical analysis of reactions reported to be amenable for DEL synthesis. Out of 41 reaction, 13 reactions belong to the protecting group chemistry, three reactions allow for functional groups transformations, appendage reactions compose the largest cluster numbering 20 reactions, and DNA-compatible heterocyclic chemistry gave access to 14 different heterocyclic structures.

Among protecting group chemistry, ten reactions include deprotection of amines (Table 1, entries 1-10) and three reactions include deprotection of carboxylic acids (Table 1, entries 11-13). However, only five out of 13 deprotection reactions were reported to be used in DEL synthesis (Fig. 1.8). Probably the most often used were Fmoc-deprotection and Nvoc-deprotection (Table 1, entries 1, 3).

To access amines, two functional group transformations are available: reduction of aromatic nitro group (Table 2, entry 1) and reduction of azides (Table 2, entry 2). Besides amines, aldehydes are also available through diol oxidation (Table 2, entry 3).

For reported DNA-encoded library synthesis was used 12 out of 20 DNA-compatible appendage reactions (Figs. 1.7, 1.8). Among them, most abundant are reactions of amines with electrophiles including acylation (Table 3, entries 1a, 1b), carbamoylation (Table 3, entry 2), sulfonylation (Table 3, entry 3), reductive alkylation (Table 3, entry 4b), nucleophilic aromatic substitution (Table 3, entries 5a, 5b), nucleophilic substitution (Table 3, entry 6), aminolysis of epoxides (Table 3, entry 19), and C-N cross coupling reactions: Buchwald-Hartwig amination (Table 3, entry 17), and “Ullmann-type” reaction (Table 3, entry 18). Thus, reactions of amines with electrophiles compose 75 % of all DNA-compatible appendage reactions which were used for library synthesis. Other appendage reactions used in

synthesis of DELs are Suzuki-Miyaura C-C cross-coupling reaction (Table 3, entry 9), Cu(I)-catalyzed alkyne-azide cycloaddition (Table 3, entry 8b), which was as well as Wittig olefination (Table 3, entry 13) used for macrocyclization.

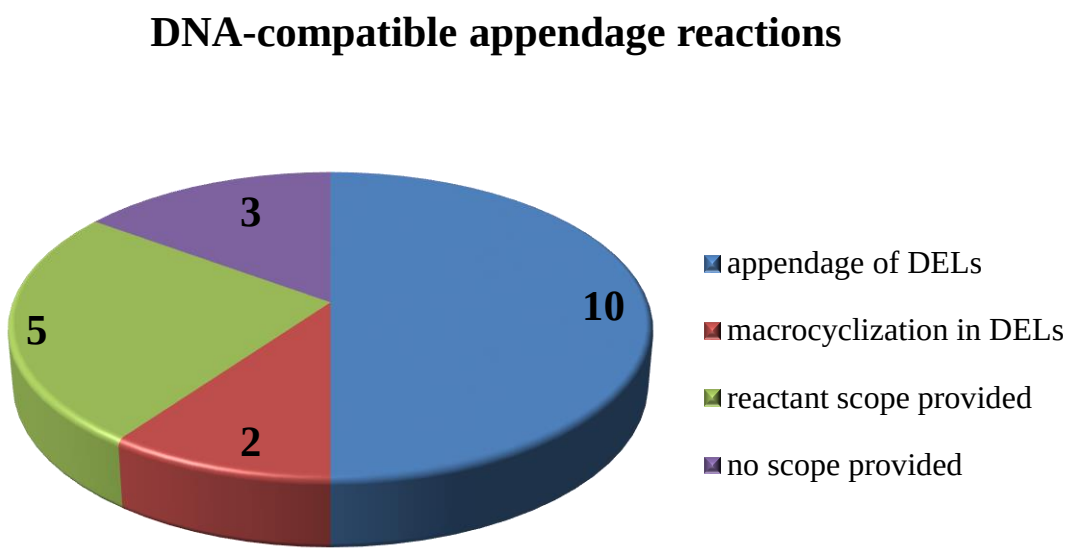

Figure 1.7. Statistical analysis of DNA-compatible appendage reactions. Out of 20 DNA-compatible appendage reactions, a synthesis of reported DELs was shown with 12 reactions: ten reactions were used for appendage of DELs and two reactions were used for macrocyclization in DELs. Proof of concept was shown for eight DNA-compatible appendage reactions, and for five of them the reactant scope was provided, while for three DNA-compatible appendage reactions the reactant scope was not provided.

Reactions which demonstrated compatibility with DNA, but were not used in the synthesis of reported DELs (Fig. 1.7) are two C-C cross-coupling reaction: Sonogashira- and Heck coupling (Table 3, entries 10, 16), Henry reaction- a C-C bond forming reaction between nitroalkanes and aldehydes or ketones (Table 3, entry 12), Michael addition (Table 3, entry 7), and Horner-Wadsworth-Emmons reaction with reactive phosphonium yilds (Table 3, entry 14). For three DNA-compatible appendage reactions: aldol condensation- a reaction of enolates and carbonyl compounds to conjugated enones (Table 3, entry 11), alkene-alkyne oxidative coupling (Table 3, entry 15), and ruthenium-catalyzed cross-metathesis reaction (Table 3, entry 20), the reactant scope was not provided (Fig. 1.7).

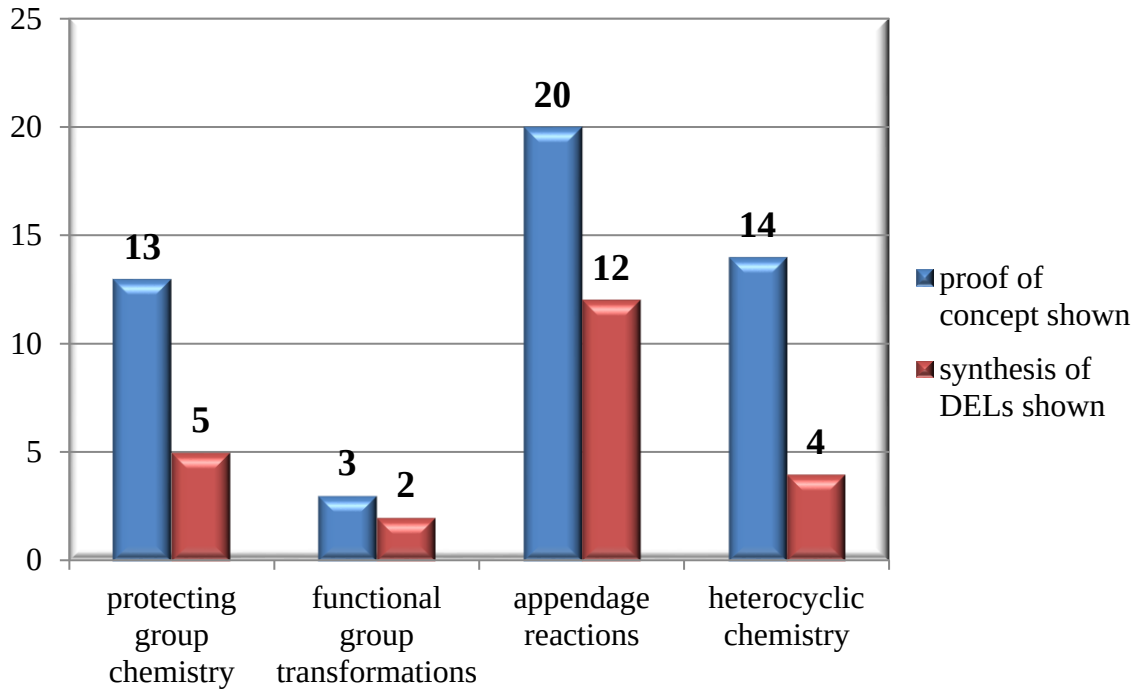

Figure 1.8. Number of DNA-compatible reactions per cluster group (protecting group chemistry, functional group transformations, appendage reactions, and heterocyclic chemistry) reported to be amenable for DEL synthesis (marked in blue) compared with number of reactions that were actually used in the synthesis of reported DNA-encoded libraries (DELs) (marked in red).

According to the published data with technical details provided on the synthesis, DNA-compatible heterocyclic chemistry allowed access to 14 different DNA-conjugated heterocycles (Table 4), and most of them were synthesized by condensation reactions. However, only four heterocycles are reported to be used for synthesis of DELs, and these are: benzimidazole (Table 4, entry 1), oxazolidin-2-one (Table 4, entry 9), morpholin-3-one (Table 4, entry 10), and tetrahydroisoindolinone (Table 4, entry 12) synthesized by Diels-Alder cycloaddition.

Table 1. DNA-compatible protecting group chemistry.

Protecting group chemistry			
No.	reaction	scheme	conditions
1	Fmoc deprotection	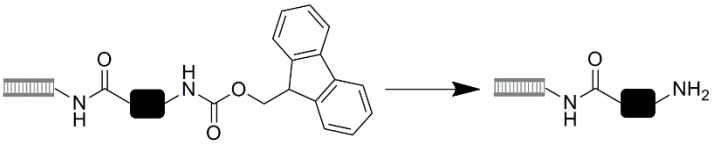	10 % piperidine, H_2O, 25 °C, 4 h [18]
2	Alloc deprotection	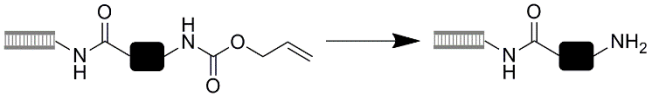	$Pd(PPh_3)_4$, $NaBH_4$, borate buffer, pH= 7.5, DMA, MeCN, 25 °C, 2 h [56]
3	Nvoc deprotection	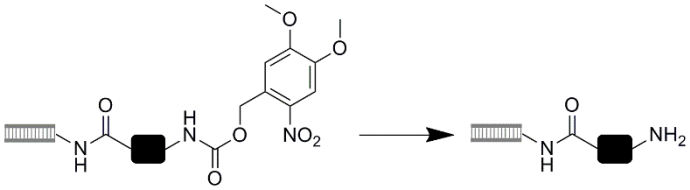	100 mM AcOH, pH= 4.5, H_2O, 365 nm, 4 °C, 16 h [16]
4	trityl deprotection	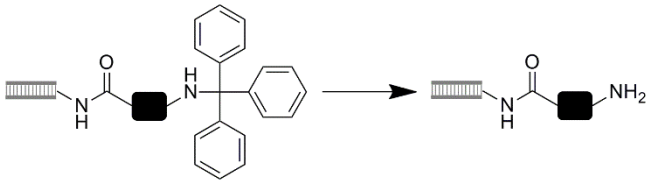	20 mM $MgCl_2$, 70 °C, 3-12 h [57]
5	4-cyano-2-nitrophenyl deprotection	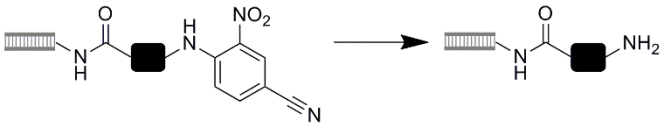	DEAE resin, mercapto-ethanol, DBU, DMF, 60 °C, 30 min [57]
6	Msec deprotection	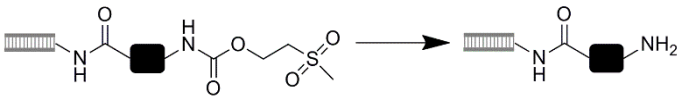	borate buffer, pH= 10, hν, 40 °C, 3 h [58]
7	nosylamide deprotection	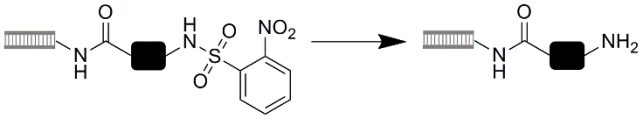	DEAE resin, mercapto-ethanol, DBU, DMF, 60 °C, 30 min [57]

Protecting group chemistry			
No.	reaction	scheme	conditions
8	pentenoyl deprotection	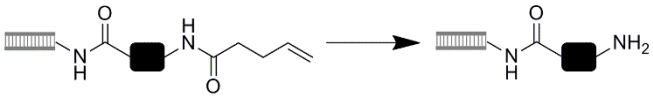	NaOAc buffer, pH= 5, THF/H_2O (1:1), 37 °C, 2 h [58]
9	trifluoro-acetamide deprotection	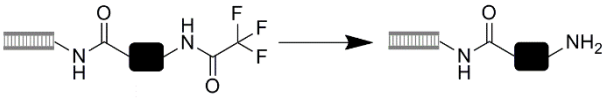	H_2O, 45 °C, 18 h [58]
10	Boc deprotection	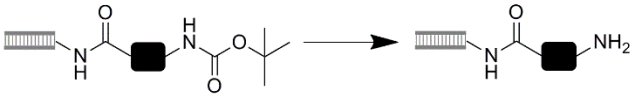	borate buffer, pH= 9.4, 90 °C, 16 h [56]
11	methyl/ethyl ester hydrolysis	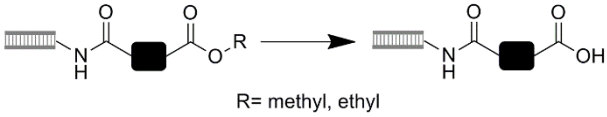	borate buffer, pH= 9.4, 100 mM NaOH, 60 °C, 2 h [56]
12	*tert*-butyl ester hydrolysis		borate buffer, pH= 9.4, 80 °C, 2 h [56]
13[a]	photo-uncaging of carboxylic acids	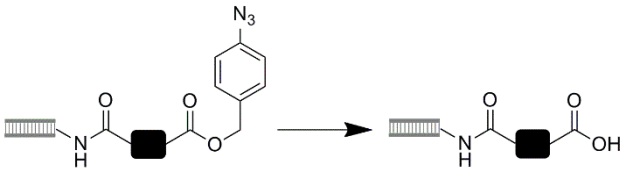	$Ru(bpy)_3Cl_2$, Na-ascorbate, Tris-Cl buffer, pH= 7.4, hν, 25 °C, 10 min [59]

Table 2. Functional group transformations on DNA.

Functional group transformations			
No.	reaction	scheme	conditions
1	nitro reduction	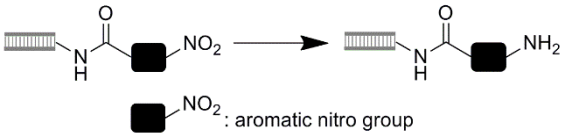	Raney Ni, hydrazine, H_2O, 25 °C, 2-24 h [56]
2[a]	azide reduction		$Ru(bpy)_3Cl_2$, Na-ascorbate, Tris-Cl buffer, pH= 7.4, hν, 25 °C, 10 min [59]
3[a]	diol oxidation	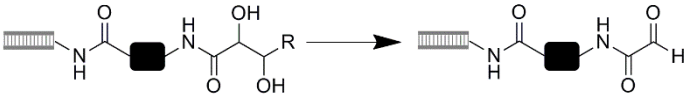	$NaIO_4$, NaOAc buffer, pH= 3.7-4, 25 °C, 1 min-2 h [22,60,61]

[a] reactions were performed only in DNA-templated format.

Probably, the most exploited appendage reactions for synthesis of DNA-encoded libraries are carbonyl reactions like acylation, carbamoylation, and reductive amination, together with sulfonylation (Table 3, entries 1a-4b).[16,18,19,22,28,38,39,62] Most of DELs are constructed by use of at least one acylation step between amino-modified DNA and carboxylic acid building blocks, thus it does not surprise that protocols for the amide coupling are continuously improving.[63] Nucleophilic aromatic substitution (Table 3, entries 5a, 5b) was also extensively used for the synthesis of DELs. It allowed for construction of a four billion-membered and a 800 million-membered triaminotriazine libraries by stepwise substitution of cyanuric chloride.[16,18] Nucleophilic substitution has shown to work with reactive aliphatic halides as well (Table 3, entry 6). Samain *et al*. synthesized a DEL by substitution of chloroacetamide functionalized DNA with amine building blocks, followed by acylation with a set of carboxylic acids in the second appendage step.[38] Wrenn *et al*. successfully employed a similar synthesis strategy to synthesize a 100 million-membered peptoid library on ion-exchange resin.[64] Gartner *et al*. reported nucleophilic substitution in DNA-templated format (DTS).[65]

Table 3. DNA-compatible appendage reactions.

Appendage reactions[a]			
No.	reaction	scheme	conditions
1a	acylation with carboxylic acid building blocks	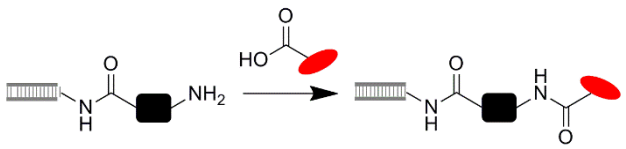	EDC, HOAt, DIPEA, MOPS buffer, pH= 8, DMSO, 25 °C, 22 h [63]
1b	acylation with amine building blocks	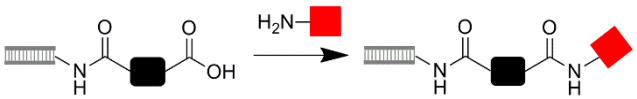	DMT-MM, 200 mM HCl, phosphate buffer, pH= 5.5, MeCN, H_2O, 25 °C, 72 h [18]
2	carbamoylation with isocyanates and isothiocyanates	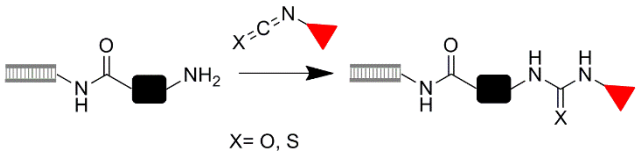	borate buffer, pH= 9.4, MeCN, 25 °C, 16 h [16]
3	sulfonylation	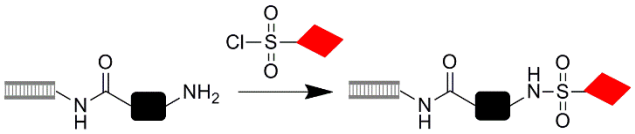	borate buffer, pH= 9.4, MeCN, 25 °C, 16 h [16]
4a	reductive mono-alkylation of primary amines	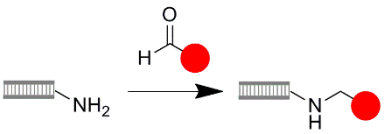	1. borate buffer, pH= 9.4, DMA, 25 °C, 1 h; 2. $NaBH_4$, MeCN, 25 °C, 1 h [56]
4b	reductive alkylation of secondary amines	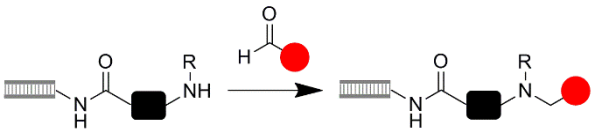	$NaBH_3CN$, phosphate buffer, pH= 5.5/DMF/ MeCN (2:1:1), 25 °C, 16 h [16]
5a	nucleophilic aromatic substitution (cyanuric chloride and amine building blocks)	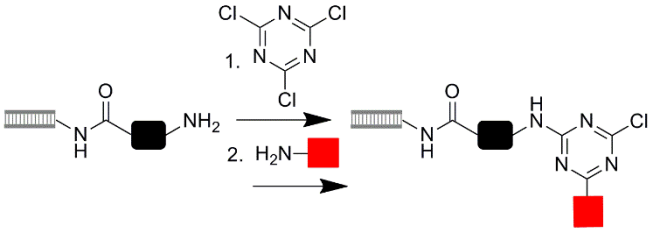	1. borate buffer, pH= 9.4, MeCN, 4 °C, 1 h; 2. 45 °C, 6 h [18]

Appendage reactions[a]			
No.	reaction	scheme	conditions
5b	nucleophilic aromatic substitution (hetarylhalide building blocks)	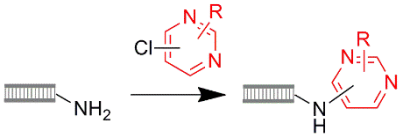	borate buffer, pH= 9.4, DMA, 60 °C, 12 h [56]
6	nucleophilic substitution	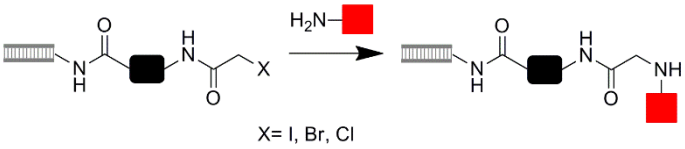	H_2O, DMA, 25 °C, 1 h [56]
7[b]	Michael addition		MOPS buffer, pH= 7.5, 250 mM NaCl, 25 °C, 10-75 min [65]
8a	CuAAC with azide building blocks	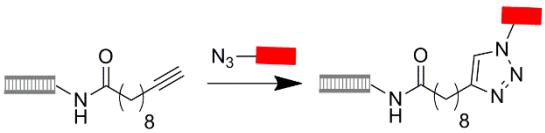	$Cu(OAc)_2$, sodium ascorbate, 25 °C, 3 h [66]
8b	CuAAC with alkyne building blocks	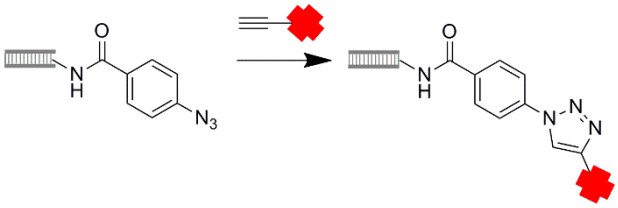	CuBr, TBTA, DMA/H_2O (3:4), 25 °C, 16 h [56]
9	Suzuki-Miyaura reaction	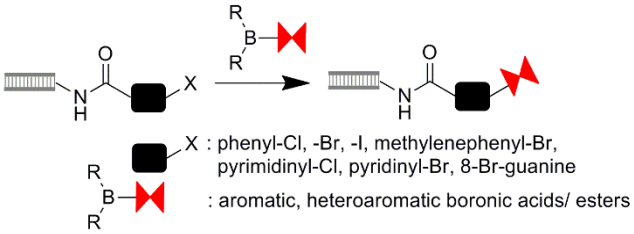	air stable Pd(II)-complex, KOH, H_2O, DMA, 80 °C, 3-4 h [67]
10	Sonogashira reaction	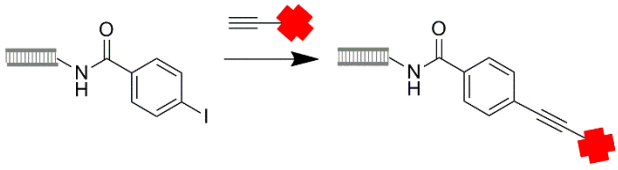	$Pd(OAc)_2$, pyrrolidine, TPPTS, DMA, H_2O, 65 °C, 2 h [56]

Appendage reactions[a]			
No.	reaction	scheme	conditions
11[b]	aldol condensation	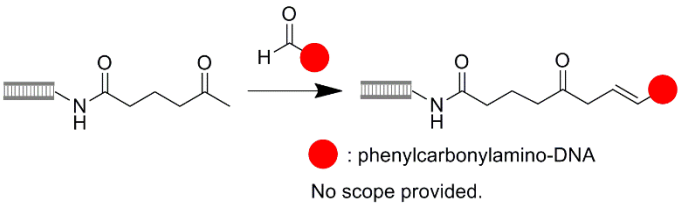	pyrrolidine, MeCN/H_2O (95:5), 25 °C, 16 h [68]
12[b]	Henry reaction	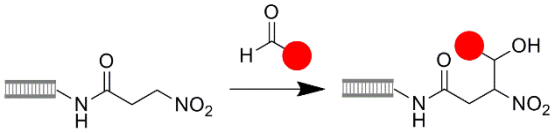	TAPS buffer, pH= 8.5, 300 mM NaCl, 25 °C, 12 h [69]
13[b]	Wittig olefination	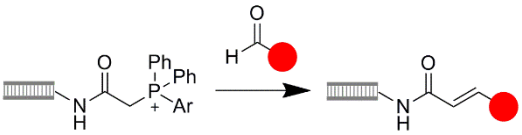	TAPS buffer, pH= 8.5, 1 M NaCl, 55 °C, 1.5 h [69]
14	Horner-Wadsworth-Emmons	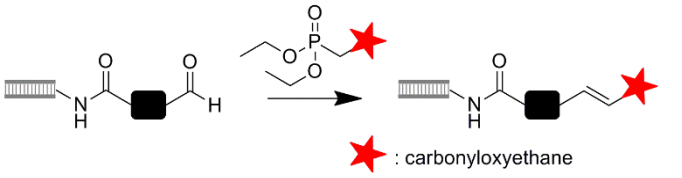	borate buffer, pH= 9.4, Cs_2CO_3, DMA, 25 °C, 16 h [56]
15[b]	alkene-alkyne oxidative coupling	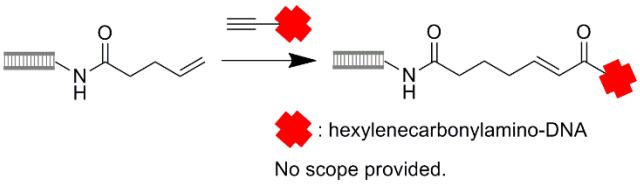	Na_2PdCl_4, MOPS buffer, pH= 7, 1 M NaCl, 37 °C, 1 h [70]
16[b]	Heck reaction	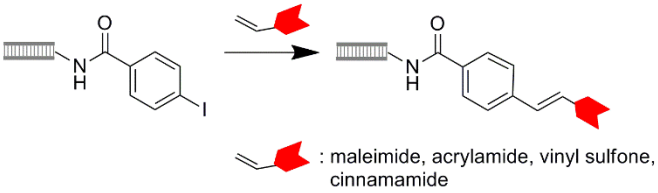	Na_2PdCl_4/ P(*p*-$SO_3C_6H_4$)$_3$ (1:2), phosphate buffer, pH= 5, 75 mM NaCl, 25 °C, 2 h [69]
17	Buchwald-Hartwig amination	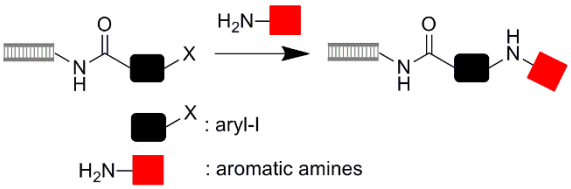	*t*-BuXPhos Pd G1, DMA, 5 M CsOH in H_2O, 100 °C, 3 h [71]

Appendage reactions[a]			
No.	reaction	scheme	conditions
18	"Ullmann-type" reaction	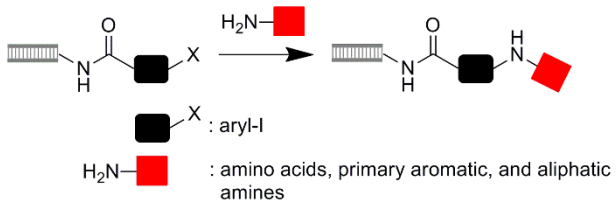	$CuSO_4$* $5H_2O$, sodium ascorbate, KOH, DMA, H_2O, 100 °C, 2 h [71]
19	aminolysis of epoxides	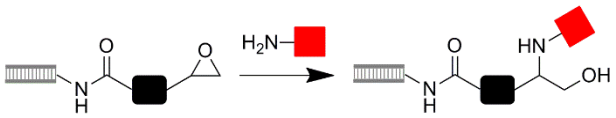	$Zr(DS)_4$, MeCN, H_2O, 50 °C, 16 h [62]
20	cross-metathesis reaction	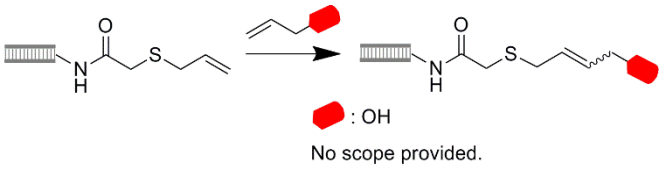	$MgCl_2$, *t*-BuOH, H_2O [72]

[a] different shapes indicate the different nature of building blocks; [b] reactions were performed only in the DNA-templated format.

In the same publication, the authors described the Michael addition (Table 3, entry 7) in DTS format as well, using maleimides and vinyl sulfones as Michael acceptors.[65] Cu(I)-catalyzed alkyne-azide cycloaddition (CuAAC) can also be used for DEL synthesis (Table 3, entries 8a, 8b), and it showed compatibility with DNA-templated[59,66] and DNA-recorded format.[56,59] The Cu(I)-catalyzed alkyne-azide cycloaddition (CuAAC) was also used for macrocyclization and synthesis of a 160.000-membered cyclic peptidomimetic DNA-templated library.[48] In last few years interest in transition metal-catalyzed cross-coupling reactions compatible with DNA has grown, especially with respect to Pd-catalyzed Suzuki-Miyaura cross-coupling. (Table 3, entry 9). In 2011, Omumi *et al*. reported Suzuki-Miyaura cross-coupling in the presence of DNA.[73] In the context of DNA-encoded libraries, Suzuki-Miyaura cross-coupling was first time published in 2014 by Ding *et al*.[74] In 2015, a publication reported on the synthesis of 334- and 34.7 million-membered libraries that were synthesized through three appendage reaction cycles which included introduction of boronic acid/ester building blocks by Suzuki cross-coupling in the second and the third cycle, respectively.[19,39] In 2016, a new catalytic system for DNA-compatible Suzuki-Miyaura cross-coupling with challenging

phenyl- and pyrimidinyl chlorides was developed.[67] Satz *et al*. described a DNA-compatible Pd-catalyzed Sonogashira cross-coupling reaction between a DNA-conjugated aryl iodide and an alkynes which were derived from an aldehydes *in situ* (Table 3, entry 10).[56] Although, DNA-templated version of Sonogashira coupling between alkyne and boronic acid was reported already in 2004 by Kanan *et al*.[70] Aldol condensation and Henry reaction were used only in DTS format (Table 3, entries 11, 12).[68,69] In contrast to the Henry reaction, aldol condensation did not proceed in aqueous solution but 95 % of acetonitrile was required.[68] Wittig olefination between phosphorus ylids and aldehydes provided the corresponding olefins in DTS format (Table 3, entry 13).[68,69,75] The reaction proceeded successfully in both, aqueous[69,75] and organic solvents.[68] In the same format, Wittig olefination was also used for macrocyclization[22,60,61] and as a ring-closing reaction efficiently delivered a 13.000-membered macrocycle library.[22] Another reaction to access olefins on DNA is the Horner-Wadsworth-Emmons reaction between reactive phosphonium yilds and aldehydes (Table 3, entry 14).[56] A DNA-templated reaction-discovery system identified alkyne-alkene oxidative coupling (Table 3, entry 15) as a novel reaction compatible with aqueous and organic solvents potentially allowing for the synthesis of macrocyclic enones.[70] Even before the development of protocols for DNA-encoded Suzuki- and Sonogashira-reaction, respectively, the first C-C cross coupling reaction that showed compatibility with DNA was the Heck reaction (Table 3, entry 16). It had been used then in the DTS format.[68,69] Heck cross-coupling can be performed in aqueous solvent, and in that case it is mediated by water soluble Na_2PdCl_4 catalyst. Using this reaction conditions, aryl iodide and activated olefins including maleimides, acryl amides, vinyl sulfones, and cinnamamides provided Heck coupling products on DNA.[69] In contrast, $Pd_2(dba)_3$-mediated Heck reaction allowed coupling of aryl iodides and unactivated alkenes but only in organic solvents, as $Pd_2(dba)_3$-complex is water insoluble.[68] Recently, first C-N cross coupling reactions for DNA-conjugated aryl iodides were developed, including Pd promoted Buchwald-Hartwig amination with aromatic amines (Table 3, entry 17), and Cu(I) promoted “Ullmann-type” coupling with amino acids and aliphatic amines (Table 3, entry 18).[71] Both reactions were used for DEL synthesis.[71] At the beginning of 2017, Fan *et al*. reported zirconium(IV)-catalyzed aminolysis of DNA-epoxide conjugates with aliphatic amines and anilines leading to DNA-encoded ß-amino alcohols (Table 3, entry 19).[62] Lewis acid-catalyzed ring opening of epoxides was successfully employed for DNA-encoded library synthesis.[62] Recently, the first ruthenium promoted cross-metathesis reaction on DNA was published, although the reactant scope was not provided (Table 3, entry 20).[72]

Table 4. DNA-compatible heterocyclic chemistry.

Heterocyclic chemistry[a]			
No.	heterocycle	scheme	conditions
1	benzimidazole	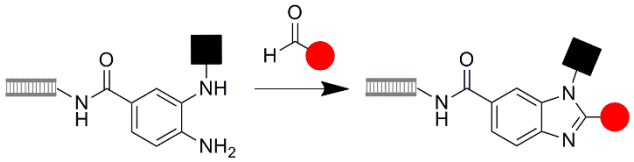	borate buffer, pH= 9.4, DMA, 60 °C, 18 h [56]
2	imidazolidinone	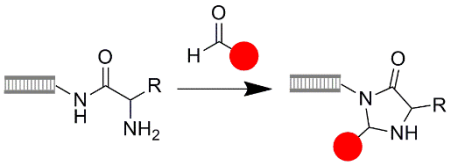	borate buffer, pH= 9.4, MeOH DMA, 60 °C, 18 h [56]
3	quinazolinone	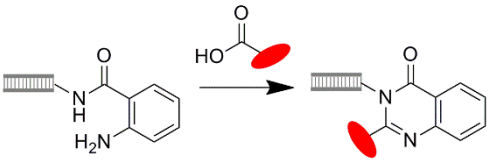	borate buffer, pH= 9.4, 1 N NaOH, 90 °C, 14 h [56]
4	isoindolinone	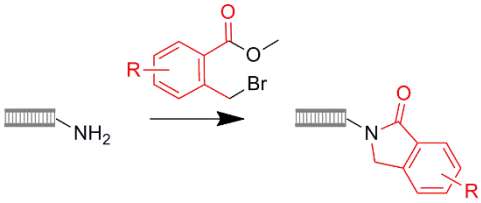	borate buffer, pH= 9.4, DMA, 60 °C, 2 h [56]
5	thiazole	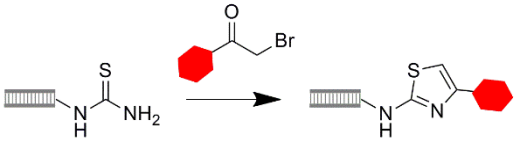	borate buffer, DMA, 25 °C, 24 h [56]
6	imidazopyridine	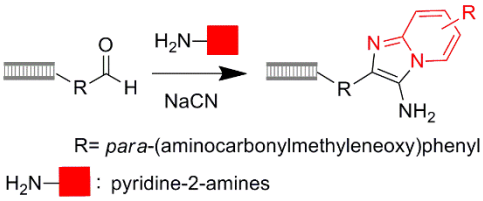 R= *para*-(aminocarbonylmethyleneoxy)phenyl H_2N— : pyridine-2-amines	borate buffer, pH= 9.4, DMA, 90 °C, 10 h [56]
7[b]	*N*-acyl-oxazolidine	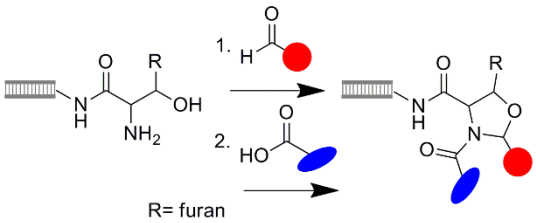 R= furan	1. MOPS buffer, pH= 7, 1 M NaCl, 25 °C, 6 h; 2. DMT-MM, 37 °C, 16 h [61]

Heterocyclic chemistry[a]			
No.	heterocycle	scheme	conditions
8[b]	*N*-acyl-thiazolidine	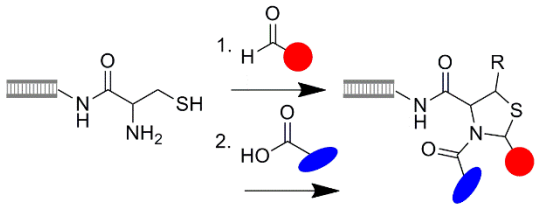	1. MOPS buffer, pH= 7, 1 M NaCl, 25 °C, 6 h; 2. DMT-MM, 25 °C, 12 h [66]
9	oxazolidin-2-one	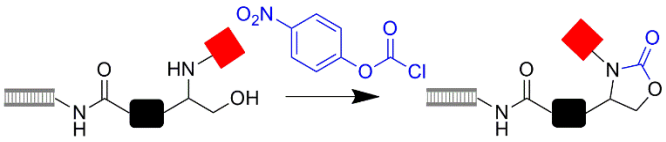	1. borate buffer, pH= 9.4, DIPEA, MeCN, 25 °C, 30 min; 2. EtOH precipitation; 3. borate buffer, pH= 12, 80 °C, 1 h [62]
10	morpholin-3-one	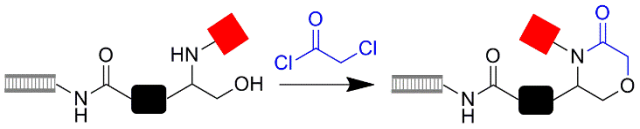	1. borate buffer, pH= 9.4, DIPEA, MeCN, 25 °C, 30 min; 2. EtOH precipitation; 3. borate buffer, pH= 12, 80 °C, 1 h [62]
11[b]	isoxazolidine	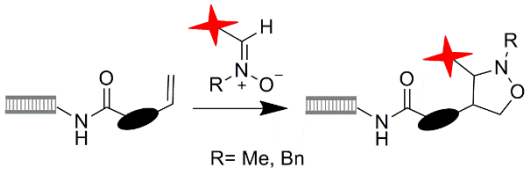	MOPS buffer, pH= 7.5, 2.8 M NaCl, 25 °C, 22 h [69]
12	tetrahydro-isoindolinone	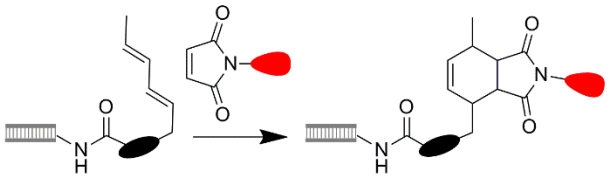	DMF, acetate buffer, pH= 4.7, 30 °C, 16 h [76]
13	spirocycle	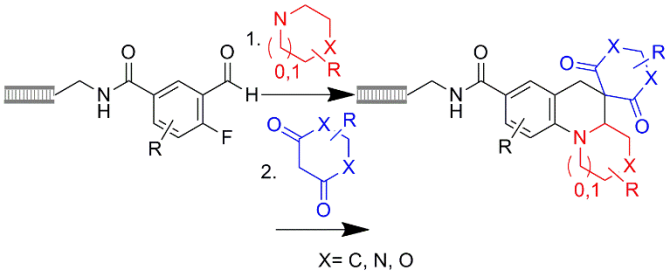	1. borate buffer, pH= 9.5, 60 °C; 2. DIPEA, dioxane, H_2O, 60 °C, 30 min [77]

Heterocyclic chemistry[a]			
No.	heterocycle	scheme	conditions
14	small saturated heterocycles and large 14- and 16-membered macrocycles	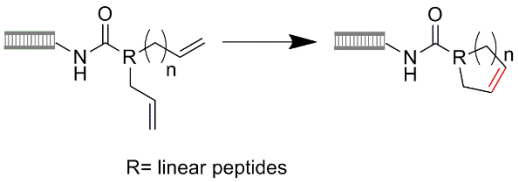	Ru catalyst, H_2O/*t*-BuOH (3:2), 25 °C, 1 h [72]

[a] different shapes indicate the different nature of building blocks; [b] reactions were performed only in the DNA-templated format.

Most heterocycles synthesized on DNA were accessed by condensation reactions. These are foremost benzimidazoles,[78] oxazolidin-2-ones,[62] and morpholin-3-ones.[62] Synthesis of *N*-acylthiazolidines was used only for construction of model 18-membered library in a DNA-templated format.[66] Another reaction that has been used for synthesis of a heterocycle on DNA in DNA-templated format (DTS) is nitrone 1,3-dipolar cycloaddition between nitrones and olefins to isoxazolidines (Table 4, entry 11). The isoxazolidines were obtained with maleimides, vinyl sulfones, and acrylamides, un-activated alkenes also furnished corresponding products but rather in low yields. In 2008, Buller *et al*. employed the Diels-Alder cycloaddition of 2,4-hexadienes and maleimide derivatives, which were either commercially available or generated *in situ* from corresponding primary amines and maleic anhydrides, to synthesize a 4000-membered tetrahydroisoindolinone DNA-encoded library (Table 4, entry 12).[76] This work demonstrated for the first time the *in situ* formation of building blocks for DEL synthesis. In 2016, Tian *et al*. brought stereochemical complexity of DNA-encoded heterocycles in focus through development of the tertiary amino-effect reaction (T-reaction) in DEL format (Table 4, entry 13).[77] The T-reaction is a cascade reaction involving a Knoevenagel condensation, subsequent [1,5]-hydride shift, and a final Mannich cyclization yielding variously substituted spirocycles. Along with the Diels-Alder cycloaddition, the T-reaction is one of a few reactions that allow formation of multiple C-C bonds on DNA. Recently, Lu *et al*. developed a DNA-compatible protocol for ruthenium-promoted ring-closing metathesis in the presence of $MgCl_2$ for the synthesis of small saturated 5-, 6-, 7-, and 8-membered heterocycles, and 14- and 16-membered macrocycles, respectively (Table 4, entry 14).[72] The authors suggested that Mg^{2+} cations bound to the phosphate

backbone thereby preventing its interaction with ruthenium ions and potential DNA decomposition.[72] Blakskjaer *et al.* reported a 2.4 million-membered dihydropyridine library synthesized by the well-known Hantzsch procedure, but technical details were not reported.[79] Arico-Muendel mentioned a broad set of DNA-compatible chemical transformations available at encoded library technology (ELT) platform in GlaxoSmithKline including cyclization and annulation reactions to pyrazoles, pyrazolines, oxadiazoles, tetrazoles, pyridones, (imino)hydantoins, imidazoles, purines, and benzothiazepinones, but with no technical details provided.[54]

1.3. Privileged scaffolds in drug discovery

In 1988, Evans *et al*. recognized that certain structural motifs are capable of acting as a ligands for diverse receptors, and to these motifs they ascribed the term "privileged structures".[80a]

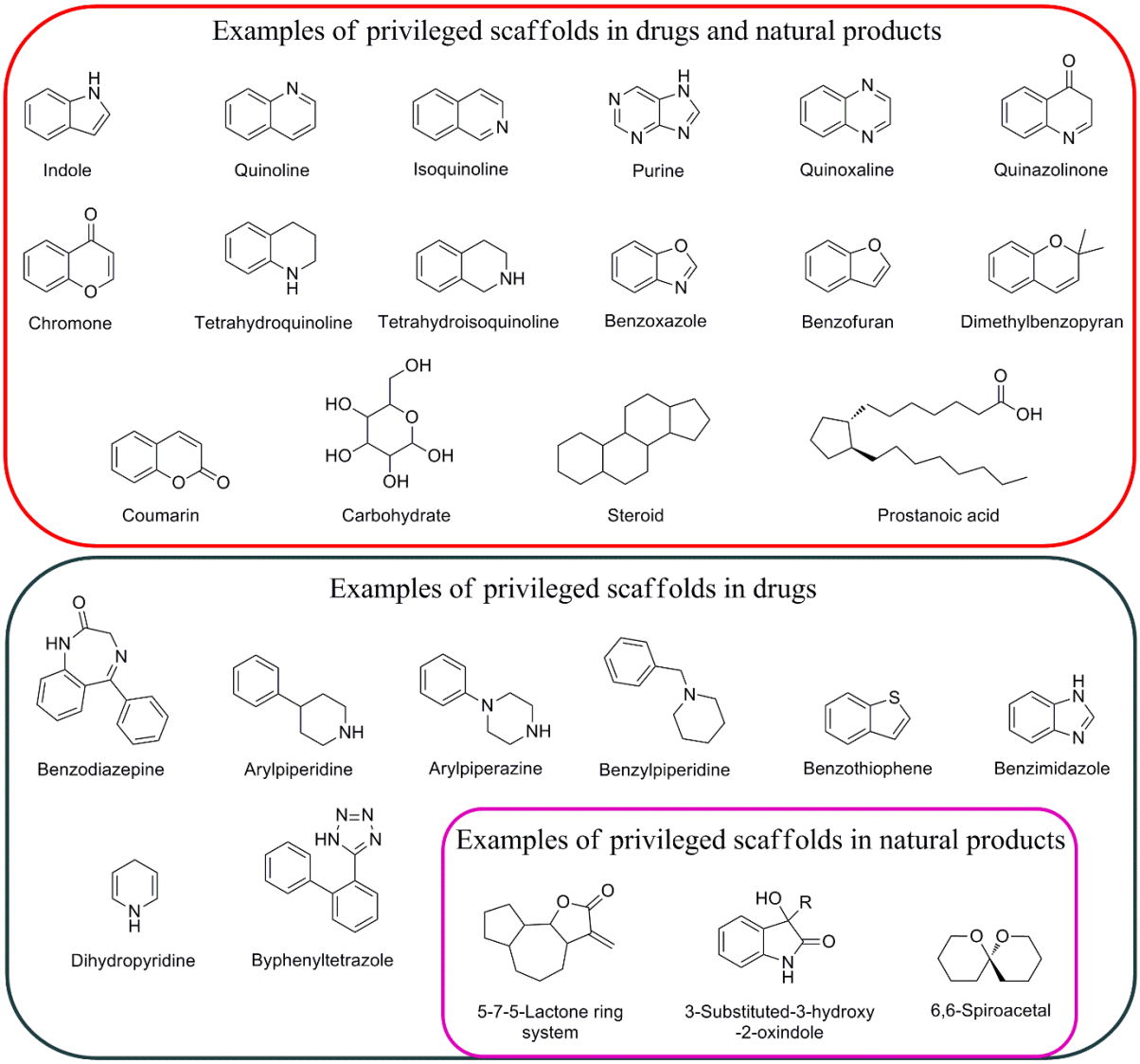

Figure 1.9. Examples of privileged scaffolds in drugs and in natural products.

The authors suggested the intriguing potential of "privileged structures" as templates for functionalization to improve the probability of discovery of small molecule protein binder. Evans *et al*. were referring to the benzodiazepine as to the "privileged structure". However, in the last 30 years several more small molecule structures were given the term "privileged".[80b] Welsch *et al*. provided a comprehensive list of "privileged scaffolds" found in drugs, as well as in natural products, a number of these are shown in Figure 1.9. They encompass e.g.

indole, quinoline, purine, chromone, coumarin, benzimidazole, dihydropyridine, and many others.

Selection of scaffold represents an important parameter of DNA-encoded library design. Therefore, we decided to base our libraries on scaffolds that are highly represented among bioactive compounds: pyrazolopyrimidine, pyrazole, and pyrazoline scaffold. A number of bioactive compounds based on these scaffolds will be described in more detail in the following chapters.

1.3.1. The pyrazolo[3,4-d]pyrimidine structure - a privileged scaffold for kinase inhibition

Pyrazolo[3,4-*d*]pyrimidine **18** is heterocyclic ring system which consists of a fused 5-membered pyrazole and a 6-membered pyrimidine ring (Fig. 1.10). It mimics the purine nucleobase adenine **19**, and can be considered as adenine bioisostere. Thus it does not surprise that pyrazolo[3,4-*d*]pyrimidine derivatives are exhaustively investigated as adenosine triphosphate (ATP) **20** competitive inhibitors of various kinases.

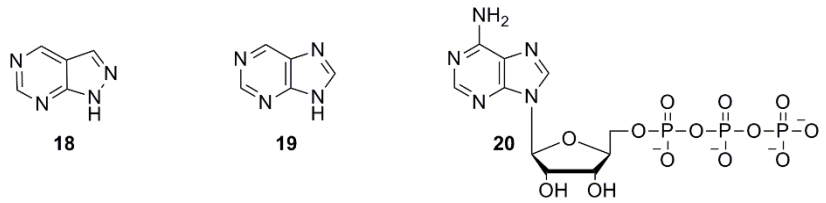

Figure 1.10. Structure of pyrazolo[3,4-*d*]pyrimidine **18**, adenine **19**, and adenosine triphosphate (ATP) **20**.

The majority of pyrazolo[3,4-*d*]pyrimidine based kinase inhibitors such as **21**-**32** presented in Figure 1.11, act as a ligands for ATP binding site in the active conformation of the enzyme. Mammalian target of rapamycin (mTOR) is serine-threonine kinase, and a member of phosphatidylinositol 3-kinase-related kinases (PIKK) family.[81] mTOR has a crucial role in the phosphatidylinositol 3-kinase (PI3K) pathway, the protein kinase B (Akt/PKB) pathway, and the Rat sarcoma (Ras)/extracellular signal regulated kinase (ERK) pathway. Therefore, mTOR is involved in cell growth, motility, proliferation, survival, protein synthesis, and transcription.[82] Intracellular mTOR exists in two complexes: mTOR complex 1 (mTORC1) and mTOR complex 2 (mTORC2). mTORC1 is regulated by growth factors (i.e. IGF1 and IGF2) over PI3K and Akt/PKB pathways,[83] and its activity is mainly mediated through

activation of p70 S6 ribosomal kinase 1 (p70S6K1)[84] and eukaryotic initiation factor 4E-binding protein 1 (4E-BP1).[85] It is engaged in regulation of cyclins, cyclin-dependent kinases (CDKs), protein phosphatases, and RNA polymerases.[86]

mTORC2 is involved in regulation of cytoskeleton functions.[87] It is activated by growth factors, and it activates Akt which in turn activates mTORC1 that stimulates cell growth and proliferation.[88] mTOR activity is frequently deregulated in human diseases, and especially in malignancies.[89] Wyeth Pharmaceuticals, Inc. (part of Pfizer, Inc. since 2009) developed mTOR inhibitor WYE-132 **21** (IC_{50}= 0.21 nM) with 5619-fold selectivity over PI3Kγ.[90] Compound **21** (Fig. 1.11) exhibited potent antitumor activity against breast carcinoma cell line MDA361, glioma carcinoma cell line U87MG, lung carcinoma cell lines A549 and H1975, and renal carcinoma cell lines A498 and 786-O.[90]

The PI3K family includes 15 lipid kinases that belong to the same signaling pathway as mTOR. They phosphorylate 3-hydroxy position of membrane phospholipid phosphatidylinositol 4,5-diphosphate to phosphatidylinositol 3,4,5-triphosphate, which regulates cell shape, growth, motility, differentiation, and survival through Akt phosphorylation.[88] They exist in four different classes: IA, IB, II and III.[91] Class IA PI3K consists of one PI3K catalytic subunit (PI3Kα, PI3Kß or PI3Kγ), and p85 regulatory subunit. The gene encoding the PI3Kα is found mutated and/or overexpressed in breast, ovarian, colorectal, brain, and gastric cancers, therefore PI3K has arisen as promising anticancer target.[88] Wyeth Pharmaceuticals, Inc. patented dual mTOR/PI3K inhibitors, as it was found that selective inhibition of mTOR pathway led to activation of PI3K pathway.[92] Wyeth identified pyrazolopyrimidine **22** (Fig. 1.11) with inhibitory activity towards PI3Kα, PI3Kγ, and mTOR (IC_{50}= 1 nM, 68 nM, and 13 nM, respectively).[93]

The mitogen-activated protein kinase (MAPK) pathway relates to the Ras-Rapidly Accelerated Fibrosarcoma (Raf)-MAPK/ERK kinase (MEK)-ERK pathway. These pivotal kinases transmit extracellular signals that regulate cell growth, differentiation, proliferation, apoptosis, and migration.[88] For example, B-Raf is the main MEK activator. It is one of the most frequent anticancer targets. The p38α family of MAPKs is mainly involved in the inflammatory response,[94] and regulates the production of pro-inflammatory cytokines, like tumor necrosis factor TNF-α, interleukin-1 (IL-1), and interleukin-6 (IL-6). Therefore, p38α MAPK is considered to be a valuable target for the treatment of rheumatoid arthritis, pain, and respiratory diseases.[95] Genetech, Inc. (a member of Roche group) reported a patent on pyrazolopyrimidine based inhibitors of B-Raf.[96,97] Compound **23** (Fig. 1.11) was among the most potent inhibitors against mutant B-Raf-V600E (IC_{50}= 0.9 nM). Pyrazolopyrimidine **24**

(Fig. 1.11) developed by Bristol-Myers Squibb exhibited low nanomolar potency against p38α in the enzymatic assay (IC_{50}= 5 nM), and against TNF-α production in human peripheral blood mononuclear cells (IC_{50}= 6 nM).[98]

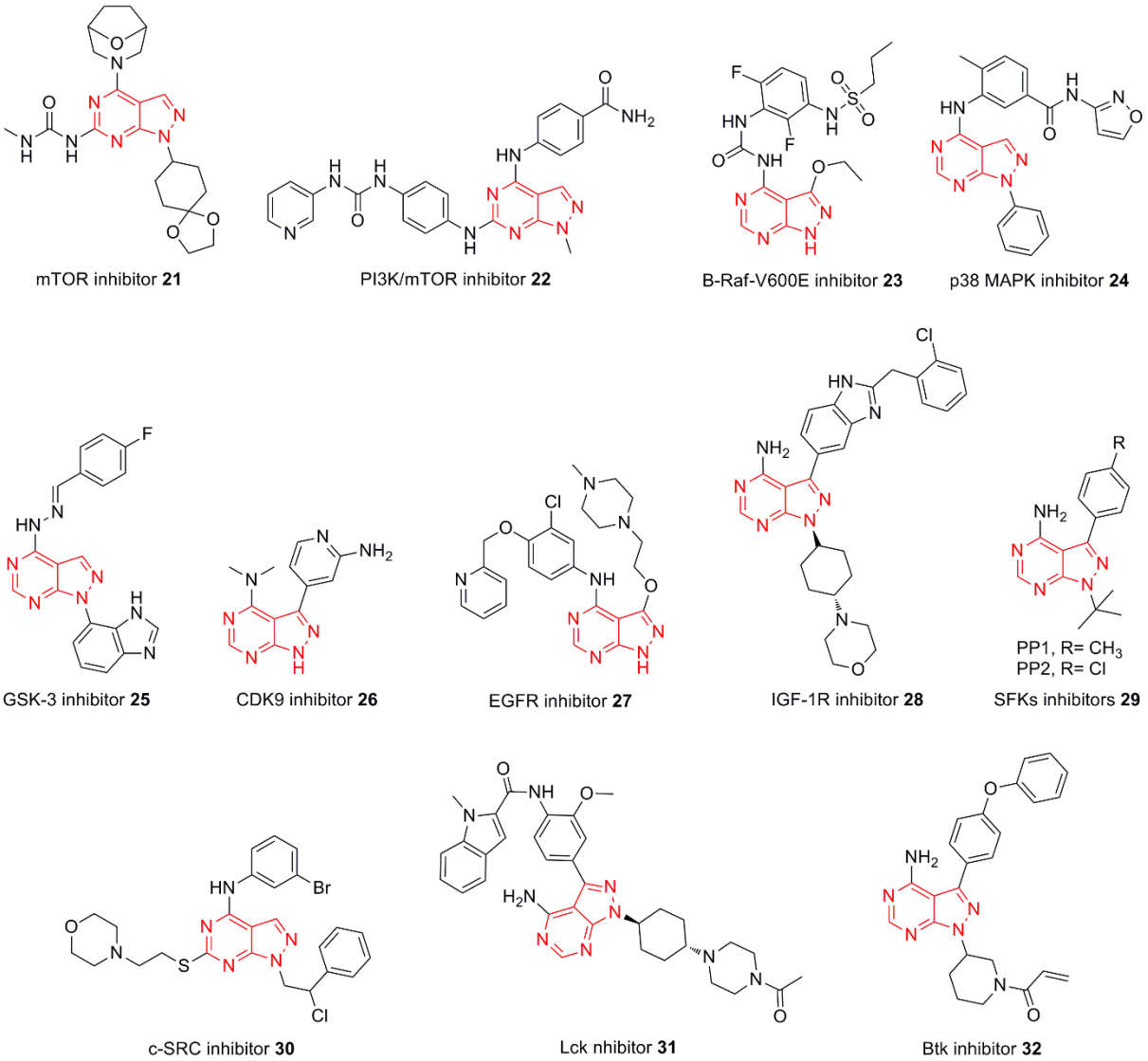

Figure 1.11. Pyrazolo[3,4-*d*]pyrimidine derivatives and their kinase targets.

Glycogen Synthase kinase-3 (GSK-3) is serine-threonine protein kinase phosphorylating more than 40 different proteins.[99] GSK-3 has an important role in cell proliferation, migration, glucose regulation, and apoptosis. It exists in two different isoforms GSK-3α and GSK-3ß. GSK-3 is highly expressed in diabetes-2 patients, thus it is potential therapeutic target for the treatment of type-2 diabetes mellitus.[88] It also phosphorylates cytoskeletal protein Tau. Hyperphosphorylated Tau may lead to neurodegenerative disorders.[100] GSK-3 is also involved in Wnt pathway and nuclear factor κB pathway, both associated with

malignancies.[101] GlaxoSmithKline developed a class of pyrazolopyrimidines bearing hydrazone motif as potential GSK-3 inhibitors. SAR studies revealed compound **25** (Fig. 1.11) with potent inhibitory activity against GSK-3 (pIC_{50}= 8.2).[102]

The family of cyclin dependent kinases (CDKs) includes at least nine serine-threonine protein kinases that together with their regulatory subunits (cyclins) control cell-cycle progression.[103] Alterations in the genes encoding CDKs, their cyclin partners, or their endogenous peptide inhibitors (CKIs) are often associated with tumorigenesis.[104] Exelixis Inc. patented a series of pyrazolopyrimidines that are active against CDKs, and some of them are especially active against CDK9[105] which plays an important role in immune cell function. Compound **26** (Fig. 1.11) showed low nanomolar activity against CDK9 in enzymatic assay (IC_{50}= 1 nM), and antitumor activity towards NCI H460 human lung cancer cell line.

Tyrosine kinases (TKs) catalyze the phosphate transfer from ATP to specific tyrosine residues of protein substrates. TKs regulate cell growth, differentiation, migration, adhesion, and apoptosis.[106] There are two subfamilies of TKs: receptor tyrosine kinases (RTKs), and cytoplasmic nuclear nonreceptor tyrosine kinases (nRTKs). RTKs consist of three domains: extracellular domain for binding of ligands (growth factors, cytokines, hormones), hydrophobic transmembrane domain, and C-terminal cytoplasmic intracellular domain.[107] Ligand binding triggers autophosphorylation of a specific tyrosine residue placed in the intracellular region, thus activates the kinase and subsequent signal transduction within the cell.[108] Epidermal growth factor receptor (EGFR, ErbB1, Her1) is a TK which belongs to the ErbB (erythroblastic leukemia viral oncogene) family together with ErbB2 (Her2), ErbB3 (Her3), and ErbB4 (Her4).[109] Insufficient ErbB signaling is related to neurodegenerative disorders, while excessive signaling is linked with human cancers. The overexpression of EGFR and ErbB2 is associated with development of epithelial tumors, and epidermal proliferative disorders.[88] AstraZeneca reported pyrazolopyrimidine **27** (Fig. 1.11) with low nanomolar activity against ErbB2 (IC_{50}= 1 nM), EGFR (IC_{50}= 5 nM), and breast carcinoma cell line HT474C (IC_{50}= 16.6 nM).[110]

Insulin-like growth factor 1 receptor (IGF-1R) is a RTK which is part of IGF pathway. The pathway also involves insulin receptor (IR), insulin-like growth factor I/II (IGF-I/IGF-II), and six insulin-like growth factor-binding proteins.[111] IGF-1R exists as homodimer of IGF-1R, or heterodimer of IGF-1R and IR. The homodimer is activated by binding of IGF-I and IGF-II, while the heterodimer is also activated by binding of insulin.[112] IGF-1R is involved in suppression of apoptosis. It simultaneously activates the antiapoptotic PI3K/Akt pathway and the mitogenic ERK/MAPK pathway.[88] Abbott Laboratories identified a number of

pyrazolopyrimidine based IGF-1R inhibitors. Compound optimization led to A-928605 **28** (Fig. 1.11) that inhibited IGF-1R *in vitro* (IC_{50}= 37 nM).[113] Pyrazolopyrimidine **28** also inhibited cellular IGF-1R phosphorylation (IC_{50}= 90 nM) induced by IGF1 in A431 epidermoid carcinoma cells,[113] and the growth of neuroblastoma xenografts *in vivo*.[114]

Cytoplasmic nuclear nonreceptor TKs are located inside the cell. They have an important role in regulation of cell growth, differentiation, proliferation, migration, metabolism, and apoptosis.[88] They are overexpressed and/or hyperactivated in many solid tumors, and alterations in their functions are probably promoting metastasis too.[115,116] They can be activated by binding of growth factor receptors, integrins and other adhesion receptors, G-protein-coupled receptors (GPCRs), cytokine receptors, and ion channels. Their activity is mediated through phosphorylation of different downstream targets. Important nRTKs are Src family kinases (SFKs). In 1996, Pfizer, Inc. reported the SFK inhibitors **29** (Fig. 1.11): PP1 and PP2.[117] These compounds inhibited all SFKs in a low nanomolar range. Because of that reason and potential toxicity, PPI and PPII were rather used as a chemical biology probes than in clinic.

c-Src kinase belongs to the Src family of kinases. It is engaged in cell proliferation, migration, invasion, and angiogenesis.[118] c-Src is overexpressed and/or hyperactivated in many cancer cell lines,[119] and some studies suggest its involvement in the development of drug resistance.[120] Hyperactivated c-Src plays a crucial role in the differentiation, cell adhesion, and survival of neuroblastoma cells (NB),[121] and it is likely involved in the progression of aggressive NB forms.[122] Tintori *et al*. developed the potent c-Src inhibitor **30** (Fig. 1.11) (IC_{50}= 130 nM) that inhibited SH-SY5Y neuroblastoma cell proliferation (IC_{50}= 340 nM) *in vivo*.[119]

Lymphocyte specific protein tyrosine kinase (Lck) is also a member of SFK family. It is mainly located in T-lymphocytes, and has essential role in T-lymphocyte activation and differentiation.[123] Lck is critical for T-cell antigen receptor (TCR) signaling pathway. As it plays crucial role in immune responses, Lck is evaluated as a potential target for treatment of autoimmune diseases and organ transplant rejection.[88] Abbot Laboratories developed pyrazolopyrimidine A-770041 **31** (Fig. 1.11) as a potent Lck inhibitor (IC_{50}= 147 nM) with 300-fold selectivity over Fyn, a kinase involved in T-cell signaling.[124] The compound's selectivity might result from compound **31** binding to the inactive conformation of Lck.

Bruton's tyrosine kinase (Btk) is nRTK that belongs to the TEC protein tyrosine kinase family (TEC). Btk is crucial for B-cell antigen receptor (BCR) signaling pathway, and regulates proliferation and survival of various B-cell malignancies.[125] Pharmacyclics, Inc. (acquired by

AbbVie, Inc. in 2015) patented a series of irreversible Btk inhibitors. Among these pyrazolopyrimidine derivatives the most interesting was ibrutinib **32** (Fig. 1.11) which covalently binds to the cysteine 481 in the active site of Btk (IC_{50}= 0.5 nM).[126] It also inhibited interleukin-2-inducible T-cell kinase (ITK), a member of TEC family,[127] and displayed oral activity against different B-cell malignancies. Ibrutinib (Imbruvica® Capsules) was approved by the Food and Drug Administration (FDA) in 2013 for treatment of mantle cell lymphoma in patients who had received at least one previous therapy, and in 2014 for treatment of chronic lymphocytic leukemia in patients who had received at least one previous therapy. In 2015, it was approved for the treatment of patients with Waldenström's macroglobulinemia.

1.3.2. Pyrazoles and pyrazolines

Pyrazoles **33** are heterocyclic five-membered rings composed of three carbon and two neighbouring nitrogen atoms (Fig. 1.12). They are aromatic compounds with 6 delocalized π-electrons that are coming from 4 π-electrons and one lone electron pair on the -NH nitrogen. This nitrogen is also known as "pyrrole-like" and it is non-basic, while neighbouring nitrogen is "pyridine-like" and it is basic.

Figure 1.12. Pyrazole **33** and pyrazoline **34**.

The non-aromatic counterpart of pyrazole is 4,5-dihydropyrazole also known as pyrazoline **34** (Fig. 1.12). Both, pyrazoles and pyrazolines undergo tautomerism (Figs. 1.13, 1.14). While pyrazole tautomers (Fig. 1.13) have similar energies,[128] in case of pyrazolines one tautomer is more stable than the others.

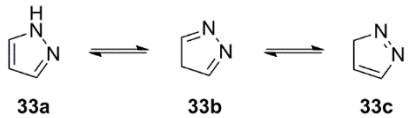

Figure 1.13. Tautomerization of pyrazole **33**.

The Δ^2-pyrazoline (4,5-dihydro-1*H*-pyrazole, **34b**) is more stable then the Δ^1-pyrazoline (4,5-dihydro-3*H*-pyrazole, **34a**), and the least stable is Δ^3-pyrazoline (2,3-dihydro-1*H*-pyrazole, **34c**). For example, the *N*-methyl group stabilizes the Δ^3-pyrazolines, but with some exceptions only 1,2-disubstituted Δ^3-pyrazolines are known.[128]

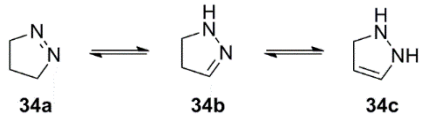

Figure 1.14. Tautomerization of pyrazoline **34**.

1.3.2.1. Bioactive pyrazoles

Plenty of bioactive compounds can be found within the pyrazole compound class, not only in the early research phase but also among marketed drugs (Fig. 1.15). As pyrazole derivatives were investigated for their hypoglycemic, analgesic, anti-inflammatory, antimicrobial, anticonvulsant, antidepressant, anthelmintic, antioxidant, and antitumor activities, one can call the pyrazole scaffold a "privileged scaffold".[80]

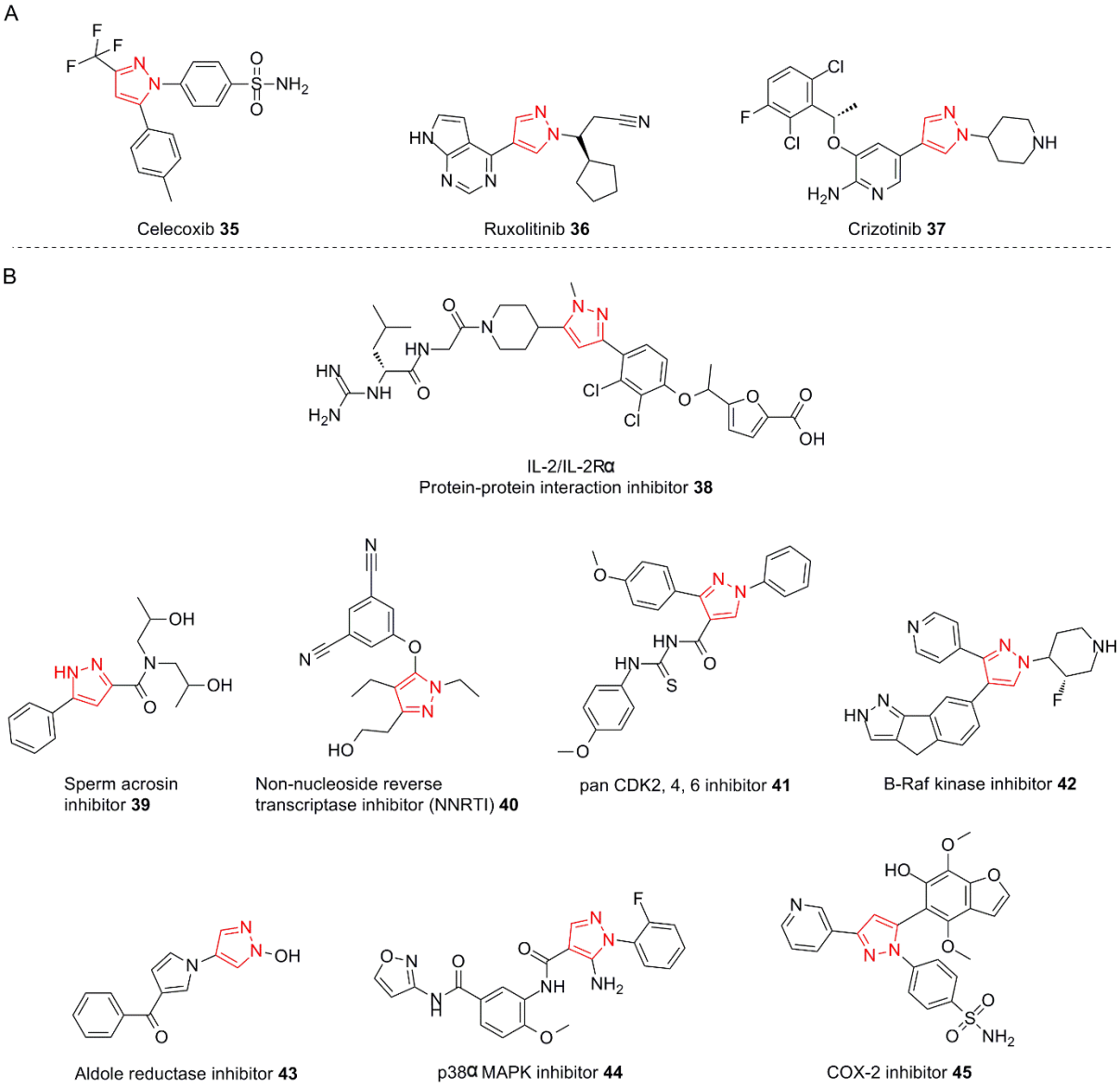

Figure 1.15. Marketed drugs and bioactive compounds based on pyrazole scaffold. A) Marketed drugs with pyrazole core structure; B) pyrazole derivatives with different biological activities.

Celecoxib (Celebrex®, Pfizer, Inc.) **35** (Fig. 1.15A) is non-steroidal anti-inflammatory drug (NSAID) acting as selective cyclooxygenase 2 (COX-2) inhibitor (IC_{50}= 40 nM). It is used to treat arthritis, acute pain, menstrual pain, juvenile rheumatoid arthritis, and hereditary polyps in the colon. NSAIDs inhibit the biosynthesis of prostaglandins (PGs), and cyclooxygenases (COXs) catalyze the conversion of arachidonic acid to prostaglandin H2 (PGH2). Two isoforms of COX are known: COX-1 and COX-2. COX-1 is produced in most of the tissues, and it is responsible for synthesis of cytoprotective PGs in gastrointestinal tract, normal renal function, vascular homeostasis, and the biosynthesis of proaggregatory thromboxane 2 (TXA2) in blood platelets.[129-132] On the other hand, COX-2 makes significant contribution to the production of inflammatory PGs. Its inhibition decreases the expression of inflammatory mediators such as TNF-α, inducible nitric oxide synthase (iNOS), and interleukin 1ß (IL-1ß),[133,134] and it reduces the activity of transcriptional noncanonical nuclear factor κB (NF-κB).[135] Thus, development of selective COX-2 inhibitors is of great interest as dual COX-1/COX-2 inhibition downregulates PGs formation in most of the healthy tissues as well, consequently delivering adverse side-effects.

Ruxolitinib (Jakafi®, Incyte Corp.) **36** (Fig. 1.15A) is the first approved inhibitor of Janus kinases (JAK1 and JAK2, IC_{50}= 3.3 nM, and 2.8 nM in cell-free assays, respectively). It is used for treatment of polycythemia vera (PV), a rare myeloproliferative neoplasm, and for myelofibrosis.[136] Janus kinases (JAKs) are non-receptor tyrosine kinases that have four members: JAK1, JAK2, JAK3 that are ubiquitously expressed, and Tyrosine kinase 2 (Tyk2) which is mainly located in hematopoietic cells. JAKs are activated by binding of cytokines to their receptors. Upon activation they activate signal transducers and activators of transcription family (STATs).[137] JAKs are involved in regulation of cell production, differentiation, proliferation, and survival. They represent potential therapeutic targets for treatment of inflammatory diseases, and hematopoietic malignancies.

Crizotinib (Xalkori®, Pfizer, Inc.) **37** (Fig. 1.15A) is the first approved inhibitor of anaplastic lymphoma kinase (ALK, IC_{50}= 24 nM) and MET proto-oncogene-encoded kinase (c-MET, IC_{50}= 5-20 nM).[138] It also inhibits ROS proto-oncogene 1-encoded kinase (ROS1).[138] It is first anti-cancer drug used for treatment of patients with metastatic non-small cell lung cancer (NSCLC). ALK, MET, and ROS1 (member of insulin receptor (IR) family) belong to the receptor tyrosine kinases (RTKs), thus they control signal transmission from cellular surface into the cell, and they are involved in regulation of many signal transduction pathways. Therefore, alterations in their functions are associated with many human cancers.

IL-2Rα is one of the three trans-membrane proteins: IL-2Rα, IL-2Rß, and IL-2Rγ, subunits of the pro-inflammatory cytokine, interleukine-2 (IL-2). IL-2Rα is expressed along with IL-2 following T-cell receptor (TCR) activation. IL-2 is produced upon immune stimulation of T-cells mediated by TCR and major histocompatibility complexes (MHC) I and II.[139] T-cells recognize different pathogenic threats in form of complexes between peptides derived from pathogenic proteins and MHC molecules, formed on cell surface. MHC class I molecules bind peptide antigens with intracellular origin, while MHC class II molecules bind to extracellular pathogens.[139] Braisted *et al*. and Raimundo *et al*. discovered SP4206 **38** (Fig. 1.15B), a small molecule that bound to IL-2 with high affinity (K_i= 68.8 nM), and consequently blocked the interaction between IL-2 and its natural receptor IL-2Rα (K_i= 10.5 nM).[140] IL-2/IL-2Rα protein-protein interaction (PPI) inhibitor **38** bound to IL-2 using one third of contact residues that IL-2Rα does, but it displayed highly focused electrostatic interactions. In complex with **38** IL-2 provided deeper cavities that contributed to the high ligand binding efficiency of small molecule **38**.[140c]

Sperm acrosin is a trypsin-like protease which likely plays role in fertilization,[141] and therefore can be considered as potential target for contraception in men.[142] Tian *et al*. synthesized a series of novel 5-phenyl-1*H*-pyrazole-3-carboxylic acid amide derivatives that were evaluated for their sperm acrosin inhibitory activity *in vitro*.[142] Among all tested pyrazoles, compound **39** (Fig. 1.15B) exhibited the most potent inhibitory activity (IC_{50}= 0.01 µM) and very good ADMET properties.

Reverse transcriptase (RT) is a DNA polymerase which inhibition is very important in the treatment of HIV infections, and NNRTI are non-competitive RT inhibitors binding to the allosteric site of the enzyme. As this site is not present in the RT of normal cells, NNRTI are more specific for viral enzyme.[143] Pfizer, Inc. developed the potent non-nucleoside reverse transcriptase inhibitor (NNRTI) **40** (Fig. 1.15B) with good aqueous solubility and metabolic stability.[143] Compound **40** was developed as a pyrazole isomer of lersivirine- a promising investigational drug, but withdrawn from phase IIb of clinical trials due to non-superiority over existing therapies. A major problem of NNRTI is development of viral resistance caused by mutations in RT. Therefore pyrazole **40** was designed as inhibitor of clinically relevant Y181C mutant enzyme (IC_{50}= 0.029 µM).[144,145]

The cyclin-dependent kinases (CDKs) are a family of serine-threonine protein kinases that are important players in cell-cycle progression. Alterations in cell cycle are often associated with malignancy. CDK2 was found to be relevant in many cancers probably due to the fact that it plays vital role in the process of G1 to S phase transition. Thus, inhibition of CDK2 holds

promise for the treatment of cancers.[146,147] Sun *et al*. synthesized a series of novel pan-CDK inhibitors as potential antitumor agents.[148] Inspired by known CDKs inhibitors that share the pyrazole core, AT7159 (CDK1, 2, 4, 5 inhibitor)[149] and PNU-292137 (CDK1, 2, 4 inhibitor),[150] the authors decided to base their inhibitor on the pyrazole scaffold as well, and substitute it with a bulky thiourea substituent to increase potency.[148] Pyrazole **41** (Fig. 1.15B) displayed highest inhibitory activity as CDK2, CDK4, and CDK6 inhibitor (IC_{50}= 0.025 µM, 0.035 µM, and 0.029 µM, respectively). It also showed anti-proliferative activity against carcinomic human alveolar basal epithelial cell A549 (IC_{50}= 0.75 µM).

B-Raf is one of the three isoforms of Raf kinases, along with A-Raf and C-Raf (Raf-1), which are all part of the mitogen-activated protein kinase pathway (MAPK). In general, Raf-kinases have critical role in cell proliferation and survival.[151,152] B-Raf gained a lot of attention in medicinal chemistry as it is mutated in 7 % of human cancers. Array BioPharma and Genetech, Inc. developed pyrazole based B-Raf inhibitors that incorporated an oxime moiety.[153] This compound series exhibited very high potency and selectivity, but suffered from chemical instability and metabolic liability.[154] The authors found that replacing of oxime moiety with a fused pyrazole structure retained high enzyme activity, with encouraging cellular potency, and led to the higher chemical stability when compared to the oxime-displaying compounds. Finally, pyrazole **42** (Fig. 1.15B) potently inhibited B-Raf (IC_{50}= 0.0014 µM), showed modest oral adsorption in mice, and good kinase selectivity as well.

Aldose reductase 2 (ALR2) is cytosolic NADPH dependent oxidoreductase. It catalyzes the NADPH dependent reduction of glucose to sorbitol dehydrogenase (SDH) in the presence of NAD+. It drew interest as a target in medicinal chemistry as it is hypothesized to play a pivotal role in many pathologies.[155] It is implicated in diabetes mellitus long-term complications. Redundant flow through this pathway can result in elevated osmotic and oxidative stress.[156,157] Besides, ALR2 was also identified as key mediator in various inflammatory diseases and cancer. [158-160] There are mainly two compound classes that act as aldose reductase inhibitors (ARIs): spiroimides and carboxylic acid derivatives with limited bioavailability. Papastavrou *et al*. reported the synthesis of 1-hydroxypyrazoles as a bioisosteres of the carboxylic acid moiety in a series of ALR2 inhibitors.[161] Pyrazole **43** (Fig. 1.15B) was identified as a potent lead compound (IC_{50}= 1.136 ± 0.020 µM) with good physiochemical properties.

Much activity in drug research is directed towards identification of potent and selective p38α mitogen-activated protein kinase (MAPK) inhibitors due to the implication of this enzyme in inflammatory diseases.[162] Bristol-Myers Squibb reported 5-aminopyrazoles as potent and

selective p38α inhibitors.[163] Before aminopyrazoles they investigated pyrazolo-pyrimidines.[164] X-ray co-crystallographic studies of their representative pyrazolopyrimidine complexed with p38α showed lack of any productive interaction of the pyrimidine ring with the enzyme, therefore they decided to reduce the scaffold to the pyrazole core. SAR optimization led to the pyrazole **44** (Fig. 1.15B) as highly potent and selective p38α inhibitor (IC_{50}= 0.002 µM) with high potency for inhibition of tumor necrosis factor TNF-α release (IC_{50}= 0.001 µM) in human peripheral blood mononuclear cells (PBMCs). Pyrazole **44** also demonstrated oral efficacy in an acute murine model of TNF-α inhibition.

Hassan *et al*. designed and synthesized analogs of Celecoxib **35** (Fig. 1.15A) bearing functionalized benzofurans, and evaluated them for potential COX-2 inhibitory activity.[165] The pyrazole core was substituted with bulky benzofuran moiety in order to maximize interactions with hydrophobic residues in COX-2 active site, and enhance COX-2 selectivity. Pyrazole **45** (Fig. 1.15B) was subsequently identified as potent and selective COX-2 inhibitor (IC_{50}= 0.36 µM) with equipotent anti-inflammatory activity compared to the reference Celecoxib, but with improved gastrointestinal safety profile.

1.3.2.2. Bioactive pyrazolines

Structurally related to pyrazoles, pyrazolines also exhibit diverse biological activities (Fig. 1.16). The CB_1 cannabinoid receptor is expressed at high levels in brain including hippocampus, cortex, cerebellum, and basal ganglia, as well as in periphery tissues like urinary bladder, testis, and ileum.[166] CB_1 receptor antagonists may have potential in the treatment of different diseases such as neuroinflammatory disorders,[167] cognitive disorders,[168] septic shock,[168] obesity,[168,169] psychosis,[168,170] addiction,[171] and gastrointestinal disorders.[172] In 2004, Solvay Pharmaceuticals, Inc. published novel 3,4-diarylpyrazoline series as potent and selective CB_1 cannabinoid receptor antagonists.[166] Lead optimization led to pyrazolines **46** and **47** (Fig. 1.16) that showed pharmacological activity *in vitro*, and *in vivo* after oral administration. Diarylpyrazolines **46** (K_i= 0.0359 ± 0.0108 µM) and **47** (K_i= 0.0078 ± 0.0014 µM) also exhibited high selectivity for CB_1 receptor vs. CB_2 receptor which is mainly located in the immune system.

5-Hydroxytryptamine 6 receptor (5-HT_6R) is mainly expressed in brain,[173] where it indirectly regulates different cholinergic, monoaminergic, and excitatory amino acid neurotransmitters.[174,175] It is probably related to central nervous system (CNS)

disorders.[176,177] Abbott Laboratories discovered *N'*-(arylsulfonyl)pyrazoline-1-carboxamidines as novel (5-HT_6R) antagonists.[178] Lead optimization led to the pyrazoline **48** (K_i= 0.0241 ± 0.0052 µM) (Fig. 1.16) that was profiled as very selective, CNS available, high-affinity 5-HT_6R antagonist with good metabolic stability.

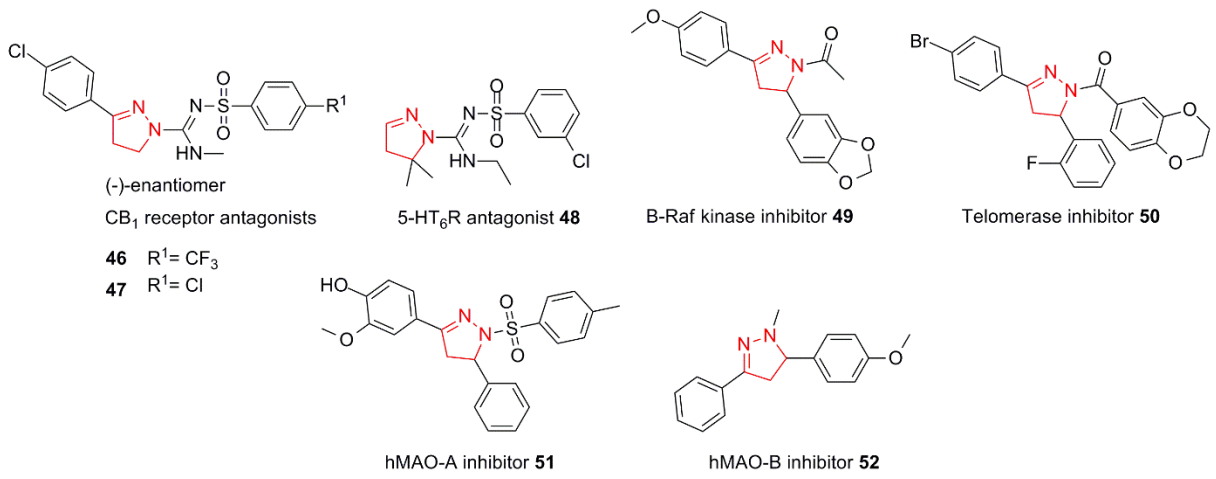

Figure 1.16. Bioactive pyrazolines.

V600E is the most frequent mutation in the active segment of B-Raf.[179,180] Yang *et al*. designed arylpyrazoline derivatives bearing 1,4-benzodioxane moiety as potential B-Raf^{V600E} inhibitors.[181] The authors identified pyrazoline **49** (Fig. 1.16) as inhibitor of B-Raf^{V600E} kinase (IC_{50}= 0.9 µM) and WM266.4 human melanoma cell line (GI_{50}= 0.58 µM).

In the same lab, Luo *et al*. designed similar pyrazoline derivatives as potential telomerase inhibitors which hold promise in anticancer therapies.[182] Among the compounds that were tested for their inhibitory activity, pyrazoline **50** (Fig. 1.16) was identified as the most potent inhibitor of telomerase (IC_{50}= 0.9 µM) with activity against human melanoma cell line B16-F10 (IC_{50}= 5.34 µM).

hMAO-A is one of the isoforms of human monoamine oxidases (hMAO), together with hMAO-B. They belong to the protein family of flavin-containing amine oxidoreductases, and they are mainly located on the outer mitochondrial membrane. Serotonin, adrenaline, and noradrenaline are preferably metabolized by hMAO-A,[183] thus selective hMAO-A inhibitors have potential in the treatment of depression and anxiety disorders.[184] hMAO-B is considered to be a major dopamine metabolizing enzyme which selective inhibitors are employed in the treatment of neurodegenerative disorders, like Parkinson's disease.[185,186] In 2016, Badavath *et al*. identified pyrazoline **51** (Fig. 1.16) as a potent and selective hMAO-A

inhibitor (K_i= 0.06 ± 0.003 µM) with better potency and selectivity then moclobemide, a well know hMAO-A inhibitor.[187]

Fioravanti *et al*. discovered potent and selective hMAO-B inhibitor **52** (IC_{50}= 0.0096 µM) (Fig. 1.16).[188] The authors analyzed the SAR of this compound class and concluded that a small methyl substituent at *N*1-position and unsubstituted 3-phenyl ring are essential to obtain selectivity towards hMAO-B.

2. DNA-Encoded Library based on the pyrazolopyrimidine scaffold

This chapter describes design, synthesis strategy development, and synthesis of 8568-membered structurally focused DNA-encoded library (DEL) based on the pyrazolopyrimidine scaffold.[189]

As a core structure of the DEL, the pyrazolopyrimidine scaffold contained functionalities which allowed DNA-encoded library synthesis. A carboxylic acid moiety served for coupling of the scaffold to 5'-amino-linker modified DNA. For combinatorial library synthesis the scaffold contained an amino function that had to be appended with carboxylic acid building blocks, and a terminal alkyne that was reacted with azide building blocks to yield triazoles. Thus, for library synthesis I used highly yielding DNA-compatible reactions with broad reactant scope: amide coupling and Cu(I)-catalyzed azide-alkyne cycloaddition (CuAAC).

Both sets of building blocks were selected with the help of chemoinformatic methods as we aimed for high diversity and controlled physiochemical properties of projected library members. Also, all building blocks with possible unwanted reactivity were removed from the library synthesis. The set of carboxylic acid building blocks included desthiobiotin for validation of the pyrazolopyrimidine DEL synthesis.

The DNA-encoded library was synthesized using “split-and-pool” approach. It was initiated with coupling of a PEG linker to the controlled pore glass (CPG) solid support bound 5'-amino-linker modified DNA, followed by coupling of the trifunctionalized pyrazolopyrimidine scaffold. In the next step, carboxylic acid building blocks were coupled to the DNA-pyrazolopyrimidine conjugate on solid support. All library members were purified to a single peak by ion pair reverse-phase HPLC, and then characterized to ascertain their purity and identity. Library synthesis proceeded with T4-DNA ligation of DNA-small molecule conjugates with scaffold and carboxylic acid building block dsDNA barcodes. After encoding, conjugates were pooled and split into a 96well plate. Enzymatic encoding was completed by T4-DNA ligation with azide building block coding dsDNA sequences. The 8568-membered pyrazolopyrimidine DNA-encoded library was finalized by introducing of pre-validated azide building blocks in the second appendage cycle.

2.1. Design and synthesis of trifunctionalized pyrazolopyrimidine scaffold

The pyrazolopyrimidine **53** displayed functionalities for DNA-encoded library synthesis (Fig. 2.1): a carboxylic acid to couple the scaffold to 5'-(C6)-amino-linker modified DNA, an Fmoc-protected amine for appendage of carboxylic acid building blocks by amide coupling, and a terminal alkyne for appendage of azide building blocks by Cu(I)-catalyzed alkyne-azide cycloaddition (CuAAC), respectively.

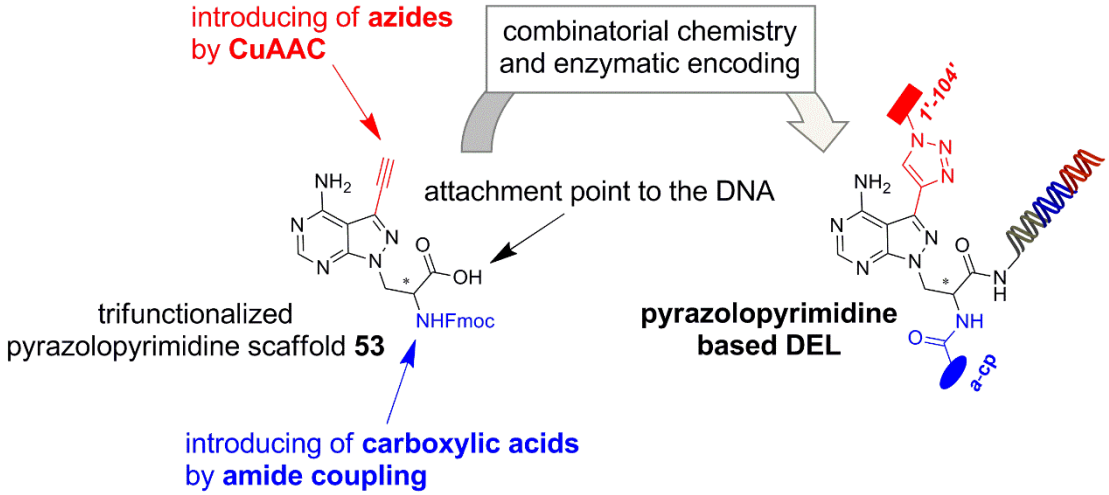

Figure 2.1. Design of trifunctionalized pyrazolopyrimidine scaffold for the DNA-encoded library (DEL) synthesis. CuAAC: Cu(I)-catalyzed alkyne-azide cycloaddition.

Amide synthesis is one of the most frequently used reaction in the synthesis of DELs, with broadly available carboxylic acid building blocks.[14,190,191] The CuAAC was less employed in reported DEL synthesis, although it is compatible with DNA.[19] It has broad functional group tolerance and does not demand protective group chemistry. For CuAAC, azide building blocks are required. Although only few azides are available[191] they are readily accessible from aryl amine and halide precursors.[192] For pyrazolopyrimidine library synthesis azides were prepared by nucleophilic substitution of corresponding halides with sodium azide *in situ*. There are only few reports on DNA encoded library synthesis where reactants were prepared *in situ*.[56,78]

Trifunctionalized pyrazolopyrimidine **53** was synthesized from 6-aminopyrazolopyrimidine **54** (Fig. 2.2). In the first step iodination of C3 carbon yielded compound **55**. Following

Mitsunobu reaction with protected serine led to pyrazolopyrimidine derivative **56** with the required carboxylic acid, and amine functionality on the core heterocycle. Sonogashira coupling with TMS-protected acetylene introduced the terminal alkyne moiety, yielding compound **57**. In the basic deprotection step that removed both the TMS-group and the *tert*-butyl ester, racemization of the amino substituent took place. Finally, Fmoc-protection yielded target pyrazolopyrimidine **53**.

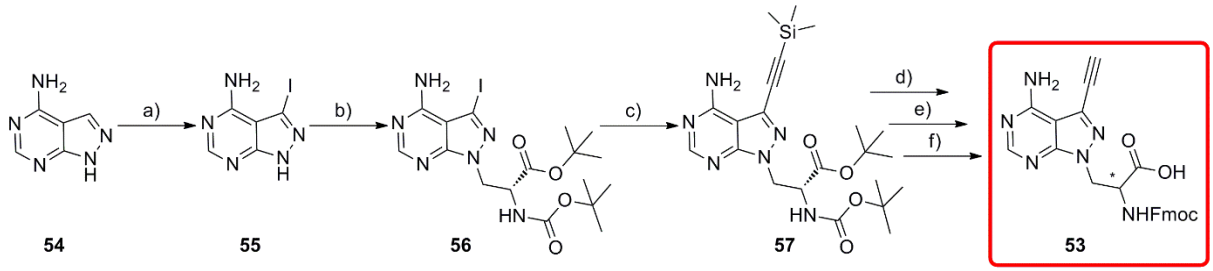

Figure 2.2. Synthesis of trifunctionalized pyrazolopyrimidine scaffold **53**. Reagents and conditions: a) *N*-iodosuccinimide, DMF, 80 °C, 14 hours; b) protected (*S*)-serine, PPh_3, DIAD, THF, room temperature, 16 hours; c) $Pd(PPh_3)_4$, CuI, TEA, TMS-acetylene, DMF, room temperature, 18 hours; d) K_2CO_3, MeOH, room temperature, 24 hours; e) TFA, CH_2Cl_2, room temperature, 20 hours; f) $NaHCO_3$, Fmoc-OSu, H_2O, 1,4-dioxane, room temperature, 20 hours.

2.2. Selection of building blocks for pyrazolopyrimidine DNA-Encoded Library

The pyrazolopyrimidine **53** allowed for combinatorial substitution with building blocks by amide coupling, and by Cu(I)-catalyzed alkyne-azide cycloaddition (CuAAC). Both reactions are high yielding, and have a broad reactant scope, two properties that are important for covering of broad chemical space, and also for library quality.[11,12,14,15,27,32,190] The fragment-sized building blocks for pyrazolopyrimidine DEL were selected by chemoinformatic filtering cascade that was applied to a database of commercially available carboxylic acids and halides. Chemoinformatic analysis of the projected pyrazolopyrimidine DEL was performed by Tuomo Kalliokoski from the Lead-Discovery Center GmbH, Dortmund.

We selected a set of 94 carboxylic acids (compounds ***a-cp***, Table 16), and 104 halides (compounds ***1'-104'***, Table 17) for the synthesis of the pyrazolopyrimidine based DNA-encoded library. Both sets of building blocks contained aliphatic, cyclic aliphatic, aromatic,

and heteroaromatic structures. Building blocks that could be engaged in side reactions with the DNA or the protein target during selection assay (PAINS)[193] were not considered for the DEL synthesis. Many of the selected building blocks (Tables 16, 17) can be found in bioactive compounds. For example, the benzopyrazole ***ai*** (Table 16) is a fragment binding to the kinase CDK2,[149] dihydrouracil ***bk*** was identified as binding motif for members of the family of PARP enzymes,[28] and the uracil ***bn*** is a structural element of a compound binding to the activated complement factor C3d.[194] Other examples included the indole ***r*** (Table 16), the benzofuran ***ac*** (Table 16), and the benzimidazole ***75*** (Table 17) that are known as "privileged" structures.[80] We added the streptavidin binder desthiobiotin to the selected building blocks to validate the pyrazolopyrimidine DEL synthesis.[17]

Table 5. Analysis of the nearest neighbours (NN)[a] of DEL in public databases and calculated physicochemical properties[b] of pyrazolopyrimidine DEL.

No.	Descriptor	Pyrazolopyrimidine DEL
1	NN-ChEMBL	CHEMBL1683-305 (**0.597**)
2	NN-Sure-ChEMBL	SCHEMBL1316 0649 (**0.605**)
3	NN-Pub-Chem	44235677 (**0.685**)
4	Mean MW	566 Da
5	Mean ClogP	1.2
6	Mean TPSA	190 $Å^2$
7	Mean NROT	11
8	Mean HBA	12
9	Mean HBD	4
10	Mean Fsp3	0.387

[a] maximum Morgan/Feat Morgan-Tanimoto-similarity in parenthesis; [b] mean molecular weight (MW), calculated logP (ClogP), topical polar surface area (TPSA), number of rotatable bonds (NROT), number of hydrogen bond acceptors (HBA), number of hydrogen bond donors (HBD), and fraction of the sp^3-carbons (Fsp3). All of these values were calculated using the combination of RDKit and ChemFP.

The nearest-neighbour (NN) Tanimoto similarities of projected pyrazolopyrimidine DEL members to the bioactivity database ChEMBL 21 (~2 million compounds), the patent database SureChEMBL (April 2016 edition, ~16 million compounds), and the bioactivity database PubChem (March 2016 edition, ~89 million compounds) were calculated using Morgan- and Feat Morgan-fingerprints (Table 5). The maximum Morgan/ Feat Morgan-Tanimoto-similarity of the chemical space described in the bioactivity databases to the pyrazolopyrimidine library was generally rather low: 0.597 in NN-ChEMBL, 0.605 in NN-Sure-ChEMBL, and 0.685 in NN-Pub-Chem, meaning that projected pyrazolopyrimidine DEL covered novel chemical space.

The library properties were analyzed by several descriptors (Table 5): mean molecular weight (566 Da), calculated logP (1.2) to assess the mean lipophilicity of the library, the topological surface area (190 $Å^2$), the number of rotatable bonds (11), the mean number of hydrogen bond donors (4) and acceptors (12), and the fraction of sp^3-hybridized carbon atoms (0.387). Regarding the likelihood of oral bioavailability of the members of the pyrazolopyrimidine based DEL, the library displayed a higher mean molecular weight and a higher mean topical polar surface area of the library then statistically associated with peroral bioavailability. However, the pyrazolopyrimidine DEL covered a large shape diversity representing a desired feature in a screening library.[195,196]

2.3. DNA-Encoded Library synthesis strategy development

With respect to the library synthesis, I coupled the pyrazolopyrimidine scaffold **53** to the coding DNA bound to the solid support controlled pore glass (CPG) by amide synthesis, and then I introduced a first set of building blocks also on solid support. In the next step, library members were purified by preparative HPLC. As before HPLC purification DNA-small molecule conjugates must be cleaved form the CPG, means that the following enzymatic encoding and second appendage reaction must take place in solution phase.

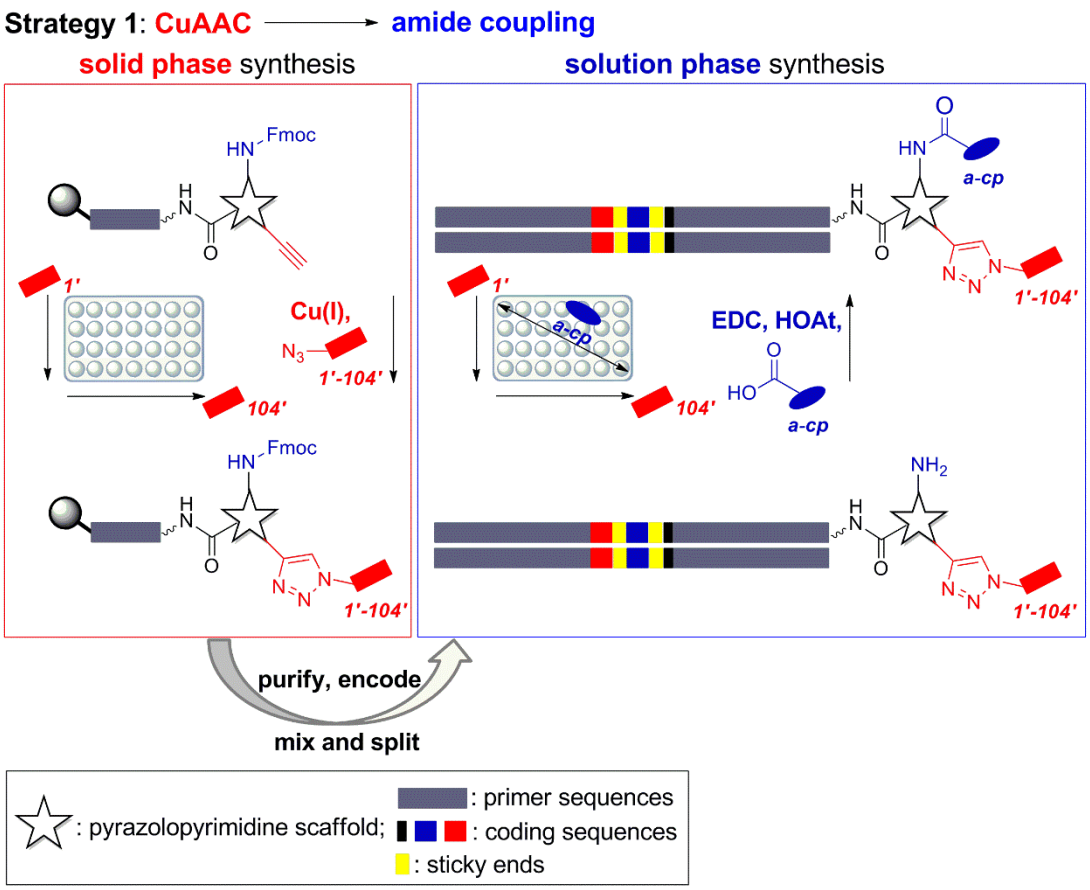

Figure 2.3. Development of DEL synthesis strategy – strategy 1. Filled grey circle denotes solid support (controlled pore glass, CPG); wavy bond to DNA: 5'-(C6)-amino-linker; bold bond: connection from the DNA oligonucleotide to the CPG.

I investigated the most convenient synthetic route to the pyrazolopyrimidine DEL (Figs. 2.3, 2.4). The first strategy for DEL synthesis consisted of introducing azide building blocks as first set of building blocks to the DNA-scaffold conjugate by CuAAC ("click" reaction) and

of amide coupling as a second appendage reaction (Fig. 2.3). In this strategy, techniques required for the DEL synthesis were CuAAC on solid support and amide coupling in solution. The second strategy rested on the reverse reaction sequence (Fig. 2.4). Thus, techniques required for the DEL synthesis were amide coupling on solid support and "click" reaction in solution. The second reaction can be performed either in aqueous solution or on DEAE (diethylamino ethanol) sepharose which is known as pseudo-solid support.[57] DEAE sepharose is a positively charged anion exchange resin that forms ion interactions with negatively charged phosphate groups of DNA. The advantage of DEAE sepharose over solution phase is the possibility of extensive washing of DNA conjugates with different organic solvents prior their elution from the sepharose with a high salt buffer.[57]

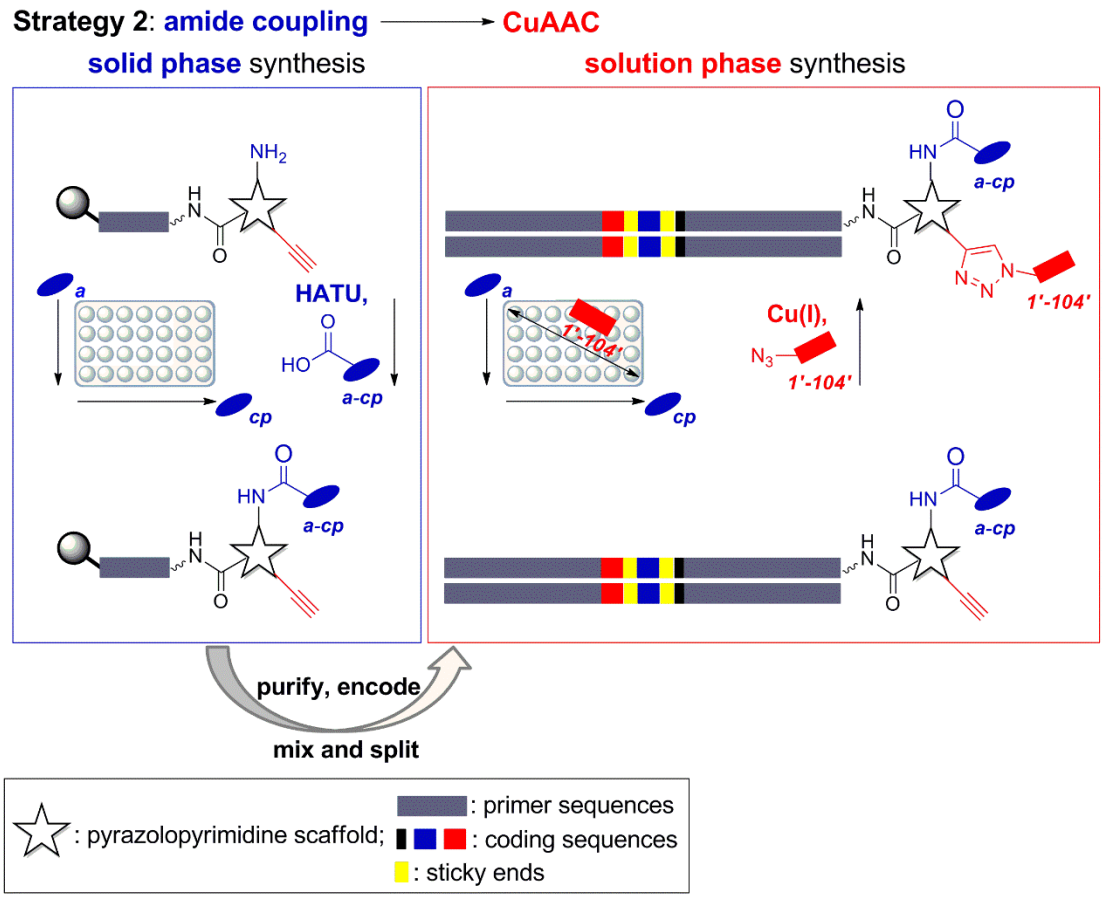

Figure 2.4. Development of DEL synthesis strategy – strategy 2. Filled grey circle denotes solid support (controlled pore glass, CPG); wavy bond to DNA: 5'-(C6)-amino-linker; bold bond: connection from the DNA oligonucleotide to the CPG.

To ensure high quality of the library it is very important to finalize the DEL synthesis with a high yielding reaction. After extensive exploration of both strategies and accordingly required techniques, I decided to use the second strategy for the pyrazolopyrimidine DEL synthesis.

Amide formation worked better on solid support than in solution and on DEAE sepharose, while “click” reaction gave higher yields on DEAE sepharose than on solid support.

2.4. Synthesis of the pyrazolopyrimidine DNA-Encoded Library

The synthesis of the pyrazolopyrimidine DNA-encoded library is depicted in Figure 2.5.

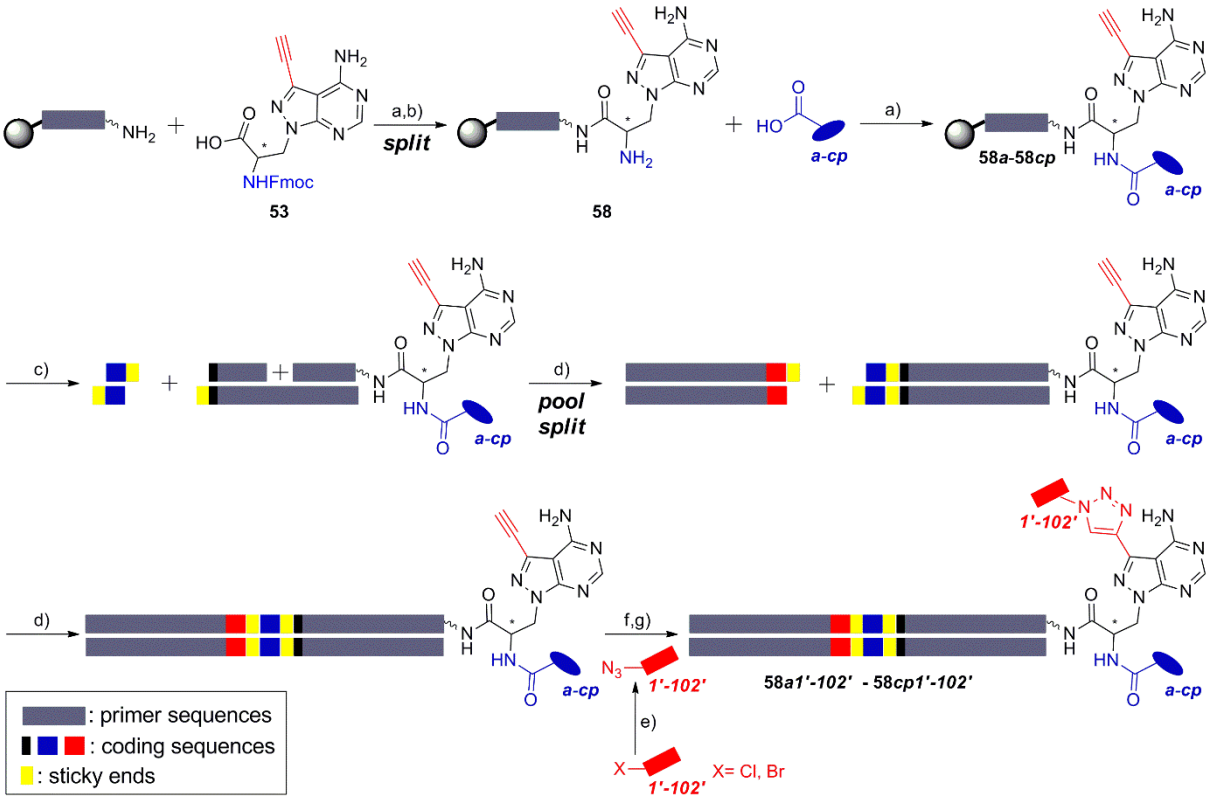

Figure 2.5. Synthesis of the pyrazolopyrimidine DEL by a two stage synthesis strategy. Reagents and conditions: a) HATU, DIPEA, DMF, room temperature, 4 hours; b) 20 % piperidine in DMF, 5 min; c) AMA (aqueous ammonia (30 %)/ aqueous methylamine (40 %), 1:1, vol/vol), 4 hours, room temperature; d) encoding by T4-DNA ligation; e) NaN_3, TBAI, DMF; f) DEAE sepharose, Cu(I), TBTA, Na-ascorbate, $MeOH/H_2O/DMF$ (2:2:1), 45 °C, 16 hours; g) 3 M sodium acetate buffer (pH= 4.75), room temperature, 30 min. Filled grey circle denotes solid support (controlled pore glass, CPG); wavy bond to DNA: 5'-(C6)-amino-PEG(4)/PEG(8) linker; bold bond: connection from the DNA oligonucleotide to the CPG.

Pyrazolopyrimidine **53** was coupled to a fully protected, solid phase-bound 5’-(C6)-amino-linker modified single-strand 23mer or 14mer DNA sequence to yield conjugate **58**. After removal of the Fmoc-group, 94 carboxylic acid building blocks ***a-cp*** (Table 16) were coupled by amide formation to the DNA-pyrazolopyrimidine conjugate **58**.[190,194] All conjugates **58*a*-**

58*cp* were cleaved from the solid support, and purified by ion pair reversed phase HPLC in order to synthesize the DNA-encoded library from a uniform set of DNA conjugates. Purified conjugates **58*a*-58*cp*** were then encoded with double-stranded DNA sequences by two consecutive DNA ligation reactions using T4 ligase in combinatorial manner. The pyrazolopyrimidine DEL was finalized with set of validated azide building blocks ***1'-102'*** (Table 17) that were introduced by copper(I)-catalyzed alkyne-azide cycloaddition on DEAE sepharose.[57,192]

2.4.1. Synthesis of the pyrazolopyrimidine DNA-Encoded Library - amide coupling on solid phase

I initiated the library synthesis with amide coupling of a protected amino-PEG-carboxylic acid using HATU as coupling reagent to 1 µmol of a solid phase-bound 5'-(C6)-amino-linker modified 23mer DNA containing the primer and scaffold code (sequence: 5'-GTC TTG CCG AAT TCC GCT GCA CT-3'). PEG linker was used as spacer between the small molecule and the DNA barcode as we wanted to reduce interactions between barcode DNA and the protein target during selection assays. I found both MMt-protected amino-PEG(8) linker and Fmoc-protected amino-PEG(4) linker suitable. Before removal of the protecting group of the PEG linker, unreacted amines were capped with acetic acid anhydride.

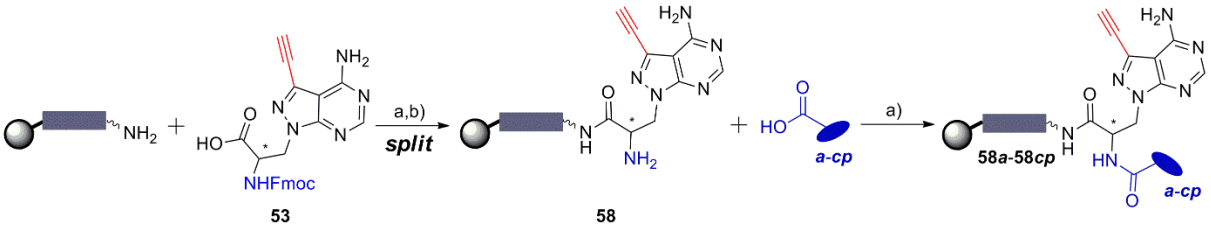

Figure 2.6. Synthesis of pyrazolopyrimidine DEL – amide coupling on solid phase: synthesis of DNA-pyrazolopyrimidine conjugate **58**, and first appendage reaction with carboxylic acids ***a-cp*** (Table 16) to conjugates **58*a*-58*cp***. Reagents and conditions: a) HATU, DIPEA, DMF, room temperature, 4 hours; b) 20 % piperidine in DMF, 5 min. Filled grey circle denotes solid support (controlled pore glass, CPG); wavy bond to DNA: 5'-(C6)-amino-linker-PEG(4)/PEG(8) linker; bold bond: connection from the DNA oligonucleotide to the CPG.

I coupled pyrazolopyrimidine scaffold **53** to the pegylated DNA yielding DNA-PEG-pyrazolopyrimidine conjugate **58** (Fig. 2.6). Unreacted amines were capped followed by Fmoc-deprotection of the conjugate **58** (Fig. 2.6).

Library synthesis continued with the first appendage step. The solid support containing the Fmoc-deprotected conjugate **58** was suspended in DMF, and split in 20 nmol aliquots into a 96well plate. Then, I coupled carboxylic acids ***a-cp*** (Table 16) to the DNA-pyrazolopyrimidine conjugate **58** (Fig. 2.6) in a way that in total 20 reactions were run in parallel, using again HATU as coupling reagent. The solid support-bound DNA conjugates **58*a*-58*cp*** were transferred to a 96well filter plate, thoroughly washed, deprotected and cleaved from the CPG with aq. ammonia/ methylamine (AMA) on the filter plate which was connected to a receiver plate, and sealed with parafilm.

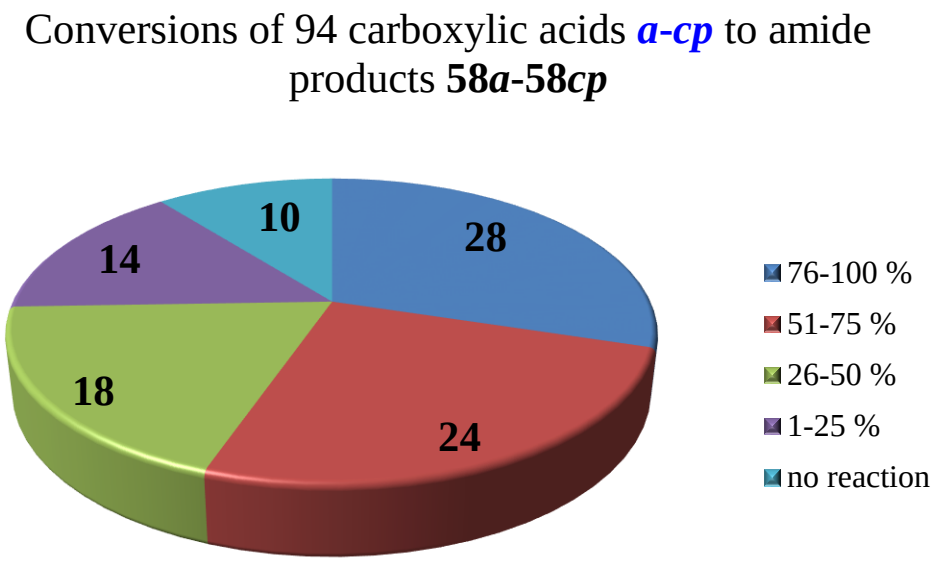

Figure 2.7. Statistical analysis of conversions of 94 carboxylic acids ***a-cp*** (Table 16) to the target DNA-pyrazolopyrimidine conjugates **58*a*-58*cp***. Out of 94 carboxylic acids, 28 carboxylic acids gave rise to the target pyrazolopyrimidine conjugates with 76-100 % conversion, 24 building blocks yielded corresponding amides with 51-75 % conversion, 18 acids afforded the target amides with 26-50 % conversion, 14 acids afforded the target pyrazolopyrimidine conjugates with conversion lower than 25 %, while ten carboxylic acids did not yield the target amide products.

To obtain the library of high quality, the conjugates **58*a*-58*cp*** were purified to a single peak by ion pair reverse-phase HPLC. After coupling of two sets of carboxylic acid building blocks (40 carboxylic acids), I observed that five of these building blocks (***h***, ***w***, ***ac***, ***ad***, ***ae***, Table 16)

did not yield the expected amide products. As amide formation in general proceeds better on shorter CPG-bound DNA oligonucleotides,[197] the initial sequence was changed from a 23mer DNA to a 14mer DNA. Four out of five carboxylic acid building blocks (***h***, ***w***, ***ad***, ***ae***) that did not work in first place successfully afforded target amides on 14mer DNA (sequence: 5'-GTC TTG CCG AAT TC-3'). Lack of detection of an amide synthesis product could either be due to low reactivity of the carboxylic acid or hydrolysis of the amide bond during cleavage of the product from the solid support in the deprotection step.[198]

Out of 94 carboxylic acids ***a-cp*** that were coupled to the DNA-pyrazolopyrimidine conjugate **58**, I obtained 84 corresponding amide products **58*a*-58*cp*** (Figs. 2.6, 2.7, Table 16). 28 carboxylic acids gave rise to the target pyrazolopyrimidine conjugates with 76-100 % conversion, 24 building blocks yielded corresponding amide conjugates with 51-75 % conversion, 18 acids led to amide formation with 26-50 % conversion, 14 acids afforded the target pyrazolopyrimidine conjugates with conversion lower than 25 %, and ten carboxylic acids did not afford the target amides at all (Fig. 2.7, Table 16). As coupling efficiencies of the carboxylic acids ***a-cp*** were very variable (Fig. 2.7, Table 16), the use of preparative HPLC to purify and isolate every conjugate was important. HPLC analysis indicated a purity of more than 95 % of the purified conjugates **58*a*-58*cp***, and MALDI-TOF/TOF-MS analysis confirmed the identity of the products (Table 16).[189]

2.4.2. Evaluation of azide building blocks

Prior library synthesis I evaluated the reactivity of the *in situ* generated azides (Fig. 2.8, Table 17) with a model 14mer DNA-alkyne conjugate **59** (sequence: 5'-GTC TTG CCG AAT TC-3').

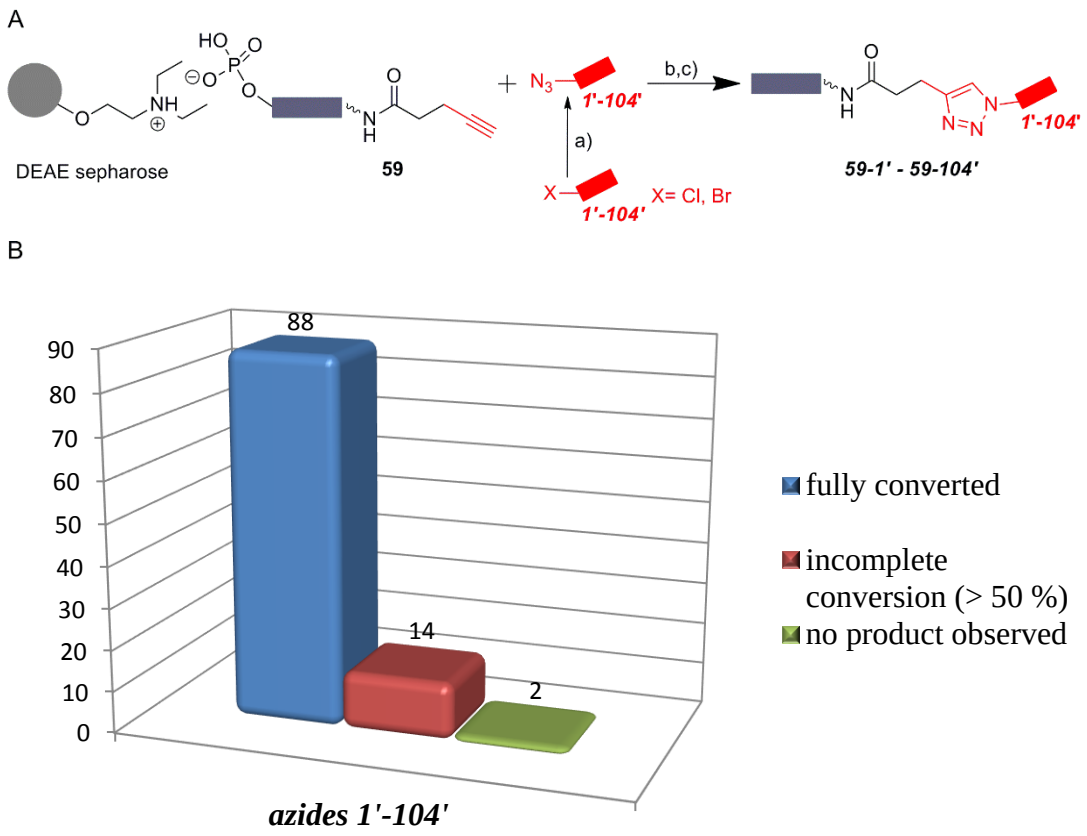

Figure 2.8. Evaluation of reactivity of azide building blocks ***1'-104'*** (Table 17) on model 14mer DNA conjugate **59**. A) Synthesis scheme for screening of azides ***1'-104'*** for their reactivity on conjugate **59** bound to the DEAE sepharose. Reagents and conditions: a) NaN_3, TBAI, DMF; b) Cu(I), TBTA, Na-ascorbate, MeOH/H_2O/DMF (2:2:1), 45 °C, 16 hours; c) 3 M sodium acetate buffer (pH= 4.75), room temperature, 30 min; B) statistical analysis of conversions of azides ***1'-104'*** to the target triazoles **59-*1'*** - **59-*104'***. Wavy bond to DNA: 5'-(C6)-amino-linker.

The azides were prepared by substitution of the halides (Table 17) with NaN_3/tetrabutylammonium iodide.[192] In the mean-time, each 400 pmol of DNA-alkyne conjugate **59** was immobilized on DEAE sepharose in 96well plate.[57] The CuAAC reaction was then performed with a 2500fold excess of the azide at 45 °C overnight.[192] After reaction was finished, the resin was extensively washed with 1 N aqueous ethylenediaminetetraacetic

acid (EDTA) solution to remove Cu-ion contaminants, and with different organic solvents to remove the excess of reagents. DNA-small molecule conjugates **59-*1'*** - **59-*104'*** were eluted from the sepharose by shaking with 3 M sodium acetate buffer for 30 minutes at room temperature, and then analyzed by MALDI-TOF/TOF-MS (Table 17). From the 104 azides tested, 102 yielded the expected triazole products (Table 17). For 82 building blocks complete conversion was detected by MALDI-MS, while in case of building blocks ***10'***, ***16'***, ***38'***, ***44'***, ***51'***, ***53'***, ***62'***, ***68'***, ***75'***, ***76'***, ***77'***, ***101'***, ***102'***, and ***104'***, I noticed incomplete conversion. These were mostly heteroaromatic structures. However, the yield exceeded 50 % as estimated by MALDI-TOF/TOF-MS analysis which I found sufficient for DEL synthesis. Azides ***6'*** and ***87'*** did not yield the target triazoles, and therefore they were excluded from the library synthesis.

I also tested azide building blocks with a model 23mer DNA-alkyne conjugate **60** (sequence: 5'-GTC TTG CCG AAT TCC GCT TAC CG-3') and detected quantitative conversions to the target triazoles by CuAAC (Fig. 2.9).

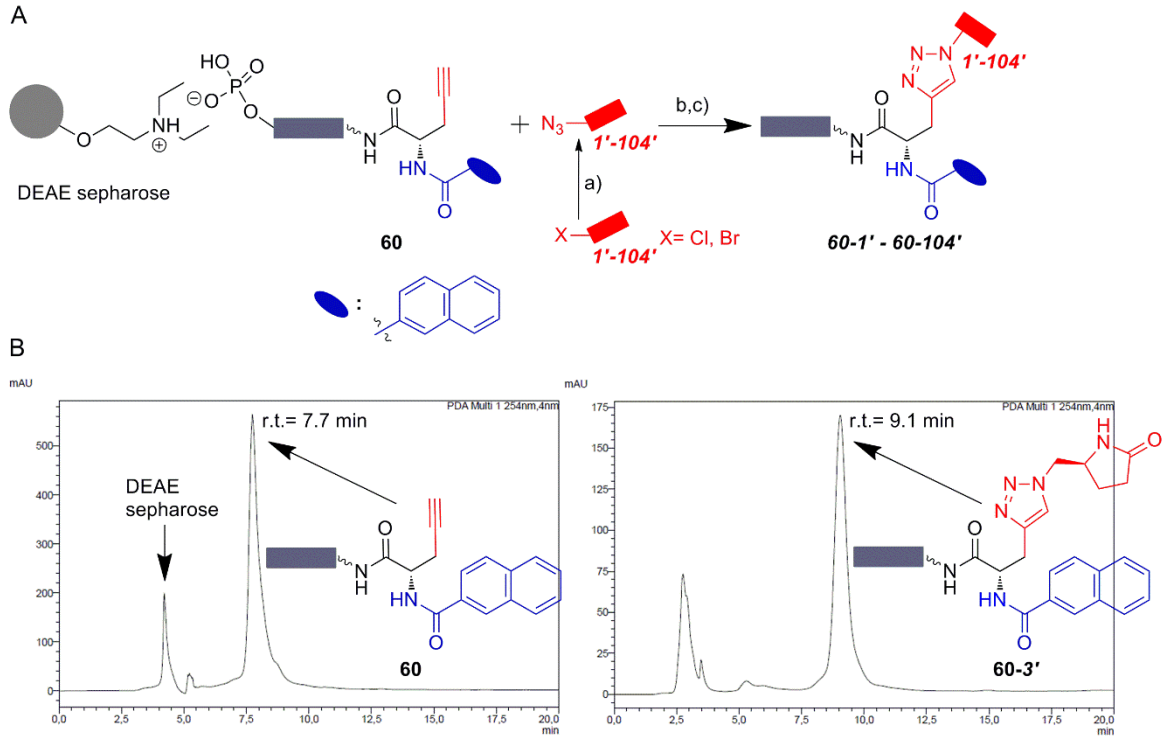

Figure 2.9. Evaluation of azide building blocks ***1'-104'*** (Table 17) for their reactivity on model 23mer DNA-alkyne conjugate **60**. A) Synthesis scheme for screening of azides ***1'-104'*** for their reactivity on conjugate **60** bound to the DEAE sepharose. Reagents and conditions: a) NaN_3, TBAI, DMF; b) Cu(I), TBTA, Na-ascorbate, MeOH/H_2O/DMF (2:2:1), 45 °C, 16 hours; c) 3 M sodium acetate buffer (pH= 4.75), room temperature, 30 min; B) HPLC analysis of DNA conjugate **60**, and of DNA conjugate **60-*3'*** synthesized by CuAAC between conjugate **60**, and azide generated *in situ* from halide building block ***3'*** (Table 17). Left hand: HPLC trace of the

starting material (DNA conjugate **60**) upon binding to DEAE sepharose followed by immediate elution from the resin; right hand: HPLC analysis of the crude DNA conjugate **60-*3'***. Wavy bond to DNA: 5'-(C6)-amino-linker.

2.4.3. Finalization of the pyrazolopyrimidine DNA-Encoded Library - solution phase synthesis

The purified set of DNA-small molecule conjugates **58*a*-58*cp*** was enzymatically encoded by T4-DNA ligation (Fig. 2.10).[18,199] In the first encoding step, 40 pmol of each purified and characterized DNA conjugate **58*a*-58*cp*** was ligated in one pot with a 5'-phosphorylated dsDNA that contained the scaffold code and PCR primer sequence, and 5'-phosphorylated 12mer dsDNA with code for carboxylic acid building blocks ***a-cp***.[189] The ligation reactions were pooled, and the DNA was precipitated with 70 % ethanol at -80 °C overnight. The pellet was dissolved in water, and split into 102 wells of two 96well plates, and ligated with a set of 102 dsDNA sequences containing the code for the azide building blocks ***1'-102'***, and the reverse primer sequence. Encoding of the library by T4-DNA ligation was done in our laboratory by Kathrin Jung.

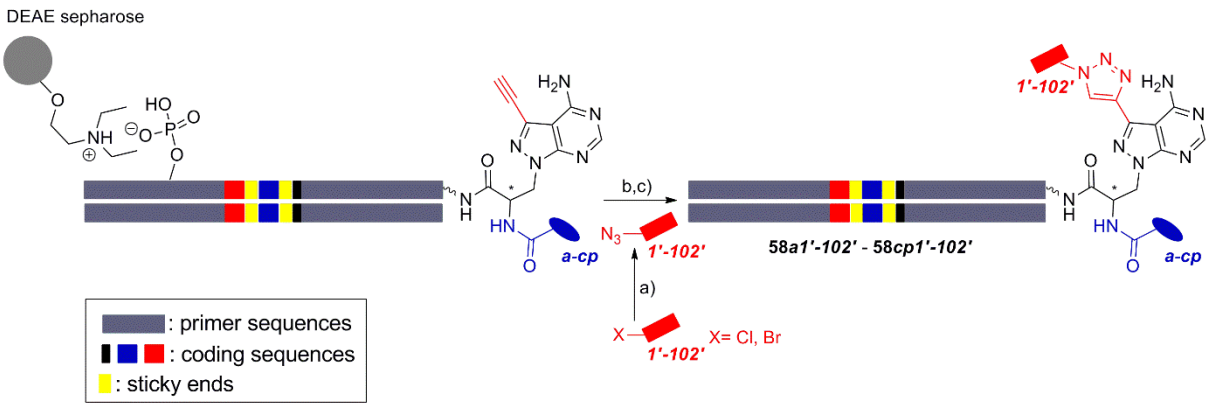

Figure 2.10. Finalization of the pyrazolopyrimidine DEL with set of azide building blocks ***1'-102'*** (Table 17) that were introduced by copper(I)-catalyzed alkyne-azide cycloaddition (CuAAC) on DEAE sepharose. Reagents and conditions: a) NaN_3, TBAI, DMF; b) DEAE sepharose, Cu(I), TBTA, Na-ascorbate, MeOH/H_2O/DMF (2:2:1), 45 °C, 16 hours; c) 3 M sodium acetate buffer (pH= 4.75), room temperature, 30 min. Wavy bond to DNA: 5'-(C6)-amino-PEG(4)/PEG(8) linker.

Thus, with DNA-encoded pyrazolopyrimidine conjugates **58*a*-58*cp***, and with a validated set of azide building blocks in hand I went into finalization of the pyrazolopyrimidine DEL (Fig. 2.10). The encoded DNA-conjugates **58*a*-58*cp*** were transferred to DEAE sepharose, and

reacted with the azides ***1'-102'*** (Table 17) as described above to yield the 8568-membered pyrazolopyrimidine DEL. After the CuAAC reaction, the library was eluted from the resin, pooled, and twice precipitated with 70 % ethanol at -80 °C overnight.

2.5. Summary

We designed and synthesized a kinase-targeted DNA-encoded library (DEL) based on pyrazolopyrimidine scaffold. The pyrazolopyrimidine scaffold displayed three functionalities which allowed coupling of the scaffold to 5'-amino-linker modified DNA and subsequent combinatorial library synthesis. Library building blocks were selected with chemoinformatic tools to improve the diversity of the library, and control its calculated physicochemical properties. Despite the broad prevalence of pyrazolopyrimidine scaffold among bioactive compounds, chemoinformatic analysis indicated that the pyrazolopyrimidine DEL covered novel chemical space.

The DNA-encoded library synthesis started with solid phase synthesis of DNA-pyrazolopyrimidine conjugate. This conjugate was appended with carboxylic acid building blocks that were introduced in parallel by amide coupling on solid support. These library members were purified by ion pair reverse-phase HPLC, and characterized. Of 94 carboxylic acids tested, 84 yielded the target amide products in variable yields, justifying the effort to purify these DNA conjugates by preparative HPLC. Uniform library members were enzymatically encoded by T4-DNA ligation with coding dsDNA sequences. The 8568-membered pyrazolopyrimidine DEL was concluded by introducing of 102 validated azide building blocks.

Currently, we are screening the pyrazolopyrimidine DNA-encoded library to identify novel target protein binders.

3. Expanding chemical space of DNA-Encoded Libraries by "hexT"-approach

3.1. The challenge: chemical instability of DNA

DNA is a molecule of life which is composed of nucleosides that are linked through phosphodiester bonds. Each nucleotide consists of a purine or pyrimidine nucleobase connected via *N*-glycosidic bond to β-D-2' deoxyribose which is phosphorylated in 3'- and 5' positions in a DNA strand (Fig. 3.1). The purine DNA nucleobases are adenine and guanine, the pyrimidine DNA nucleobases are cytosine and thymine (Fig. 3.1).

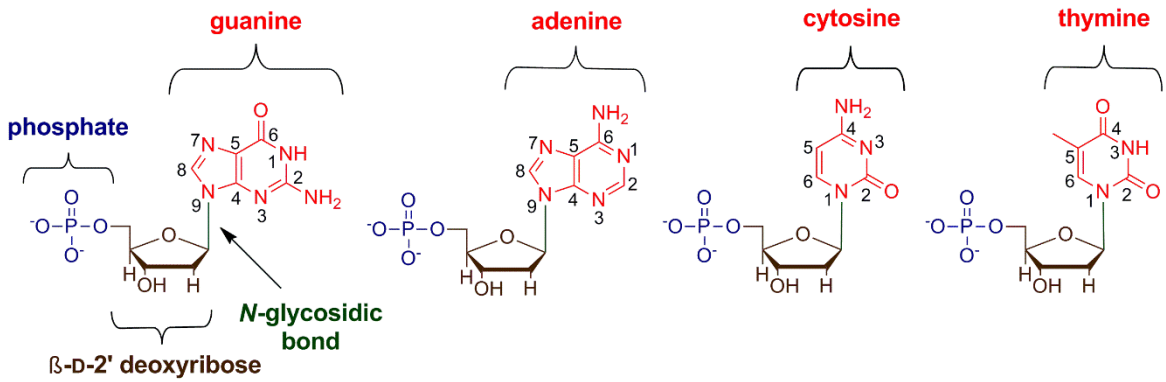

Figure 3.1. Four different DNA nucleotides consisting of purine or pyrimidine nucleobase (marked in red) which is linked to β-D-2' deoxyribose (marked in brown) via *N*-glycosidic bond (marked in dark green). Sugar moiety is phosphorylated (marked in dark blue) in the 5' position.

DNA is a complex molecule displaying multiple functionalities and reactivities. For instance, the phosphodiester backbone can be hydrolyzed by strong bases. However, an (in)famous reactivity of DNA is the so-called depurination reaction. Hydrolytic cleavage of *N*-glycosidic bond of purine nucleosides, commonly known as depurination is triggered under acidic conditions (pH < 5) by protonation of the purine nucleobase. Protonation primarily takes place at the *N7* position of guanine, and *N1*/*N7* position of adenine causing a *N7*-*N9* tautomerism that ultimately leads to cleavage of the *N*-glycosidic bond. A similar mechanism can be effected by coordination of transition metals to these positions as well.[200] In single stranded DNA they can theoretically coordinate to any electron-rich position, but are very prone to coordinate to the very basic nitrogen *N7* in guanine and adenine.[201] Upon coordination, transition metal ions (M) cause redistribution of electrons in the heterocyclic ring. Consequently, the basicity of endocyclic and exocyclic nitrogens decreases, while acidity of endocyclic nucleobase protons increases.[201] Coordination of transition metal ions can follow nucleobase deprotonation. In that case, negative charge resulting from

deprotonation is not relocalized in the M-N interaction, thus, the nucleobase basicity increases. Therefore, transition metal ions show preferences towards deprotonated, metalated nucleobases which then undergo multiple metalation reactions.[202]

It was found that coordination of transition metal ions to *N7* in guanine, and *N1*/*N7* in adenine retards the acid-catalyzed depurination, as the metal ion competes with protons for binding sites. However, when protonation of the nucleobase does not occur anymore, the coordination of the transition metal ion facilitates the spontaneous depurination.[200,203] For example, Pt(II) retards the acid-catalyzed hydrolysis of *N*-glycosidic bond in guanine at pH < 4, while at pH > 4 it accelerates the spontaneous depurination. In adenine nucleosides the first protonation occurs at *N1* site, while transition metal ions prefer coordination to *N7* site. Therefore, in pH ranges where nucleobase protonation takes place, transition metal ions indeed can retard depurination of adenine nucleosides, but not as prominent as of guanine nucleosides, and only when the metal ion coordinates to both, *N1* and *N7* site.[200,203]

Other irreversible degradation reactions of the DNA code related to the coordination of transition metal ions are deamination and DNA oxidation. Deamination is hydrolysis reaction which involves conversion of an exocyclic amine group of a nucleobase to an exocyclic carbonyl group. For example, in cytosine Pt(II) coordinates to nucleobase nitrogen *N3*, and under basic conditions it accelerates deamination leading to corresponding uracil-metal complex.[200] In comparable manner, platinated adenine is converted to hypoxanthine.[200]

Transition metal ions can also produce reactive radical oxygen species and in that manner be involved in DNA oxidation. Guanine has the lowest ionization potential of all nucleobases, and therefore is more susceptible to oxidation leading primarily to 8-oxo-7,8-dihydroguanine (8-OxoG).[200,204]

3.2. Development of the Thymidine-initiated DNA-Encoded Chemistry (TiDEC) concept

In DNA-encoded libraries integrity of the genetic information during library synthesis and handling is a key requirement. Preserving the DNA code, keeping it amplifiable, sequencable, and finally decodable is the basis of successful DEL selections. Thus, design and synthesis of DELs must be adapted to this requirement. So far, the synthesis strategies for construction of DELs relied on DNA-compatible chemical transformations, and adaption of organic reactions to the chemistry of DNA. However, the success of DEL selection assays profoundly depends on the chemical space covered by DELs. The fact that DNA does not tolerate acid, and many transition metal catalysts has influenced the chemical space yet explored with DELs.

Heterocycles are often incorporated in small molecule drugs highlighting their significance in medicinal chemistry. They are often synthesized by either condensation reactions, or by transition metal catalysis.[205]

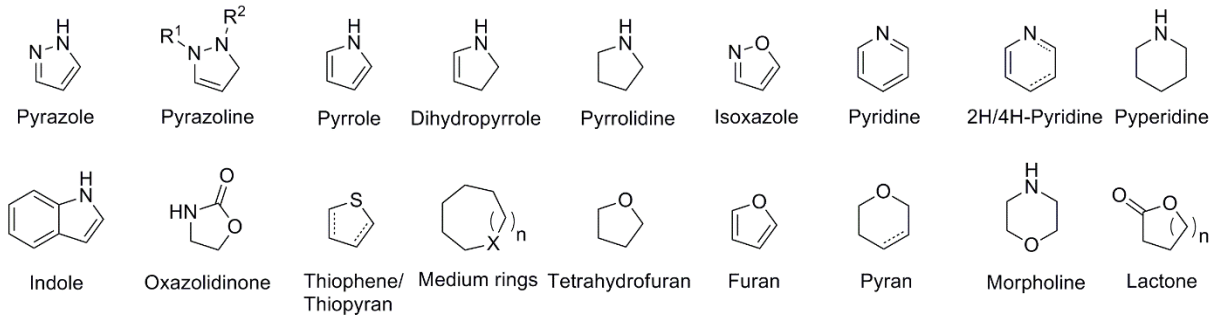

Figure 3.2. Heterocyclic structures accessed by gold catalysis.

For instance, gold-catalyzed transformations allow access to a large number of heterocycles (Fig. 3.2).[206,207] Gold catalysts tolerate aerobic conditions, moisture, and different functional groups making them efficient in synthesis of diverse chemical structures from simple starting materials.[206]

Being interested in application of Au(I) catalysis in a DEL format, we decided to adapt our DNA to transition metal catalysis. We excluded purine nucleobases from the DNA sequence as they are more prone to degradation than pyrimidine nucleobases. At thymine, transition metal ions can coordinate to exocyclic oxygen sites *O2* and *O4*, and after deprotonation to endocyclic nitrogen site *N3* as well (Fig. 3.1). At cytosine, transition metal ions can coordinate to *N3* and *O2* site, and following proton loss also to *N4* and *C5* sites (Fig. 3.1).[202]

Binding of metal ions to exocyclic oxygens (i.e. *O2* and *O4* in thymine, and *O2* in cytosine) leads to thermodynamically less stable compounds.[202] This changes only when the base is deprotonated.[202] As deprotonation of thymine occurs at pH values higher than 9 (pKa value of the 3-*N*-*H*: 9-10),[202,208] the *N3* in thymine might be of less concern regarding the use of a Au(I) catalysts than the nucleophilic *N3* in cytosine, which does not require deprotonation for binding to metal ions and is thus more susceptible towards coordination of transition metal ions, i.e. Au(I). Nevertheless, Au(I) is a soft acid that prefers to coordinate to nitrogen as it is softer base then oxygen. In conclusion: if Au(I) catalysis would be performed on DNA the nucleobase which would interact the least with the soft Au(I) metal ion is thymine. Therefore, we designed the hexathymidine oligonucleotide adapter **"hexT"** as a chemostable adapter oligonucleotide (Fig. 3.3).[209]

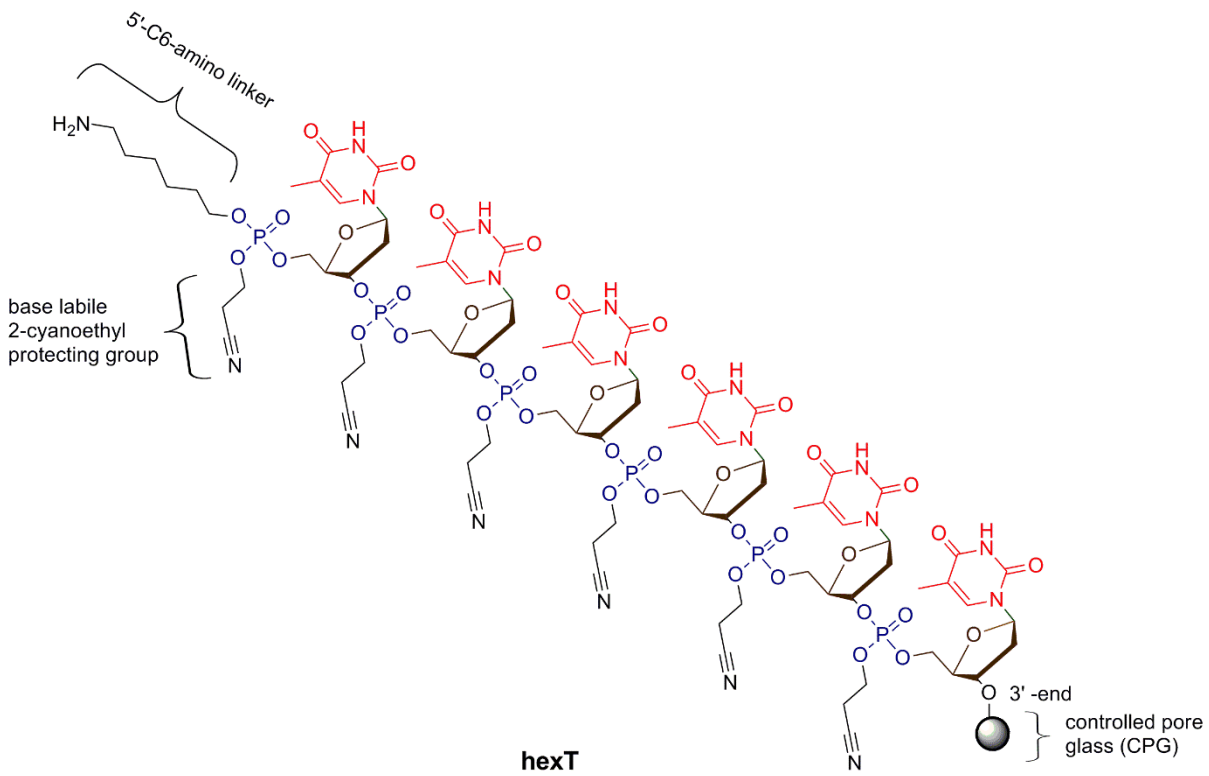

Figure 3.3. Hexathymidine oligonucleotide adapter **"hexT"**.

HexT is an oligonucleotide consisting of six thymidines. We usually use it as controlled pore glass (CPG) support bound DNA. We hypothesized that a hexathymidine DNA **"hexT"** would be stable enough to allow transition metal catalysis (and acid catalysis) to convert hexT conjugates of simple starting materials into hexT-heterocycle conjugates, and also be recognized by T4 ligase to record the synthesis step with coding DNA sequences (Fig. 3.4).[209] Accordingly, we called this synthesis strategy "TiDEC" (Thymidine-initiated DNA-

Encoded Chemistry), and library initiated with synthesis on hexT-oligonucleotide adapter we called tiDEL (oligothymidine-initiated DNA-Encoded Library).[209]

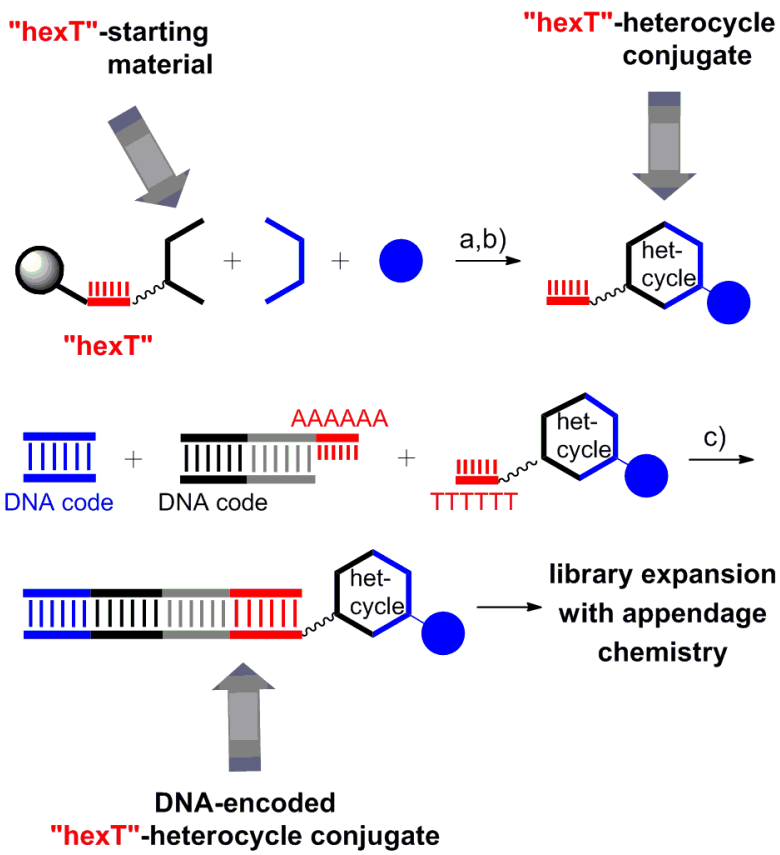

Figure 3.4. Outline of the Thymidine-initiated DNA-Encoded Chemistry (TiDEC) strategy. The TiDEC concept to DNA-encoded libraries; a) heterocyclic chemistry; b) isolation of hexT conjugates; c) DNA ligation. Filled grey circle denotes controlled pore glass (CPG) solid support; wavy bond to hexT denotes 5'-amino-PEG(4)-linker, bold bond denotes connection to CPG solid support.

Indeed, we were able to obtain hexT-pyrazol(in)es by a Au(I)-mediated cascade reaction from simple, readily available starting materials for subsequent encoded library synthesis,[210] as well as hexT-6-oxa-1,2-diazaspiro-[4.4]nonanes by a Au(I)-mediated [3+2]-cycloaddition reaction.[211]

3.3. Approaches towards synthesis of pyrazoles and pyrazolines

Due to the outstanding interest in pyrazol(in)es in medicinal chemistry, in crop-sciences, and also in the chemical industry with respect to their potential in development of dyes and catalysts, it does not surprise that there is a plethora of approaches towards their synthesis. Most commonly used are reactions of 1,3-diketones with hydrazines, reactions of α,ß-unsaturated aldehydes or ketones with hydrazines, and reactions of 1,3-dipolar cycloadditions of hydrazines or hydrazones with alkynes. In spite of many well established synthetic routes to variously substituted pyrazol(in)es, they still represent attractive synthetic targets. In the throng of standard reactions, some reactions stand out, and some of these will be described below in more detail.

In 2006, Martin *et al.* reported an interesting Cu(I)-catalyzed domino amination/ hydroamination sequence to produce pyrazoles.[212] Iodoenynes **61** were used as the precursors and bis(Boc) hydrazine **62** as the nucleophile. The authors discussed two possible mechanisms for the Cu(I)-catalyzed domino reaction (Fig. 3.5).

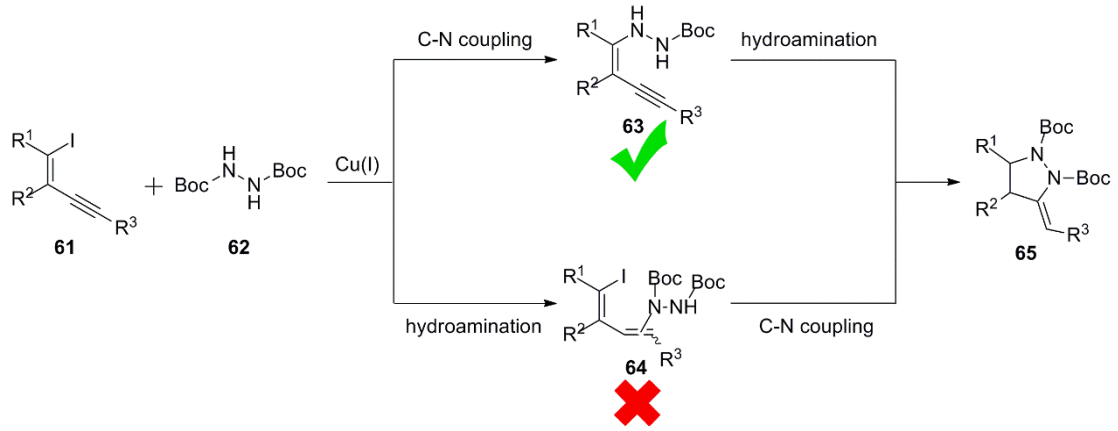

Figure 3.5. Possible mechanisms for the Cu(I)-catalyzed domino reaction to densely substituted pyrazoles.

NMR mechanistic studies confirmed that the process started with C-N coupling (amination) leading to the intermediate **63**. Subsequent 5-*exo-dig* intermolecular cyclization led to the final cascade product **65**. During mechanistic studies, the hypothetical intermediate **64** was not observed (Fig. 3.5).

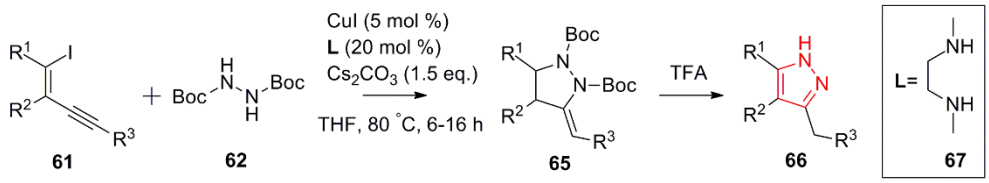

Figure 3.6. Synthesis of pyrazoles **66** through Cu(I)-catalyzed amination/ hydroamination of iodoenynes **61** with bis(Boc) hydrazine **62**, followed by Boc-deprotection of crude intermediate **65**.

Reaction conditions were optimized with respect to identification of the most suitable ligand (**L**) for this Cu(I)-catalyzed reaction. The reactions were performed in THF with CuI as the precatalyst and Cs_2CO_3 as the base at 80 °C for 12 hours. Among all tested ligands, *N*,*N'*-dimethylethylenediamine ligand **67** demonstrated the highest activity (Fig. 3.6). Regarding reactant scope, different substituents were tolerated at alkyne and alkene part of the iodoenyne **61**, but the reaction led to decomposition with substrates bearing terminal alkyne (R^3= H). Instead, the use of terminal acetylene substituted with a trimethylsilyl group was successful. In the last step, crude intermediates **65** were treated with trifluoroacetic acid to afford target pyrazoles **66** in good to excellent overall yields. Depending on the iodoenyne substitution pattern, mono-, di-, and trisubstituted pyrazoles **66** were accessed using this approach.

In 2015, Sun *et al*. reported the first Au(I)-catalyzed diazo cross-coupling reaction by selective and ligand controlled denitrogenation/ cyclization cascade to produce *N*-substituted pyrazoles (Fig. 3.7).[213] The authors were initially interested in the synthesis of *Z*-selective tetrasubstituted alkenes **70** by Au(I)-catalyzed cross-coupling of vinyldiazoacetates **68** and aryldiazoacetates **69** catalyzed by $IPrAuNTf_2/NaBAr_F$. Indeed, reaction led to expected dienes **70** with *para*- and *meta*-substituted aryldiazoacetates, but *ortho*-substituted aryldiazoacetates surprisingly afforded pyrazoles **71** (Fig. 3.7). An additional intriguing finding was related to the use of $PPh_3AuCl/NABAr_F$ catalyst that led to the pyrazoles **72** rather than dienes **70** (Fig. 3.7). Reactions to both pyrazoles took place in dichloromethane at room temperature.

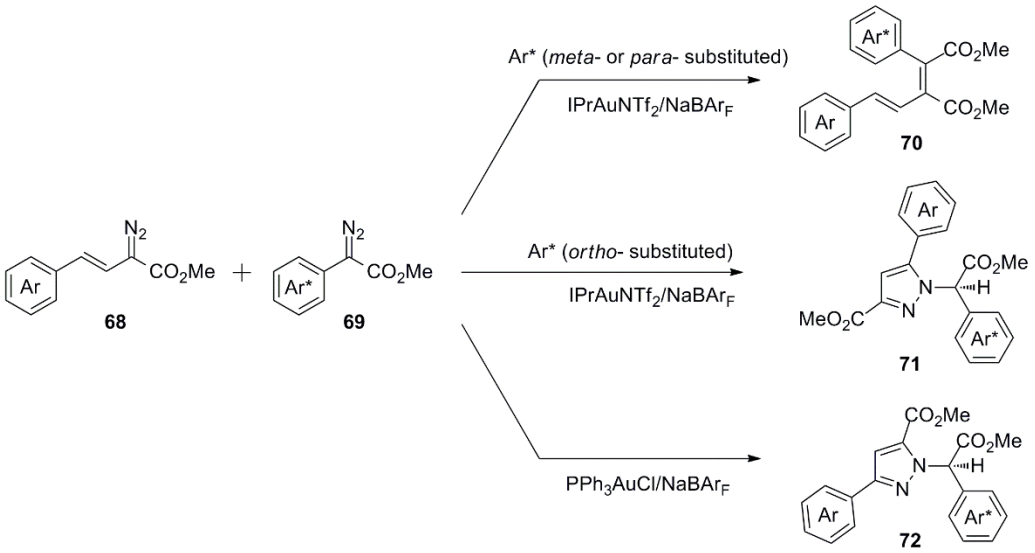

Figure 3.7. Au(I)-catalyzed cross-coupling of vinyldiazoacetates **68** and aryldiazoacetates **69** yielding three different products: diene **70**, and pyrazoles **71** and **72**.

Optimization of reaction conditions revealed $(ArO)_3PAuCl/NaBAr_F$ (BAr_F= tetrakis[3,5-bis(trifluoromethyl)phenyl]borate) as the best catalyst for synthesis of the pyrazoles **72**. For synthesis of pyrazoles **71**, steric properties of aryldiazoacetate component **69** played a crucial role (Fig. 3.8), therefore the reaction succeeded only when *ortho*-substituted substrates **69** were used.

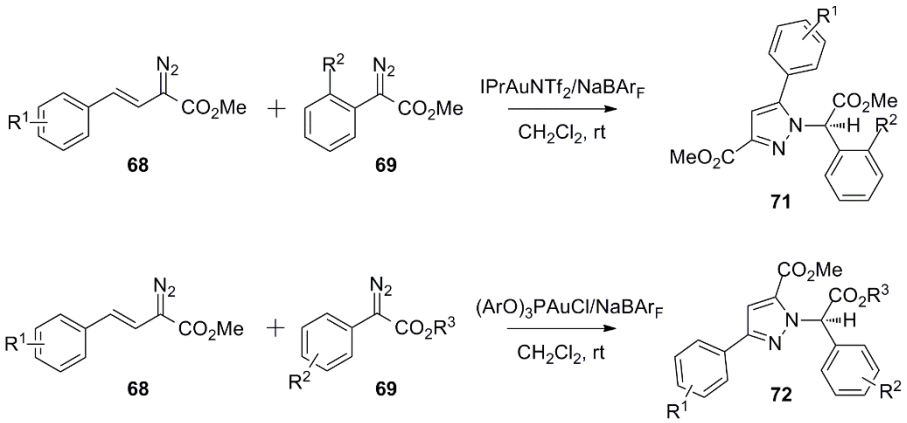

Figure 3.8. A selective and ligand controlled Au(I)-catalyzed cross-coupling of diazo compounds **68** and **69** to *N*-substituted pyrazoles **71** and **72**.

Nevertheless, different electronic properties of *ortho* substituent (-R^2) were tolerated leading to diverse pyrazoles **71** in moderate to high yields. Also, the reaction mode was not influenced by the substituent in position R^1 on the aryl ring of vinyldiazoacetates **69**. Use of alkyl vinyldiazoacetates **69** afforded corresponding pyrazoles **71** in low yield. Examination of

reactant scope for $(ArO)_3PAuCl/NaBAr_F$ catalyzed reaction with optimal reaction conditions showed that vinyl- and aryldiazoacetates, **68** and **69**, respectively, with *ortho*, *meta*, and *para* substituents ($-R^1$, $-R^2$) successfully yielded corresponding pyrazoles **72**. In addition, various carboxylates of aryldiazoacetates **69** ($-R^3$) demonstrated similar reactivity (Fig. 3.8).

Hashimoto *et al*. published the first catalytic asymmetric three component 1,3-dipolar cycloaddition (1,3-DC) of hydrazides **73**, aldehydes **74,** and terminal alkynes **75** leading to 1,2,4,5-substituted pyrazolines **78**.[214] The 1,3-DC relied on formation of azomethine imine **76** with 1,3-dipolar character, and on *in situ* generated copper acetylide **77** with 1,3-dipolarophile character (Fig. 3.9). The major concern regarding this Cu(I)-catalyzed three-component reaction was possible formation of three different compounds. Two of them are products of 1,3-DC and these are regioisomers 1,2,3,4- and 1,2,3,5-substituted pyrazolines, **78** and **79**, respectively (path a), and the third one is the alkynylation product, propargyl hydrazine **80** (path b). Upon further activation propargyl hydrazine **80** can undergo nucleophilic cyclization (path c) leading exclusively to pyrazoline **79** (Fig. 3.9).

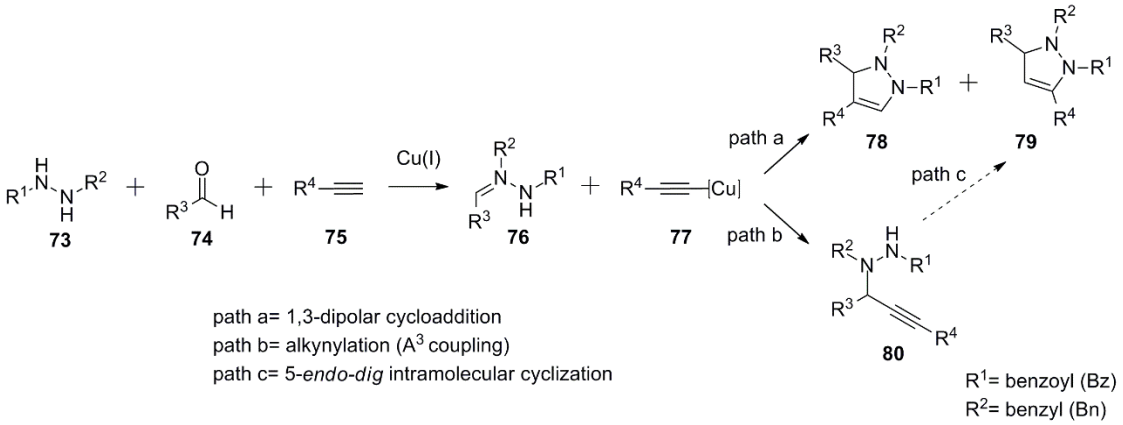

Figure 3.9. Cu(I)-catalyzed 1,3-dipolar cycloaddition of azomethine imine **76** and copper acetylide **77**.

Optimization of reaction conditions revealed CuOAc/pybox **81** and axially chiral dicarboxylic acid **82** co-catalyst as combination favouring 1,3-DC over alkynylation (Fig. 3.10).

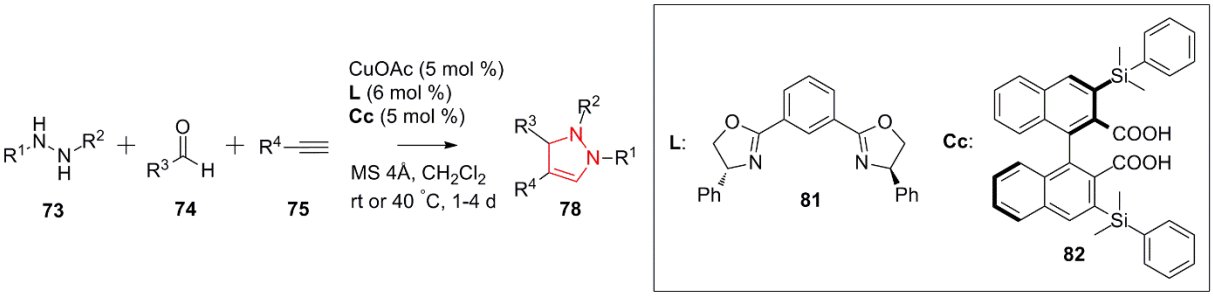

Figure 3.10. Synthesis of pyrazolines **78** by three-component Cu(I)-catalyzed 1,3-dipolar cycloaddition of hydrazines **73**, aldehydes **74**, and alkynes **75**.

Reaction proceeded in a regiospecific manner, with excellent enantioselectivities, and with broad reactant scope. Regarding hydrazide scope, substitution of benzoyl with carboxybenzyl (Cbz) group (-R^1) successfully provided the target pyrazoline **78**, as well as displacement of benzyl with butyl group (-R^2). Target pyrazolines **78** were furnished with linear and branched aliphatic aldehydes, and aromatic aldehydes of different electronic and steric properties (-R^3). Reaction also succeeded with aliphatic and aromatic, although not sterically demanding alkynes (-R^4).

3.3.1. Synthesis of pyrazolines by Au(I)-catalyzed annulation reaction

Inspiration for tiDEL synthesis was found in work published by the Ohno group, that described Au(I)-catalyzed synthesis of 1,2,3,5-substituted pyrazolines **79** (Fig. 3.11).[215] This work was very attractive not just due to regioselective synthesis of densely substituted pyrazolines, but because the reaction used for their synthesis was a multicomponent reaction (MCR). Among the many advantages that MCRs bear compared to sequential multistep synthesis, like being atom economic, efficient, convergent, exhibit high bond-forming index, especially library synthesis benefits from the ready accessibility of starting materials.[216] In addition, successful translation of a Au(I)-catalyzed reaction to an encoded library format would set a precedent for the translation of further reactions of this type to drug-like scaffolds to the encoded library format.

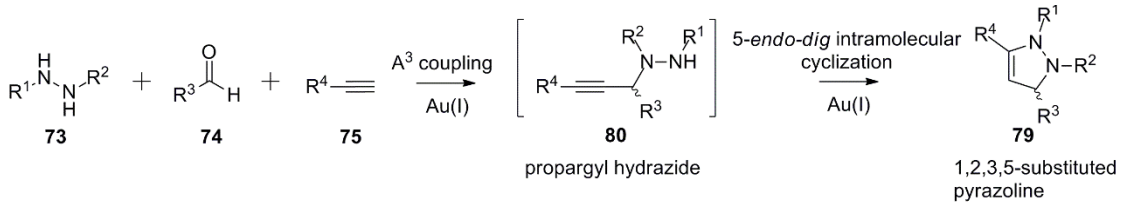

Figure 3.11. Three-component Au(I)-catalyzed annulation reaction of hydrazides **73**, aldehydes **74**, and alkynes **75** to 1,2,3,5-substituted pyrazolines **79** consisting of A^3 coupling followed by 5-*endo-dig* intramolecular cyclization.

The 1,2,3,5-substituted pyrazolines **79** are formed by a Au(I)-catalyzed three-component annulation reaction of hydrazides **73**, aldehydes **74**, and alkynes **75**. The reaction consists of A^3 coupling (alkynylation) that consists of the coupling of an alkyne, an aldehyde, and an amine component- in this case hydrazide, followed by 5-*endo-dig* intramolecular cyclization (hydroamination) of the propargyl hydrazide intermediate **80** (Fig. 3.11). The proposed reaction mechanism is described in Figure 3.12.

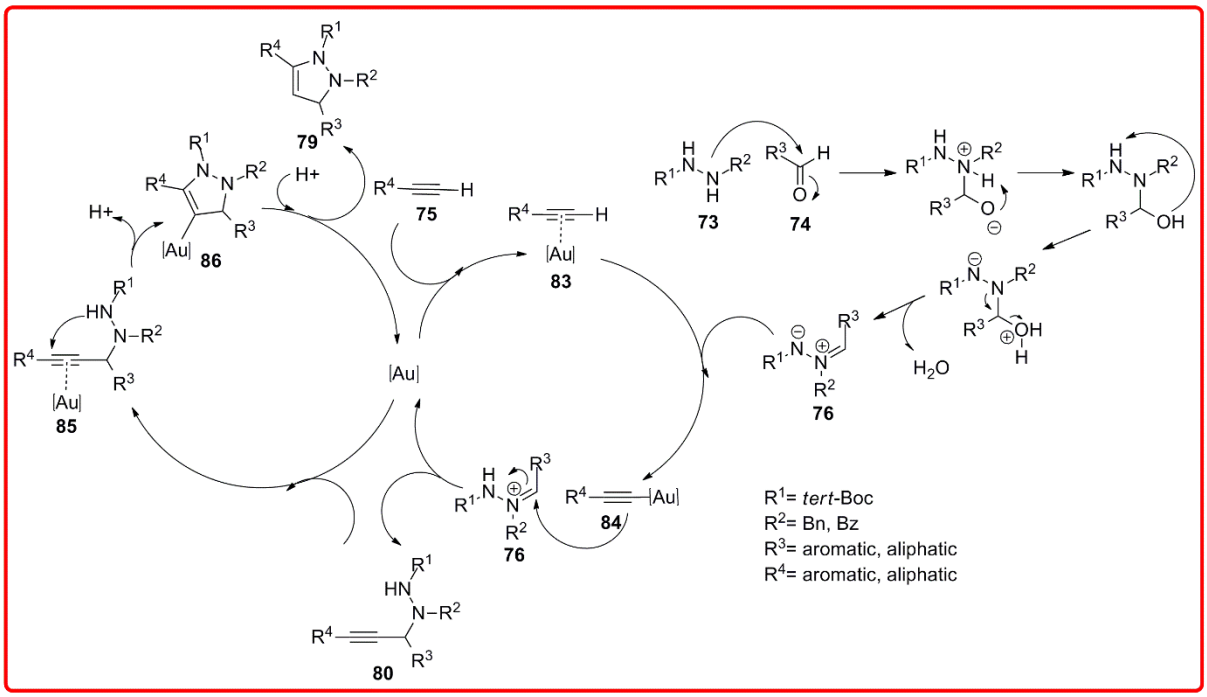

Figure 3.12. Proposed reaction mechanism of the three-component Au(I)-catalyzed annulation reaction of hydrazides **73**, aldehydes **74**, and alkynes **75** leading to pyrazolines **79**.

Condensation of hydrazide **73** and aldehyde **74** yields the azomethine imine **76** *in situ*, analogously to imine formation. But as hydrazides possess two nitrogen atoms these must have different electronic character, so that only one nitrogen can act as a nucleophile towards the carbon atom of the aldehyde carbonyl. To make a clear distinction between the nitrogen's

nucleophilicity, one of them has to be connected to an electron-withdrawing group, for example a Boc group. A Au(I) catalyst coordinates to the alkyne **75** yielding Au(I)-alkyne π-complex **83**. The nucleophilic nitrogen of azomethine imine **76** deprotonates the activated alkyne resulting in formation of a nucleophilic σ-organogold intermediate, gold acetylide **84**. Gold acetylide **84** reacts with azomethine imine **76** through nucleophilic addition leading to propargyl hydrazide **80**. Further coordination of the Au(I) catalyst to the alkyne bond of intermediate **80** leads to π-complex **85**. Upon coordination of the Au(I) catalyst, the alkyne bond becomes more electron deficient, therefore more electrophilic and more prone towards nucleophilic attack, thus activated towards intramolecular hydroamination leading to vinyl-gold intermediate **86** along with liberation of proton.[217] Protodeauration in the last step affords the target pyrazoline **79**.

Optimization of reaction conditions revealed Au(I) bearing *N*-heterocyclic carbene ligand (NHC) ***C*** (Fig. 3.13) in combination with silver triflate, IPrAuCl/AgOTf as the best catalyst for described annulation reaction. Best reaction conditions included 1,2-dichloroethane (1,2-DCE) as a solvent, reaction temperature of 50 °C, and 1 hour reaction time. Performing the reaction at room temperature led only to the alkynylation product **80**.

The reactant scope was evaluated with different hydrazides **73**, aldehydes **74**, and alkynes **75** (Fig. 3.13).

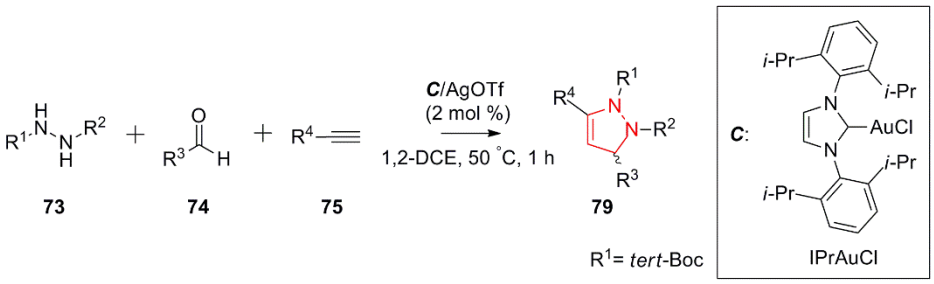

Figure 3.13. Synthesis of pyrazolines **79** by three-component Au(I)-catalyzed annulation of hydrazides **73**, aldehydes **74**, and alkynes **75**.

One of the hydrazide nitrogens must bear an electron-withdrawing substituent (-R^1), and for that purpose *tert*-butyloxycarbonyl (Boc) group was used. The neighbouring nitrogen was substituted with a phenyl group instead of benzyl (-R^2) as well. With respect to the aldehyde **74** scope, different aliphatic and aromatic aldehydes (-R^3) gave the target pyrazolines **79**, although with aromatic aldehydes the annulation reaction proceeded better in glacial acetic acid. Instead of aldehydes, ketones were also used in this reaction, but in that case catalyst loading needed to be increased (5 mol %). For alkynes **75** various substituents (-R^4) were tolerated including a phenyl bearing an electron-withdrawing or electron-donating groups.

Also branched aliphatic alkynes were tolerated, while linear aliphatic alkynes led to the mixture of regioisomers.[215]

Taking into consideration 1,3-dipolar nature of azomethine imine **76** and dipolarophile nature of gold-acetylide **84**, the Au(I)-catalyzed reaction described above could also be driven by 1,3-DC (Fig. 3.14). That mechanism could theoretically lead to a mixture of 1,2,3,4- and 1,2,3,5-substituted pyrazolines **78** and **79**, respectively, as discussed for Cu(I)-catalyzed reaction to pyrazolines (Fig. 3.10). Because of the electron density distribution of azomethine imine **76**, 1,3-dipolar cycloaddition to the pyrazoline **79** would be favoured (path b, Fig. 3.14).

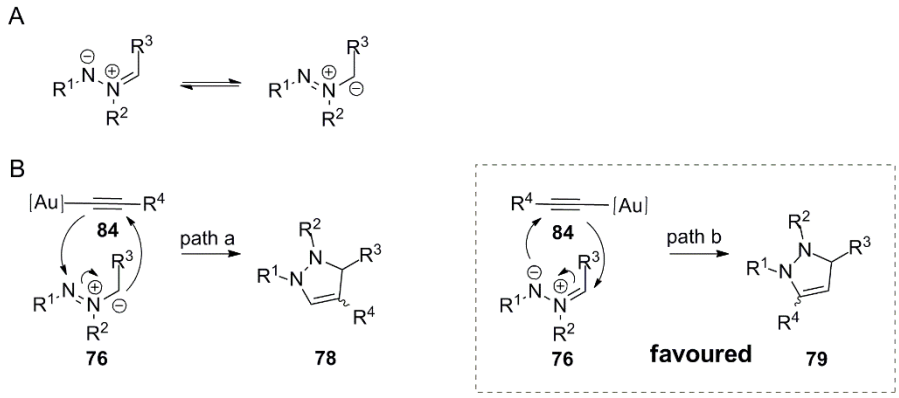

Figure 3.14. A) Zwitterionic resonance structure of azomethine imine; B) proposed Au(I)-catalyzed 1,3-DC leading to pyrazolines **78** and **79**.

However, propargyl hydrazide **80** formation was demonstrated in the literature, clearly suggesting that the Au(I)-catalyzed annulation proceeds rather via A^3 coupling followed by nucleophilic intramolecular cyclization yielding exclusively pyrazoline **79** (Fig. 3.11).[215]

3.4. Synthesis of the hexathymidine-pyrazol(in)e conjugates by the Au(I)-mediated annulation reaction

3.4.1. Optimization of the Au(I)-mediated annulation reaction

The CPG-bound alkyne **hexT-87** (see Chapter 5.4.1), isobutyric aldehyde **T**, and hydrazide **88** served to investigate the accessibility of the hexT-pyrazoline conjugate **hexT-89T** by Au(I)-mediated annulation. Systematic exploration of reaction parameters yielded four distinct, isolatable products in different rations: the pyrazoline **hexT-89T**, the pyrazole **hexT-90T**, the propargyl hydrazide **hexT-91T**, and **hexT-92** as the product of water addition to phenylacetylene conjugate **hexT-87** (Fig. 3.15, Table 6).

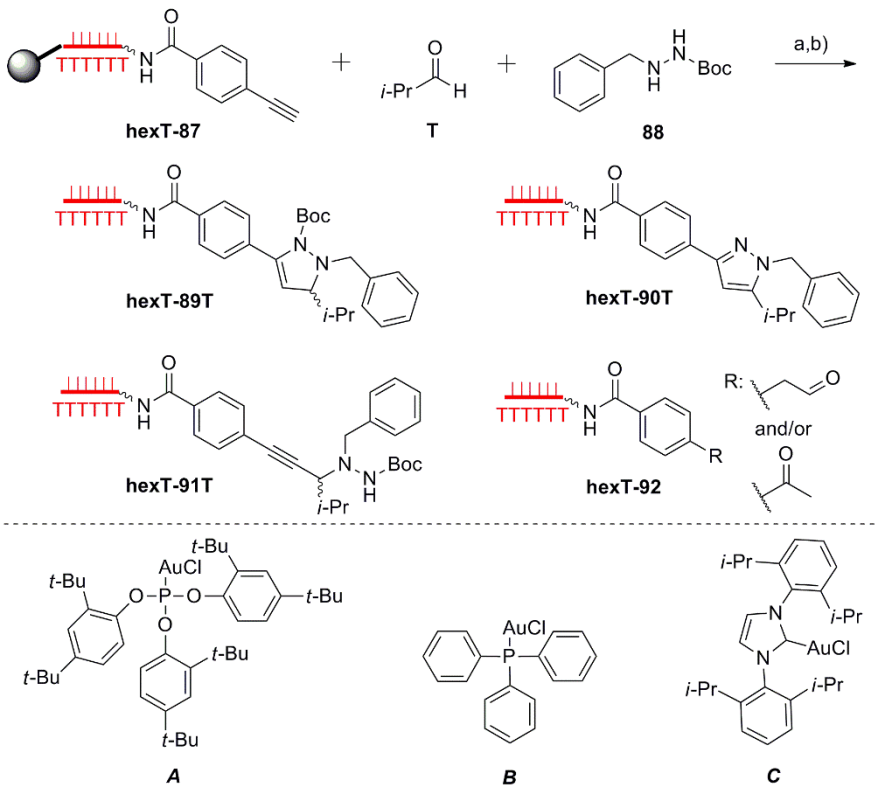

Figure 3.15. Adapting a Au(I)-mediated annulation reaction to TiDEC.[215] a) For conditions see Table 6; b) AMA (aqueous ammonia (30 %)/ aqueous methylamine (40 %), 1:1, vol/vol), 30 min, room temperature. Figures 3.16-3.22 show HPLC traces of the crude reaction mixtures (preparative HPLC). Filled grey circle denotes solid support (controlled pore glass, CPG); wavy bond to hexT: 5'-(C6)-amino-linker; bold bond: connection from the hexT-oligonucleotide to the CPG.

Table 6. Optimization of reaction conditions for the Au(I)-mediated annulation reaction to furnish hexT-pyrazol(in)e conjugates **hexT-89**.

	No.	hydrazide and aldehyde [eq][a]	catalyst [eq][a]	solvent	T [°C]	catalyst	**hexT-89** [%][b]	**hexT-90** [%][b]	**hexT-91** [%][b]	**hexT-92** [%][b]
a) equivalents of catalyst ***A***/$AgSbF_6$	**1**	1000	5	THF	50	***A***/$AgSbF_6$	-	-	-	-
	2	1000	50	THF	50	***A***/$AgSbF_6$	15	-	55	-
	3	1000	250	THF	50	***A***/$AgSbF_6$	50	-	25	10
b) solvent	**1**	1000	250	THF	50	***A***/$AgSbF_6$	50	-	25	10
	2	1000	250	$C_2H_4Cl_2$	50	***A***/$AgSbF_6$	40	-	10	50
	3	1000	250	CH_2Cl_2	50	***A***/$AgSbF_6$	20	-	10	50
	4	1000	250	toluene	50	***A***/$AgSbF_6$	50	15	15	15
	5 (A)	1000	250	MeCN	50	***A***/$AgSbF_6$	75	-	25	-
	6	1000	250	DMF	50	***A***/$AgSbF_6$	10	-	20	10
	7	1000	250	AcOH	50	***B***/AgOTf	10	55	10	-
c) temperature	**1**	1000	250	$C_2H_4Cl_2$	45	***A***/$AgSbF_6$	40	-	25	30
	2	1000	250	$C_2H_4Cl_2$	50	***A***/$AgSbF_6$	40	-	10	50
	3	1000	250	$C_2H_4Cl_2$	55	***A***/$AgSbF_6$	40	15	20	20
	4	1000	250	$C_2H_4Cl_2$	60	***A***/$AgSbF_6$	15	35	<5	35
	5	1000	250	toluene	50	***A***/$AgSbF_6$	50	15	15	15
	6	1000	250	toluene	55	***A***/$AgSbF_6$	30	25	10	30
	7	1000	250	MeCN	50	***A***/$AgSbF_6$	75	-	25	-
	8	1000	250	MeCN	55	***A***/$AgSbF_6$	75	-	25	-
	9	1000	250	MeCN	60	***A***/$AgSbF_6$	70	20	-	-
	10 (B)	1000	250	AcOH	50	***B***/AgOTf	10	55	10	-
	11 (C)	1000	250	AcOH	60	***B***/AgOTf	<5	90	-	-
	12	1000	250	MeCN	rt	***A***/$AgSbF_6$	-	-	-	-
d) catalyst	**1**	1000	250	toluene	50	***B***	-	-	5	-
	2	1000	250	toluene	50	AgOTf	40	-	60	-
	3	1000	250	$C_2H_4Cl_2$	50	***B***/AgOTf	85	-	-	-
	4	1000	250	$C_2H_4Cl_2$	50	***C***/AgOTf	85	-	-	-

[a] *versus* the solid support-bound hexathymidine-alkyne conjugate **hexT-87**; [b] HPLC analysis of the crude, missing percentage to 100 %: **hexT-87**.

3.4.1.1. Exploration of catalyst concentration

Performing the reaction with a 250fold excess of the Au(I) catalyst ***A***/$AgSbF_6$[218] *versus* hexathymidine-alkyne conjugate **hexT-87** at 50 °C yielded a 2:1:0.4 mixture of pyrazoline **hexT-89T**, propargyl hydrazide **hexT-91T**, and the hydration product **hexT-92** (Fig. 3.16d, Table 6a, entry 3). While 250fold excess of the catalyst ***A***/$AgSbF_6$ yielded predominantly pyrazoline **hexT-89T**, 50fold excess of the Au(I) catalyst reduced the yield of cyclization product **hexT-89T** in favour of A^3 coupling product **hexT-91T** (Figs. 3.16c, 3.17, Table 6a, entry 2).[215] This finding suggests that 50fold excess of the Au(I) catalyst was sufficient to activate the alkyne towards alkynylation of azomethine imine, but not completely sufficient for further activation of the triple bond towards nucleophilic attack of the carbamate nitrogen. Reducing the excess of the catalyst to 5fold (Table 6a, entry 1),[215] and lowering the temperature to 25 °C returned only starting material (Table 6c, entry 12).

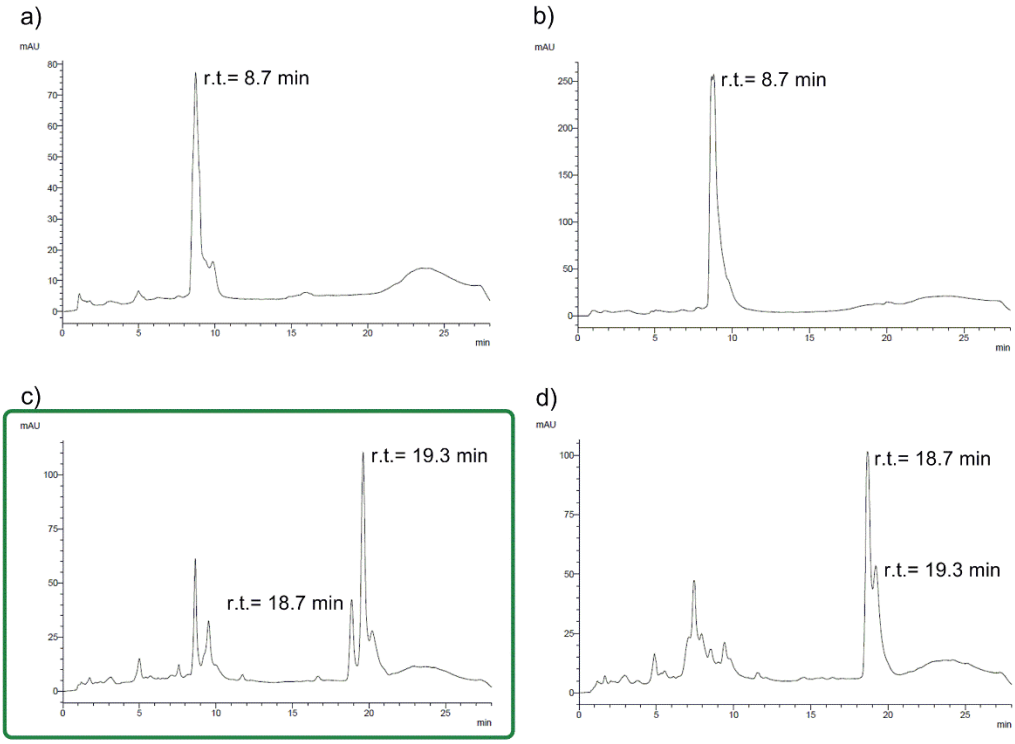

Figure 3.16. Exploration of catalyst concentration for the Au(I)-mediated MCR of the hexathymidine-alkyne conjugate **hexT-87**, isobutyraldehyde **T**, and hydrazide **88**, for reaction conditions see Table 6a. a) HPLC trace of the starting material (hexathymidine-alkyne conjugate **hexT-87**); b) HPLC trace of experiment **No. 1**, no product formation visible; c) HPLC trace of experiment **No. 2**, formation of a product mixture with the later eluting component **hexT-91T** (r.t.= 19.3 min) as main product; d) HPLC trace of experiment **No. 3**, formation of a product mixture with the earlier eluting component **hexT-89T** (r.t.= 18.7 min) as main product.

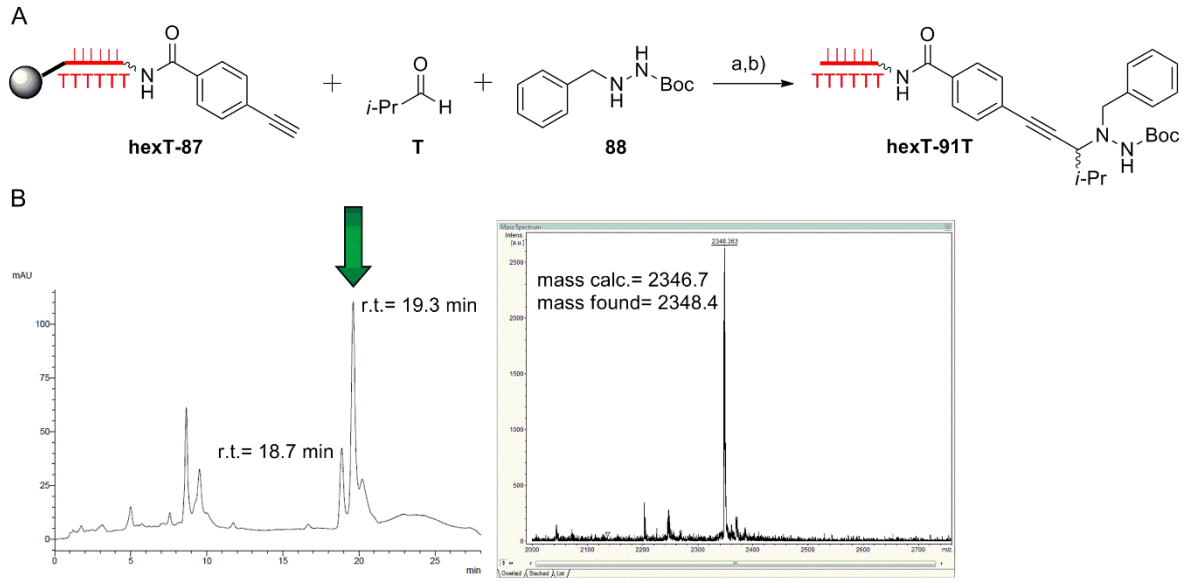

Figure 3.17. MALDI-TOF/TOF-MS of the isolated propargyl hydrazide **hexT-91T** (r.t.= 19.3 min) from Figure 3.16c. A) Reaction scheme of the propargyl hydrazide formation; a) reaction condition **No. 2** (Table 6a); b) AMA (aqueous ammonia (30 %)/ aqueous methylamine (40 %), 1:1, vol/vol), 30 min, room temperature; B) MALDI-TOF/TOF-MS of the isolated hexathymidine conjugate **hexT-91T**. Filled grey circle denotes solid support (controlled pore glass, CPG); wavy bond to hexT: 5'-(C6)-amino-linker; bold bond: connection from the hexT-oligonucleotide to the CPG.

3.4.1.2. Exploration of solvents

Changing the solvent at 50 °C had a profound effect on the product ratio (Fig. 3.18).

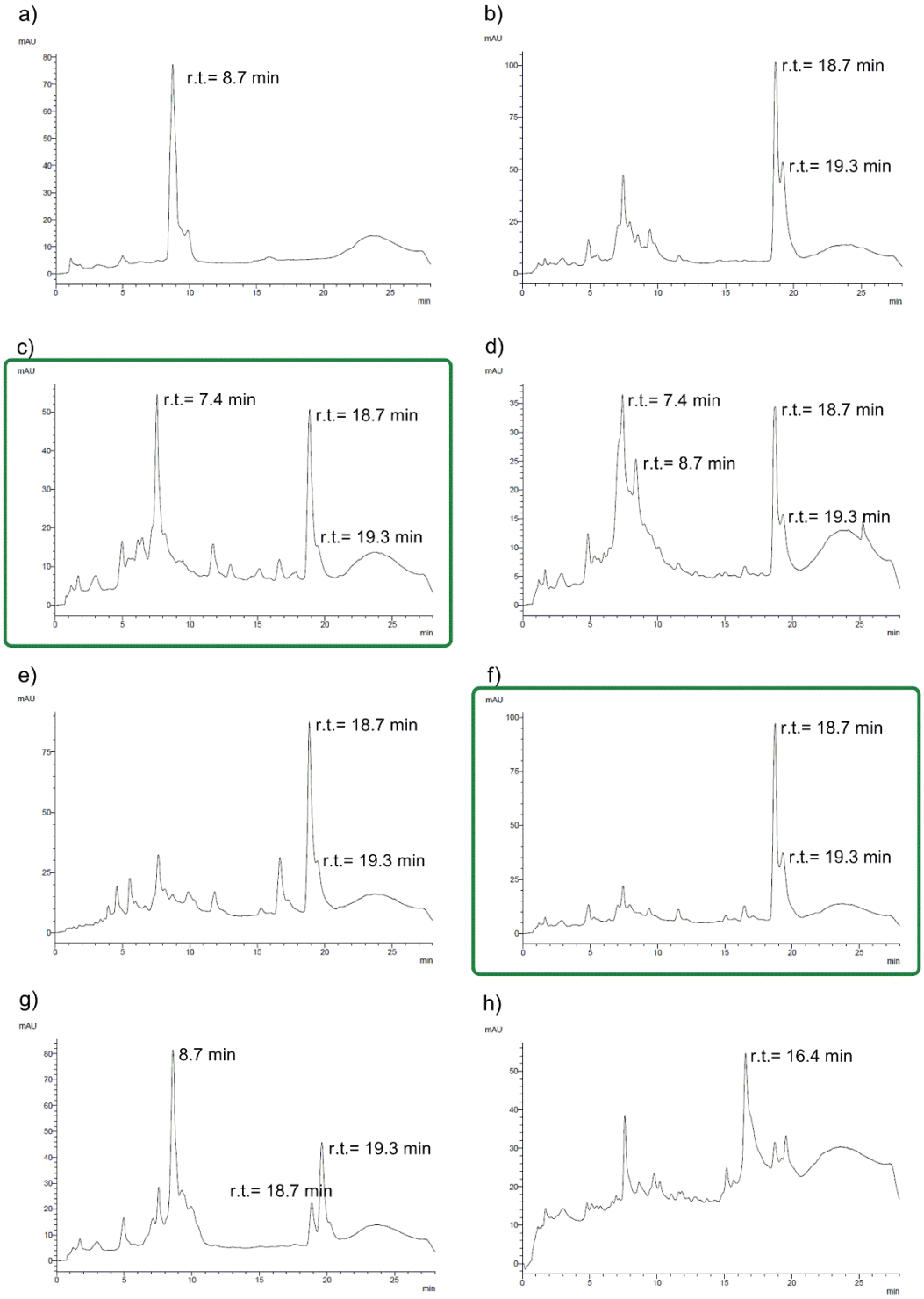

Figure 3.18. Exploration of different solvents for the Au(I)-mediated MCR of the hexathymidine-alkyne conjugate **hexT-87**, isobutyraldehyde **T**, and hydrazide **88**, for reaction conditions see Table 6b. a) HPLC trace of the starting material (hexathymidine-alkyne conjugate **hexT-87**); b) HPLC trace of experiment **No. 1** (same experiment as Figure 3.16d); c) HPLC trace of experiment **No. 2**, formation of a product mixture with the

pyrazoline **hexT-89T** and the hydration product **hexT-92** (r.t.= 7.4 min) as main products; d) HPLC trace of experiment **No. 3**, similar result as experiment **No. 2**; e) HPLC trace of experiment **No. 4**, formation of the pyrazoline **hexT-89T** as main product, formation of the oxidized pyrazole **hexT-90T** as a side product (r.t.= 16.4 min); f) HPLC trace of experiment **No. 5(A)**, formation of the earlier eluting pyrazole **hexT-90T** as main product; g) HPLC trace of experiment **No. 6**, low conversion to the target heterocycle; h) HPLC trace of experiment **No. 7**, formation of the pyrazole **hexT-90T** as a main product (r.t.= 16.4 min).

MeCN yielded a 3:1 mixture of pyrazoline **hexT-89T** and propargyl hydrazide **hexT-91T** (Figs. 3.18f, 3.19, Table 6b, entry 5). Performing the reaction in THF and toluene afforded pyrazoline **hexT-89T** in the same conversion, but in toluene pyrazole **hexT-90T** was detected as a minor product (Table 6b, entries 1, 4).

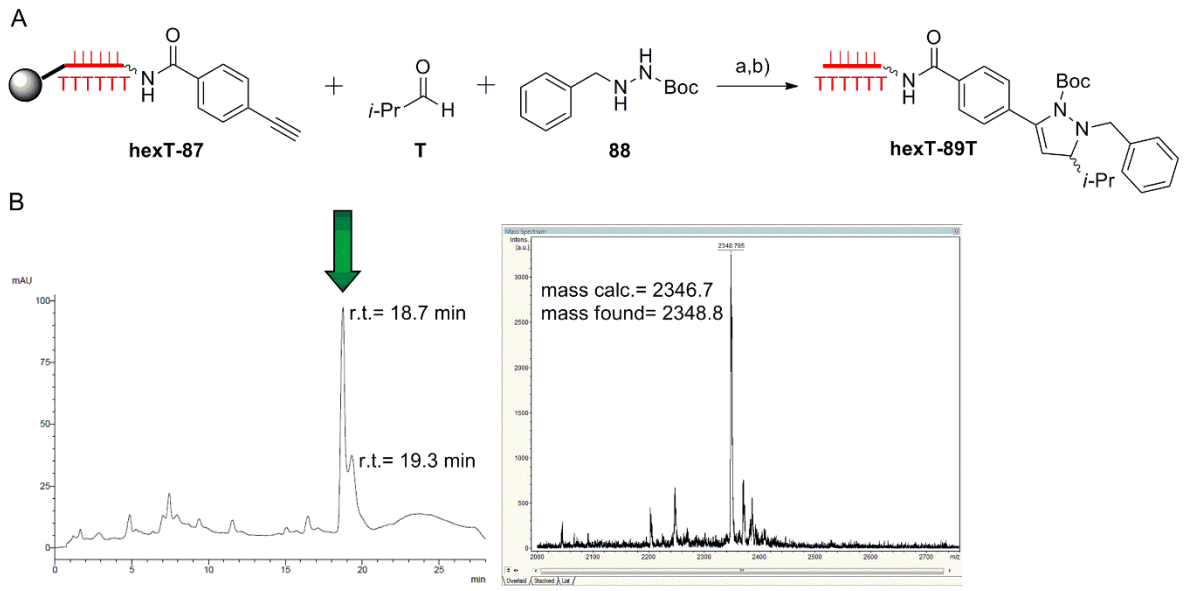

Figure 3.19. MALDI-TOF/TOF-MS of the isolated pyrazoline **hexT-89T** (r.t.= 18.7 min) from Figure 3.18f. A) Reaction scheme of the pyrazoline formation; a) reaction condition **No. 5** (Table 6b); b) AMA (aqueous ammonia (30 %)/ aqueous methylamine (40 %), 1:1, vol/vol), 30 min, room temperature; B) MALDI-TOF/TOF-MS of the isolated hexathymidine conjugate **hexT-89T**. Filled grey circle denotes solid support (controlled pore glass, CPG); wavy bond to hexT: 5'-(C6)-amino-linker; bold bond: connection from the hexT-oligonucleotide to the CPG.

A similar yield of **hexT-89T** was obtained in 1,2-dichloroethane. Although, as in dichloromethane, hydration of the alkyne **hexT-87** was profound, yielding a substantial amount of **hexT-92** (Figs. 3.18c, d, 3.20, Table 6b, entries 2, 3). Hydration product **hexT-92** also occurred as a minor product in THF, toluene, and DMF. On contrast to other organic solvents, hydration of alkyne **hexT-87** did not take place in MeCN (Table 6b, entry 9). In glacial acetic acid with catalyst ***B***/AgOTf formation of pyrazole **hexT-90T** through ring

closure, oxidation, and Boc-group removal was found as major reaction (Fig. 3.18h, Table 6b, entry 7).

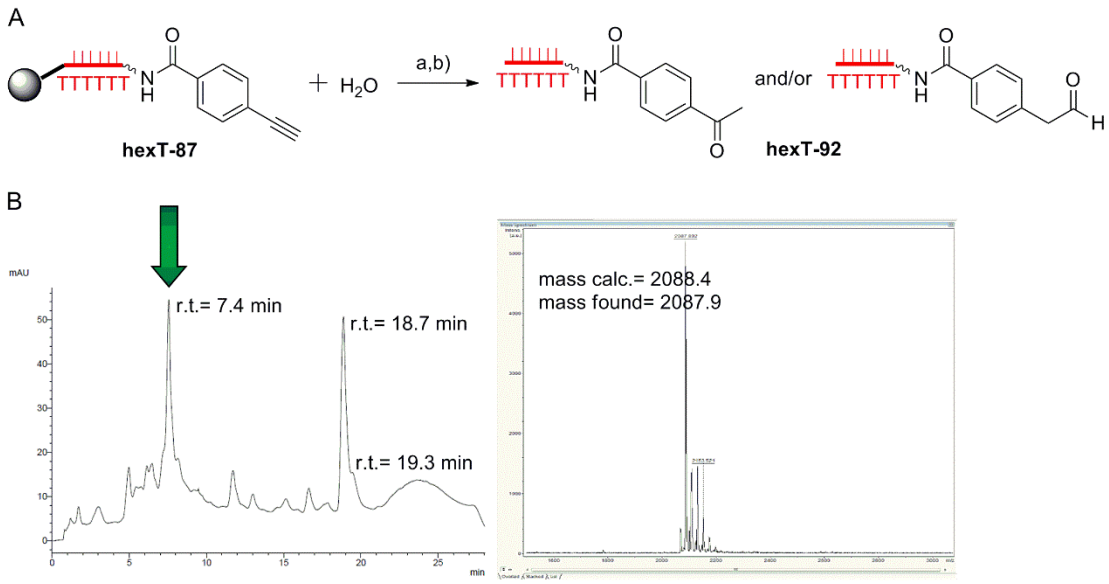

Figure 3.20. MALDI-TOF/TOF-MS analysis of the isolated hydration product **hexT-92** (r.t.= 7.4 min) from Figure 3.18c. A) Reaction scheme of the hydration reaction; a) reaction condition **No. 2** (Table 6b); b) AMA (aqueous ammonia (30 %)/ aqueous methylamine (40 %), 1:1, vol/vol), 30 min, room temperature; B) MALDI-TOF/TOF-MS of the isolated hexathymidine conjugate **hexT-92**. Filled grey circle denotes solid support (controlled pore glass, CPG); wavy bond to hexT: 5'-(C6)-amino-linker; bold bond: connection from the hexT-oligonucleotide to the CPG.

In general, formation of hexT-phenylacetaldehyde and/or hexT-phenylacetophenon **hexT-92** in the Au(I)-mediated annulation reaction (Fig. 3.20) is not surprising. Condensation of 1000 equivalents of both, hydrazide and aldehyde, will yield not just 1000 equivalents of azomethine imine, but also 1000 equivalents of water that can act as a nucleophile towards the electron-deficient alkyne. High catalyst loading and elevated temperature might contribute to this reaction.[219]

3.4.1.3. Exploration of solvents and temperature

It is worth to mention that hydration of the alkyne **hexT-87** did not take place in MeCN even upon increasing of the reaction temperature to 60 °C (Table 6c, entry 9).

Increasing the temperature from 50 °C to 55 °C, and then to 60 °C in glacial acetic acid, 1,2-dichloroethane, toluene, and MeCN led to elevated oxidative aromatization of the pyrazoline ring (Fig. 3.21, Table 6c, entries 1-9). As a result, Au(I)-mediated annulation in glacial acetic acid at 60 °C afforded exclusively pyrazole **hexT-90T** (Figs. 3.21k, 3.22, Table 6c, entry 11). However, aromatization was less profound in MeCN then in other solvents (Figs. 3.21g-i).

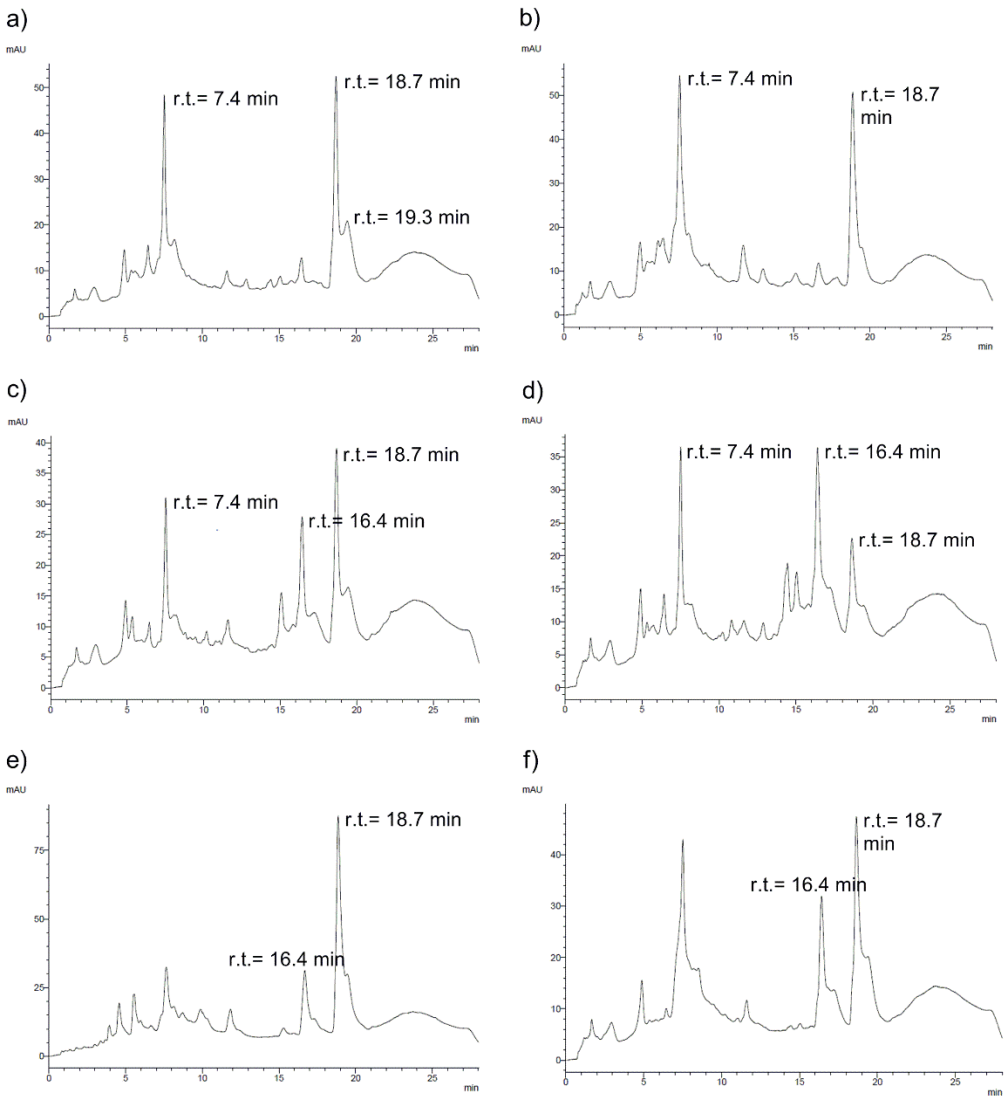

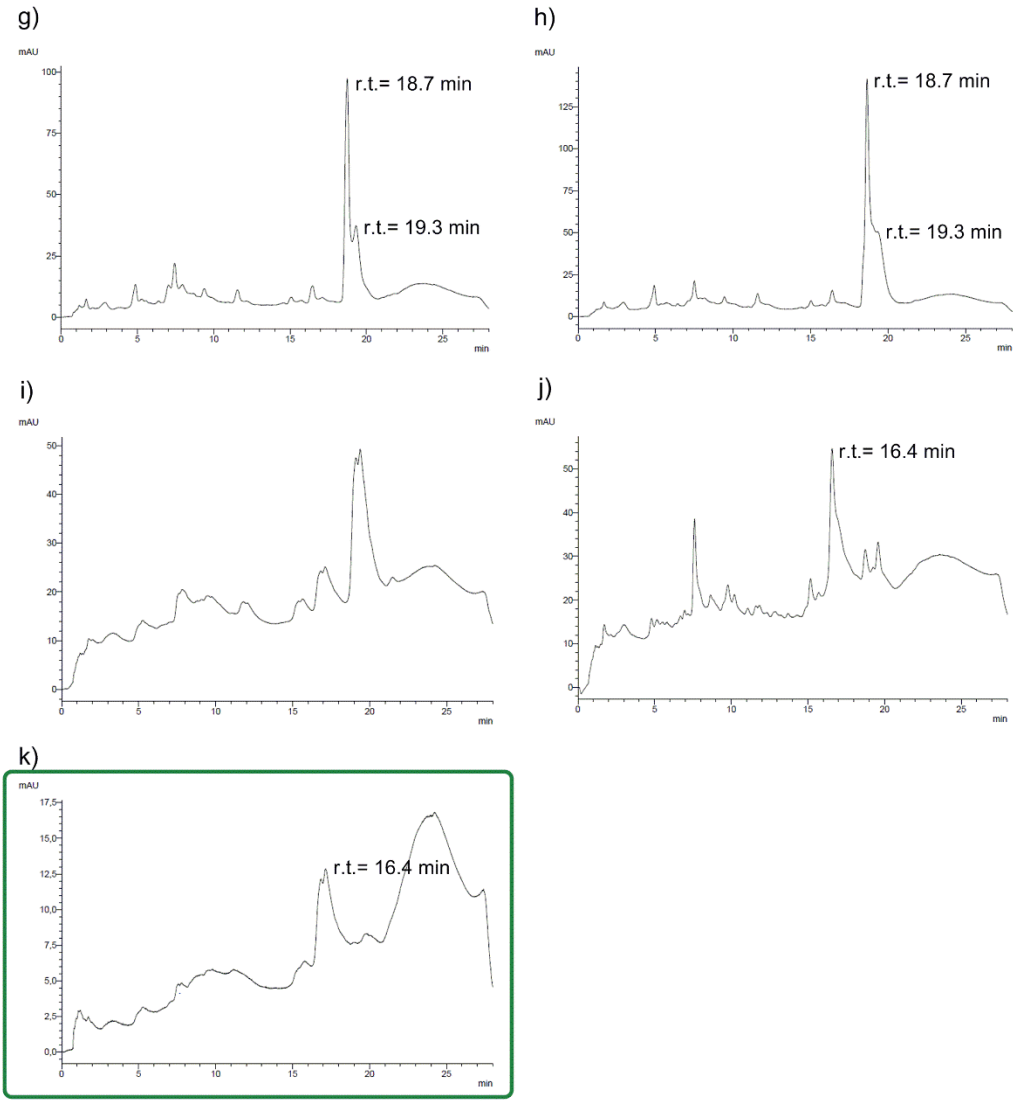

Figure 3.21. Exploration of different solvents and temperatures for the Au(I)-mediated MCR of the hexathymidine-alkyne conjugate **hexT-87**, isobutyraldehyde **T**, and hydrazide **88**, for reaction conditions see Table 6c. a) HPLC trace of experiment **No. 1**, formation of a mixture of products **hexT-89T**, **hexT-91T** and **hexT-92**; b) HPLC trace of experiment **No. 2**, formation of a mixture of products **hexT-89T** and **hexT-92**, less formation of **hexT-91T** than in **No. 1**; c) HPLC trace of experiment **No. 3**, formation of a mixture of products **hexT-89-92**, at 55 °C formation of the pyrazole **hexT-89T** becomes notable; d) HPLC trace of experiment **No. 4**, the pyrazole **hexT-90T** and the hydration product **hexT-92** are the main products formed under these conditions; e) HPLC trace of experiment **No. 5**, formation of compound **hexT-89T** as main product, formation of the oxidized pyrazole **hexT-90T** as a side product (r.t.= 16.4 min); f) HPLC trace of experiment **No. 6**, formation of a mixture of products **hexT-89-92**; g) HPLC trace of experiment **No. 7**, formation of compound **hexT-89T** as main product; h) HPLC trace of experiment **No. 8**, formation of compound **hexT-89T** as main product; i) HPLC trace of experiment **No. 9**, formation of a mixture of products **hexT-89-92**; j) HPLC trace of experiment **No. 10**, formation of pyrazole **hexT-90T** as main product; k) HPLC trace of experiment **No. 11**, formation of pyrazole **hexT-90T** as main product.

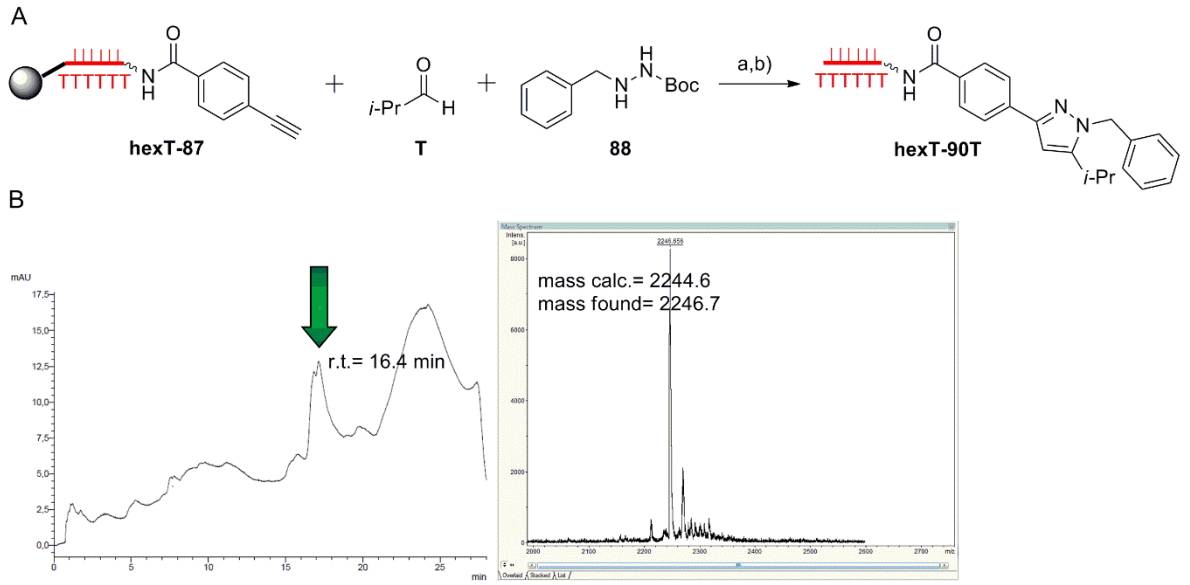

Figure 3.22. MALDI-TOF/TOF-MS of the isolated pyrazole **hexT-90T** (r.t.= 16.4 min) from Figure 3.21k. A) Reaction scheme of the pyrazole formation; a) reaction condition **No. 11** (Table 6c); b) AMA (aqueous ammonia (30 %)/ aqueous methylamine (40 %), 1:1, vol/vol), 30 min, room temperature; B) MALDI-TOF/TOF-MS of the isolated hexathymidine conjugate **hexT-90T**. Filled grey circle denotes solid support (controlled pore glass, CPG); wavy bond to hexT: 5'-(C6)-amino-linker; bold bond: connection from the hexT-oligonucleotide to the CPG.

3.4.1.4. Exploration of catalysts

Finally, the triphenylphosphine- and *N*-heterocyclic carbene-based Au(I) catalysts ***B*** and ***C*** (Fig. 3.15), respectively, yielded the pyrazoline **hexT-89T** as sole detectable product (Fig. 3.23d, Table 6d, entries 3, 4).[215] Ag(I), which reportedly afforded propargylamine by a Mannich-type reaction,[215] gave the cyclization product **hexT-89T** and propargyl hydrazide **hexT-91T** in a 4:6 ratio, likely due to the high catalyst concentration (Fig. 3.23c, Table 6d, entry 2). One needs to be careful with interpretation of that result in the context of Au(I)-mediated reaction discussed above. Many of commonly used Au(I) precatalysts (on example ***A***, ***B***, and ***C***) possess chloride as coordination ion. These catalysts are activated upon addition of a silver salt (for example $AgSbF_6$ or AgOTf) by AgCl precipitation. Much attention in the field of gold catalysis is directed towards explanation of the "silver effect" which relates to the role of the silver salts used as a halide scavengers in Au(I) catalysis.[220-222] Recent mechanistic experimental studies of Maier *et al.*[223] on "silver effects" in Au(I)-catalyzed hydroalkoxylation of alkynes shed some light on that topic, clarifying the innocence of Ag(I) regarding the mechanism of the catalytic process itself, and stating that in Au(I)-catalyzed hydroalkoxylation where a Ag(I) salt is used to activate the catalyst, Au(I) is indeed the active

catalyst, and not Ag(I).[223] According to the authors, this should be valid also for many other Au(I)-catalyzed reactions,[223] so it could be valid for the Au(I)-catalyzed annulation, as it consists of hydroamination where organogold intermediates are of similar origin as these of hydroalkoxylation.[223,224] It is very important to distinguish the "silver effect" in Au(I) catalysis, from the use of Ag(I) as a catalyst, i.e. the direct participation of Ag(I) in a catalytic process[220] (Fig. 3.23c, Table 6d, entry 2).

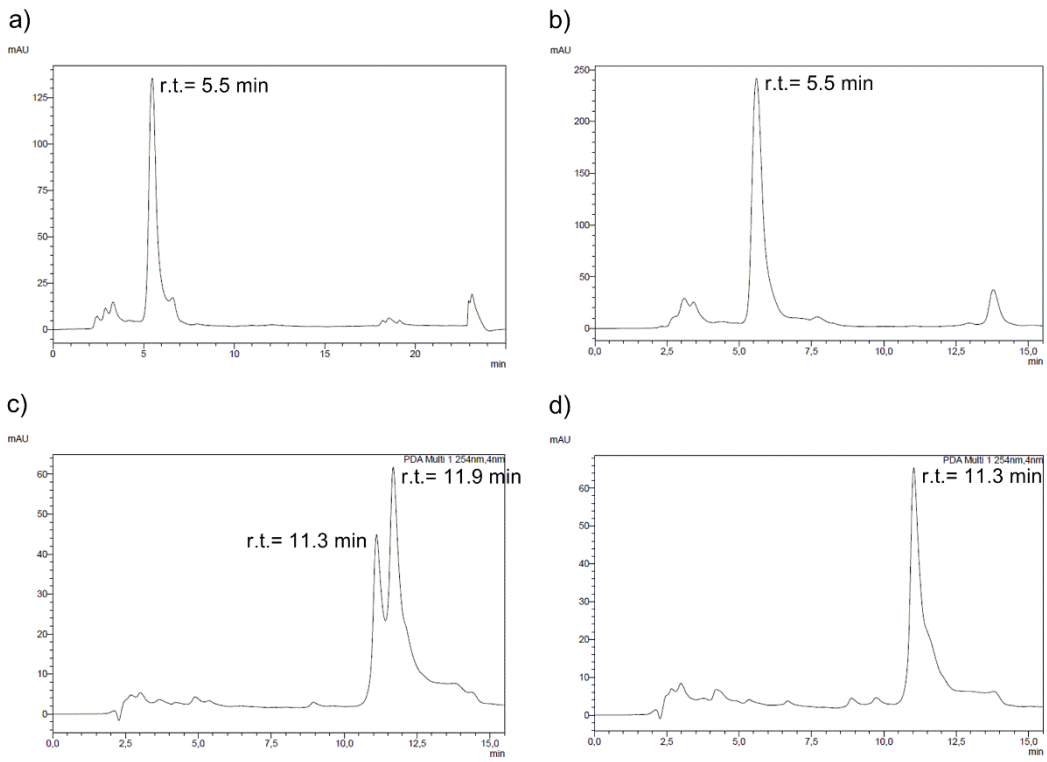

Figure 3.23. Exploration of different catalysts for the Au(I)-mediated MCR of the hexathymidine-alkyne conjugate **hexT-87**, isobutyraldehyde **T**, and hydrazide **88**, for reaction conditions see Table 6d. a) HPLC trace of the starting material **hexT-87**; b) HPLC trace of experiment **No. 1**, no product formation upon reaction with catalyst ***B*** alone; c) HPLC trace of experiment **No. 2**, catalysis with AgOTf gave rise to a mixture (40:60) of products **hexT-89T** and **hexT-91T**; d) HPLC trace of experiment **No. 3**, the pyrazoline **hexT-89T** was formed as the sole product under these conditions; experiment **No. 4** gave the same result as experiment **No. 3**. Experiments a-d) were analyzed on a different HPLC system: ion pair reverse phase high-pressure liquid chromatography (HPLC, Shimadzu Prominence) using a C18 stationary phase (Phenomenex, Gemini; 5 µm, C18, 110 Å, 100*4.6 mm) and a gradient of 10 mM aqueous triethylammonium acetate/MeOH (30-90 % over 15.5 min). HPLC trace a) shows column washing, and equilibration, too.

3.4.2. Synthesis of reference molecules: pyrazoline, propargyl hydrazide, and pyrazole

To prove that the Au(I)-mediated MCR to pyrazolines indeed leads to the proposed hexT conjugates, reference molecules were synthesized. Au(I)-mediated annulation proceeds via A^3 coupling, and therefore in addition to reference pyrazoline **PL-C**, the propargyl hydrazide intermediate **PH-C** was also synthesized.[215] The identity of both small molecules was confirmed by ^{1}H and ^{13}C NMR, and they were coupled to hexT by amide formation, yielding **ref-hexT-89T** and **ref-hexT-91T**, respectively (Fig. 3.24).

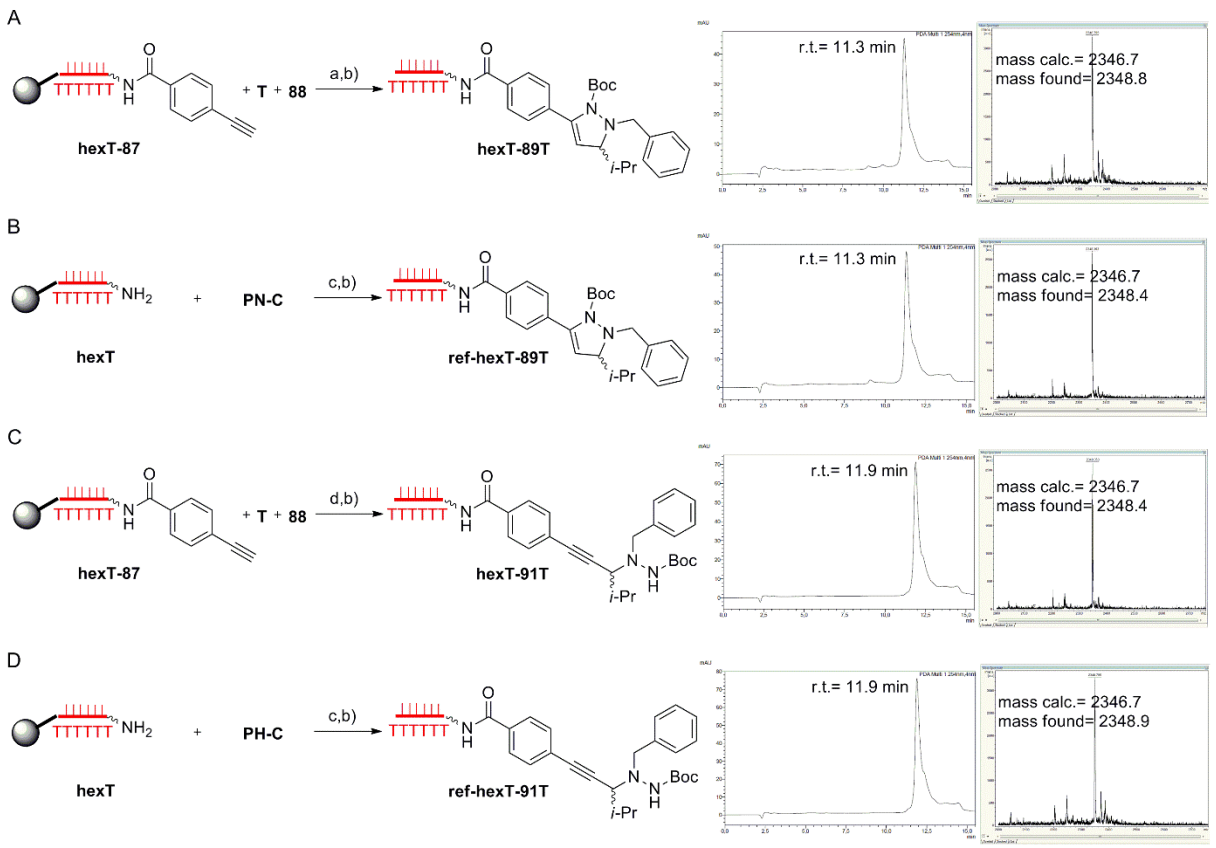

Figure 3.24. Comparison of the hexT-pyrazoline **hexT-89T** synthesized from the hexT-alkyne conjugate **hexT-87** by the Au(I)-mediated annulation reaction (Fig. 3.15) with the reference hexT-pyrazoline **ref-hexT-89T** synthesized from the pyrazoline **PL-C**, and 5'-(C6)-amino-linker modified **hexT** by amide coupling, and comparison of the propargyl hydrazide **hexT-91T** with the reference compound **ref-hexT-91T** synthesized by amide coupling of the propargyl hydrazide **PH-C** with the 5'-(C6)-amino-linker modified **hexT**. A) Scheme for the synthesis of the hexT-pyrazoline conjugate **hexT-91T** and analysis of the product; conditions: a) method **A** (Table 6b, entry 5); b) AMA (aqueous ammonia (30 %)/ aqueous methylamine (40 %), 1:1, vol/vol), 30 min, room temperature); B) scheme for the synthesis of the hexT-pyrazoline conjugate **ref-hexT-89T** by amide coupling and analysis of the product; conditions: c) HATU, DIPEA, room temperature, 4 hours; b) AMA (aqueous ammonia (30 %)/ aqueous methylamine (40 %), 1:1, vol/vol), 30 min, room temperature); C) scheme

for the synthesis of the hexT-propargyl hydrazide conjugate **hexT-91T** and analysis of the product; conditions: d) AgOTf, toluene; b) AMA (aqueous ammonia (30 %)/ aqueous methylamine (40 %), 1:1, vol/vol), 30 min, room temperature); D) scheme for the synthesis of the hexT-propargyl hydrazide conjugate **ref-hexT-91T** by amide coupling and analysis of the product; conditions: c) HATU, DIPEA, room temperature, 4 hours; b) AMA (aqueous ammonia (30 %)/ aqueous methylamine (40 %), 1:1, vol/vol), 30 min, room temperature. Filled grey circle denotes solid support (controlled pore glass, CPG); wavy bond to hexT: 5'-(C6)-amino-linker; bold bond: connection from the hexT-oligonucleotide to the CPG.

Comparison of analytical HPLC and MALDI-TOF/TOF-MS data of **hexT-89T** and **ref-hexT-89T** suggested that pyrazoline conjugates accessed either by Au(I)-mediated MCR, or by amide coupling (Fig. 3.24A, B) are identical. The same holds true for propargyl hydrazides **hexT-91T** and **ref-hexT-91T** synthesized by Ag(I) catalysis, and by amide coupling, respectively (Fig. 3.24C, D).

As screening of different reaction conditions suggested that some conditions led to oxidative aromatization and Boc-deprotection of pre-formed pyrazoline **hexT-89T** yielding corresponding pyrazole **hexT-90T**, the analogous molecule **P-C** was synthesized and coupled to the hexT by amide formation, yielding **ref-hexT-90T**. Both, analytical HPLC and MALDI-TOF/TOF-MS data suggested that **hexT-90T** and **ref-hexT-90T** are identical compounds (Fig. 3.25A, B).

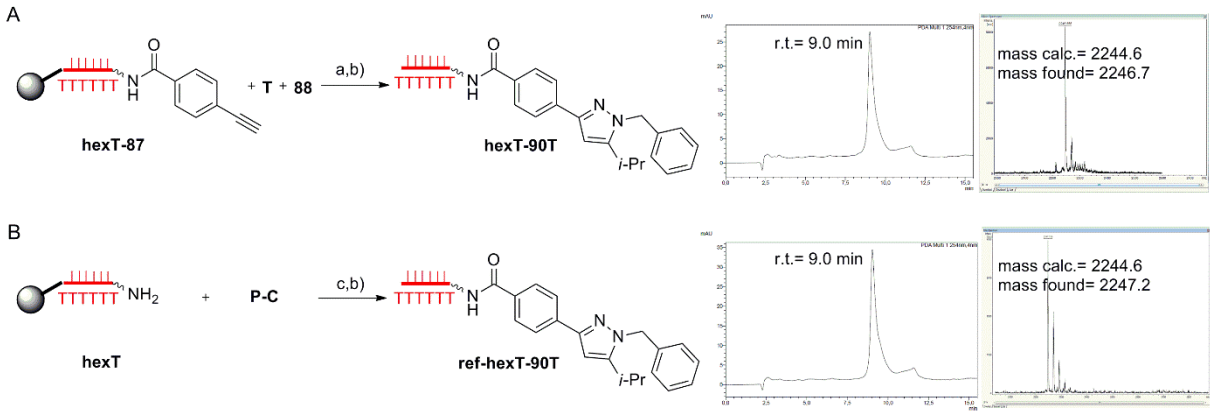

Figure 3.25. Comparison of the hexT-pyrazole **hexT-90T** synthesized from the hexT-alkyne conjugate **hexT-87** by the Au(I)-mediated annulation reaction with the reference hexT-pyrazole **ref-hexT-90T** synthesized from the pyrazole **P-C**, and 5'-(C6)-amino-linker modified **hexT** by amide coupling. A) Scheme for the synthesis of the hexT-pyrazole conjugate **hexT-90T** and analysis of the product; conditions: a) method **C** (Table 6c, entry 11); b) AMA (aqueous ammonia (30 %)/ aqueous methylamine (40 %), 1:1, vol/vol), 30 min, room temperature); B) scheme for the synthesis of the hexT-pyrazole conjugate **ref-hexT-90T** by amide coupling and analysis of the product; conditions: c) HATU, DIPEA, room temperature, 4 hours; b) AMA (aqueous ammonia (30 %)/ aqueous methylamine (40 %), 1:1, vol/vol), 30 min, room temperature).

3.4.3. Synthesis of hexathymidine-pyrazole conjugates by oxidative aromatization of hexathymidine-pyrazolines

Treatment of pyrazoline **hexT-89T** with 10 % TFA in dry CH_2Cl_2 for 4 hours afforded Boc-deprotected pyrazoline **hexT-93T** (Fig. 3.26A), showing that Δ^2-pyrazolines are easily accessible as hexT conjugates as well, potentially increasing the diversity of a tiDEL.

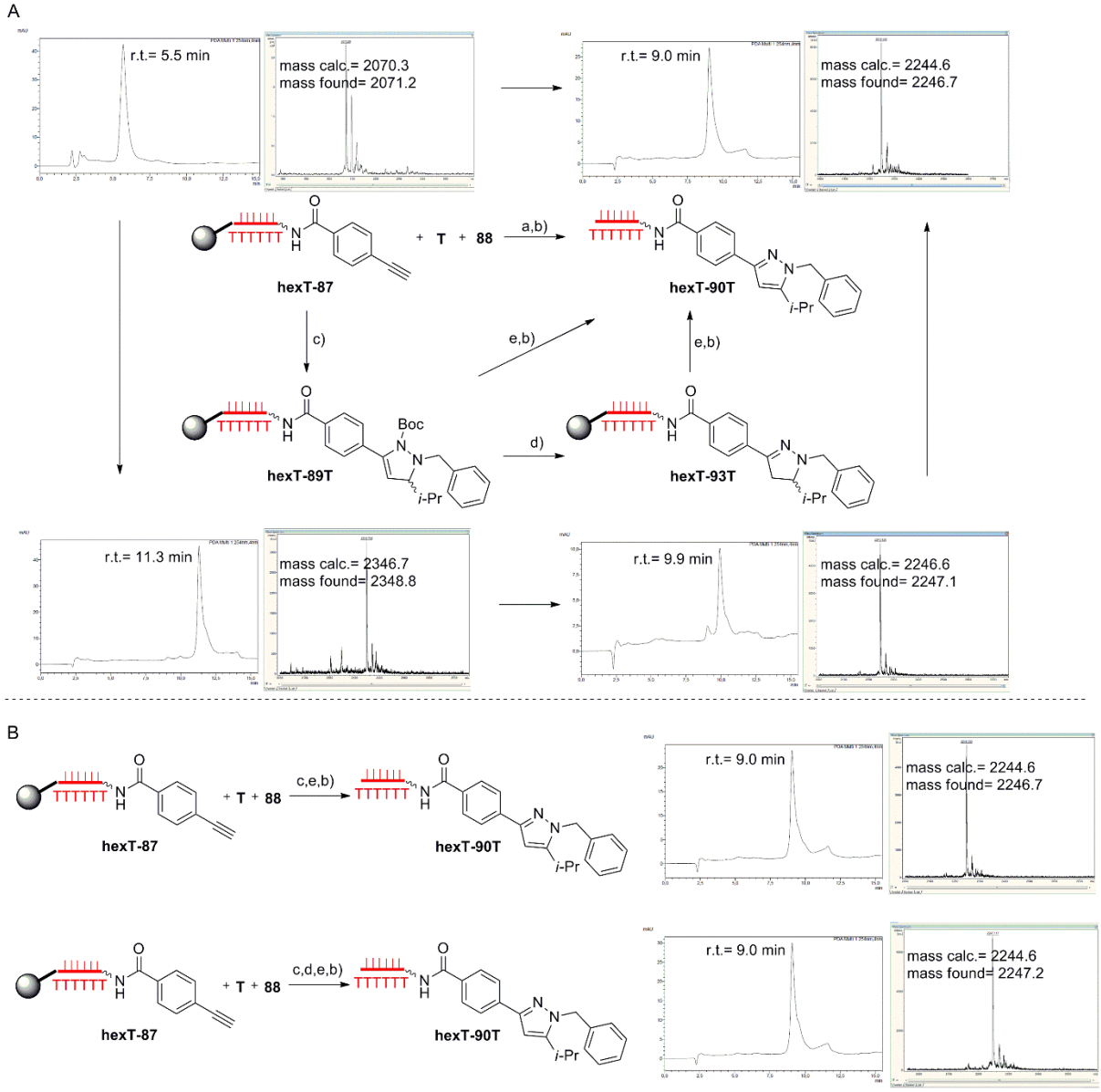

Figure 3.26. Synthesis of the hexT-pyrazole conjugate **hexT-90T** from the hexT-alkyne conjugate **hexT-87** by the Au(I)-mediated annulation reaction in glacial acetic acid at 60 °C (Fig. 3.15), and synthesis of the same conjugate from the pyrazoline conjugates **hexT-89T** and **hexT-93T** by oxidative aromatization with DDQ. A) Synthesis scheme for the synthesis of the hexT-pyrazole conjugate **hexT-90T** from **hexT-87**, **hexT-89T**, and **hexT-93T**. See above or below each hexT conjugate a corresponding HPLC trace and MALDI-TOF/TOF-MS spectrum of the compound; conditions: a) method **C** (Table 6c, entry 11); b) AMA (aqueous ammonia (30 %)/

aqueous methylamine (40 %), 1:1, vol/vol), 30 min, room temperature; c) method **A** (Table 6b, entry 5); d) 10 % TFA, CH_2Cl_2; e) 100 eq. of DDQ, toluene, room temperature, 30 min; B) synthesis scheme and analytical data for hexT-pyrazole conjugate **hexT-90T** synthesized from the pyrazoline conjugates **hexT-89T** and **hexT-93T** by oxidative aromatization. Filled grey circle denotes solid support (controlled pore glass, CPG); wavy bond to hexT: 5'-(C6)-amino-linker; bold bond: connection from the hexT-oligonucleotide to the CPG.

The pyrazoline **hexT-93T** was stable upon storage in water at -20 °C over several weeks, as well as upon storage at room temperature for several days. Oxidation to the pyrazole **hexT-90T** was not observed by analytical HPLC.

In general, pyrazoles can be synthesized by oxidation of corresponding pyrazolines with different oxidizing agents.[225] Therefore, in addition to the Au(I)-mediated annulation in glacial acetic acid at 60 °C (Figs. 3.22, 3.26A), hexT-pyrazoles can also be accessed by oxidative aromatization of related hexT-pyrazolines (Fig. 3.26). Quantitative conversion of pyrazolines **hexT-89T** and **hexT-93T** to the corresponding pyrazole **hexT-90T** was achieved with 100 equivalents of DDQ in toluene at room temperature after 30 minutes reaction time. The integrity of the hexT-oligonucleotide adapter was preserved under these reaction conditions.

3.4.4. Reaction conditions controlled access to hexathymidine-pyrazolines and hexathymidine-pyrazoles

Screening of different reaction conditions for Au(I)-mediated cascade reaction revealed access to two different scaffolds as hexT conjugates. Control of reaction conditions provided access to densely substituted hexT-pyrazolines and hexT-pyrazoles from the same starting materials, thereby adding diversity to projected library synthesis in a highly efficient manner (Fig. 3.27).

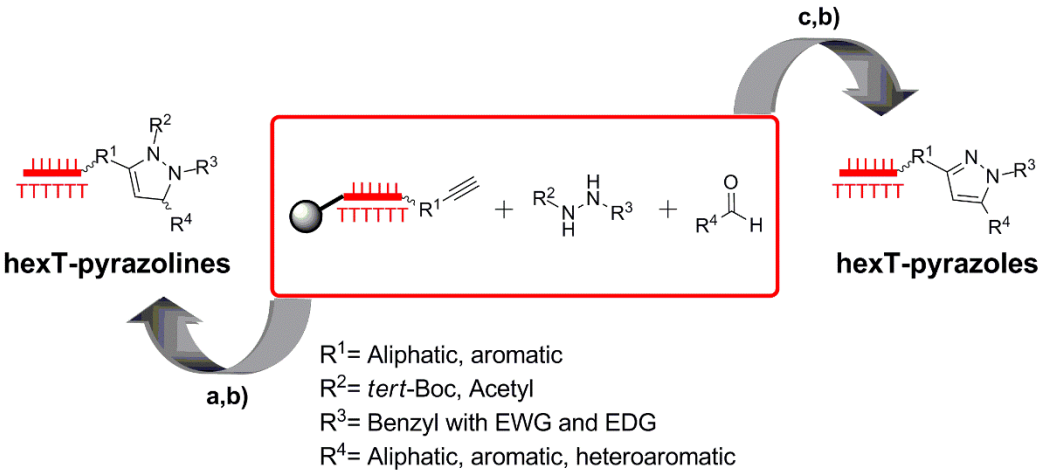

Figure 3.27. Reaction conditions controlled synthesis of the hexT-pyrazol(in)e conjugates using the same starting materials: an alkyne component conjugated to the hexT, an aldehyde, and a hydrazide component. Reagents and conditions: a) ***A***/$AgSbF_6$, MeCN, 50 °C, overnight; b) aq. NH_3/$MeNH_2$, room temperature, 30 min; c) ***B***/AgOTf, AcOH, 60 °C, overnight; EDG= electron-donating group; EWG= electron-withdrawing group. Filled grey circle denotes solid support (controlled pore glass, CPG); wavy bond to hexT: 5'-(C6)-amino-linker; bold bond: connection from the hexT-oligonucleotide to the CPG.

Optimization of reaction conditions afforded the target hexT-pyrazolines when the reaction was mediated by a Au(I) phosphite precatalyst ***A*** (Fig. 3.15) activated with silver hexafluoroantimonate in acetonitrile at 50 °C overnight (Fig. 3.27, Table 6, entry 5), while Au(I) phosphine precatalyst ***B*** (Fig. 3.15) in combination with silver triflate in glacial acetic acid at 60 °C overnight afforded access to the hexT-pyrazoles (Fig. 3.27, Table 6, entry 11).

3.4.5. Exploration of the scope of unsymmetrically substituted hydrazides for Au(I)-mediated pyrazol(in)e synthesis

HexT-pyrazol(in)es were successfully synthesized with several unsymmetrically substituted hydrazides (Table 7). Besides the *tert*-Boc group, an acetyl (-R^1) group was also tolerated (Table 7, entry 4), yielding amides that are in general more stable than carbamates.

Table 7. Reaction scope of unsymmetrically substituted hydrazides.

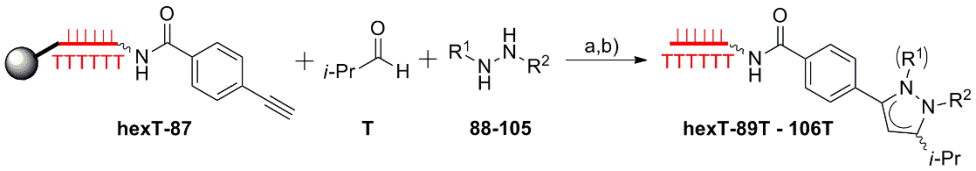

Conditions: a) method **A** (Table 6b, entry 5), b) AMA (aqueous ammonia (30 %)/ aqueous methylamine (40 %), 1:1, vol/vol), 30 min, room temperature.

entry	hydrazide	hexT	R^1	R^2	yield [nmol][a]	conversion [%][b,c]	mass calc. mass found[d]
1	**88**	**hexT-89T**	*tert*-Boc	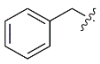	4.4	75 (25)	2346.7 2345.3
2[e]	**94**	**hexT-95T**	*tert*-Boc	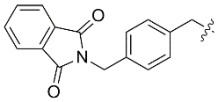	4.9	80 (15)	2375.8 2375.5
3[e,f]	**94**	**hexT-96T**	*tert*-Boc	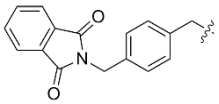	5.0	90 (0)	2273.6 2272.4
4[e]	**97**	**hexT-98T**	acetyl	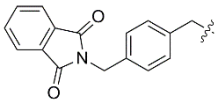	4.0	95 (0)	2317.7 2317.6
5	**99**	**hexT-100T**	*tert*-Boc	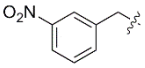	4.0	80 (10)	2391.7 2392.3
6	**101**	**hexT-102T**	*tert*-Boc	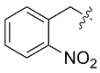	4.1	75 (0)	2391.7 2392.4
7	**103**	**hexT-104T**	*tert*-Boc	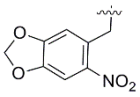	0.9	25 (35)	2435.7 2437.2 2257.7[g]
8	**105**	**hexT-106T**	*tert*-Boc	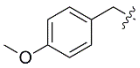	4.7	30 (15)	2376.7 2377.8

[a] measured by Nanodrop; [b] % conversion estimated based on the area under the curve of the product peak versus the educt peak in the HPLC-trace (preparative HPLC), missing percentage to 100 %: **hexT-87**; [c]

conversions in parentheses show those of corresponding propargyl hydrazides; [d] measured by MALDI-TOF/TOF-MS; [e] phthalimide group removed in the product; [f] product synthesized by method **C** (Table 6c, entry 11), thus leading to the oxidized compound **hexT-96T**; [g] loss of the photolabile 3,4-methylendioxy-6-nitrobenzyl group upon irradiation in the mass spectrometer. Filled grey circle denotes solid support (controlled pore glass, CPG); wavy bond to hexT: 5'-(C6)-amino-linker; bold bond: connection from the hexT-oligonucleotide to the CPG.

But, even acetyl protection could not prevent aromatization of the pyrazoline when the Au(I)-mediated MCR was performed in glacial acetic acid at 60 °C overnight. Both, electron donating and electron withdrawing groups of benzyl substituent (-R^2) were tolerated. For purpose of tiDEL synthesis, readily available aldehydes represented one diversification point, therefore a second diversification point had to be installed in the hydrazide component. Alternative to introducing of different hydrazides, as they all have to be synthesized *de novo*, was the selection of one hydrazide that contains an additional functionality that will allow for further modification required for library synthesis. Thus, amine-displaying hydrazide **94** (Fig. 3.28) was selected. During cleavage of hexT-pyrazol(in)e conjugates from the solid support, by treatment with aq. ammonia/ methylamine (AMA), phthalimide deprotection took place yielding free benzylic amine suitable for introducing of different carboxylic acids as a second set of a building blocks by amide coupling (Fig. 3.28).

3.5. Towards oligothymidine-initiated DNA-Encoded Library (tiDEL) based on the pyrazol(in)e scaffold

3.5.1. Exploration of aldehyde scope for the Au(I)-mediated pyrazol(in)e synthesis

The synthesis of **23 hexT-pyrazolines** and **48 hexT-pyrazoles** (Fig. 3.28) succeeded with cyclic and acyclic branched aliphatic aldehydes, variously substituted benzaldehydes, and some heteroaromatic aldehydes (Tables 18, 19).

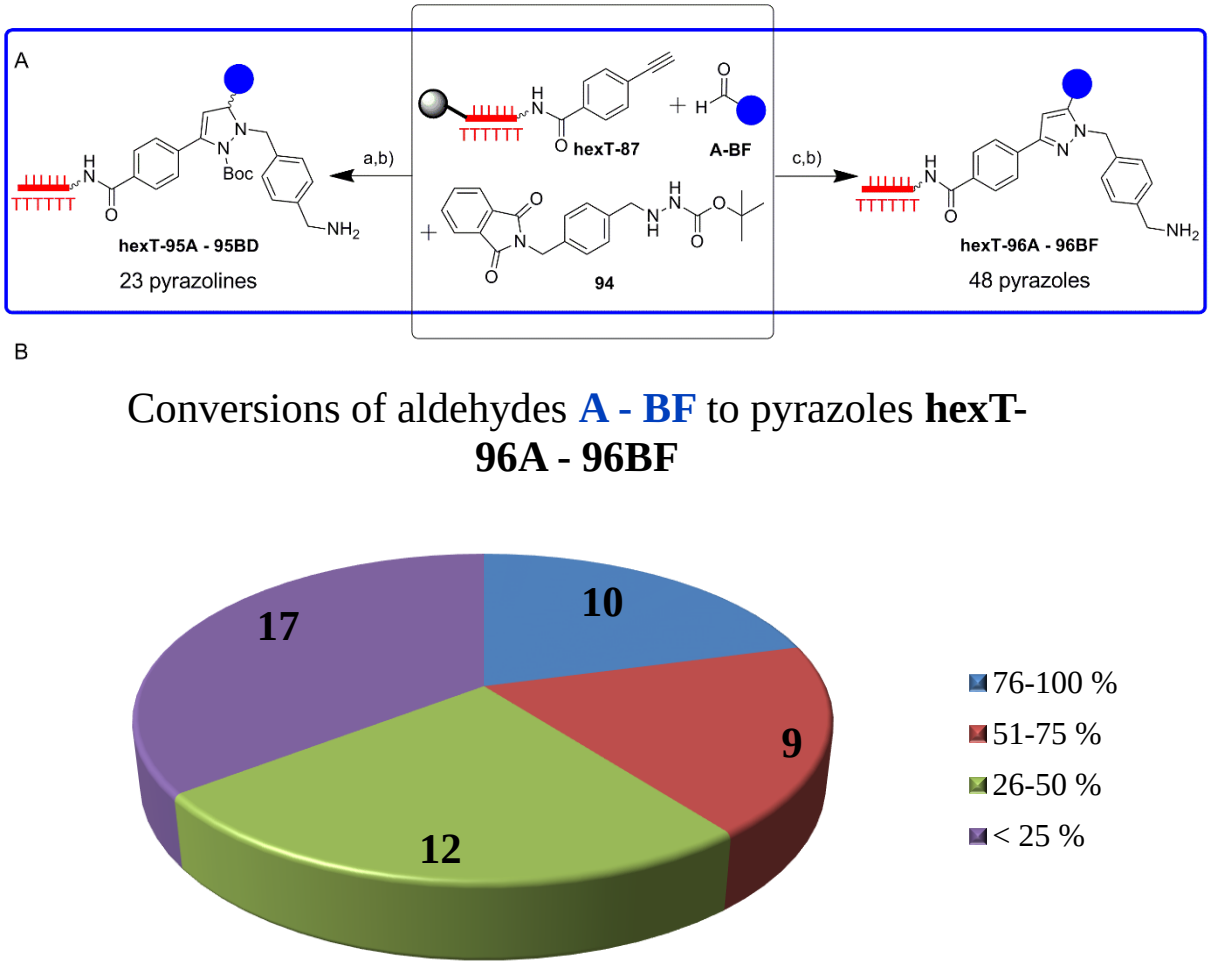

Figure 3.28. Reaction conditions controlled synthesis of hexT-pyrazol(in)e conjugates and statistical analysis of conversions of aldehydes **A - BF** to the target hexT-pyrazoles. A) Synthesis scheme for reaction conditions controlled synthesis of hexT-pyrazol(in)e conjugates using the same starting materials: hexT-phenylacetylene **hexT-87**, hydrazide **94**, and 48 different aldehydes **A - BF**. Reagents and conditions: a) ***A***/$AgSbF_6$, MeCN, 50 °C, overnight; b) aq. NH_3/$MeNH_2$, room temperature, 30 min; c) ***B***/AgOTf, AcOH, 60 °C, overnight; B)

statistical analysis of conversions of 48 different aldehydes **A - BF** to the target pyrazoles **hexT-96A - 96BF** by Au(I)-mediated annulation reaction (Table 19). Out of 48 aldehydes, ten aldehydes gave rise to the target pyrazoles with 76-100 % conversion, nine aldehydes led to the target pyrazoles with 51-75 % conversion, 12 aldehydes yielded corresponding pyrazoles with 26-50 % conversion, while 17 aldehydes afforded the target pyrazoles with conversion lower that 25 %. Filled grey circle denotes solid support (controlled pore glass, CPG); wavy bond to hexT: 5'-(C6)-amino-linker; bold bond: connection from the hexT-oligonucleotide to the CPG.

Although 60 % of aldehydes (**A - BF**) afforded the target pyrazoles in conversion lower than 50 % (Fig. 3.28B), and the same is true even for 73 % of aldehydes (**A - BD**) involved in the pyrazoline synthesis, the total yields of both (Tables 18, 19) were more than sufficient as 40 pmol of each conjugate was required for library synthesis. All pyrazol(in)e conjugates were purified by preparative HPLC, and analyzed by analytical HPLC and MALDI-TOF/TOF-MS to provide pure authentic samples for tiDEL synthesis (Tables 18, 19).
Linear aliphatic and several heteroaromatic aldehydes did not give the expected products. Heteroaromatic aldehydes might poison the Au(I) catalyst, while in case of the Au(I)-mediated annulation with linear aliphatic aldehydes, the lack of product formation might be explained by dimerization of the acyclic azomethine imine **76** (Fig. 3.29).[214]

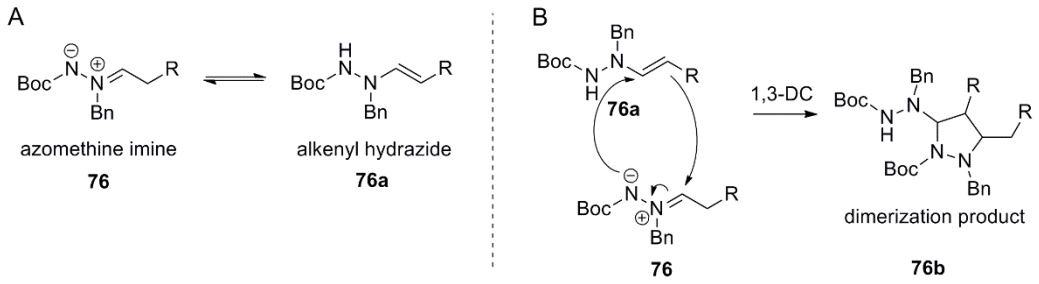

Figure 3.29. Dimerization of azomethine imine **76**. A) Tautomerization of azomethine imine **76** to alkenyl hydrazide **76a**; B) [3+2]-cycloaddition of azomethine imine **76** and alkenyl hydrazide **76a** leading to dimerization product **76b**.

When aliphatic aldehyde is used as a substrate then tautomerization of corresponding azomethine imine **76** produces alkenyl hydrazide **76a** (Fig. 3.29A) that itself is not reactive towards a π-activated alkyne. Instead, it can act as dipolarophile towards azomethine imine **76** yielding [3+2]-cycloaddition product **76b** (Fig. 3.29B). This scenario is very possible as both hydrazide and aldehyde are added in 1000fold excess to solid-support bound alkyne **hexT-87**. As small molecule side product, dimerization product **76b** would not be bound to the CPG, and therefore would not be detected by preparative HPLC as it would be washed away during standard solid-support synthesis work-up procedure.

3.5.2. Evaluation of carboxylic acids reactivity for library synthesis

The in total **71 hexT-pyrazol(in)e** conjugates were synthesized using hydrazide **94** displaying benzylic amine serving as a site for introducing of different carboxylic acids as a second set of building blocks. My aim was to synthesize a high quality library. Therefore, before the real library synthesis 106 carboxylic acids were selected from a previously published diversity set of carboxylic acids,[189]. and then they were screened for their reactivity (Fig. 3.30, Table 20).

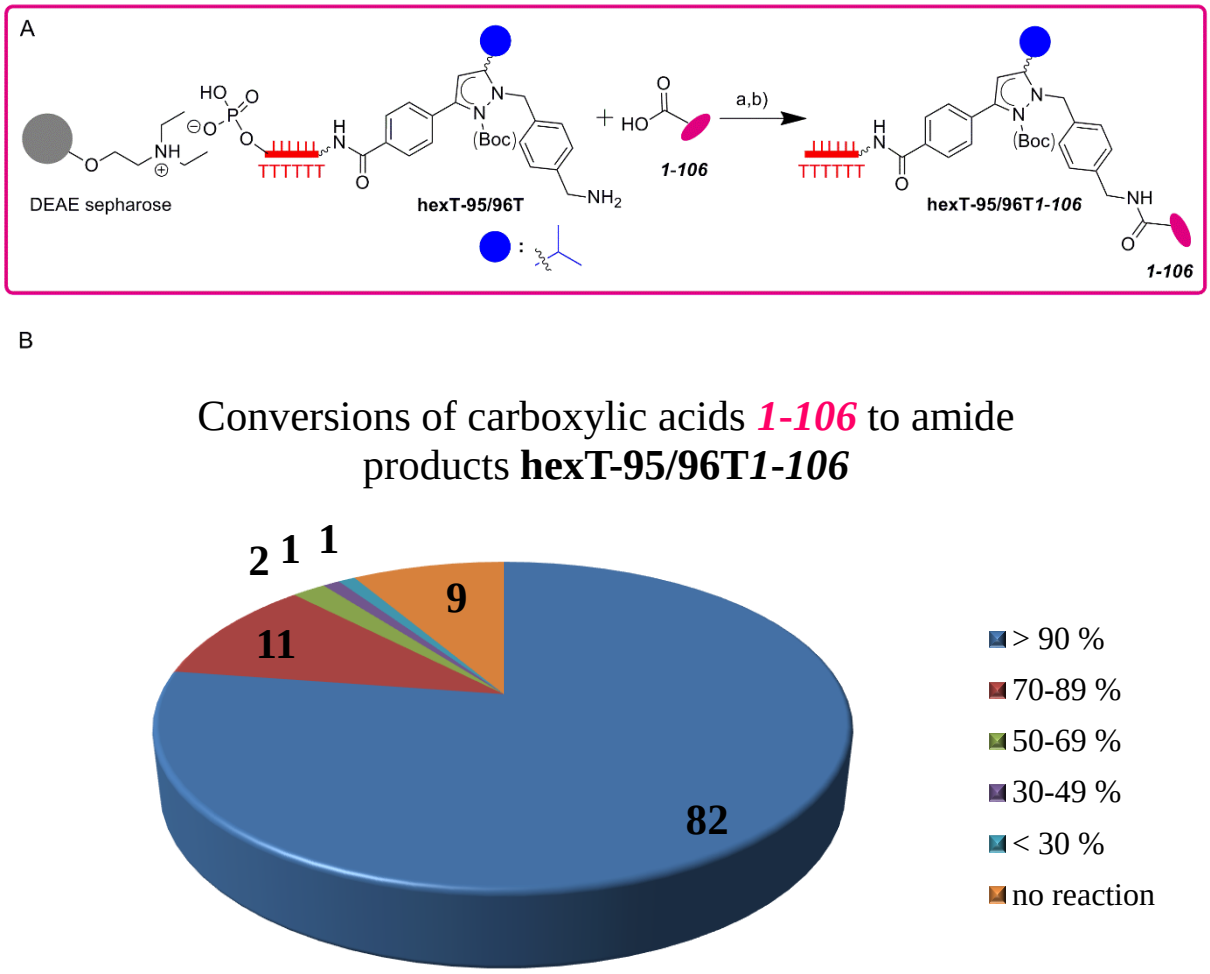

Figure 3.30. Evaluation of carboxylic acid building blocks. A) Synthesis scheme for screening of carboxylic acids for their reactivity on model conjugates: **hexT-95-PEG(4)-T**, **hexT-95T**, and **hexT-96T** bound to the DEAE sepharose. Reagents and conditions: a) HOAt, EDC × HCl, DMSO/ddH_2O (70/30), room temperature, overnight; b) 3 M sodium acetate buffer (pH= 4.75), room temperature, 30 min; B) statistical analysis of conversions of carboxylic acids ***1-106*** to the target amides. Out of 106 carboxylic acids, 82 carboxylic acids afforded the target amides with conversion higher that 90 %, 11 carboxylic acids yielded corresponding amides with 70-89 % conversion, two carboxylic acids yielded the target amides with 60 % conversion, one carboxylic

acid was coupled with 30 % conversion, and one with 10 % conversion. Nine carboxylic acids did not yield the expected products.

Carboxylic acids (Table 20) reactivity was evaluated with model hexT-pyrazol(in)e conjugates. Carboxylic acids ***28***, ***29***, ***32***, ***37***, ***39***, ***41***, ***42***, ***43***, ***46***, ***56***, and ***93*** were coupled to the hexT-pyrazoline conjugate **hexT-95-PEG(4)-T** containing a PEG(4) linker serving as spacer between hexT and pyrazoline scaffold, while carboxylic acids ***4***, ***30***, ***31***, ***33***, ***34***, ***44***, ***45***, ***47***, ***48***, ***49***, ***51***, ***77***, ***82***, ***84***, ***85***, ***86***, ***87***, ***89***, and ***91*** were coupled to the hexT-pyrazole conjugate **hexT-96T**. All other carboxylic acids (76) were coupled to the hexT-pyrazoline conjugate **hexT-95T**. The aim was to exclude carboxylic acids that would not give a corresponding amide product or that would give it in a low conversion from the tiDEL synthesis. All reactions were performed on 500 pmol scale, and they all took place on DEAE sepharose.[57] After the reactions were finished, sepharose was extensively washed with different organic solvents to remove excess of reagents. At the end, the DNA was eluted from the resin by 30 minutes shaking with 3 M sodium acetate buffer (pH= 4.75). Reactions were analyzed by MALDI-MS. All samples were taken directly from eluates, therefore sodium adducts were detected, too (Chapter 5.4.6.1). Out of 106 carboxylic acids, 97 carboxylic acids or 92 % of all carboxylic acids, gave the expected amide products, while nine carboxylic acids, or 8 % of all acids, did not yield the target amides at all (Fig. 3.30). To be more precise, 82 carboxylic acids afforded the target amides with conversion higher that 90 %, 11 carboxylic acids yielded the target amides with 70-89 % conversion, two carboxylic acids (***36*** and ***57***) were coupled with 60 % conversion, and one carboxylic acid (***75***) was coupled with 30 % conversion (Table 20). Carboxylic acids ***1***, ***8***, ***11***, ***14***, ***16***, ***26***, ***51***, ***89***, and ***106*** did not yield the expected products, and therefore they were not included in the tiDEL synthesis as well as carboxylic acid ***65*** that gave the target amide in only 10 % conversion.

3.5.3. *Enzymatic encoding of hexathymidine-pyrazol(in)e conjugates by T4-DNA ligase*

For encoding of hexT-pyrazol(in)e conjugates T4-DNA ligation was used, as well established DNA-encoding method.[18] Encoding of hexT-pyrazol(in)es is described in Figure 3.31, and designation of the sequences in Tables 8 and 9. I encoded all hexT-pyrazol(in)e conjugates ***I*** with heterocycle-encoding DNA sequences ***II/II`***, and aldehyde-encoding DNA sequences ***III/III`*** *in one pot* to duplex DNAs ***I-II-III/II`-III`***, and then with carboxylic acid-encoding DNA sequences ***IV/IV`*** to fully encoded conjugates ***I-II-III-IV/II`-III`-IV`*** (Fig. 3.31).

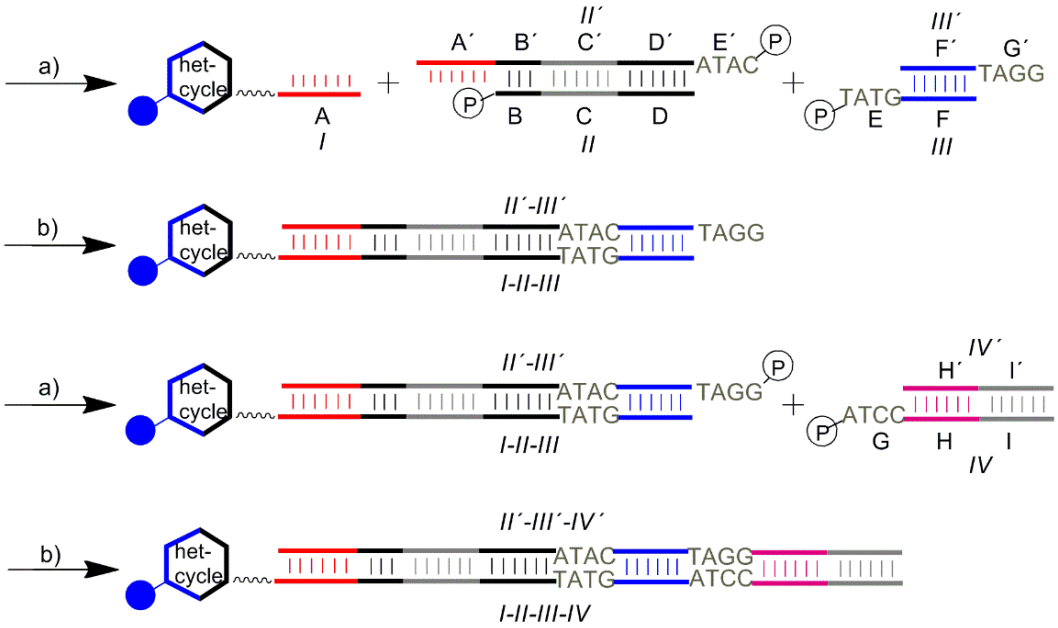

Figure 3.31. Scheme for enzymatic ligation of hexT conjugates (sequence ***I***), for the designation of the sequences see Tables 6 and 7; a) 5'-end phosphorylation and annealing; b) T4-DNA ligation. hetcycle: pyrazoline or pyrazole scaffold.

Heterocycle-encoding sequences ***II/II`*** contained hexaadenine overhang **A`**, EcoR1 restriction site **B** and complementary region **B`**, primer sequence **C** and complementary region **C`**, the scaffold code **D** and complementary region **D`**, and a region complementary to the overhang for T4 ligation **E`**. Aldehyde-encoding sequences ***III/III`*** contained the overhang for T4 ligation **E**, code for aldehyde building block **F** and complementary region **F`**, and a region complementary to the overhang for T4 ligation **G`**. Beside carboxylic acid code **H** and complementary region **H`**, carboxylic acid-encoding DNA sequences ***IV/IV`*** contained the

overhang for T4 ligation **G**, and reverse primer sequence **I** and the complementary region **I`** (Fig. 3.31, Tables 8, 9).

Table 8. Sequences of DNA oligonucleotides ***I – IV/IV'***

DNA	partial sequences (5'-3')	length	sequence (5'-3')[a]
I	A („hexT“ sequence)	6mer	*5'AM*-TTT TTT
II	B-C-D	30mer	GAA TTC AGG TCG GTG TGA ACG GAT TTG XXX
II'	E'-D'-C'-B'-A'	40mer	ATA CXX XCA AAT CCG TTC ACA CCG ACC TGA ATT CAA AAA A
III	E-F	12mer	GTA TXX XXX XXX
III'	G'-F'	12mer	TAG GXX XXX XXX
I-II-III	A-B-C-D-E-F	48mer	*5'AM*-TTT TTT GAA TTC AGG TCG GTG TGA ACG GAT TTG XXX GTA TXX XXX XXX
II´-III´	G'-F'-E'-D'-C'-B'-A'	52mer	TAG GXX XXX XXX ATA CXX XCA AAT CCG TTC ACA CCG ACC TGA ATT CAA AAA A
IV	G-H-I	35mer	CCT AXX XXX XXX TGA CCT CAA CTA CAT GGT CTA CA
IV'	I´-H´	31mer	TGT AGA CCA TGT AGT TGA GGT CAX XXX XXX X
I-II-III- IV	A-B-C-D-E-F-G-H-I	83mer	*5'AM*-TTT TTT GAA TTC AGG TCG GTG TGA ACG GAT TTG XXX GTA TXX XXX XXX CCT AXX XXX XXX TGA CCT CAA CTA CAT GGT CTA CA
II´-III´-IV´	I´-H´-G'-F'-E'-D'-C'-B'-A'	83mer	TGT AGA CCA TGT AGT TGA GGT CAX XXX XXX XTA GGX XXX XXX XAT ACX XXC AAA TCC GTT CAC ACC GAC CTG AAT TCA AAA AA

[a] *5'-AM* denotes (C6)-amino-linker; X denotes coding region.

Table 9. Functions of the partial sequences of oligonucleotides ***I*** – ***IV/IV'***

partial sequence	function of partial sequence	length	sequence (5'-3')
A	hexT	6mer	*5'AM*-TTT TTT
A´	complementary sequence to A	6mer	AAA AAA
B	EcoRI restriction site	6mer	GAA TTC
B´	complementary sequence to B	6mer	GAA TTC
C	forward primer sequence	21mer	AGG TCG GTG TGA ACG GAT TTG
C´	complementary sequence to C	21mer	CAA ATC CGT TCA CAC CGA CCT
D	scaffold code	3mer	XXX
D´	complementary sequence to D	3mer	XXX
E	overhang for T4 ligation	4mer	GTA T
E´	complementary sequence to E	4mer	ATA C
F	codes for aldehyde synthons[a]	8mer	XXX XXX XX
F´	complementary sequence to F	8mer	XXX XXX XX
G	overhang for T4 ligation	4mer	CCT A
G´	complementary sequence to G	4mer	TAG G
H	codes for carboxylic acid synthons[b]	8mer	XXX XXX XX
H´	complementary sequence to H	8mer	XXX XXX XX
I	reverse primer sequence	23mer	TGA CCT CAA CTA CAT GGT CTA CA
I´	complementary sequence to I	23mer	TGT AGA CCA TGT AGT TGA GGT CA

[a] see Tables 18, 19; [b] see Table 20.

Prior encoding of the library, encoding protocols established in our group were tested for their suitability with four different pyrazolines **hexT-95** (**A**, **T**, **AD**, **AO**) and four different pyrazoles **hexT-96** (**A**, **C**, **Z**, **AC**). In the first experiment selected **hexT-95**, **-96** conjugates ***I*** (Fig. 3.31) were ligated just to heterocycle-encoding DNA ***II***/***II`*** (Fig. 3.32A), and in another experiment they were ligated in parallel to heterocycle- and aldehyde-encoding DNA ***II***/***II`*** and ***III***/***III`*** (Fig. 3.32B). In general, encoding of hexT conjugates consisted of three steps: 5`-phosphorylation, annealing, and ligation. First, the single stranded oligonucleotides ***II***, ***II`*** and ***III*** were phosphorylated at 5`-ends with T4 polynucleotide kinase (PNK) at 37 °C for 30 minutes, and then inactivated at 75 °C for 10 minutes. After that, oligonucleotides **hexT-95**/ **-96**, ***II*** and ***II`***, and **hexT-95**/ **-96**, ***II***, ***II`***, ***III*** and ***III`*** were annealed at 85 °C for 10 minutes and slowly cooled down to 25 °C. Upon addition of T4-DNA ligase to each of the two oligonucleotide combinations, ligation reactions took place at 25 °C overnight, followed

by heat inactivation at 75 °C for 10 minutes. All reactions were performed at 40 pmol scale. The ligation products were analyzed by agarose gel electrophoresis (Fig. 3.32C, D).

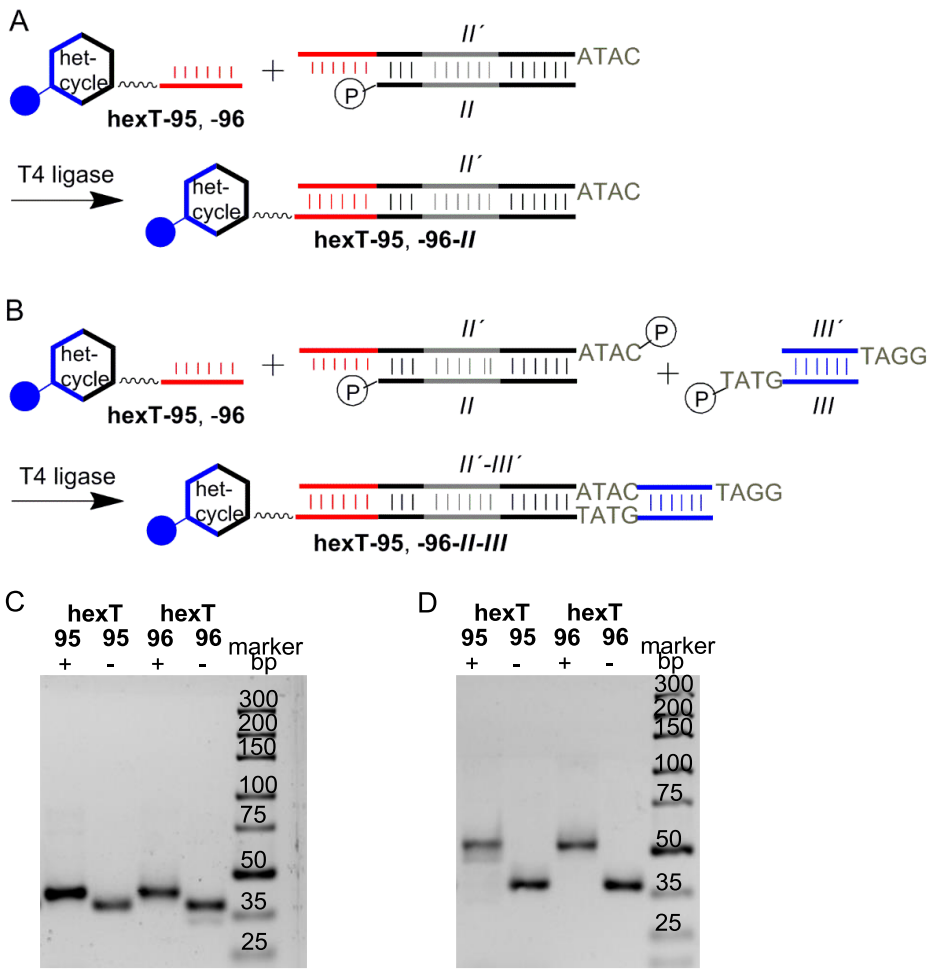

Figure 3.32. Overnight ligation of four hexT-pyrazoline conjugates **hexT-95** (**A**, **T**, **AD**, **AO**), and four hexT-pyrazole conjugates **hexT-96** (**A**, **C**, **Z**, **AC**) to the duplex ***II***/***II´***, and to the duplexes ***II***/***II´*** and ***III***/***III´*** *in one pot* (Table 8); A) ligation scheme for the ligation to the duplex ***II***/***II´***; B) ligation scheme for the ligation to the duplexes ***II***/***II´*** and ***III***/***III´*** *in one pot*; C) for analysis of the ligation reactions each four reactions were pooled and analyzed by gel electrophoresis, gel shows the ligation of each four conjugates **hexT-95**, **-96** to the duplex ***II***/***II´***, D) for analysis of the ligation reactions each four reactions were pooled and analyzed by gel electrophoresis, gel shows the ligation of each four conjugates **hexT-95**, **-96** to the duplexes ***II***/***II´*** and ***III***/***III´*** *in one pot*; - denotes w/o ligase; + denotes ligation reaction for 16 h at 25 °C. hetcycle: pyrazoline or pyrazole scaffold.

All hexT conjugates were ligated to heterocycle-encoding DNA sequences (Fig. 3.32C), and in parallel to heterocycle-, and aldehyde-encoding DNA sequences with excellent yields (Fig. 3.32D).

3.5.4. Synthesis of the oligothymidine-initiated DNA-Encoded Library (tiDEL)

For the tiDEL synthesis, the in total 71 hexT-conjugates **hexT-95**, and **hexT-96** (Tables 18, 19) were successfully ligated in parallel to heterocycle-, and aldehyde-encoding DNA sequences (Figs. 3.31, 3.33).

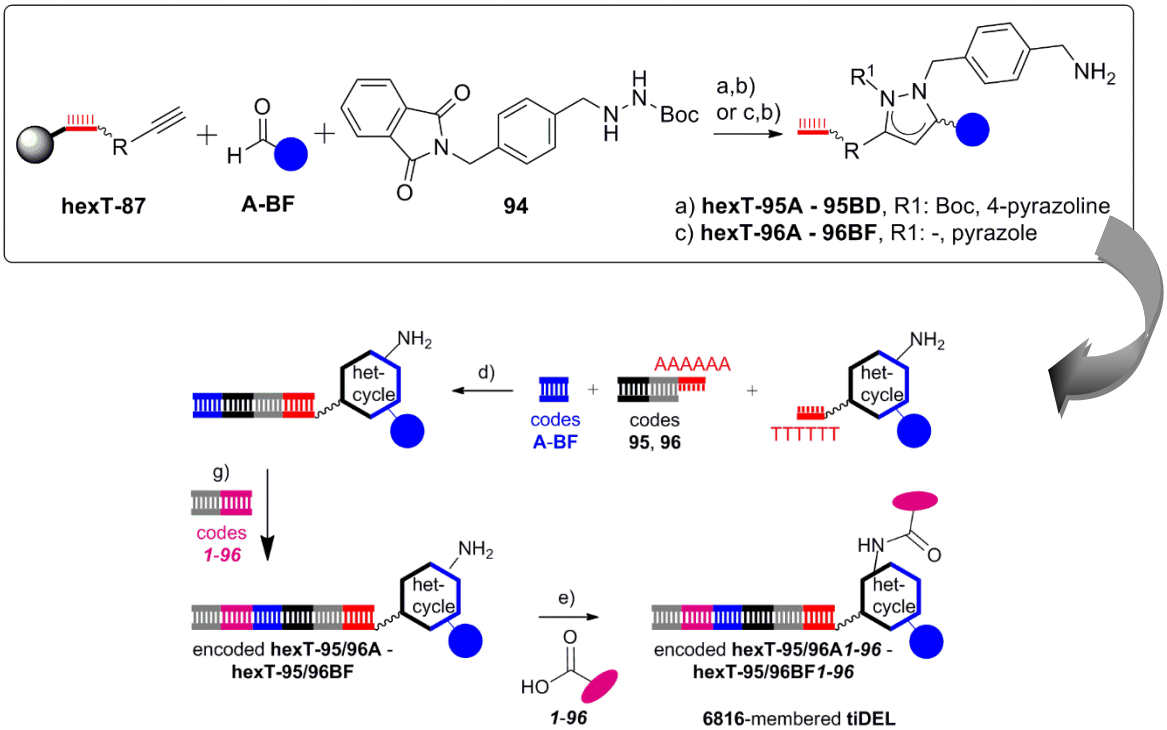

Figure 3.33. Synthesis of pyrazol(in)e tiDEL; reagents and conditions: a) ***A***/$AgSbF_6$, MeCN, 50 °C, overnight; b) aq. NH_3/$MeNH_2$, room temperature, 30 min; c) ***B***/AgOTf, AcOH, 60 °C, overnight; d) T4-DNA ligase, room temperature, overnight; e) EDC, HOAt, DEAE sepharose, room temperature, overnight. R= aminocarbonylphenyl. Filled grey circle denotes solid support (controlled pore glass, CPG); wavy bond to hexT: 5'-(C6)-amino-PEG(4) linker; bold bond: connection from the hexT-oligonucleotide to the CPG. hetcycle: pyrazoline or pyrazole scaffold.

To control the success of the ligation reactions an aliquot of 0.5 µL was taken from each reaction, pooled, and analyzed by agarose gel electrophoresis (Fig. 3.34A). The remaining ligation products were pooled by precipitation. The DNA pellet was dissolved, split in a 96well plate, and successfully ligated to sequences containing the reverse primer, and code for 96 carboxylic acids (Figs. 3.31, 3.33). All encoded library constituents were transferred to DEAE sepharose in a 96well plate, and reacted with the validated 96 carboxylic acids (Table 20) in parallel overnight. Washing steps removed the excess of reagents, and elution of the

DNA conjugates with a high-salt buffer, followed by pooling, and desalting provided a combined tiDEL with **6816 compounds** based on pyrazoline and pyrazole scaffold. The library was analyzed by gel electrophoresis (Fig. 3.34B).

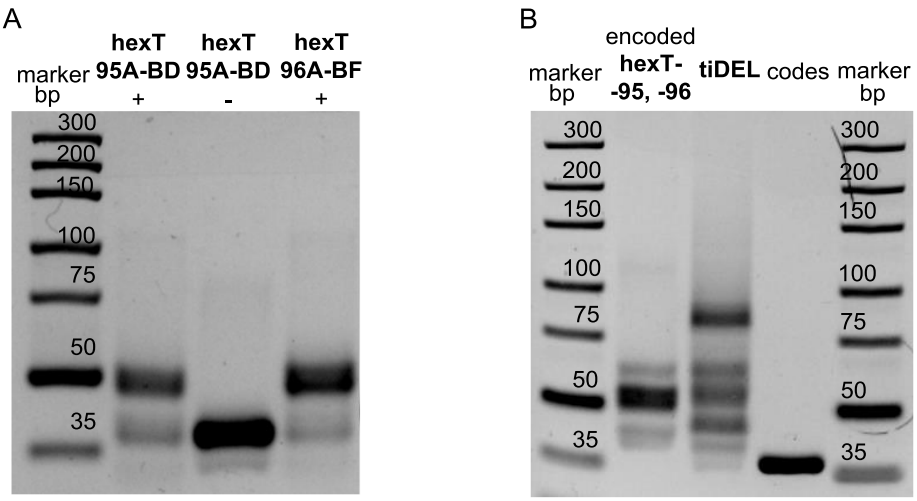

Figure 3.34. Analysis of the tiDEL, for the encoding scheme see Figure 3.31. A) Gel electrophoresis of the ligation of hexT conjugates to DNA duplexes ***II***/***II´*** and ***III***/***III´*** *in one pot* yielding the duplex ***I-II-III/II´-III´***; lane 1: ligation of duplexes ***II***/***II´*** and ***III***/***III´*** to pyrazolines **hexT-95** (Table 18) yielding the duplex **hexT-95-*II-III/II´-III´***; lane 2: negative control for two compounds w/o T4 ligase; lane 3: ligation of duplexes ***II***/***II´*** and ***III***/***III´*** to pyrazoles **hexT-96** (Table 19) yielding the duplex **hexT-96-*II-III/II´-III´***; B) ligation of DNA duplex sequences ***I-II-III/II´-III´*** to the DNA duplex ***IV***/***IV´*** to encode carboxylic acid building blocks; lane 1: gel electrophoresis of the pool of all encoded hexT conjugates (DNA duplex sequences ***I-II-III/II´-III´***); lane 2: gel electrophoresis of the ligation of DNA duplex sequences ***I-II-III/II´-III´*** to the DNA duplexes ***IV***/***IV´*** to encode carboxylic acid building blocks ***1-96*** (Table 20); lane 3: gel electrophoresis of a duplex sequence ***IV***/***IV´***.

3.5.5. Quality control of the pyrazol(in)e library: PCR amplification and streptavidin pull-down experiment

The pyrazol(in)e based tiDEL was PCR-amplified at two concentrations with barcoded primers (forward primer: 5'- TAC ACG ACG CTC TTC CGA TCT CGATGT AGG TCG GTG TGA ACG GAT TTG; reverse primer: 5'- CAG ACG TGT GCT CTT CCG ATC CGA TGT TGT AGA CCA TGT AGT TGA GGT CA)[226] (Fig. 3.35A).

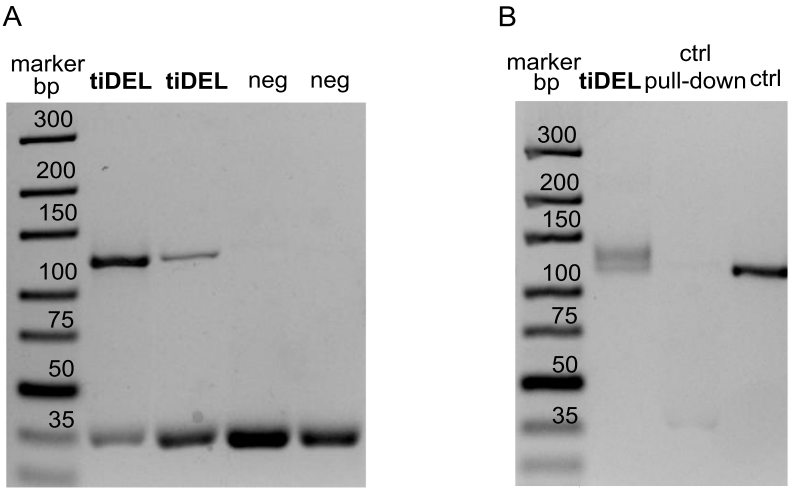

Figure 3.35. PCR amplification and streptavidin pull-down of the tiDEL. A) PCR amplification of the pooled tiDEL; lane 1: amplification of 10 pM of the tiDEL; lane 2: amplification of 100 fM of the tiDEL; lane 3: negative control, amplification of the primers without template; lane 4: negative control, gel electrophoresis of primers; B) streptavidin pull-down of the tiDEL; lane 1: gel electrophoresis of the streptavidin pull-down of the tiDEL; lane 2: gel electrophoresis of the streptavidin pull-down of 10 fmol of a 69mer duplex DNA corresponding to duplex ***I-II-III-IV/II´-III´-IV´*** (Table 8) serving as negative control. Only a faint trace of this DNA is visible on the gel after the streptavidin pull-down; lane 3: PCR amplification of the negative control 69mer DNA (10 fmol total amount).

As ca. one percent of the library members contained the streptavidin binder desthiobiotin (carboxylic acid building block ***93***, Table 20), the tiDEL was subjected to a streptavidin pull-down experiment *versus* a control DNA (Fig. 3.35B). Streptavidin pull-down was performed with 0.1 pmol of the tiDEL, corresponding to ca. 1 fmol of streptavidin-binding desthiobiotin-conjugates according to a previously published procedure.[189] PCR amplification indicated that a substantial part of the tiDEL was retained on the affinity matrix whereas only traces of the control DNA were detectable, suggesting the functionality of the tiDEL.

3.6. Increasing structural complexity of hexathymidine-heterocycle conjugates

Reports on synthesis of (hetero)cyclic structures based on Diels-Alder cycloaddition,[76] condensation reactions[56] as well as report on synthesis of spirocycles[77] are hinting at an interest in expansion of DEL chemical space. One strategy for expansion of chemical space relies on expansion of synthesis methodology for DEL synthesis. The oligothymidine-initiated DNA-encoded chemistry (TiDEC) approach already proved the compatibility with Au(I) catalysis. With the TiDEC methodology in our hands, the idea was to go for more complex chemical structures in a DNA-encodable format.

A higher level of structural complexity is already possible to reach by simple exchange of a single component in a three component Au(I)-mediated synthesis of pyrazolines **79**. By replacement of alkyne **75** with alkynol component **107** one can move from 5-membered pyrazoline ring **79** to a more complex 6-oxa-1,2-diazaspiro[4.4]nonane **108** which can be classified as [*N*,*O*]-spiroacetal (Fig. 3.36).

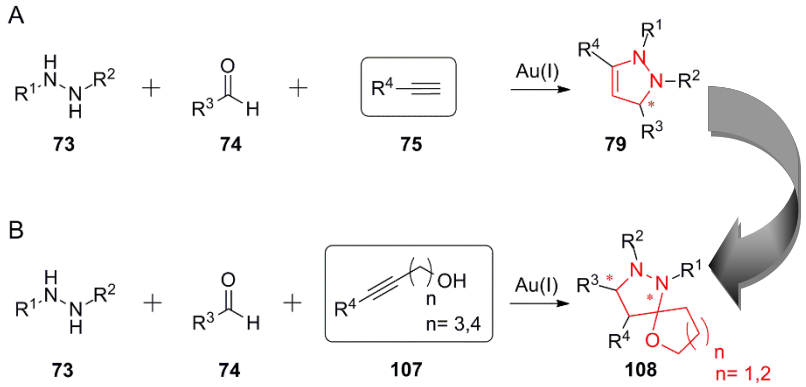

Figure 3.36. Au(I)-mediated synthesis of pyrazoline **79** and 6-oxa-1,2-diazaspiro[4.4]nonane **108**. A) Au(I)-mediated annulation of hydrazide **73**, aldehyde **74**, and alkyne **75** to pyrazoline **79**; B) exchange of alkyne **75** with alkynol **107** opens access to structurally more complex 6-oxa-1,2-diazaspiro[4.4]nonane **108**.

Recently published by Wagner *et al.*, the [*N*,*O*]-spiroacetals **108** represent a new compound class.[218]

3.6.1. [N,O]-spiroacetals and their accessibility

[*N*,*O*]-spiroacetals can be found in natural products. Important examples are the marine toxine azaspiracid-1 **109** isolated from the blue mussels (*Mytilus edulis*),[227] and tomatidine **110** found in the stems and leaves of tomato plants, and in the fruit of green tomatoes (Fig. 3.37).

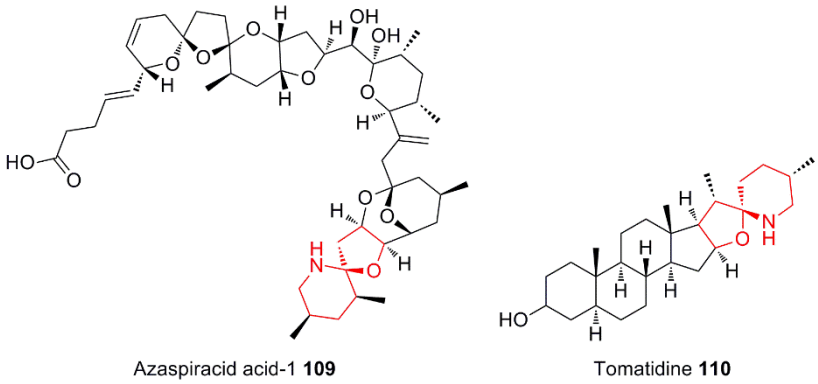

Figure 3.37. Natural products containing [*N*,*O*]-spiroacetals.

The 6-oxa-1,2-diazaspiro[4.4]nonane **108** is synthesized by a Au(I)-mediated three-component reaction of hydrazide **73**, aldehyde **74** (or ketone), and alkynol **107a** (Fig. 3.38). The proposed reaction mechanism is described in Figure 3.38. This reaction likely consists of three steps: 5-*exo-dig* intermolecular cyclization of alkynol **107a** to enol ether **111**, condensation of hydrazide **73** and aldehyde **74** to azomethine imine **76**, and [3+2]-cycloaddition of enol ether intermediate **111** and azomethine imine **76**. Coordination of the Au(I) catalyst to the triple bond of the substrate **107a** leads to the π-complex **112**. As a result, the alkyne bond is more electron-deficient, and therefore more prone towards nucleophilic attack of the alkynol oxygen (hydroalkoxylation). Upon nucleophilic attack, the π-complex **112** is transformed into the protonated vinyl gold intermediate **113** that undergoes proton liberation. Finally, protodeauration gives rise to the enol ether **111** (Fig. 3.38A).

Condensation of hydrazide **73** and aldehyde **74** yields the azomethine imine **76** (Fig. 3.12) with 1,3-dipolar character. As enol ether **111** acts as dipolarophile they react through a 1,3-dipolar cycloaddition, which may proceed in a concerted manner (path a) or stepwise (path b) (Fig. 3.38B), both leading to 6-oxa-1,2-diazaspiro[4.4]nonane **108**.[218]

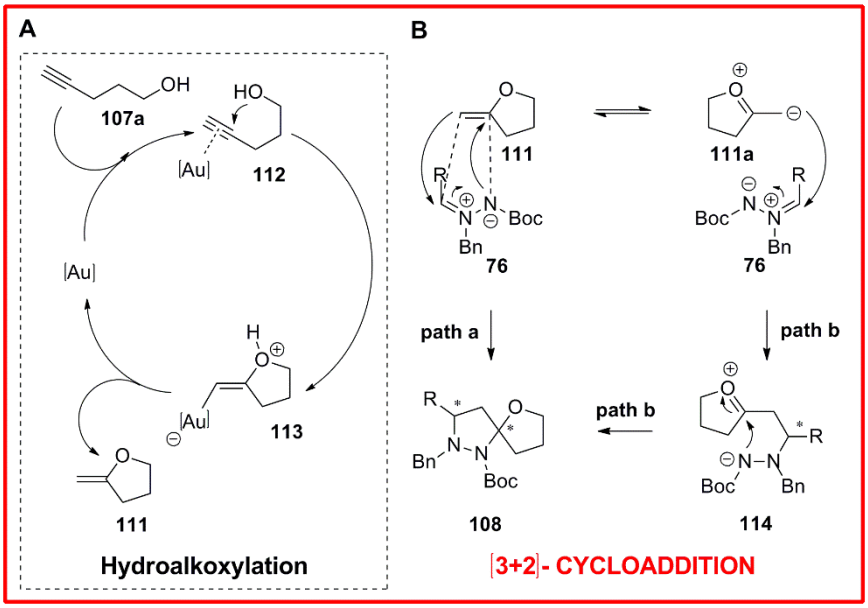

Figure 3.38. Proposed mechanism for the Au(I)-mediated reaction consisting of enol ether **111** formation, and synthesis of the 6-oxa-1,2-diazaspiro[4.4]nonane **108** by [3+2]-cycloaddition. A) Reaction mechanism for cycloisomerization of alkynol **107a** to the corresponding enol ether **111**; B) [3+2]-cycloaddition of enol ether **111** and azomethine imine **76** can proceed in a concerted manner (path a) or stepwise via liner intermediate **114** (path b). Both pathways lead to the 6-oxa-1,2-diazaspiro[4.4]nonane **108**.

3.6.2. Synthesis of the hexathymidine-6-oxa-1,2-diazaspiro[4.4]nonane conjugates

Inspired by the new spirocycle[218] we went into exploration of possibilities for translating this chemistry to the TiDEC strategy (Fig. 3.39). We were interested to explore the impact of connectivity between hexT and small molecule on the synthesis of 6-oxa-1,2-diazaspiro[4.4]nonane by Au(I)-mediated [3+2]-cycloaddition. As above described the Au(I)-mediated reaction is a three-component reaction, thus, accessibility of 6-oxa-1,2-diazaspiro[4.4]nonane as hexT conjugate was investigated starting from three different hexT conjugates (Figs. 3.39, 3.40B). Therefore, aldehyde **hexT-115**, hydrazide **hexT-119**, and alkynol **hexT-127** were synthesized (Chapter 5.5.1), and used as starting materials for the synthesis of spirocycles **hexT-116**, **hexT-120**, and **hexT-128**, respectively (Fig. 3.39).

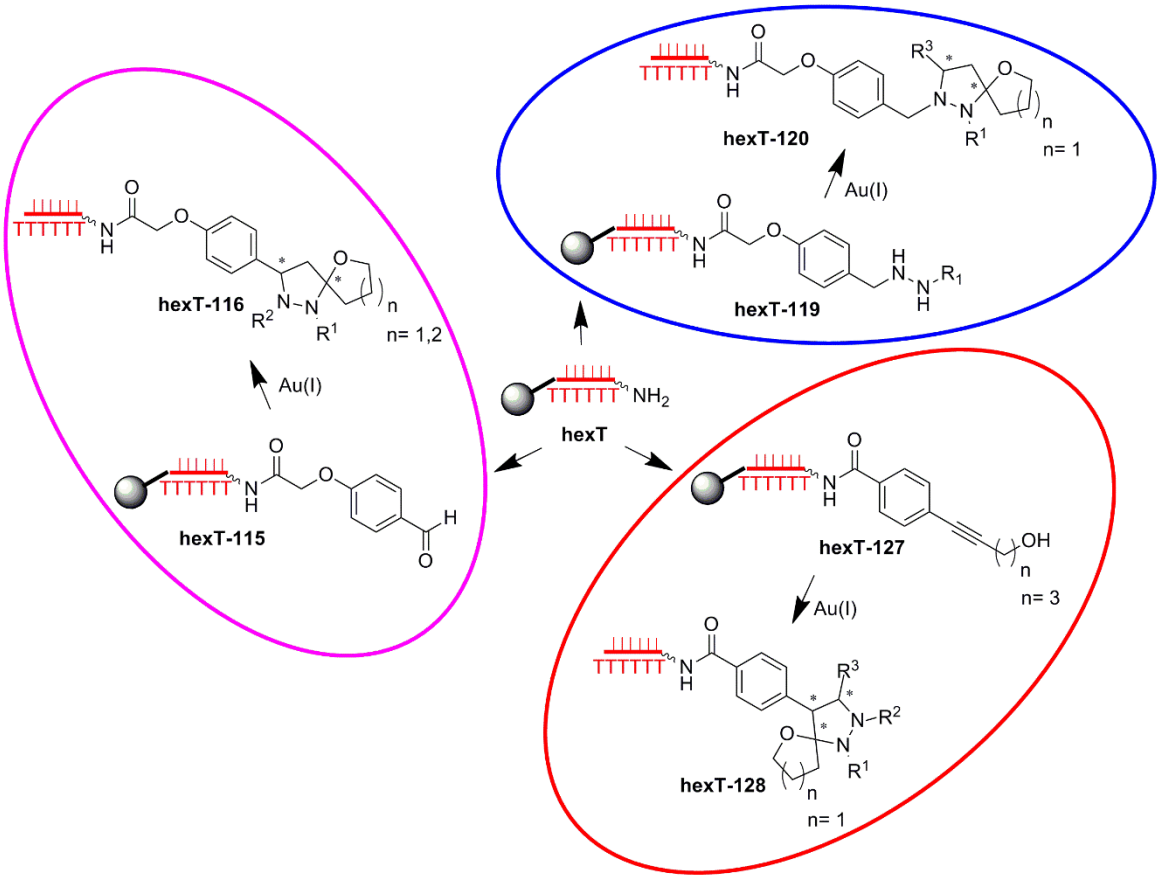

Figure 3.39. Synthesis of hexT-6-oxa-1,2-diazaspiro[4.4]nonanes **hexT-116**, **-120**, and **-128** starting from three different hexT conjugates: aldehyde **hexT-115**, hydrazide **hexT-119**, and alkynol **hexT-127**. Filled grey circle denotes solid support (controlled pore glass, CPG); wavy bond to hexT: 5'-(C6)-amino-linker; bold bond: connection from the hexT-oligonucleotide to the CPG.

Au(I)-mediated synthesis of hexT-pyrazol(in)es (Fig. 3.40A) represented a breakthrough in application of Au(I) catalysis for synthesis of various scaffolds in a DNA-encodable manner. My aim was to use the same catalytic system, replace an alkyne with an alkynol component, and explore the accessibility of a more complex, three-dimensional spirocycle as hexT conjugate (Figs. 3.39, 3.40B).

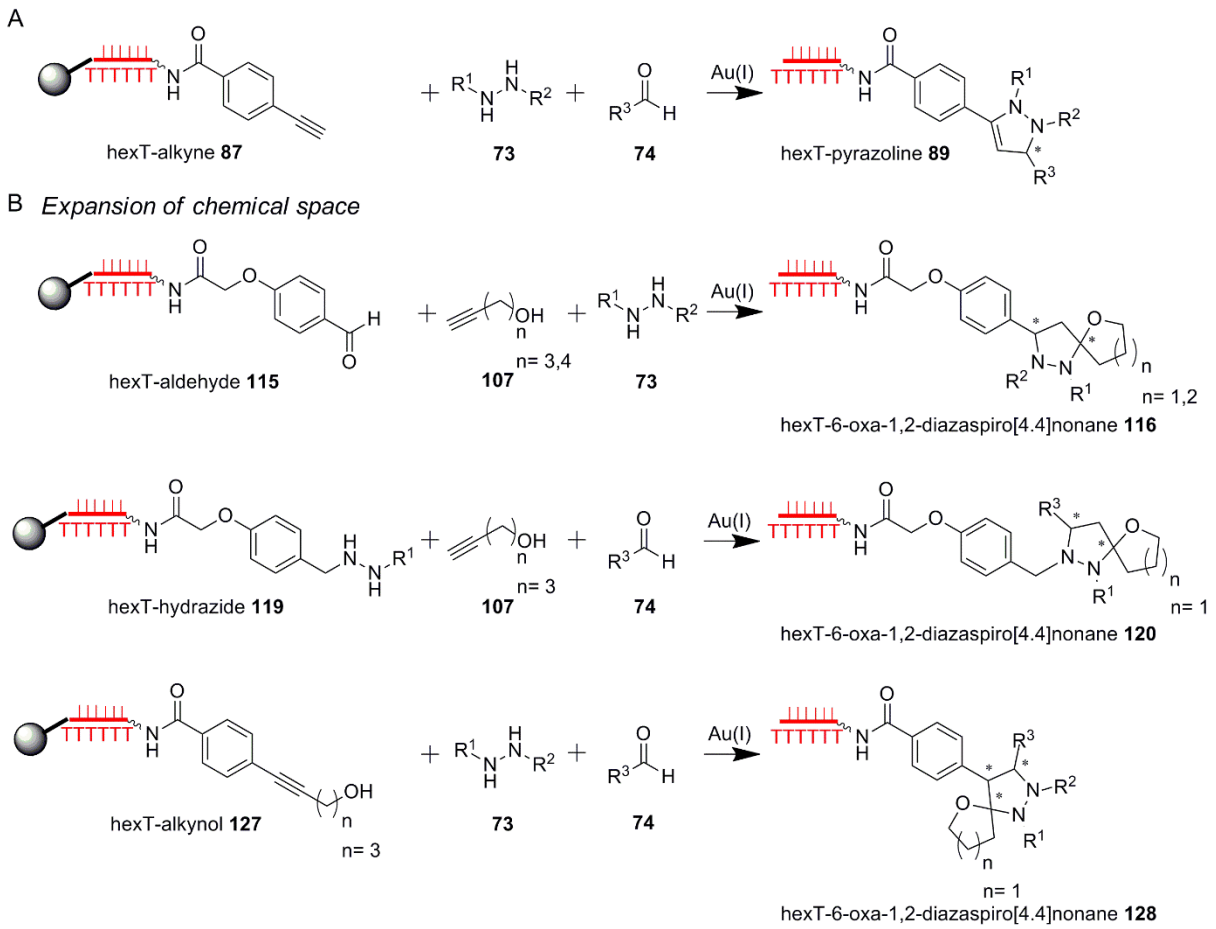

Figure 3.40. Au(I)-mediated synthesis of hexT-pyrazolines and hexT-6-oxa-1,2-diazaspiro[4.4]nonanes. A) Au(I)-mediated annulation of hexT-alkyne **87**, hydrazide **73**, and aldehyde **74** yielding hexT-pyrazoline **89**; B) Au(I)-mediated synthesis of 6-oxa-1,2-diazaspiro[4.4]nonanes using three different hexT conjugates: aldehyde **hexT-115**, hydrazide **hexT-119**, and alkynol **hexT-127**, leading to hexT-6-oxa-1,2-diazaspiro[4.4]nonanes **hexT-116**, **hexT-120**, and **hexT-128**, respectively. Filled grey circle denotes solid support (controlled pore glass, CPG); wavy bond to hexT: 5'-(C6)-amino-linker; bold bond: connection from the hexT-oligonucleotide to the CPG.

3.6.2.1. The impact of the aldehyde component as connectivity between hexathymidine DNA and small molecule on the reaction outcome

The CPG-bound aldehyde **hexT-115**, *tert*-butyl 2-benzylhydrazinecarboxylate **88**, and pent-4-yn-1-ol **107a** served to investigate the accessibility of the hexT-6-oxa-1,2-diazaspiro[4.4]nonane conjugate **hexT-116a** by Au(I)-mediated [3+2]-cycloaddition reaction (Fig. 3.41). Systematic exploration of reaction parameters yielded three distinct, isolatable products in different rations: the 6-oxa-1,2-diazaspiro[4.4]nonane **hexT-116a**, the suggested Mannich-type product **hexT-117**, and plausible azomethine imine intermediate **hexT-118** as the product of condensation of aldehyde **hexT-115** and hydrazide **88** (Fig. 3.41, Table 10).

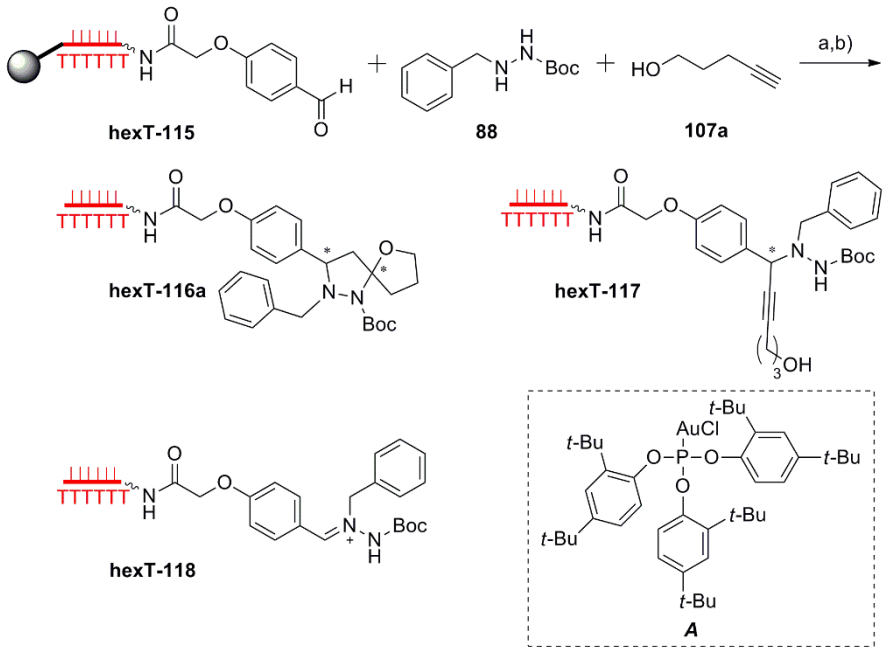

Figure 3.41. Au(I)-mediated synthesis of hexT-6-oxa-1,2-diazaspiro[4.4]nonane conjugate **hexT-116a** from hexT-aldehyde conjugate **hexT-115**. a) For conditions see Table 10; b) AMA (aqueous ammonia (30 %)/ aqueous methylamine (40 %), 1:1, vol/vol), 30 min, room temperature. Figures 3.42-3.47 show HPLC traces of the crude reaction mixtures. Filled grey circle denotes solid support (controlled pore glass, CPG); wavy bond to hexT: 5'-(C6)-amino-linker; bold bond: connection from the hexT-oligonucleotide to the CPG.

Table 10. Optimization of reaction conditions for the Au(I)-mediated MCR to furnish hexT-6-oxa-1,2-diazaspiro[4.4]nonane conjugate **hexT-116a**.

	No.	hydrazide [eq.][a]	alkynol [eq.][a]	catalyst [eq.][a]	time/h	solvent	T/[°C]	catalyst	**hexT-116a** [%][b]	**hexT-118** [%][b]
a) equivalents of reagents and catalyst[c]	**1**	100	200	10	20	THF	25	***A***/$AgSbF_6$	-	-
	2	500	1000	10	20	THF	25	***A***/$AgSbF_6$	-	-
	3	500	1000	50	20	THF	25	***A***/$AgSbF_6$	40	-
	4	500	1000	100	20	THF	25	***A***/$AgSbF_6$	50	-
	5	500	1000	250	20	THF	25	***A***/$AgSbF_6$	90	-
	6	-	-	250	20	THF	25	***A***/$AgSbF_6$	-	-
	7	500	1000	-	20	THF	25	-	-	-
b) solvent	**1**	500	1000	250	14	MeOH	25	***A***/$AgSbF_6$	0	90
	2	500	1000	250	14	DMF	25	***A***/$AgSbF_6$	0	75
	3	500	1000	250	14	MeCN	25	***A***/$AgSbF_6$	45	45
	4	500	1000	250	14	THF	25	***A***/$AgSbF_6$	55	35
	5	500	1000	250	14	$C_2H_4Cl_2$	25	***A***/$AgSbF_6$	10	55
	6	500	1000	250	14	toluene	25	***A***/$AgSbF_6$	15	50
	7	500	1000	250	14	CH_2Cl_2	25	***A***/$AgSbF_6$	10	70
c) time	**1**	500	1000	250	14	THF	25	***A***/$AgSbF_6$	55	35
	2	500	1000	250	18	THF	25	***A***/$AgSbF_6$	75	20
	3	500	1000	250	20	THF	25	***A***/$AgSbF_6$	90	<5

[a] *versus* the solid support-bound hexathymidine-aldehyde conjugate **hexT-115**; [b] % conversion estimated based on the area under curve of the product peak *versus* the starting material peak in the HPLC-trace of the crude; [c] note that the conjugates contain PEG(4) linker.

3.6.2.1.1. Exploration of catalyst concentration

Different equivalents of the hydrazide **88**, the alkynol **107a**, and the catalyst ***A***/$AgSbF_6$ (Fig. 3.42, Table 10a) were investigated in a first series of reactions run in THF at room temperature for 20 hours. Performing the reaction with 500fold excess of **88**, 1000fold excess of **107a**, and 100fold excess of the catalyst ***A***/$AgSbF_6$ *versus* **hexT-115** gave 50 % conversion of the aldehyde **hexT-115** into the target 6-oxa-1,2-diazaspiro[4.4]nonane **hexT-116a** (Table 10a, entry 4).

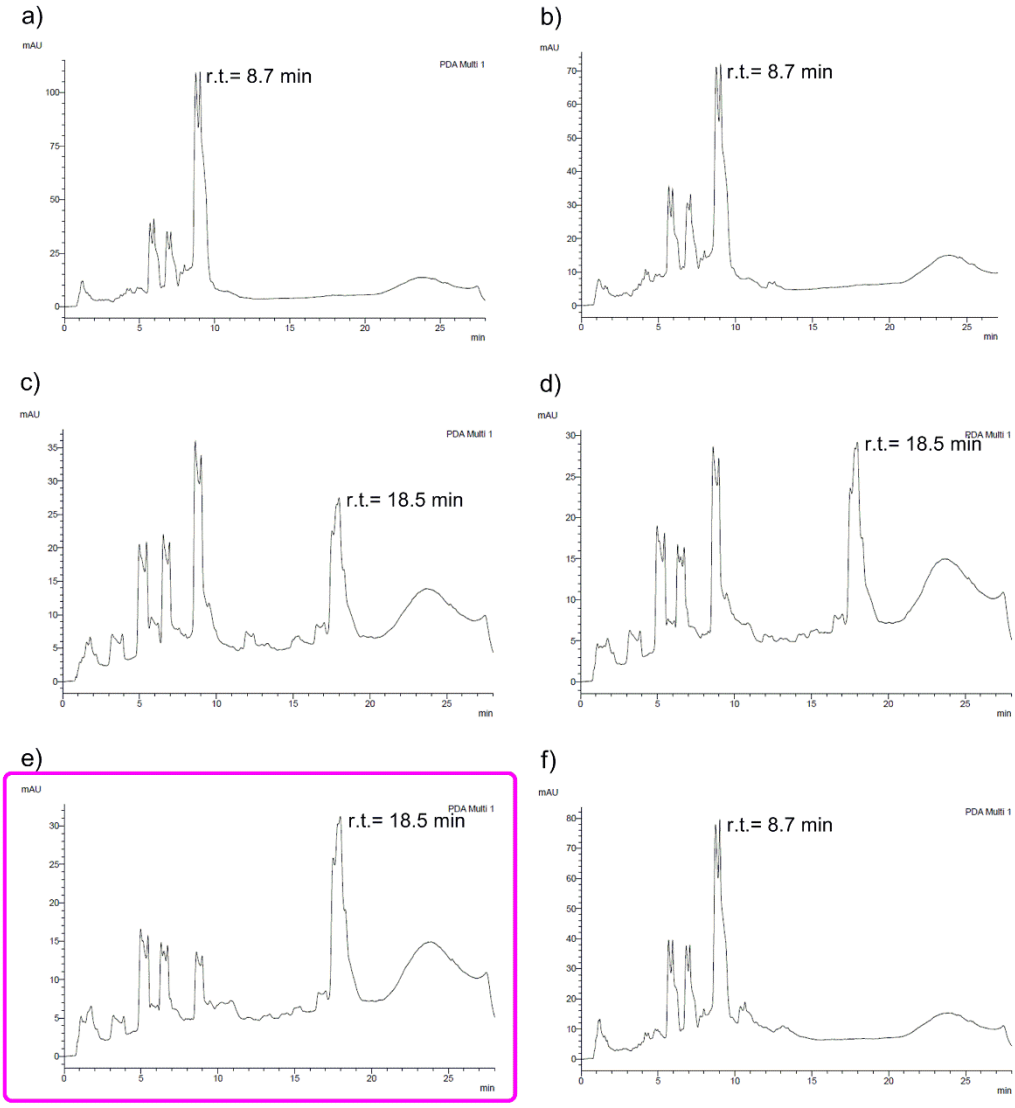

Figure 3.42. Exploration of different equivalents of reactants, and catalyst for the Au(I)-mediated MCR of the hexathymidine-aldehyde conjugate **hexT-115**, hydrazide **88**, and alkynol **107a**, for reaction conditions see Table 10a. a) HPLC trace of the starting material (aldehyde conjugate **hexT-115**); b) HPLC trace of experiment **No. 1**; formation of the target spirocycle **hexT-116a** was not observed (same result: experiment **No. 2**); c) HPLC trace of experiment **No. 3**; 40 % conversion of the starting material to the target spirocycle **hexT-116a**; d) HPLC trace

of experiment **No. 4**; 50 % conversion of the starting material to the target spirocycle **hexT-116a**; e) HPLC trace of experiment **No. 5**; 90 % conversion of the starting material to the target spirocycle **hexT-116a**; f) HPLC trace of experiment **No. 6** and **No. 7**; formation of the target spirocycle **hexT-116a** was not observed.

Reducing the excess of the catalyst to 50fold lowered the conversion of the **hexT-115** into the spirocycle **hexT-116a** to 40 % (Table 10a, entry 3), while 10fold excess of the catalyst gave no product at all (Table 10a, entries 1, 2). The highest, 90 % conversion of the **hexT-115** into the spirocycle **hexT-116a** was achieved when 250fold excess of the catalyst ***A***/$AgSbF_6$ was used (Fig. 3.42.e, Table 10a, entry 5). The same as with hexT-pyrazoline synthesis, high loading of the ***A***/$AgSbF_6$ was crucial for the reaction success.

3.6.2.1.2. Exploration of solvents

A solvent screen during reaction time of 14 hours (Fig. 3.43) revealed THF as the best solvent for the synthesis of the 6-oxa-1,2-diazaspiro[4.4]nonane **hexT-116a** with moderate conversion of 55 % (Fig. 3.43e, Table 10b, entry 4), while acetonitrile gave similar result affording **hexT-116a** in 45 % conversion (Fig. 3.43d, Table 10b, entry 3).

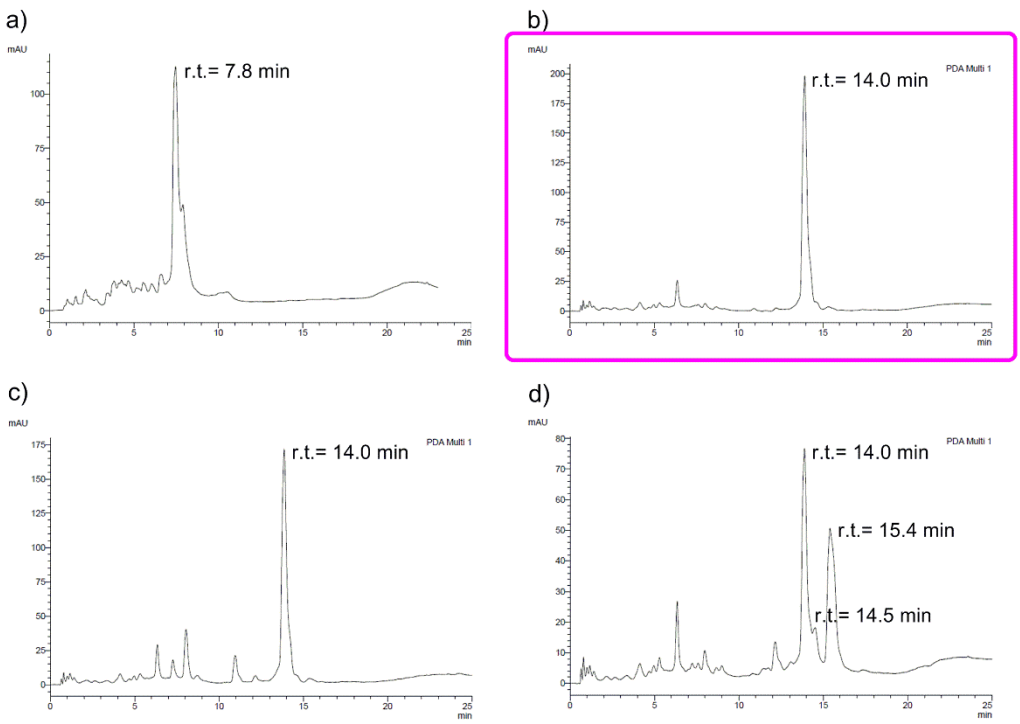

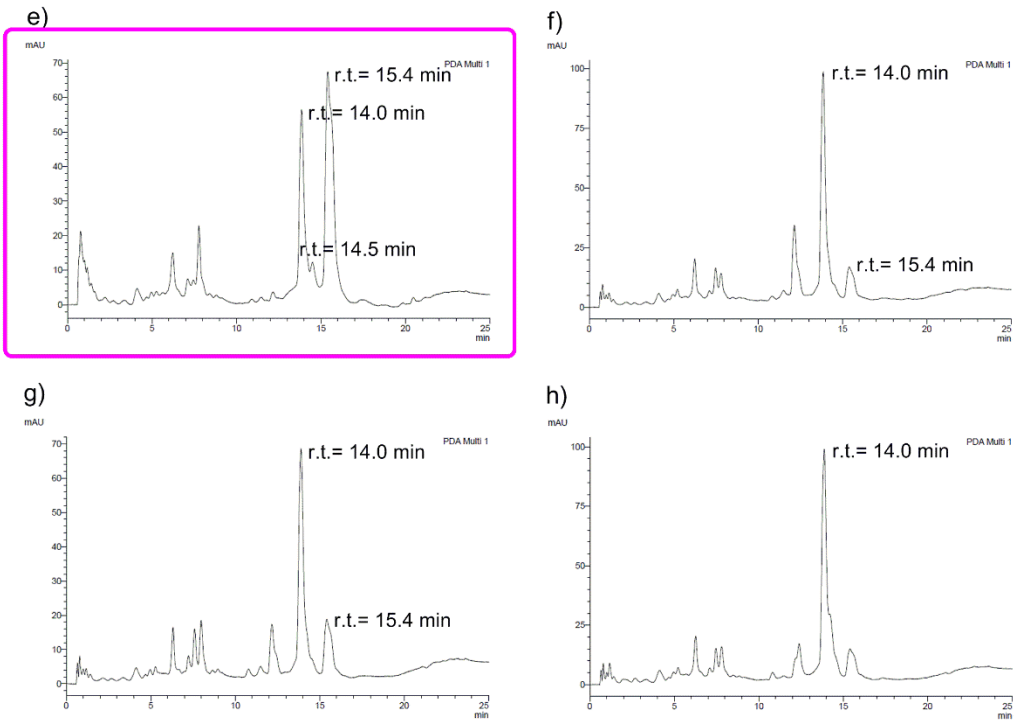

Figure 3.43. Exploration of different solvents for the Au(I)-mediated MCR of the hexathymidine-aldehyde conjugate **hexT-115**, hydrazide **88**, and alkynol **107a**, for reaction conditions see Table 10b. a) HPLC trace of the starting material (aldehyde conjugate **hexT-115**); b) HPLC trace of experiment **No. 1**; formation of condensation product **hexT-118** (r.t.= 14.0 min); c) HPLC trace of experiment **No. 2**; formation of condensation product **hexT-118**; d) HPLC trace of experiment **No. 3**; formation of mixture of condensation product **hexT-118** and spirocycle **hexT-116a** (r.t.= 15.4 min); e) HPLC trace of experiment **No. 4**; formation of mixture of condensation product **hexT-118** and spirocycle **hexT-116a**; f) HPLC trace of experiment **No. 5**; formation of condensation product **hexT-118**, target spirocycle **hexT-116a** formed as minor product; g) HPLC trace of experiment **No. 6**; formation of condensation product **hexT-118**, target spirocycle **hexT-116a** formed as minor product; h) HPLC trace of experiment **No. 7**; formation of condensation product **hexT-118**, target spirocycle **hexT-116a** formed as minor product.

In 1,2-dichloroetane, dichloromethane, and toluene Au(I)-mediated MCR afforded the 6-oxa-1,2-diazaspiro[4.4]nonane **hexT-116a** in low conversion (Table 10b, entries 5-7). In methanol and DMF the spirocycle formation was not observed at all (Table 10b, entries 1, 2), instead the plausible azomethine imine intermediate **hexT-118** was identified as a major product (Fig. 3.44). Its appearance was observed in all solvents (Fig. 3.43). The suggested Mannich-type product **hexT-117** was detected as a minor product in THF and acetonitrile (Fig. 3.43d, e).

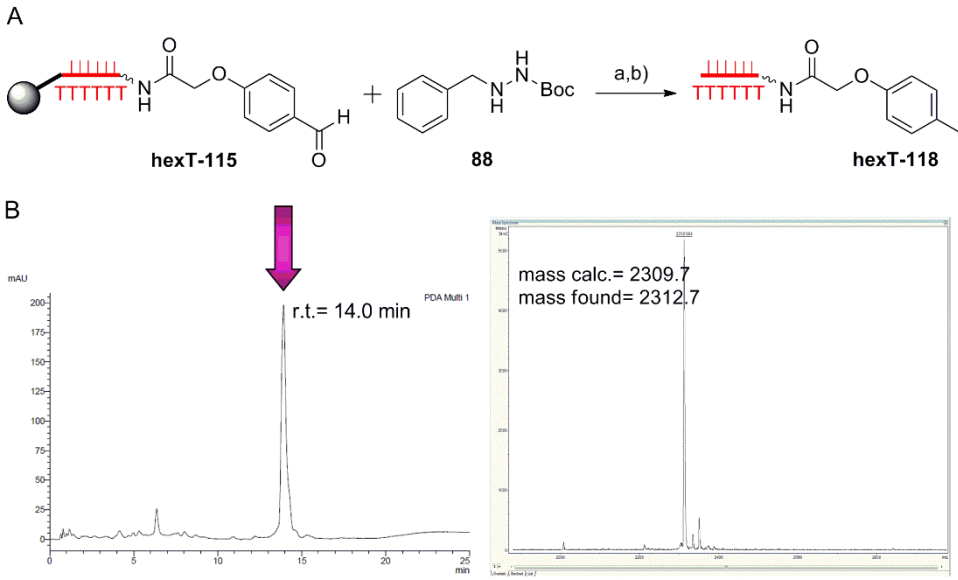

Figure 3.44. MALDI-TOF/TOF-MS of the isolated plausible azomethine imine intermediate **hexT-118** (r.t.= 14.0 min) from Figure 3.43b. A) Reaction scheme of the plausible azomethine imine **hexT-118** formation; a) reaction condition **No. 1** (Table 10b); b) AMA (aqueous ammonia (30 %)/ aqueous methylamine (40 %), 1:1, vol/vol), 30 min, room temperature; B) MALDI-TOF/TOF-MS of the isolated plausible azomethine imine intermediate **hexT-118**. Filled grey circle denotes solid support (controlled pore glass, CPG); wavy bond to hexT: 5'-(C6)-amino-linker; bold bond: connection from the hexT-oligonucleotide to the CPG.

3.6.2.1.3. Exploration of reaction time

As expected, prolongation of reaction time led to the consumption of the azomethine imine **hexT-118** in favour of the spirocycle **hexT-116a** (Fig. 3.45). As a result, 20 hours reaction time in THF at room temperature (Table 10c, entry 3) led to 90 % conversion of the starting aldehyde conjugate **hexT-115** to the target spirocycle **hexT-116a** (Figs. 3.45d, 3.46).

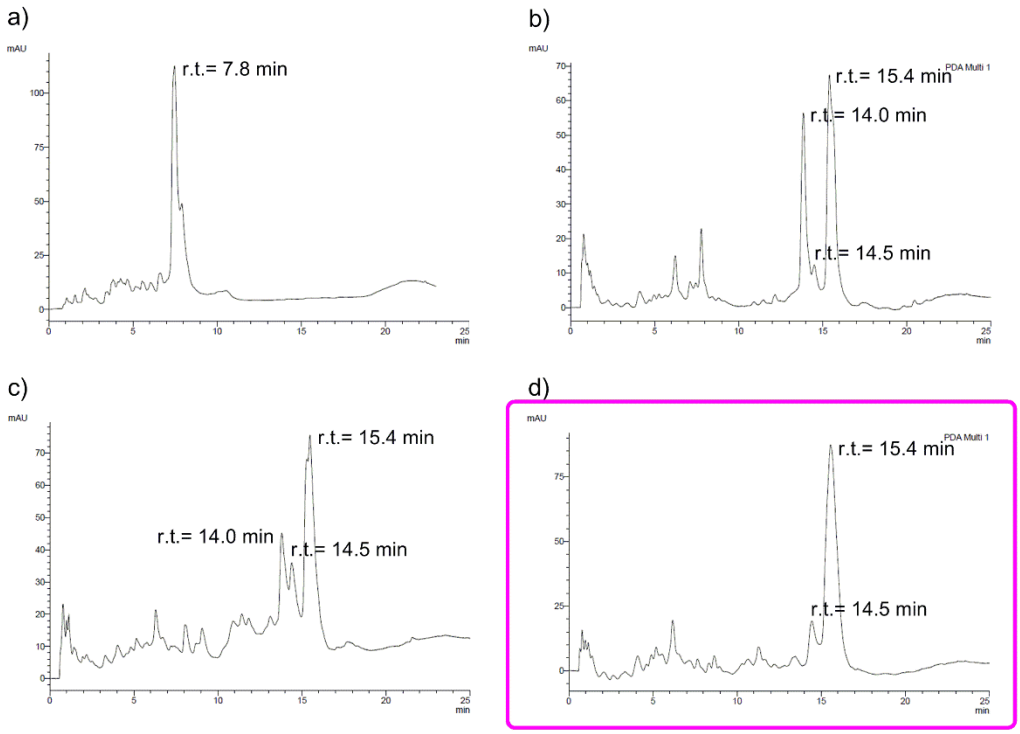

Figure 3.45. Exploration of different reaction times for the Au(I)-mediated MCR of the hexathymidine-aldehyde conjugate **hexT-115**, hydrazide **88**, and alkynol **107a**, for reaction conditions see Table 10c. a) HPLC trace of the starting material (aldehyde conjugate **hexT-115**); b) HPLC trace of experiment **No. 1**; formation of a mixture of products **hexT-116a** and **hexT-118**; c) HPLC trace of experiment **No. 2**; formation of a mixture of products **hexT-116a-118**; d) HPLC trace of experiment **No. 3**; target spirocycle **hexT-116a** formed as major product.

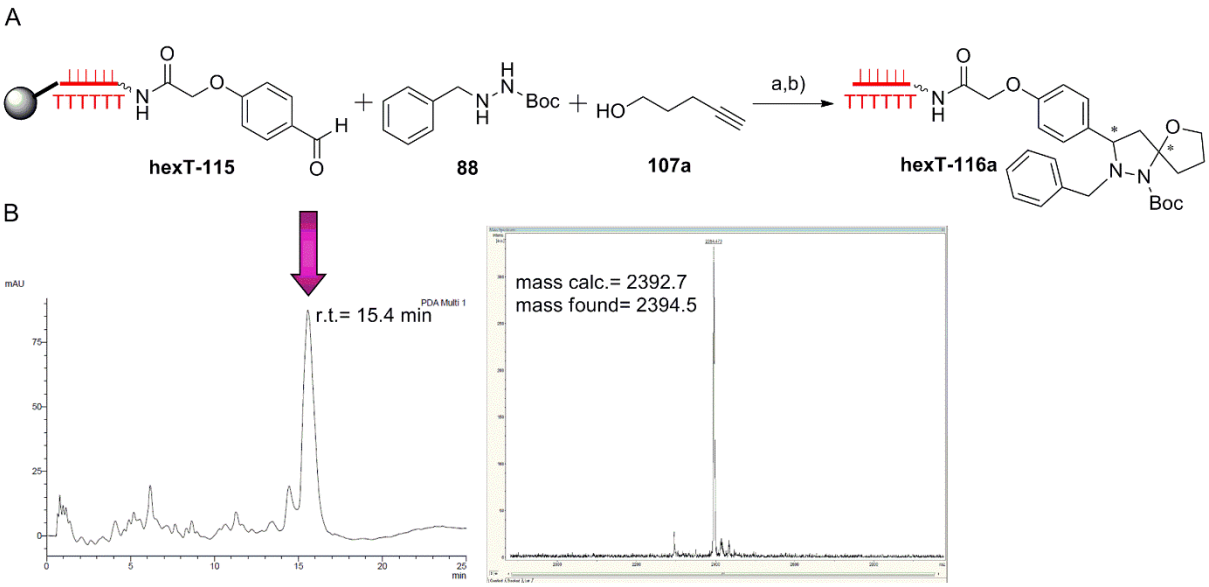

Figure 3.46. MALDI-TOF/TOF-MS of the isolated 6-oxa-1,2-diazaspiro[4.4]nonane **hexT-116a** (r.t.= 15.4 min) from Figure 3.45d. A) Reaction scheme of the 6-oxa-1,2-diazaspiro[4.4]nonane **hexT-116a** formation; a) reaction condition **No. 3** (Table 10c); b) AMA (aqueous ammonia (30 %)/ aqueous methylamine (40 %), 1:1, vol/vol), 30 min, room temperature; B) MALDI-TOF/TOF-MS of the isolated spirocycle conjugate **hexT-116a**.

Filled grey circle denotes solid support (controlled pore glass, CPG); wavy bond to hexT: 5'-(C6)-amino-linker; bold bond: connection from the hexT-oligonucleotide to the CPG.

Optimized reaction conditions (Table 10c, entry 3) afforded target spirocycle **hexT-116a** (Fig. 3.46) as a major product, and earlier eluting minor side product **hexT-117** that has the same mass as the spirocycle **hexT-116a** according to the MALDI-TOF/TOF-MS analysis. As already observed in Au(I)-mediated annulation to hexT-pyrazolines,[210] we hypothesized that the conjugate **hexT-117** might correspond to the Mannich-type product (Fig. 3.47).

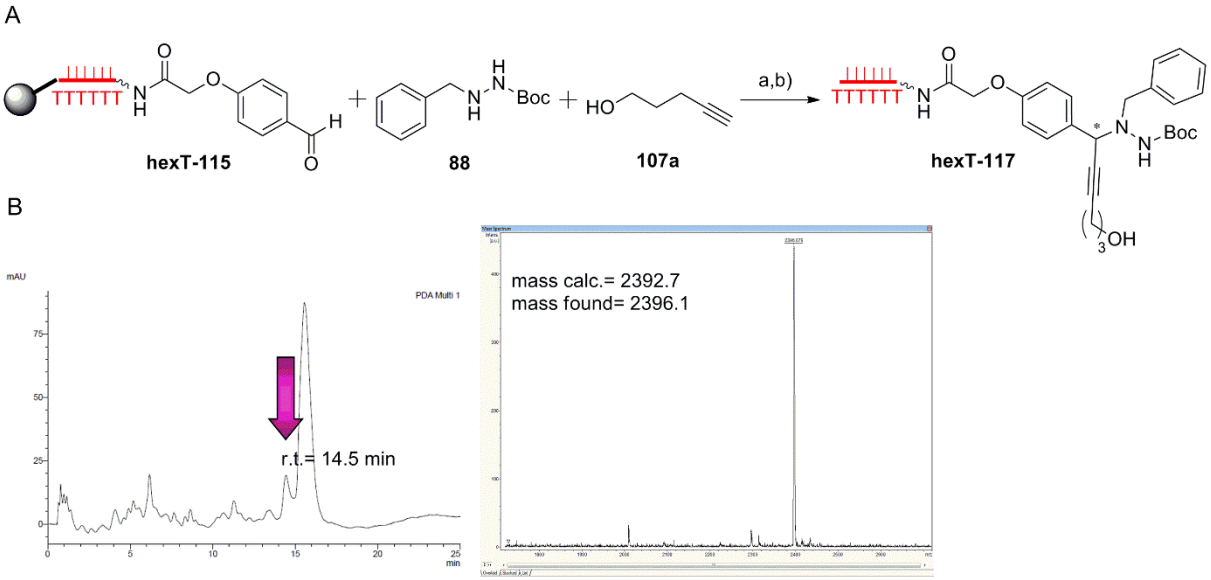

Figure 3.47. MALDI-TOF/TOF-MS of the isolated suggested Mannich-type product **hexT-117** (r.t.= 14.5 min) from Figure 3.45d. A) Reaction scheme of the suggested Mannich-type product **hexT-117** formation; a) reaction condition **No. 3** (Table 10c); b) AMA (aqueous ammonia (30 %)/ aqueous methylamine (40 %), 1:1, vol/vol), 30 min, room temperature; B) MALDI-TOF/TOF-MS of the isolated suggested Mannich-type product **hexT-117**. Filled grey circle denotes solid support (controlled pore glass, CPG); wavy bond to hexT: 5'-(C6)-amino-linker; bold bond: connection from the hexT-oligonucleotide to the CPG.

3.6.2.1.4. Synthesis of the reference molecule: 6-oxa-1,2-diazaspiro[4.4]nonane

To demonstrate that Au(I)-mediated [3+2]-cycloaddition indeed took place yielding the proposed product, the reference molecule **SP-C** for 6-oxa-1,2-diazaspiro[4.4]nonane **hexT-116a** was synthesized.[228] Identity of the 6-oxa-1,2-diazaspiro[4.4]nonane **SP-C** was confirmed by ^{1}H and ^{13}C NMR, and it was coupled to hexT by amide formation, yielding **ref-hexT-116a** (Fig. 3.48C).

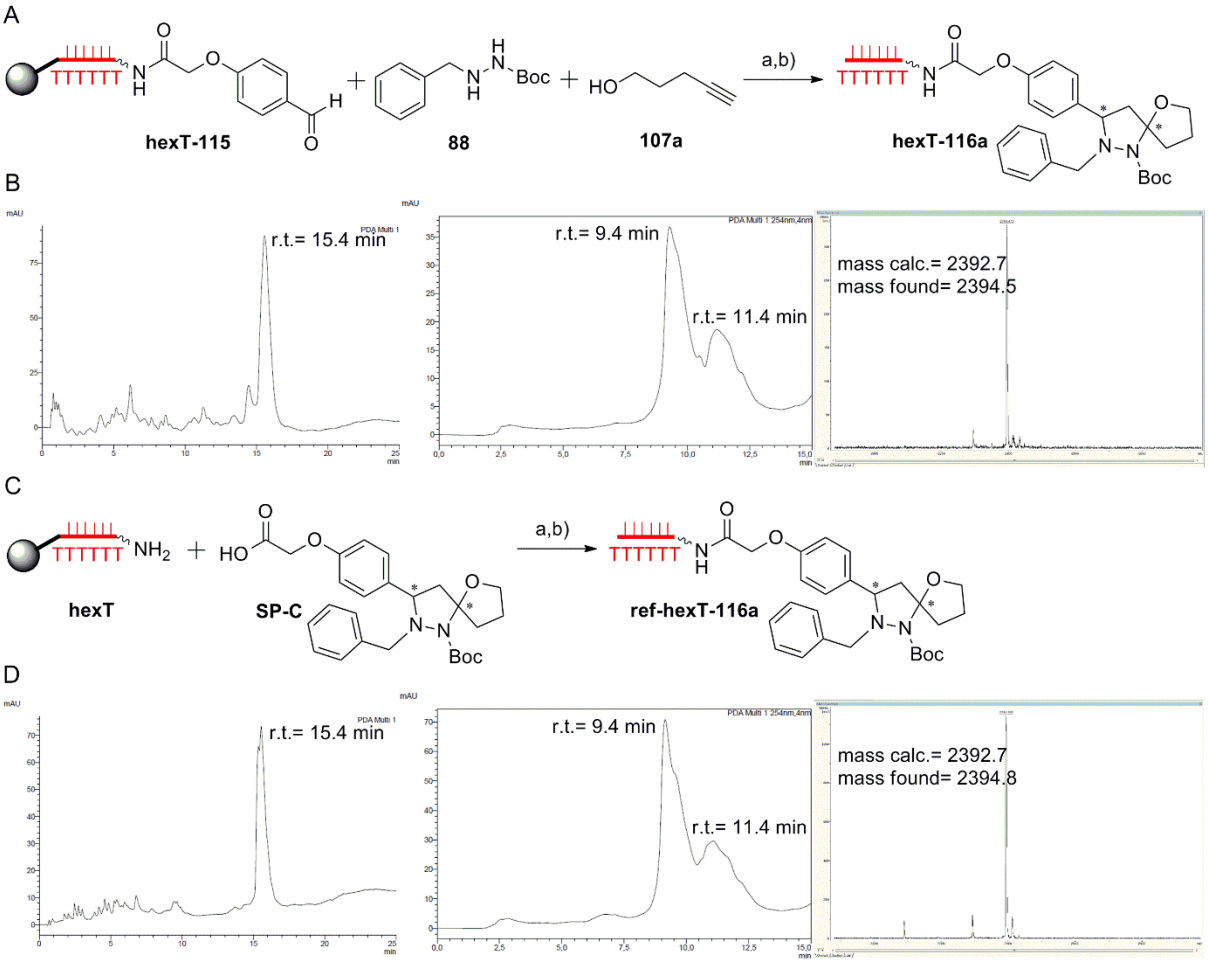

Figure 3.48. Comparison of the hexT-6-oxa-1,2-diazaspiro[4.4]nonane **hexT-116a** synthesized from the hexT-aldehyde conjugate **hexT-115** by the Au(I)-mediated reaction with the reference hexT-6-oxa-1,2-diazaspiro[4.4]nonane **ref-hexT-116a** synthesized from the 6-oxa-1,2-diazaspiro[4.4]nonane **SP-C**, and 5'-(C6)-amino-linker modified **hexT** by amide coupling. A) Scheme for the synthesis of the hexT-6-oxa-1,2-diazaspiro[4.4]nonane conjugate **hexT-116a**; conditions: a) reaction conditions **No. 3** (Table 10c); b) AMA (aqueous ammonia (30 %)/ aqueous methylamine (40 %), 1:1, vol/vol) 30 min, room temperature; B) analysis of the hexT-6-oxa-1,2-diazaspiro[4.4]nonane synthesized from the hexT-aldehyde conjugate **hexT-115**; left hand: HPLC trace (preparative HPLC) of the crude hexT-spirocycle conjugate **hexT-116a**; in the middle: HPLC trace

(analytical HPLC) of the purified hexT-spirocycle conjugate **hexT-116a**; right hand: MALDI-TOF/TOF-MS analysis of the purified hexT-spirocycle conjugate **hexT-116a**; C) scheme for the synthesis of the hexT-6-oxa-1,2-diazaspiro[4.4]nonane conjugate **ref-hexT-116a** by amide coupling; conditions: c) HATU, DIPEA, room temperature, 4 hours; b) AMA (aqueous ammonia (30 %)/ aqueous methylamine (40 %), 1:1, vol/vol) 30 min, room temperature; D) analysis of the hexT-6-oxa-1,2-diazaspiro[4.4]nonane synthesized by amide coupling; left hand: HPLC trace (preparative HPLC) of the crude hexT-spirocycle conjugate **ref-hexT-116a**; in the middle: HPLC trace (analytical HPLC) of the purified hexT-spirocycle conjugate **ref-hexT-116a**; right hand: MALDI-TOF/TOF-MS analysis of the purified hexT-spirocycle conjugate **ref-hexT-116a**. Filled grey circle denotes solid support (controlled pore glass, CPG); wavy bond to hexT: 5'-(C6)-amino-linker; bold bond: connection from the hexT-oligonucleotide to the CPG.

Comparison of HPLC traces, and MALDI-TOF/TOF-MS data of **hexT-116a** and **ref-hexT-116a** suggested that 6-oxa-1,2-diazaspiro[4.4]nonanes accessed either by Au(I)-mediated MCR (Fig. 3.48A, B), or by amide coupling (Fig. 3.48C, D) are identical products. Additionally, we saw that in Au(I)-mediated [3+2]-cycloaddition to hexT-6-oxa-1,2-diazaspiro[4.4]nonane **hexT-116a**, the hexT DNA did not impact the diastereomeric ratio of the product (Fig. 3.48B, D).

3.6.2.1.5. Exploration of the product scope of the Au(I)-mediated [3+2]-cycloaddition from the hexathymidine-aldehyde conjugate

The product scope of the Au(I)-mediated 6-oxa-1,2-diazaspiro[4.4]nonane **hexT-116** synthesis towards a projected tiDEL was investigated. Hydrazide displaying amino-substituted benzyl group (Table 11, entry 2), and a hydrazide with the photocleavable 3,4-methylenedioxy-6-nitrobenzyl protecting group successfully furnished target 6-oxa-1,2-diazaspiro[4.4]nonanes (Table 11, entry 3). Variation in alkynol component with respect to the alkyl-chain length was also tolerated (Table 11, entry 4).

Table 11. Scope of the Au(I)-mediated reaction yielding hexT-6-oxa-1,2-diazaspiro-[4.4]nonane conjugates **hexT-116**.

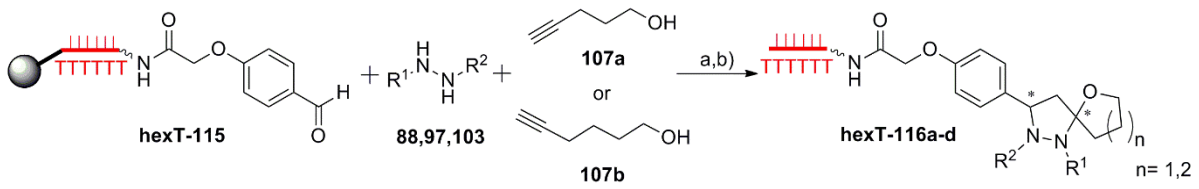

Conditions: a) Reaction condition **No. 3** (Table 10c), b) AMA (aqueous ammonia (30 %)/ aqueous methylamine (40 %), 1:1, vol/vol), 30 min, room temperature.

entry	hexT	hydrazide	alkynol	R^1	R^2	n	yield [nmol][a]	mass calc. mass found[b]
1	**hexT-116a**	**88**	**107a**	*tert*-Boc	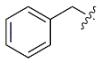	1	3.6	2392.7 2394.5
2	**hexT-116b**	**97**	**107a**	acetyl	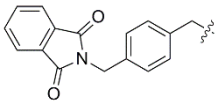	1	1.5	2363.7 2366.2[d]
3	**hexT-116c**	**103**	**107a**	*tert*-Boc	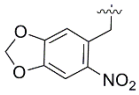	1	1.4	2302.6[c] 2305.1[c]
4	**hexT-116d**	**88**	**107b**	*tert*-Boc	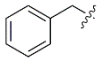	2	1.8	2406.8 2410.3

[a] measured by Nanodrop; [b] measured by MALDI-TOF/TOF-MS; [c] loss of the photolabile 3,4-methylendioxy-6-nitrobenzyl group upon irradiation in the mass spectrometer; [d] phthalimide group removed in the product. Filled grey circle denotes solid support (controlled pore glass, CPG); wavy bond to hexT: 5'-(C6)-amino-linker; bold bond: connection from the hexT-oligonucleotide to the CPG.

3.6.2.2. The impact of the hydrazide component as connectivity between hexathymidine DNA and small molecule on the reaction outcome

The successful synthesis of 6-oxa-1,2-diazaspiro[4.4]nonane **hexT-116** encouraged us further to explore the accessibility of the spirocycle **hexT-120** from the hexT-hydrazide conjugate **hexT-119**. The advantage of this approach compared to the previous one is related to the advantage of having an aldehyde component as a diversification point, as in general, aldehydes represent diverse, and easy available building blocks.

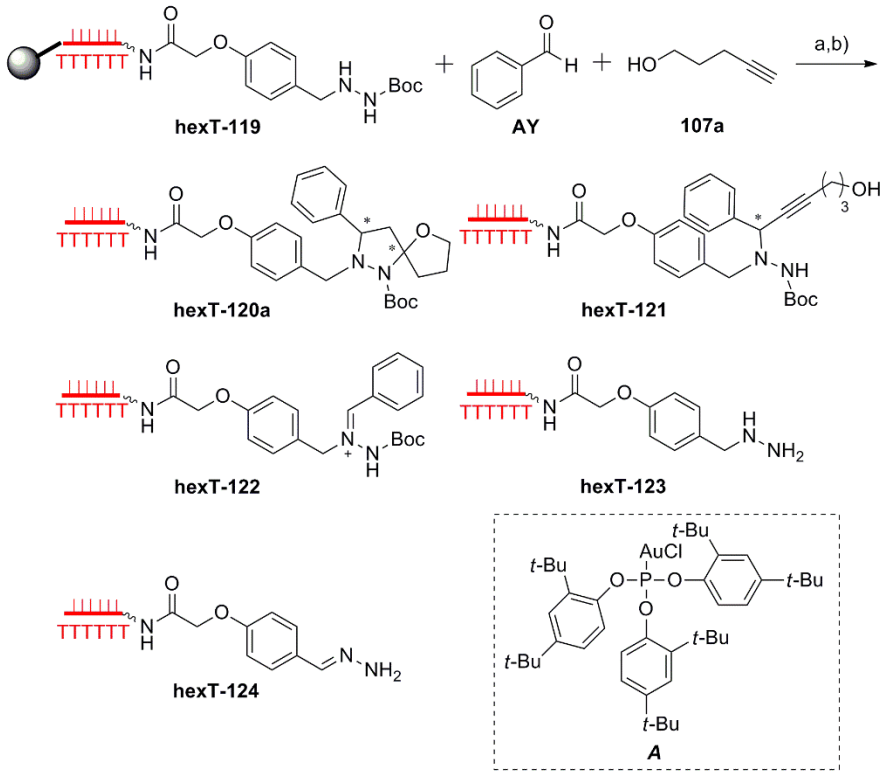

Figure 3.49. Au(I)-mediated synthesis of hexT-6-oxa-1,2-diazaspiro[4.4]nonane conjugate **hexT-120a** from hexT-hydrazide conjugate **hexT-119**. a) For conditions see Table 12; b) AMA (aqueous ammonia (30 %)/ aqueous methylamine (40 %), 1:1, vol/vol), 30 min, room temperature. Figures 3.50-3.55 show HPLC traces of the crude reaction mixtures. Filled grey circle denotes solid support (controlled pore glass, CPG); wavy bond to hexT: 5'-(C6)-amino-linker; bold bond: connection from the hexT-oligonucleotide to the CPG.

The CPG-bound hydrazide **hexT-119**, benzaldehyde **AY**, and pent-4-yn-1-ol **107a** served to investigate the accessibility of hexT-6-oxa-1,2-diazaspiro[4.4]nonane conjugate **hexT-120a** by Au(I)-mediated [3+2]-cycloaddition reaction (Fig. 3.49).

Table 12. Optimization of reaction conditions for the Au(I)-mediated MCR to furnish hexT-6-oxa-1,2-diazaspiro[4.4]nonane conjugate **hexT-120a**.

	No.	hydrazide [eq][a]	alkynol [eq][a]	catalyst [eq][a]	time/h	solvent	T/[°C]	catalyst	**hexT-120a** [%][b]	**hexT-121** [%][b]	**hexT-122** [%][b]
a) solvent	**1**	500	1000	250	20	MeOH	25	***A***/$AgSbF_6$	15	10	25
	2	500	1000	250	20	DMF	25	***A***/$AgSbF_6$	35	30	30
	3	500	1000	250	20	MeCN	25	***A***/$AgSbF_6$	25	10	30
	4	500	1000	250	20	THF	25	***A***/$AgSbF_6$	40	25	25
	5	500	1000	250	20	$C_2H_4Cl_2$	25	***A***/$AgSbF_6$	5	-	-
b) time	**1**	500	1000	250	14	THF	25	***A***/$AgSbF_6$	20	15	15
	2	500	1000	250	20	THF	25	***A***/$AgSbF_6$	40	25	25

[a] *versus* the solid support-bound hexathymidine-hydrazide conjugate **hexT-119**; [b] % conversion estimated based on the area under curve of the product peak *versus* the starting material peak in the HPLC-trace of the crude.

Systematic exploration of reaction parameters yielded five different products: the 6-oxa-1,2-diazaspiro[4.4]nonane **hexT-120a**, the suggested Mannich-type product **hexT-121**, the plausible azomethine imine intermediate **hexT-122** as the product of condensation of hydrazide **hexT-119** and aldehyde **AY**, and the co-eluting Boc-deprotected products **hexT-123** and the imine **hexT-124** (Fig. 3.49, Table 12).

As high reagent and catalyst loading was already identified as beneficial in the synthesis of 6-oxa-1,2-diazaspiro[4.4]nonane **hexT-116a**, and in the synthesis of hexT-pyrazolines, the synthesis of the spirocycle **hexT-120a** was performed in the same manner.

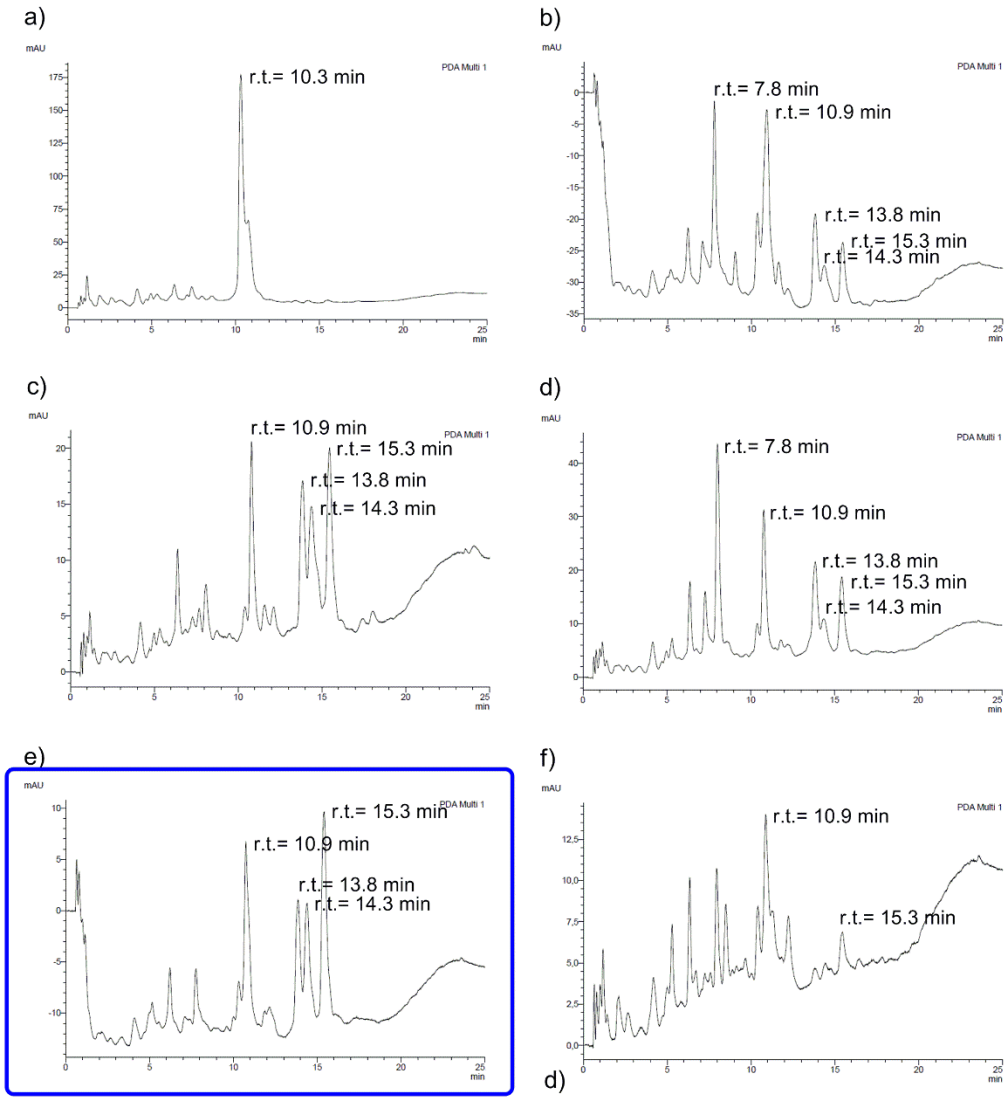

Figure 3.50. Exploration of different solvents for the Au(I)-mediated MCR of the hexathymidine-hydrazide conjugate **hexT-119**, aldehyde **AY**, and alkynol **107a**, for reaction conditions see Table 12a. a) HPLC trace of the starting material (hydrazide conjugate **hexT-119**); b) HPLC trace of experiment **No. 1**; formation of mixture of Boc-cleavage products **hexT-123** and **hexT-124** (r.t.= 7.8 min), plausible condensation product **hexT-122** (r.t.= 13.8 min), suggested Mannich-type product **hexT-121** (r.t.= 14.3 min), and spirocycle **hexT-120a** (r.t.=

15.3 min); c) HPLC trace of experiment **No. 2**; formation of mixture of products **hexT-120a-122**; d) HPLC trace of experiment **No. 3**; formation of mixture of products **hexT-120a-124**; e) HPLC trace of experiment **No. 4**; formation of mixture of products **hexT-120a-122**; f) HPLC trace of experiment **No. 5**, spirocycle **hexT-120a** formed as minor product.

A solvent screen (Fig. 3.50) displayed again THF as the best solvent for the Au(I)-mediated [3+2]-cycloaddition, although in this case I observed a rather low (40 %) conversion of the starting hydrazide conjugate **hexT-119** into the target spirocycle **hexT-120a** (Figs. 3.50e, 3.51, Table 12a, entry 4). DMF was identified as an additional solvent of choice affording **hexT-120a** in 35 % conversion (Table 12a, entry 2).

Again, longer reaction time turned out to drive product formation (Table 12b). Based on preparative HPLC chromatograms of crude reaction mixtures, it was obvious that the Au(I)-mediated [3+2]-cycloaddition to the spirocycle **hexT-120a** using hydrazide component as the connectivity between hexT and spirocycle led to much more complex reaction mixtures (Fig. 3.50) when compared to the synthesis of the spirocycle **hexT-116a**. Some of the side products were of the same nature as those ones that were identified in the synthesis of the spirocycle **hexT-116a**, the plausible azomethine imine intermediate **hexT-122** a counterpart of **hexT-118**, and the suggested Mannich-type product **hexT-121** a counterpart of **hexT-117**.

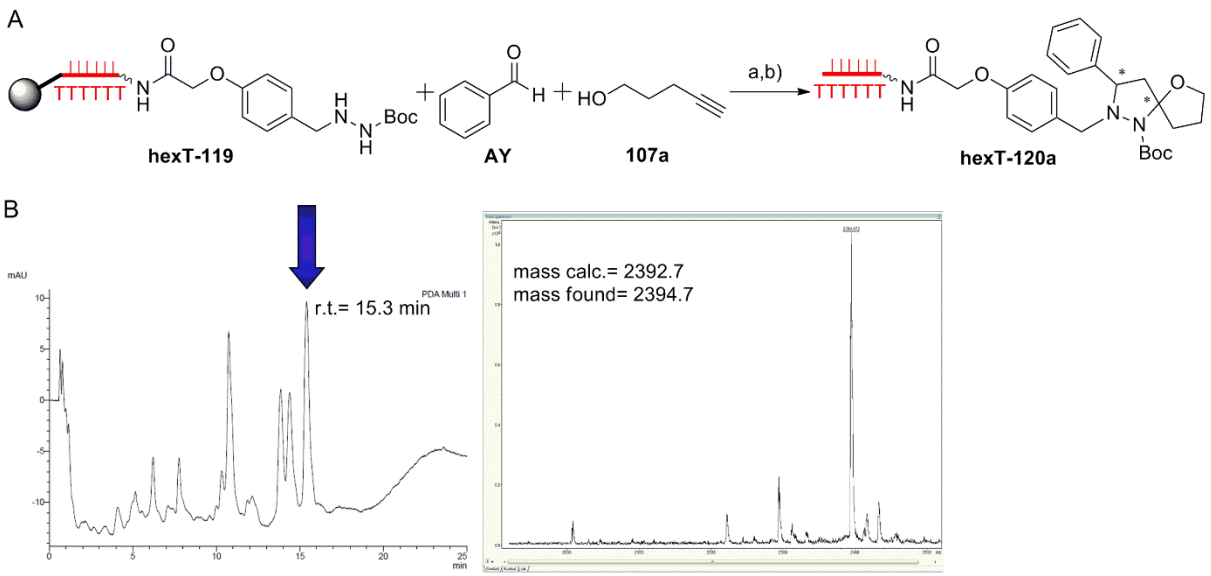

Figure 3.51. MALDI-TOF/TOF-MS of the isolated 6-oxa-1,2-diazaspiro[4.4]nonane **hexT-120a** (r.t.= 15.3 min) from Figure 3.50e. A) Reaction scheme of the 6-oxa-1,2-diazaspiro[4.4]nonane **hexT-120a** formation; a) reaction condition **No. 4** (Table 12a); b) AMA (aqueous ammonia (30 %)/ aqueous methylamine (40 %), 1:1, vol/vol), 30 min, room temperature; B) MALDI-TOF/TOF-MS of the isolated spirocycle conjugate **hexT-120a**. Filled grey circle denotes solid support (controlled pore glass, CPG); wavy bond to hexT: 5'-(C6)-amino-linker; bold bond: connection from the hexT-oligonucleotide to the CPG.

Condensation of hydrazide **hexT-119** and aldehyde **AY** led to the plausible azomethine imine intermediate **hexT-122** (Fig. 3.52) that was detected as one of the side products during optimization of reaction conditions, analogously to **hexT-118**.

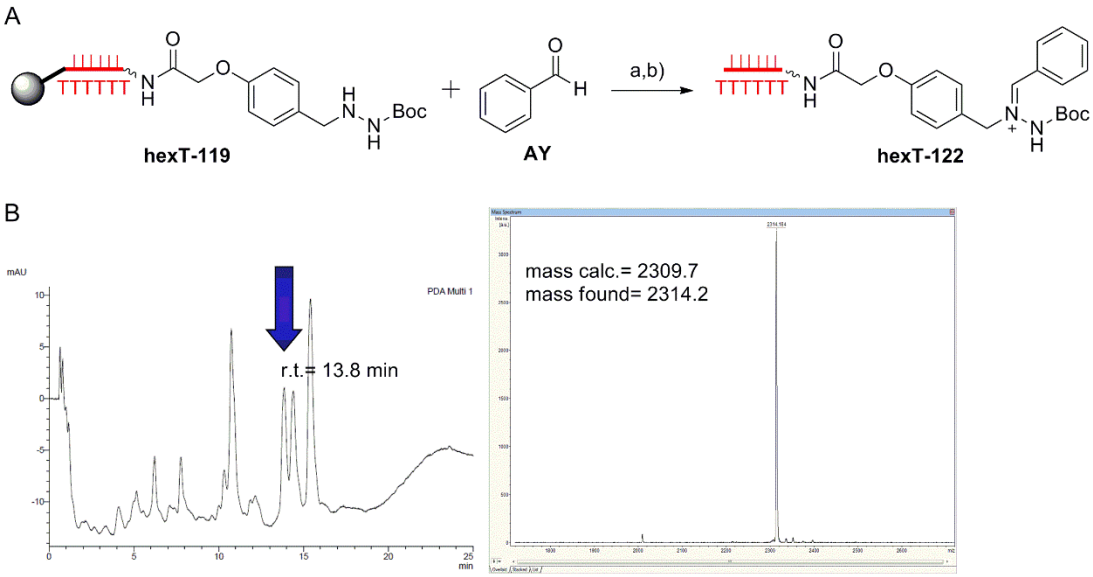

Figure 3.52. MALDI-TOF/TOF-MS of the plausible azomethine imine intermediate **hexT-122** (r.t.= 13.8 min) from Figure 3.50e. A) Reaction scheme of the plausible azomethine imine **hexT-122** formation; a) reaction condition **No. 4** (Table 12a); b) AMA (aqueous ammonia (30 %)/ aqueous methylamine (40 %), 1:1, vol/vol), 30 min, room temperature; B) MALDI-TOF/TOF-MS of the isolated plausible azomethine imine intermediate **hexT-122**. Filled grey circle denotes solid support (controlled pore glass, CPG); wavy bond to hexT: 5'-(C6)-amino-linker; bold bond: connection from the hexT-oligonucleotide to the CPG.

Besides the MALDI-TOF/TOF-MS analysis, and the reaction mechanism which includes azomethine imine formation, the identification of conjugates **hexT-118** and **hexT-122** was contributed by the fact that both conjugates were observed during Au(I)-mediated synthesis of 6-oxa-1,2-diazaspiro[4.4]nonanes **hexT-116a** and **hexT-120a** from hexT-aldehyde **115** and hexT-hydrazide **119**, respectively, and not observed when an alkynol component was used as the connectivity between the hexT and the spirocycle. This finding pointed out that the conjugates **hexT-118** and **hexT-122** must originate from an event common to both, Au(I)-mediated synthesis of **hexT-116a** and **hexT-120a**. Indeed, in both cases condensation reaction took place on the solid support bound oligonucleotide.

In contrast to the Au(I)-mediated [3+2]-cycloaddition to the spirocycle **hexT-116a**, formation of the suggested Mannich-type product **hexT-121** (Fig. 3.53) was more profound reacting the hexT-hydrazide **119** to the corresponding spirocycle, especially in THF and DMF (Fig. 3.50c, e).

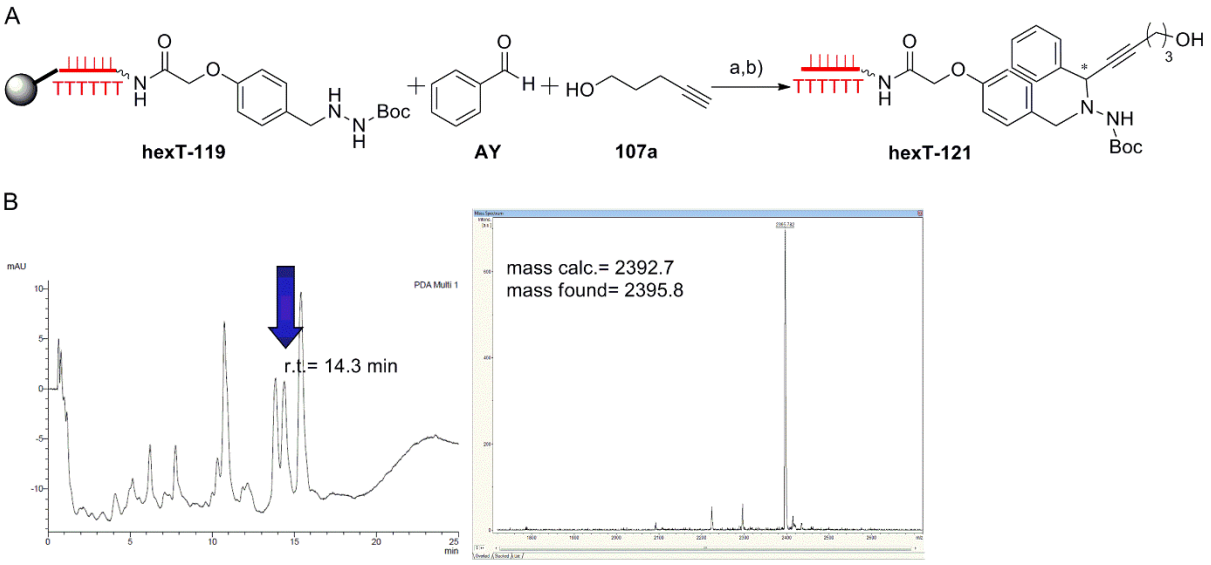

Figure 3.53. MALDI-TOF/TOF-MS of the isolated suggested Mannich-type product **hexT-121** (r.t.= 14.3 min) from Figure 3.50e. A) Reaction scheme of the suggested Mannich-type product **hexT-121** formation; a) reaction condition **No. 4** (Table 12a); b) AMA (aqueous ammonia (30 %)/ aqueous methylamine (40 %), 1:1, vol/vol), 30 min, room temperature; B) MALDI-TOF/TOF-MS of the isolated suggested Mannich-type product **hexT-121**. Filled grey circle denotes solid support (controlled pore glass, CPG); wavy bond to hexT: 5'-(C6)-amino-linker; bold bond: connection from the hexT-oligonucleotide to the CPG.

During optimization of reaction conditions, besides the suggested Mannich-type product **hexT-121** and the plausible azomethine imine **hexT-122**, a few additional side products were detected as well (Figs. 3.54, 3.55). For example, presence of hydrazone **hexT-125** was observed in all reaction mixtures (Fig. 3.54). It apparently originated from the starting hydrazide conjugate **hexT-119** as condensation of aldehyde **hexT-115** and hydrazide **126** (Fig. 3.54) yielded hydrazone prior reduction to the hydrazide. As a control experiment condensation of aldehyde **hexT-115** and hydrazide **126** was performed (Fig. 3.54). The reaction mixture was purified by preparative HPLC, and the HPLC chromatogram of the condensation reaction product was compared with HPLC chromatogram of reaction from the solvent screen for Au(I)-mediated [3+2]-cycloaddition (Fig. 3.50b). The comparison of the data confirmed the identity of the hydrazone **hexT-125** (Fig. 3.54). In general, condensation reactions of aldehydes and hydrazides are reversible; therefore re-generation of aldehyde **hexT-115** was not surprising (Figs. 3.50b, d, 3.54). I found that the aldehyde conjugate **hexT-115** was eluting together with Boc-cleavage products **hexT-123**, which formed upon removal of the Boc group from hydrazide **hexT-119**, and **hexT-124** which resulted from incomplete reduction in the preceeding step (Fig. 3.55).

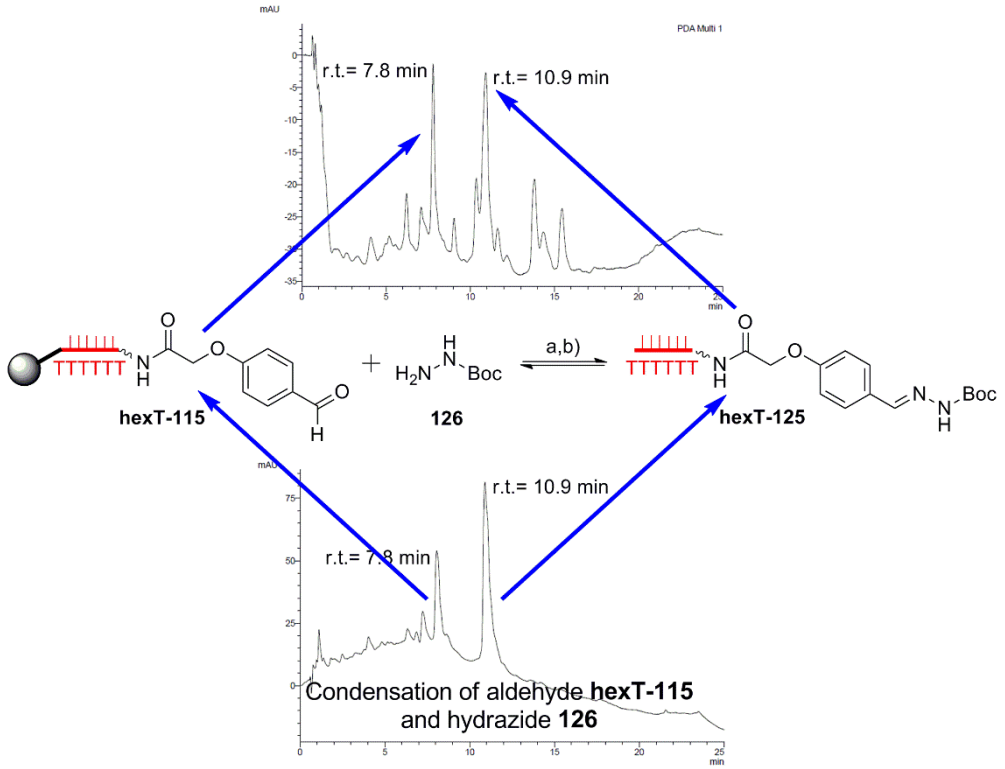

Figure 3.54. Comparison of preparative HPLC chromatograms of the crude hydrazone conjugate **hexT-125** (r.t.= 10.9 min) obtained from condensation reaction between aldehyde **hexT-115** and hydrazide **126** (below the reaction scheme), and from Figure 3.50b (above the reaction scheme). Reagents and conditions: a) 300 mM MOPS buffer, room temperature, overnight; b) AMA (aqueous ammonia (30 %)/ aqueous methylamine (40 %), 1:1, vol/vol), 30 min, room temperature. Filled grey circle denotes solid support (controlled pore glass, CPG); wavy bond to hexT: 5'-(C6)-amino-linker; bold bond: connection from the hexT-oligonucleotide to the CPG.

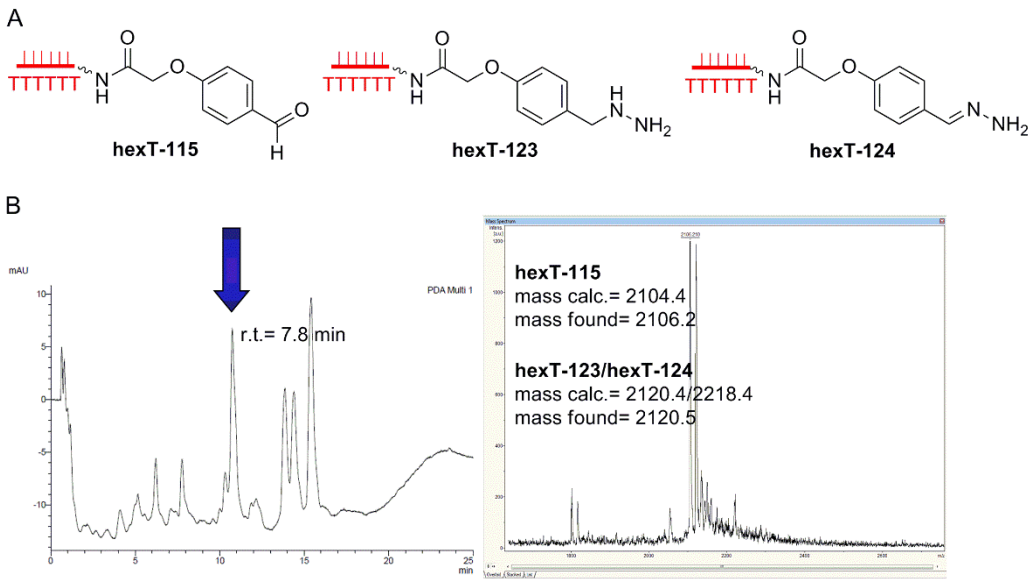

Figure 3.55. MALDI-TOF/TOF-MS of the isolated product **hexT-115** and **hexT-123/hexT-124** (r.t.= 7.8 min) from Figure 3.50b. A) Structures of starting material **hexT-115**, **hexT-123** which formed upon removal of the Boc group from hydrazide **hexT-119**, and **hexT-124** which formed upon removal of the Boc group from the

unreduced hydrazone **hexT-125**; B) MALDI-TOF/TOF-MS spectrum of the isolated mixture of hexathymidine conjugates **hexT-115** and **hexT-123/hexT-124** from experiment **No. 1** (Table 12a). Conjugates **hexT-115** and **hexT-123/hexT-124** are eluting together at r.t.= 7.8 min, and based on MALDI-TOF/TOF-MS spectrum they are present in a 1:1 mixture. Filled grey circle denotes solid support (controlled pore glass, CPG); wavy bond to hexT: 5'-(C6)-amino-linker; bold bond: connection from the hexT-oligonucleotide to the CPG.

In contrast to the Au(I)-mediated synthesis of 6-oxa-1,2-diazaspiro[4.4]nonane **hexT-116a** from hexT-aldehyde conjugate **115** where optimized reaction conditions led to the almost clean reaction, the product mixture obtained from the hexT-hydrazide conjugate **119** was much more complex. Yet, it does not represent a problem as it is possible to remove all impurities by preparative HPLC to obtain pure samples for potential tiDEL synthesis.

3.6.2.2.1. Exploration of the product scope of the Au(I)-mediated [3+2]-cycloaddition from the hexathymidine-hydrazide conjugate

The generality of the Au(I)-mediated hexT-6-oxa-1,2-diazaspiro-[4.4]nonane **hexT-120** synthesis from the hydrazide conjugate **hexT-119** was investigated with a few aldehydes. Substituted electron-rich, and electron-poor aromatic, a heterocyclic, and an aliphatic aldehyde all gave rise to the target hexT conjugates **hexT-120a-e** (Table 13).

Table 13. Scope of the Au(I)-mediated reaction yielding hexT-6-oxa-1,2-diazaspiro-[4.4]nonane conjugates **hexT-120**.

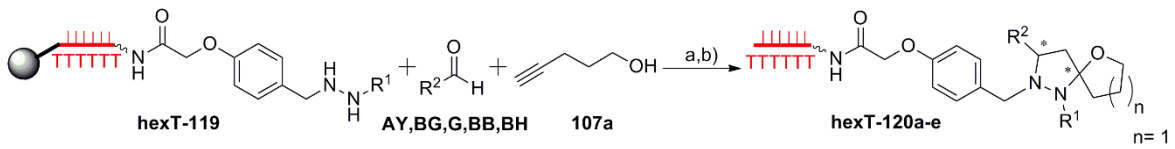

Conditions: a) Reaction condition **No. 4** (Table 12a), b) AMA (aqueous ammonia (30 %)/ aqueous methylamine (40 %), 1:1, vol/vol), 30 min, room temperature.

entry	hexT	aldehyde	R^1	R^2	yield/ [nmol][a]	mass calc. mass found[b]
1	**hexT-120a**	**AY**	*tert*-Boc	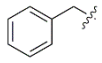	1.1	2392.7 2394.7
2	**hexT-120b**	**BG**	*tert*-Boc	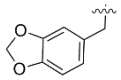	1.4	2436.8 2438.9
3	**hexT-120c**	**G**	*tert*-Boc	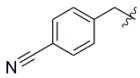	3.8	2417.8 2419.7
4	**hexT-120d**	**BB**	*tert*-Boc		1.5	2356.7 2358.4
5	**hexT-120e**	**BH**	*tert*-Boc	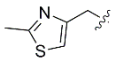	2.7	2413.8 2415.6

[a] measured by Nanodrop; [b] measured by MALDI-TOF/TOF-MS. Filled grey circle denotes solid support (controlled pore glass, CPG); wavy bond to hexT: 5'-(C6)-amino-linker; bold bond: connection from the hexT-oligonucleotide to the CPG.

3.6.2.3. *The impact of the alkynol component as connectivity between hexathymidine DNA and small molecule on the reaction outcome*

Finally, we were also interested to investigate the synthesis of the 6-oxa-1,2-diazaspiro[4.4]nonanes from a hexT-alkynol conjugate.

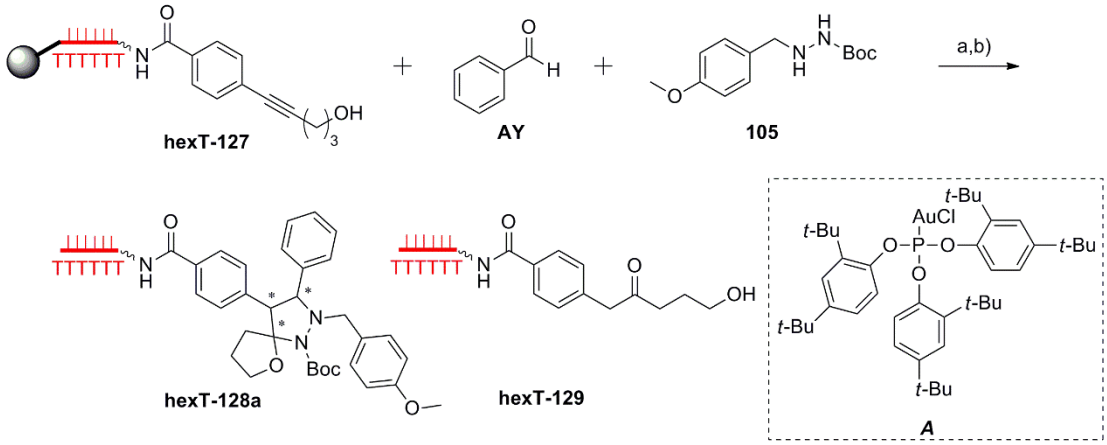

Figure 3.56. Au(I)-mediated synthesis of hexT-6-oxa-1,2-diazaspiro[4.4]nonane conjugate **hexT-128a** from hexT-alkynol conjugate **hexT-127**. a) For conditions see Table 14; b) AMA (aqueous ammonia (30 %)/ aqueous methylamine (40 %), 1:1, vol/vol), 30 min, room temperature. Figures 3.57 and 3.58 show HPLC traces of the crude reaction mixtures. Filled grey circle denotes solid support (controlled pore glass, CPG); wavy bond to hexT: 5'-(C6)-amino-linker; bold bond: connection from the hexT-oligonucleotide to the CPG.

The CPG-bound alkynol **hexT-127**, benzaldehyde **AY**, and hydrazide **105** served to investigate the accessibility of the hexT-6-oxa-1,2-diazaspiro[4.4]nonane conjugate **hexT-128a** by Au(I)-mediated [3+2]-cycloaddition reaction (Fig. 3.56). The Au(I)-mediated cycloisomerization of alkynol **hexT-127** yielded the highly reactive intermediate enol ether **hexT-130** (Fig. 3.57) which was in our initial experiments hydrolysed by the substantial amounts of water generated by the condensation reaction of aldehyde **AY** and hydrazide **105**. With alkynol **hexT-127**, water addition to the enol ether intermediate was a far more significant problem than with aldehyde **hexT-115** and hydrazide **hexT-119** as enol ether intermediate was connected to the DNA (Table 14a, Fig. 3.57). Thus, any side reaction in which enol ether took part (ex. hydration) reduced formation of the target spirocycle. On the other hand, side products that were not CPG-bound were removed during standard solid-phase synthesis work-up procedure.

Table 14. Optimization of reaction conditions for the Au(I)-mediated MCR to furnish hexT-6-oxa-1,2-diazaspiro[4.4]nonane conjugate **hexT-128a**.

	No.	hydrazide [eq][a]	aldehyde [eq][a]	catalyst [eq][a]	time [h]	solvent	drying agent	catalyst	T [°C]	**hexT-128a** [%][b]
a) solvent without drying agent	**1**	500	1000	250	17	THF	-	***A***/$AgSbF_6$	45	-
	2	500	1000	250	17	$C_2H_4Cl_2$	-	***A***/$AgSbF_6$	45	-
	3	500	1000	250	17	toluene	-	***A***/$AgSbF_6$	45	-
	4	500	1000	250	17	MeCN	-	***A***/$AgSbF_6$	45	-
	5	500	1000	250	17	DMF	-	***A***/$AgSbF_6$	45	-
b) drying agent	**1**	500	1000	250	17	MeCN	MS 5Å	***A***/$AgSbF_6$	45	40
	2	500	1000	250	17	MeCN	$MgSO_4$	***A***/$AgSbF_6$	45	35
c) solvent	**1**	500	1000	250	17	THF	MS 5Å	***A***/$AgSbF_6$	45	30
	2	500	1000	250	17	$C_2H_4Cl_2$	MS 5Å	***A***/$AgSbF_6$	45	25
	3	500	1000	250	17	toluene	MS 5Å	***A***/$AgSbF_6$	45	trace
	4	500	1000	250	17	MeCN	MS 5Å	***A***/$AgSbF_6$	45	40
	5	500	1000	250	17	DMF	MS 5Å	***A***/$AgSbF_6$	45	-
d) time	**1**	500	1000	250	17	THF	MS 5Å	***A***/$AgSbF_6$	45	30
	2	500	1000	250	41	THF	MS 5Å	***A***/$AgSbF_6$	45	10
e) temperature	**1**	500	1000	250	17	MeCN	MS 5Å	***A***/$AgSbF_6$	25	-
	2	500	1000	250	17	MeCN	MS 5Å	***A***/$AgSbF_6$	45	40
	3	500	1000	250	17	MeCN	MS 5Å	***A***/$AgSbF_6$	50	30
	4	500	1000	250	17	MeCN	MS 5Å	***A***/$AgSbF_6$	55	25
f) catalyst	**1**	500	1000	250	17	MeCN	MS 5Å	***A***	45	-
	2	500	1000	250	17	MeCN	MS 5Å	$AgSbF_6$	45	-
	3	500	1000	250	17	MeCN	MS 5Å	***A***/$AgSbF_6$	45	40

[a] *versus* the solid support-bound hexathymidine-alkynol conjugate **hexT-127**; [b] % conversion estimated based on the area under curve of the product peak *versus* the starting material peak in the HPLC-trace of the crude.

Therefore, in the synthesis of hexT-6-oxa-1,2-diazaspiro[4.4]nonane conjugate **hexT-128a** from hexT-alkynol **127** adding the water scavengers $MgSO_4$ or molecular sieves (5Å) was crucial for reaction success (Table 14b). Following experiments were performed in the presence of molecular sieves as they displayed slightly better performance than $MgSO_4$. This affected robustness of the synthesis protocol and made it less attractive for use in parallel fashion.

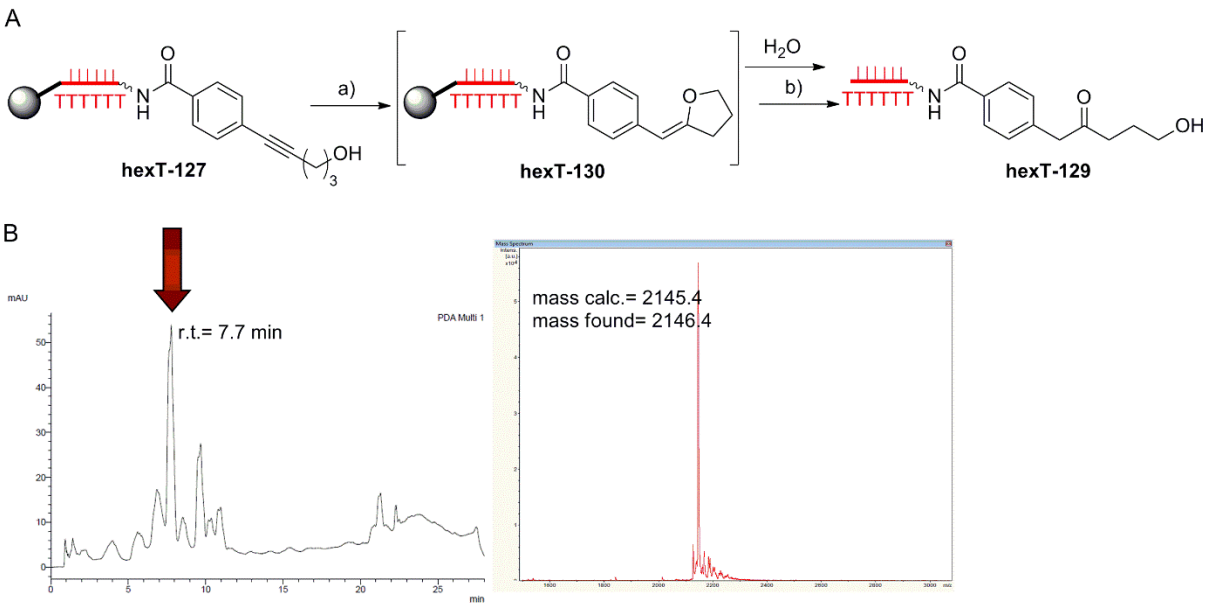

Figure 3.57. MALDI-TOF/TOF-MS analysis of the isolated water addition product **hexT-129** (r.t.= 7.7 min). A) Reaction scheme of the water addition reaction; a) reaction condition **No. 1-5** (Table 14a); b) AMA (aqueous ammonia (30 %)/ aqueous methylamine (40 %), 1:1, vol/vol), 30 min, room temperature; B) MALDI-TOF/TOF-MS of the isolated hexathymidine conjugate **hexT-129**. Filled grey circle denotes solid support (controlled pore glass, CPG); wavy bond to hexT: 5'-(C6)-amino-linker; bold bond: connection from the hexT-oligonucleotide to the CPG.

Among the solvents that were investigated in reactions run at 45 °C for 17 hours (Table 14c), the Au(I)-mediated [3+2]-cycloaddition yielded the target 6-oxa-1,2-diazaspiro[4.4]nonane **hexT-128a** in acetonitrile, THF, and 1,2-dichloroethane. The highest conversion (40 %) of the starting alkynol conjugate **hexT-127** into the target spirocycle **hexT-128a** was achieved in acetonitrile (Fig. 3.58, Table 14c, entry 4). These conditions yielded the mixture of four lipophilic products with similar retention times on preparative HPLC (Fig. 3.58). MALDI-TOF/TOF-MS analysis revealed two peaks (r.t.= 19.1 min and r.t.= 20.0 min) with the same mass corresponding to the target 6-oxa-1,2-diazaspiro[4.4]nonane **hexT-128a** (Fig. 3.58), while for other two peaks masses were not identifiable by MALDI-TOF/TOF-MS.

Further prolongation of the reaction time (Table 14d) and an increase of the temperature (Table 14e, entries 3, 4), had no positive effect on reaction outcome, and led to more side products. In contrast to the Au(I)-mediated [3+2]-cycloaddition with hexT-aldehyde conjugate **115** (Fig. 3.41.) or hexT-hydrazide conjugate **119** (Fig. 3.49), in case of alkynol **hexT-127** reaction did not take place at room temperature at all (Table 14e, entry 1). It can be explained with higher stability of vinyl gold intermediate of enol ether **hexT-130** as compared to vinyl gold intermediate **113** (Fig. 3.38) which is formed in the Au(I)-mediated synthesis of **hexT-116** and **hexT-120**. In the first case π-system is conjugated with a phenyl ring that decreases protodeauration rate.[223] Therefore, elevated temperature was required.

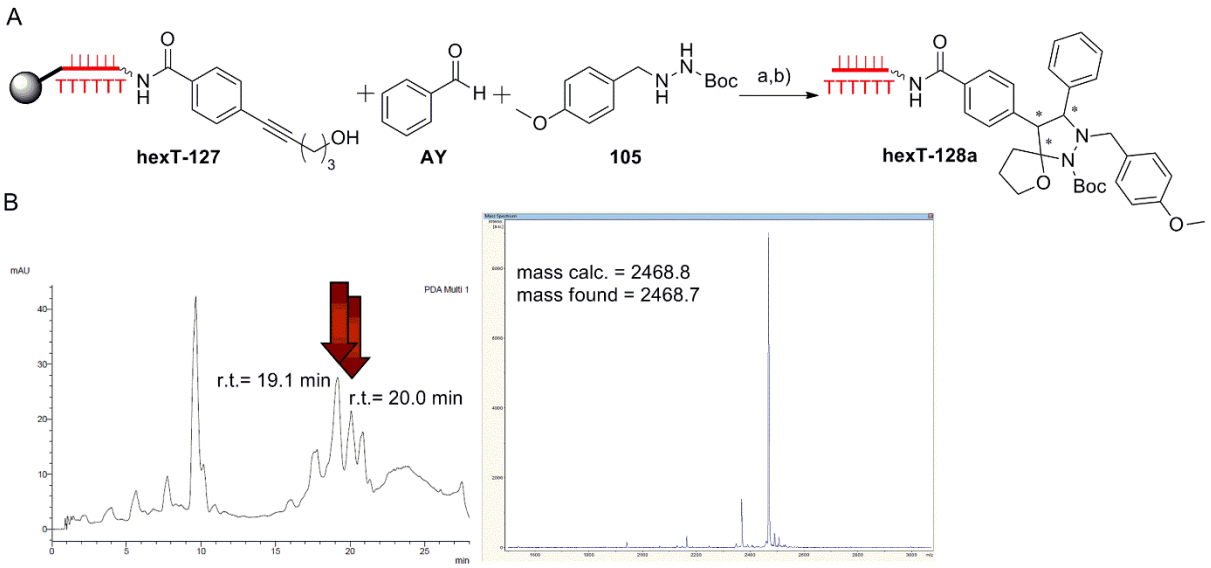

Figure 3.58. MALDI-TOF/TOF-MS of the isolated 6-oxa-1,2-diazaspiro[4.4]nonane **hexT-128a** (r.t.= 19.1 min and r.t.= 20.0 min). A) Reaction scheme of 6-oxa-1,2-diazaspiro[4.4]nonane **hexT-128a** formation; a) reaction condition **No. 4** (Table 14c); b) AMA (aqueous ammonia (30 %)/ aqueous methylamine (40 %), 1:1, vol/vol), 30 min, room temperature; B) MALDI-TOF/TOF-MS of the isolated spirocycle conjugate **hexT-128a**. Filled grey circle denotes solid support (controlled pore glass, CPG); wavy bond to hexT: 5'-(C6)-amino-linker; bold bond: connection from the hexT-oligonucleotide to the CPG.

Control reactions either without Au(I) precatalyst ***A*** (Fig. 3.56) or without silver salt ($AgSbF_6$) returned only starting material peak in the HPLC analysis as expected (Table 14f).

In contrast to the 6-oxa-1,2-diazaspiro[4.4]nonanes **hexT-116** and **hexT-120**, which are expected to form mixture of four diastereomers each, hexT-6-oxa-1,2-diazaspiro[4.4]nonane **hexT-128** gives rise to eight diastereomers, which might explain two product peaks on preparative HPLC (Fig. 3.58) that could be assigned to the target spirocycle (instead of one product peak which we observed in preparative HPLC for mixture of four diastereomers of

hexT-116 and **hexT-120**). As in this case the alkyne is an internal sub-structure, the Au(I)-acetylide cannot be formed, thus the Mannich-type product cannot be formed.

3.6.2.4. Comparison of the connectivity points between hexathymidine DNA and 6-oxa-1,2-diazaspiro[4.4]nonane on the reaction outcome

For synthesis of hexathymidine DNA conjugates of 6-oxa-1,2-diazaspiro[4.4]nonanes, we can conclude that the aldehyde component connected to the DNA **hexT-115** (Fig. 3.59A) gave the highest yields and the cleanest product conversion. Thus it represents the most feasible approach towards 6-oxa-1,2-diazaspiro[4.4]nonane library synthesis. In that case, the aldehyde building blocks would need to display an additional functionality for connection to the DNA, while a second diversification point would need to be installed on the hydrazide, e.g. amine-displaying hydrazide **94** could be exploited for library synthesis.

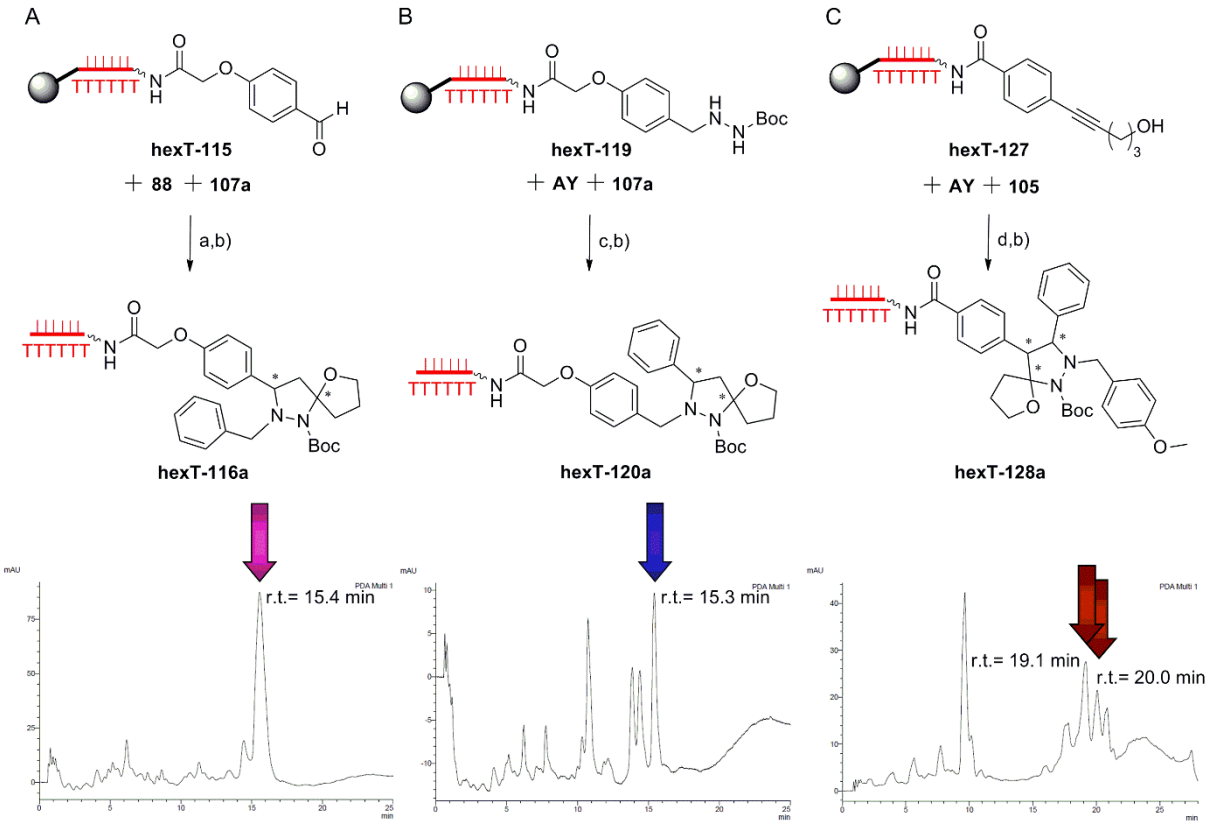

Figure 3.59. Comparison of different connectivity points for the synthesis of 6-oxa-1,2-diazaspiro[4.4]nonanes by Au(I)-mediated [3+2]-cycloaddition. A) Reaction scheme of 6-oxa-1,2-diazaspiro[4.4]nonane **hexT-116a** formation and HPLC trace of the crude 6-oxa-1,2-diazaspiro[4.4]nonane **hexT-116a** synthesized from the aldehyde conjugate **hexT-115**; a) reaction conditions **No. 3** (Table 10c); b) AMA (aqueous ammonia (30 %)/ aqueous methylamine (40 %), 1:1, vol/vol) 30 min, room temperature; B) reaction scheme of 6-oxa-1,2-

diazaspiro[4.4]nonane **hexT-120a** formation and HPLC trace of the crude 6-oxa-1,2-diazaspiro[4.4]nonane **hexT-120a** synthesized from the hydrazide conjugate **hexT-119**; c) reaction conditions **No. 4** (Table 12a); b) AMA (aqueous ammonia (30 %)/ aqueous methylamine (40 %), 1:1, vol/vol) 30 min, room temperature; C) reaction scheme of 6-oxa-1,2-diazaspiro[4.4]nonane **hexT-128a** formation and HPLC trace of the crude 6-oxa-1,2-diazaspiro[4.4]nonane **hexT-128a** synthesized from the alkynol conjugate **hexT-127**; d) reaction conditions **No. 4** (Table 14c); b) AMA (aqueous ammonia (30 %)/ aqueous methylamine (40 %), 1:1, vol/vol) 30 min, room temperature. Filled grey circle denotes solid support (controlled pore glass, CPG); wavy bond to hexT: 5'-(C6)-amino-linker; bold bond: connection from the hexT-oligonucleotide to the CPG.

Starting the 6-oxa-1,2-diazaspiro[4.4]nonane synthesis from the hydrazide conjugate **hexT-119** led to far more complex reaction mixture (Fig. 3.59B). However, the products were separable by preparative HPLC and their identity was interpreted. For that reason, this approach could be used for library synthesis as well. This option is attractive as aldehydes are abundantly available building blocks. Just the alkynol component would need to be designed in a way that it allows for further modification required for combinatorial library synthesis.

The synthesis of 6-oxa-1,2-diazaspiro[4.4]nonane scaffold with alkynol component attached to the hexT showed several disadvantages. In addition to the requirements of molecular sieves, even after optimization of reaction conditions the target spirocycle was obtained as a mixture of hardly separable products in a low conversion (Fig. 3.59C). Thus, starting tiDEL synthesis from the alkynol conjugate **hexT-127** is currently not a viable option.

3.6.2.5. Au(I)-mediated [3+2]-cycloaddition to 6-oxa-1,2-diazaspiro[4.4]nonane scaffold on different DNA sequences

Beside identification of optimal reaction conditions for diversity oriented synthesis of 6-oxa-1,2-diazaspiro[4.4]nonanes in DNA-encodable manner, we were also curious about tolerance of different DNA sequences to the optimized reaction conditions established for the synthesis of hexT-6-oxa-1,2-diazaspiro[4.4]nonane **hexT-116**.[211] Therefore, I synthesized aldehyde conjugates of hexacytidine **hexC-115**, hexapyrimidine (TCTCTC) **hexTC-115**, hexaadenosine **hexA-115**, hexaguanosine **hexG-115**, and sequence containing all four nucleobases (CAGTCG) **hexACGT-115** (Chapter 5.5.5.1). It is important to note that the amide coupling on hexA (unreacted hexA left) and hexG sequence (side products) gave lower yields as compared to other sequences. Then, I set up Au(I)-mediated [3+2]-cycloaddition to DNA-6-oxa-1,2-diazaspiro[4.4]nonane conjugates using previously optimized reaction conditions (Table 10c, entry 3).

Table 15. DNA sequence scope for the Au(I)-mediated [3+2]-cycloaddition.

entry	sequence 5'-3'	reaction	DNA-hexamer-116a [%][a]	mass calc. mass found[b]
1	TTTTTT	Au(I)-mediated [3+2]-cycloaddition	90	2392.7 2394.5
2	CCCCCC	Au(I)-mediated [3+2]-cycloaddition	60	2302.7 2304.7
3	TCTCTC	Au(I)-mediated [3+2]-cycloaddition	60	2347.7 2351.9
4	AAAAAA	Au(I)-mediated [3+2]-cycloaddition	30	2446.9 2448.7
5	GGGGGG	Au(I)-mediated [3+2]-cycloaddition	-	2542.8 -
6	CAGTCG	Au(I)-mediated [3+2]-cycloaddition	-	2421.7 -
7	TCATCT	Au(I)-mediated [3+2]-cycloaddition	40	2371.7 2374.2

[a] % conversion estimated based on the area under curve of the product peak *versus* the starting material peak in the HPLC-trace of the crude; [b] measured by MALDI-TOF/TOF-MS.

As expected, the reaction took place on hexC and hexTC sequences yielding **hexC-116a** and **hexTC-116a**, both with 60 % conversion (Table 15, entries 2, 3), while 6-oxa-1,2-diazaspiro[4.4]nonane **hexA-116a** was formed with 30 % conversion (Table 15, entry 4). However, the hexaguanosine sequence was completely destroyed under the reaction conditions (Table 15, entry 5). The 6-oxa-1,2-diazaspiro[4.4]nonane formation was not observed neither on the CAGTCG sequence (Table 15, entry 6). Next, we designed DNA sequence that did not contain nucleobase guanine (TCATCT), and I synthesized corresponding aldehyde conjugate **hexACT-115**. Then, I proceeded with Au(I)-mediated [3+2]-cycloaddition which afforded 6-oxa-1,2-diazaspiro[4.4]nonane **hexACT-116a** with 40 % conversion (Table 15, entry 7). Different reactivity of purine based nucleotides might be explained with lower ionization potential of guanine nucleobase compared to the adenine nucleobase, thus higher susceptibility towards DNA oxidation. [204]

3.6.2.5.1. *Compatibility of hexapyrimidine sequence with Au(I)-mediated annulation and acid catalyzed Pictet-Spengler reaction*

The superior stability of the hexathymidine sequence in the Au(I)-mediated [3+2]-cycloaddition over all other sequences was evident. But, although hexathymidine can be ligated to DNA sequences,[210] it cannot be a code itself. However, oligopyrimidine sequences consisting of thymidines and cytidines possess a great advantage. They could serve as a binary code in a DEL synthesis. As I demonstrated suitability of hexTC sequence for Au(I)-mediated synthesis of 6-oxa-1,2-diazaspiro[4.4]nonane **hexTC-116a**, I wanted to test whether it is convenient for synthesis of other scaffolds, and application of other chemical reactions as well (Fig. 3.60).[211]

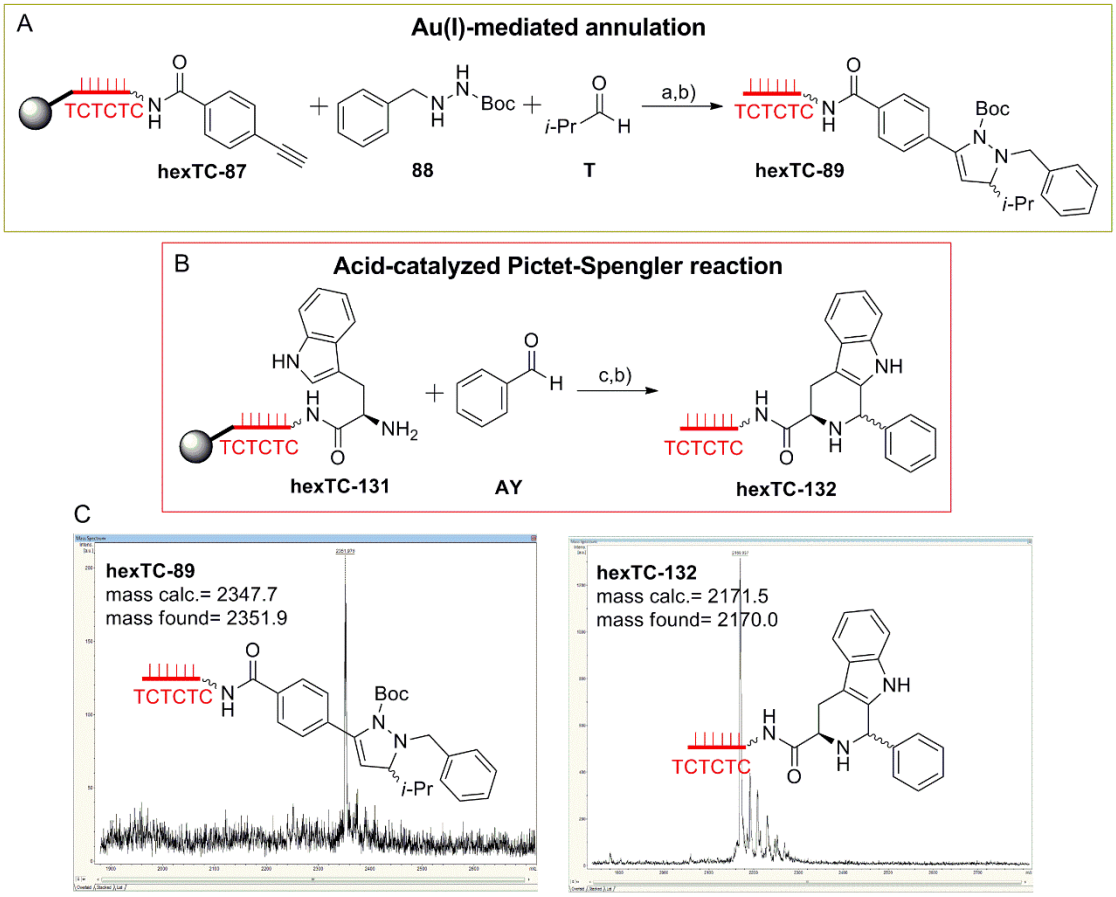

Figure 3.60. Synthesis of pyrazoline conjugate **hexTC-89** and ß-carboline conjugate **hexTC-132**. A) Reaction scheme of pyrazoline **hexTC-89** formation; a) reaction conditions **No. 5** (Table 6b); b) AMA (aqueous ammonia (30 %)/ aqueous methylamine (40 %), 1:1, vol/vol) 30 min, room temperature; B) Reaction scheme of ß-carboline **hexTC-132** formation; c) 2 % TFA, CH_2Cl_2, room temperature, 18 h; b) AMA (aqueous ammonia (30 %)/ aqueous methylamine (40 %), 1:1, vol/vol) 30 min, room temperature; C) MALDI-TOF/TOF-MS analysis of hexapyrimidine conjugates **hexTC-89** and **hexTC-132**. Filled grey circle denotes solid support

(controlled pore glass, CPG); wavy bond to hexT: 5'-(C6)-amino-linker; bold bond: connection from the hexT-oligonucleotide to the CPG.

Having already demonstrated access to hexT-pyrazolines and hexT-ß-carbolines,[210] I went for synthesis of corresponding hexTC conjugates. Optimized Au(I)-mediated annulation and Pictet-Spengler reaction,[210] allowed for synthesis of pyrazoline **hexTC-89** and ß-carboline **hexTC-132** from hexapyrimidine-alkyne conjugate **hexTC-87** and hexapyrimidine-tryptophan conjugate **hexTC-131**, respectively (Fig. 3.60).

4. Conclusion

The selection of large, pooled DNA-encoded small molecule libraries (DELs) is a validated technology for the target-based identification of bioactive compounds. We have designed and synthesized a 8568-membered adenine-binding site-directed DNA-encoded library (DEL) based on pyrazolopyrimidine scaffold. The scaffold was substituted with functional groups allowing for combinatorial DNA-encoded library synthesis using DNA-compatible, high-yielding reactions with broad reactant scope: amide coupling and Cu(I)-catalyzed azide–alkyne cycloaddition (CuAAC). The building blocks for library synthesis were selected with chemoinformatic support to filter out unwanted structural motifs, to control the physicochemical properties of the library members, and to maximize their structural diversity. The chemoinformatic analysis also indicated that pyrazolopyrimidine DEL covered novel chemical space. I investigated two different strategies to the pyrazolopyrimidine DEL. They involved either introducing of a first set of building blocks to DNA-pyrazolopyrimidine conjugate by amide coupling on solid support, followed by introduction of a second set of building blocks by CuAAC in solution phase, or the reverse reaction sequence. After investigation of both reactions on solid support, and in solution phase, we decided to introduce first the carboxylic acid building blocks on solid support, and then the azides as second set of building blocks by CuAAC on DEAE sepharose (ion-exchange resin). The library synthesis was initiated by coupling of the pyrazolopyrimidine scaffold to 5′-amino-linker modified DNA on solid support. Then, the set of carboxylic acid building blocks was appended to the DNA-pyrazolopyrimidine conjugate also by amide coupling on the solid support. Of 94 carboxylic acids, 84 acids (89 %) yielded the target products, although with variable yields, justifying their purification by Reversed-Phase High-Performance Liquid Chromatography (RP-HPLC). All conjugates were characterized by analytical HPLC and Matrix Assisted Laser Desorption/Ionization-Time of Flight/Time of Flight-Mass Spectrometry (MALDI-TOF/TOF-MS). Library synthesis proceeded with combinatorial ligation of coding dsDNA sequences by T4-DNA ligation. Finally, the library synthesis was concluded by introducing of a set of 102 validated azide building blocks (Fig. 4.1).

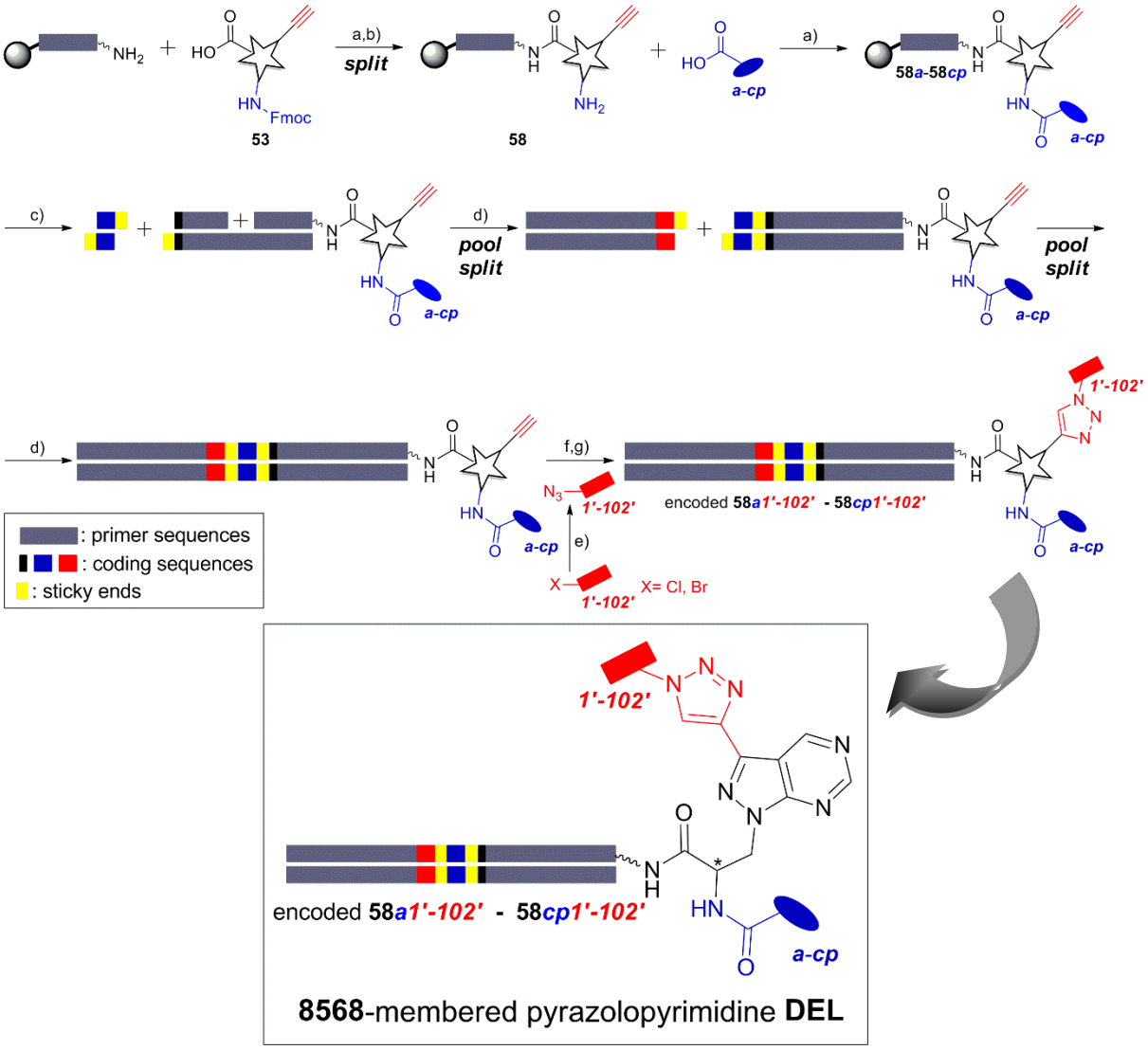

Figure 4.1. Synthesis of the 8568-membered pyrazolopyrimidine DEL. Reagents and conditions: a) HATU, DIPEA, DMF, room temperature, 4 hours; b) 20 % piperidine in DMF, 5 min; c) AMA (aqueous ammonia (30 %)/ aqueous methylamine (40 %), 1:1, vol/vol), 4 hours, room temperature; d) T4-DNA ligase, room temperature, overnight; e) NaN_3, TBAI, DMF; f) DEAE sepharose, Cu(I), TBTA, Na-ascorbate, MeOH/H_2O/DMF (2:2:1), 45 °C, 16 hours; g) 3 M sodium acetate buffer (pH= 4.75), room temperature, 30 min. Filled grey circle denotes solid support (controlled pore glass, CPG); wavy bond to DNA: 5'-(C6)-amino-PEG(4)/PEG(8) linker; bold bond: connection from the DNA oligonucleotide to the CPG.

A step further was made in the second project which aimed at evolution of the library synthesis strategy. As DNA-encoded libraries are a tool in drug discovery aiming for identification of protein binders, coverage of chemical space as broad as possible by these libraries is an important aim in the field as it might give a higher chance to identify a protein binder. A very reasonable assumption is far from being a trivial in realization. DNA sets strict limitations to chemical methods for library synthesis as the preservation of the DNA genetic

information is mandatory for operational libraries. Thus, acid organocatalysts, many transition metals, and oxidants that are known to furnish diverse drug-like structures, need to be avoided because they cause loss of genetic information primarily by depurination. Therefore we designed a hexathymidine oligonucleotide, called "hexT" serving as an adapter oligonucleotide which allows application of these classes of catalysts to access a potentially broad spectrum of structures in the initial step of library synthesis. Accordingly, we called this synthesis strategy "TiDEC" (Thymidine-initiated DNA-Encoded Chemistry). Au(I) catalysts enable access to drug-like heterocycles from simple starting materials, yet these reactions were not available for DEL synthesis until development of the TiDEC.

I investigated the access to densely substituted hexT-pyrazoline conjugates by a Au(I)-mediated annulation reaction. This reaction involved three components: an alkyne component conjugated to the hexT, an aldehyde, and a hydrazide component. Optimization of reaction conditions afforded the target pyrazolines when the reaction was mediated by a Au(I) phosphite precatalyst activated with silver hexafluoroantimonate, in acetonitrile at 50° overnight. Under harsher reaction conditions, i.e. when a Au(I) phosphine precatalyst was used in combination with silver triflate, in glacial acetic acid at 60 °C overnight, this reaction afforded access to pyrazoles. It is important to note that the glacial acetic acid alone would be sufficient to completely degrade the DNA, but still the integrity of the hexT-oligonucleotide was preserved under these harsh reaction conditions. Altogether, 71 hexT-pyrazol(in)e conjugates were synthesized using the same simple starting materials for both scaffolds: a hexT-alkyne conjugate, a set of aldehyde building blocks representing one diversification point, and an amine-displaying hydrazide designed to allow for further functionalization of hexT-pyrazol(in)e conjugates by amide coupling. All hexT conjugates were purified by preparative HPLC, and characterized by analytical HPLC and MALDI-TOF/TOF-MS.

The hexT conjugates were ligated to coding DNA sequences yielding encoded library which was finalized by introducing of a set of 96 validated carboxylic acids, yielding a 6816-membered pyrazol(in)e tiDEL (Fig. 4.2).

Using a reaction system similar to the synthesis of hexT-pyrazolines, but exchanging an alkyne with an alkynol component, we were able to establish the access to a fully saturated, highly substituted hexT-6-oxa-1,2-diazaspiro-[4.4]nonanes by Au(I)-mediated [3+2]-cycloaddition (Chapter 3.6). In general, multicomponent reactions give the opportunity to append any of the reaction components to the DNA, thereby varying the connectivity between small molecule and DNA. We appended any of the three components required for synthesis of

the target spirocycle to the hexT DNA, and optimized reaction conditions for spirocycle formation (Figs. 3.41, 3.49, 3.56).

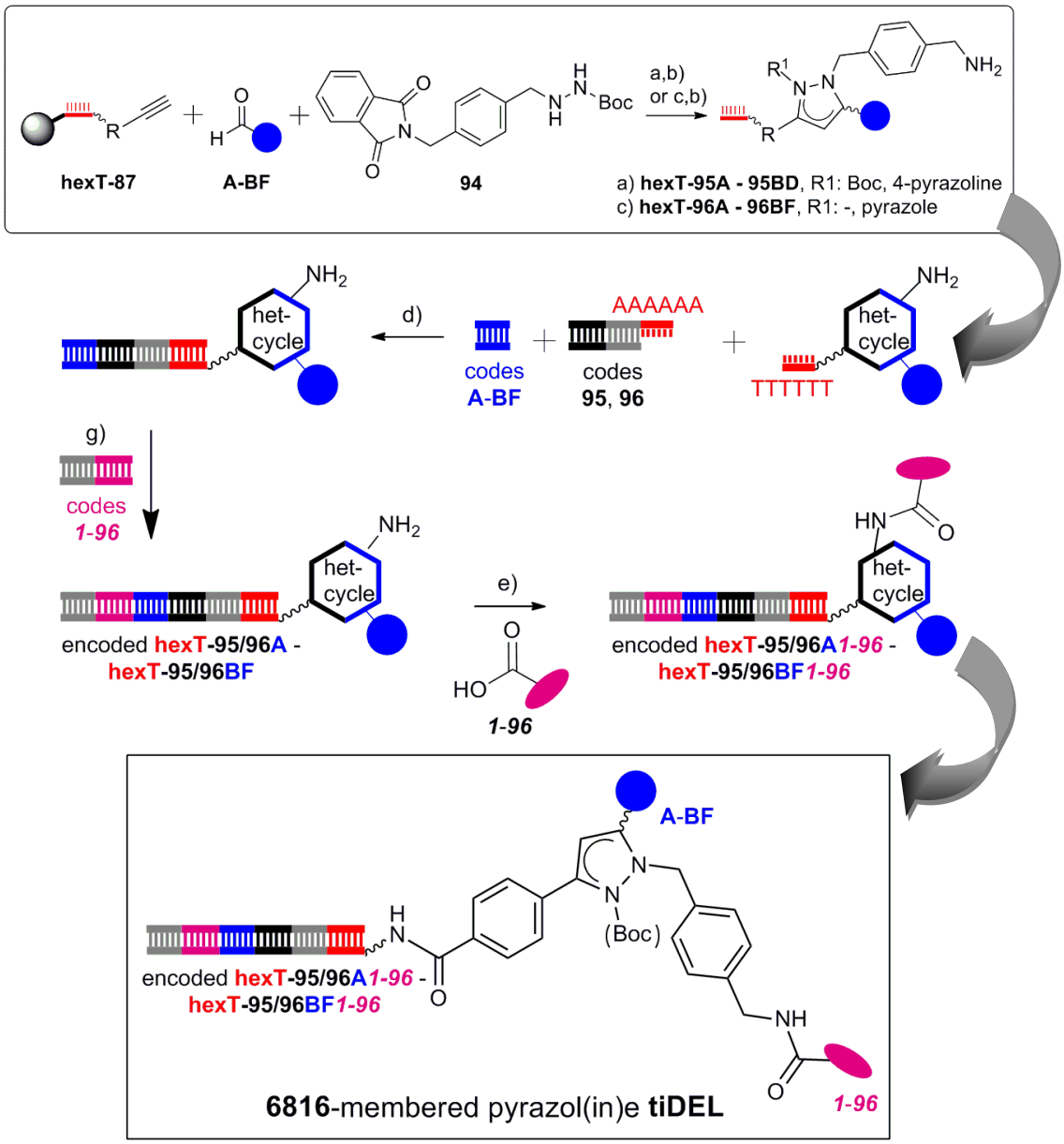

Figure 4.2. Synthesis of 6816-membered pyrazol(in)e tiDEL. Reagents and conditions: a) ***A***/$AgSbF_6$, MeCN, 50 °C, overnight; b) aq. NH_3/$MeNH_2$, room temperature, 30 min; c) ***B***/AgOTf, AcOH, 60 °C, overnight; d) T4-DNA ligase, room temperature, overnight; e) EDC, HOAt, DEAE sepharose, room temperature, overnight. R= aminocarbonylphenyl. Filled grey circle denotes solid support (controlled pore glass, CPG); wavy bond to hexT: 5'-(C6)-amino-PEG(4) linker; bold bond: connection from the hexT-oligonucleotide to the CPG. hetcycle: pyrazoline or pyrazole scaffold.

The hexT-aldehyde conjugate yielded the target spirocycle with minimal formation of side products, while the hexT-hydrazide and hexT-alkynol conjugates gave complex product

mixtures. In this project, we clearly demonstrated the influence of the connectivity between DNA and small molecule on reaction outcome in multicomponent reactions on DNA. Within this project several DNA sequences were tested for their compatibility with the Au(I)-mediated [3+2]-cycloaddition: both pyrimidine bases, and surprisingly adenine tolerated the reaction conditions.

Both aforementioned libraries contain desthiobiotin as building block to validate the synthesis and encoding strategy through selection experiments on its target protein streptavidin. Indeed, illumina sequencing data validated both libraries.

For the library of pyrazoles and pyrazolines, and the synthesis of 6-oxa-1,2-diazaspiro-[4.4]nonanes in DNA-encodable manner, we developed TiDEC, a new library synthesis strategy which rests on the use of a short chemostable adapter oligonucleotide composed of six thymidines. Likely, the development of the TiDEC strategy makes a significant contribution to the field of DNA-encoded chemistry as it extends the spectrum of organic reactions available in the initial step of the DNA-encoded library synthesis.

5. *Experimental part*

5.1. Reagents and instruments

Unless otherwise noted, chemicals were purchased from Sigma-Aldrich (Taufkirchen, Germany), Thermo Fisher Scientific (Karlsruhe, Germany), AppliChem (Darmstadt, Germany), Bachem (Bubendorf, Switzerland), and VWR (Langenfeld, Germany). MMt-NH-PEG(8)-COOH and Fmoc-NH-PEG(4)-COOH was purchased from Iris Biotech (Marktredwitz, Germany). The building blocks shown in tables 16 and 17 were selected and purchased from the Aldrich Market Select building blocks catalogue (version 2013/3). PNK was purchased from Thermo Fisher Scientific, T4-DNA ligase (Rapid) from Biozym Scientific GmbH (Hessisch Oldendorf, Germany), Taq DNA Polymerase (5 U/µL), 10 x PCR Rxn Buffer (200 mM Tris-HCl, pH= 8.4, 500 mM KCl), and $MgCl_2$ (50 mM aqueous solution) were purchased from Invitrogen (Carlsbad, CA). All primers were synthesized by Sigma-Aldrich Co. LLC (Munich, Germany). The dNTP Mix (25 mM each, 100 mM total) was obtained from Biozym Scientific GmbH. Agarose was purchased from Biozym Scientific GmbH. All PCR reactions were performed in an Eppendorf mastercycler personal (Hamburg, Germany). GeneRuler Ultra Low Range DNA marker (Thermo Fisher Scientific™) and PCR products were stained with Midori Green Direct (Nippon Genetics Europe, Düren, Germany). Gel documentation was done with Gel Doc XR+ from Bio-Rad (Hercules, CA). 5'-Amino-linker modified DNA oligonucleotides attached to controlled pore glass solid phase (CPG, 1000 Å) were synthesized by IBA (Göttingen, Germany); DNA oligonucleotides used for encoding of the library were purchased from Integrated DNA Technologies (Leuven, Belgium). Controlled pore glass solid phase was filtered on a synthesis column plugged onto a vacuum manifold (Vac-Man®, Promega). Parallel reactions for library synthesis were performed in a DESYRE vortexer in 0.5 mL glass vials (Zinsser Analytic, Franfurt a. M.). Oligonucleotide-small molecule conjugates were purified by ion pair reverse-phase high-pressure liquid chromatography (HPLC, Shimadzu Prominence) using a C_{18} stationary phase (Phenomenex, Gemini; 5 µm, C18, 110 Å, 100*10.0 mm or 50*10.0 mm) and a gradient of aqueous triethylammonium acetate buffer (100 mM, pH= 8) and methanol (20 % – 70 % of methanol over 19 min (for 100*10.0 mm column) or 20 % – 80 % of methanol over 18 min (for 50*10.0 mm column)). 23mer-, and 14mer-oligonucleotide-small molecule conjugates were analyzed by ion pair reverse-phase ultra-pressure liquid chromatography (UPLC, Agilent Technologies 1100) using a C_{18} stationary phase (Waters, Acquity UPLC® BEH, 1.7 µm, C18, 50*2.1 mm) and a gradient of 100 mM aqueous triethylammonium acetate buffer

(10 mM, pH= 8) and methanol (5 % – 20 % of methanol over 7 min). Hexamer-oligonucleotide-small molecule conjugates were analyzed by ion pair reverse-phase high-pressure liquid chromatography (HPLC, Shimadzu Prominence) using a C_{18} stationary phase (Phenomenex, Gemini; 5 µm, C18, 110 Å, 100*4.6 mm) and a gradient of aqueous triethylammonium acetate buffer (10 mM, pH= 8) and methanol (30 % – 90 % of methanol over 15 min). The oligonucleotide-small molecule conjugates were detected with a UV detector at 254 nm. Oligonucleotide concentrations were determined by UV spectroscopy using a spectrophotometer (NanoDrop 2000, Thermo Fisher Scientific). 23mer-, and 14mer-oligonucleotides were analyzed by MALDI-TOF/TOF-MS (Bruker Daltonics) using 3-HPA matrix (Dichrom). Hexamer-oligonucleotides were analyzed by MALDI-TOF/TOF-MS (Bruker Daltonics) using THAP matrix (Dichrom). ^{1}H-NMR-spectra were measured at 400 or 500 MHz on a Bruker DRX400 or Inova 500 spectrometer, respectively. ^{13}C-NMR-spectra were measured at 101 MHz or 126 MHz on a Bruker DRX400 or Inova 500 spectrometer, respectively. The pure substance was dissolved in deuterated chloroform ($CDCl_3$, 99.8 %, VWR) or dimethyl sulfoxide-d_6 (DMSO-d_6, 99.8 %, VWR, Langenfeld, Germany). Chemical shifts are listed relative to the deuterated solvent. Each proton signal was analyzed regarding its multiplicity, coupling constant J [Hz] and the amount of protons. The multiplicity was abbreviated as follows: s= singulett, d= duplet, t= triplet, q= quartet, quint= quintet, m= multiplet and br. s= broad signal. Silica gel chromatography was performed on NORMASIL 60 silica gel 40-63 µm (VWR, Langenfeld, Germany); thin layer chromatography was performed on aluminium-backed silica gel 60 F_{254} plates (Merck Millipore, Darmstadt, Germany). LC-MS analysis of low-molecular weight compounds was performed on reverse-phase high-pressure liquid chromatography (HPLC, Shimadzu Prominence) using a C_{18} column stationary phase (Phenomenex, Luna; 5 µm, C18, 100 Å, 250*4.6 mm) and a gradient of 1 % aqueous formic acid and methanol (50 % – 100 % of methanol over 13 min). High resolution mass spectrometry (ESI) was performed on a Thermo LTQ Orbitrap coupled with an Accela HPLC system.

5.2. Amide coupling on solid support

5.2.1. Amide coupling of carboxylic acids to 5'-amino-linker modified DNA

The MMt-protective group of any 5'-amino-linker modified DNA strand bound to 1000 Å controlled pore glass (CPG) solid support (1 µmol, ca. 40 mg (23mer or 14mer DNA); 1 µmol, ca. 36 mg (hexamer DNA)) was removed by addition of 3 % trichloroacetic acid in dry CH_2Cl_2 (3 x 200 µL) for 3 x 1 min. A yellow to orange color indicated successful removal of the protective group. The CPG containing the amine-deprotected DNA was washed three times with each 200 µL of 1 % TEA in MeCN, DMF, MeOH, MeCN and CH_2Cl_2. The CPG, a carboxylic acid, and HATU were then dried *in vacuo* for 15 min. Stock solutions of all reactants in dry DMF were prepared immediately before the reaction was started. To 300 µL of a solution of a carboxylic acid (100 µmol, 100 eq.) in dry DMF were added HATU (38 mg, 50 µmol, 100 eq.) dissolved in 300 µL of dry DMF and DIPEA (42.5 µL, 250 µmol, 250 eq.). This reaction mixture was shaken for 5 min and added to the solid support-bound DNA suspended in dry DMF (300 µL). The amide coupling reaction was shaken at room temperature for 4 hours. Then, the CPG containing the DNA-small molecule conjugate was filtered over a filter column and washed subsequently with each 3 x 200 µL of DMF, MeOH, MeCN, and CH_2Cl_2. Unreacted amines were capped with acetic acid anhydride (a 1:1 mixture of THF/methylimidazole, 9:1, vol/vol, and THF/pyridine/acetic acid anhydride, 8:1:1, vol/vol was used), and the CPG was washed again with each 3 x 200 µL of DMF, MeOH, MeCN, and CH_2Cl_2, and dried *in vacuo* for 15 min. For analysis, an aliquot of ca. 10 nmol of the DNA conjugate was deprotected and cleaved from the CPG by treatment with 500 µL of AMA (AMA= aqueous ammonia (30 %)/ aqueous methylamine (40 %), 1:1, vol/vol) for 30 min (DNA strands containing only pyrimidine nucleotides) or for 4 hours (DNA strands containing purine nucleotides as well) at room temperature. To this solution 20 µL of 1 M Tris buffer (pH= 7.5) were added, the mixture was dried in a SpeedVac, re-dissolved in 100 µL of distilled water, and the product was purified by RP-HPLC (Gemini, 5u, C18, 110A column; 100*10.0 mm or 50*10.0 mm) with a gradient of aqueous triethylammonium acetate buffer (100 mM, pH= 8) and methanol (20 % – 70 % of methanol over 19 min (for 100*10.0 mm column), or 20 % – 80 % of methanol over 18 min (for 50*10.0 mm column)).

5.2.2. Synthesis of DNA-PEG linker conjugates

The MMt-protective group of the 5'-amino-linker modified DNA strand bound to 1000 Å controlled pore glass (CPG) solid support (1 µmol, ca. 40 mg (23mer or 14mer DNA); 1 µmol, ca. 36 mg (hexamer DNA)) was removed by addition of 3 % trichloroacetic acid in dry CH_2Cl_2 (3 x 200 µL) for 3 x 1 min. A yellow to orange color indicated successful removal of the protective group. The CPG containing the deprotected DNA was then washed three times with each 200 µL of 1 % TEA in MeCN, DMF, MeOH, MeCN, and CH_2Cl_2. The CPG, the MMt-NH-PEG(8)-COOH linker or Fmoc-NH-PEG(4)-COOH linker, and HATU were dried *in vacuo* for 15 min. Stock solutions of all reactants in dry DMF were prepared immediately before the reaction was started. To 300 µL of a solution of the MMt-NH-PEG(8)-COOH linker (71 mg, 100 µM, 100 eq.), or to 300 µL of a solution of the Fmoc-NH-PEG(4)-COOH linker (49 mg, 100 µmol, 100 eq.) in dry DMF were added HATU (38 mg, 100 µmol, 100 eq.) dissolved in 300 µL of dry DMF and DIPEA (42.5 µL, 250 µmol, 250 eq.). This reaction mixture was shaken for 5 min and added to the solid support-bound DNA suspended in dry DMF (150 µL). The amide coupling reaction was shaken at room temperature for 4 hours. Then, the CPG containing the DNA-PEG linker conjugate was filtered over a filter column and washed subsequently with each 3 x 200 µL of DMF, MeOH, MeCN, and CH_2Cl_2. Unreacted amines were capped with acetic acid anhydride (a 1:1 mixture of THF/methylimidazole, 9:1, vol/vol, and THF/pyridine/acetic acid anhydride, 8:1:1, vol/vol was used), and the CPG was again washed with each 3 x 200 µL of DMF, MeOH, MeCN, and CH_2Cl_2, and dried *in vacuo* for 15 min. For analysis, an aliquot of ca. 10 nmol of the DNA-PEG conjugate was deprotected and cleaved from the CPG by treatment with 500 µL of AMA (AMA= aqueous ammonia (30 %)/ aqueous methylamine (40 %), 1:1, vol/vol) for 30 min (DNA strands containing only pyrimidine nucleotides), or for 4 hours (DNA strands containing purine nucleotides as well) at room temperature. To this solution 20 µL of 1 M Tris buffer (pH= 7.5) were added, the mixture was dried in a SpeedVac, re-dissolved in 100 µL of distilled water, and the product was analyzed by RP-HPLC as described above.

5.3. DNA-Encoded Library based on the pyrazolopyrimidine scaffold

5.3.1. Synthesis of the DNA-pyrazolopyrimidine conjugate

Prior coupling of the pyrazolopyrimidine scaffold **53** to the pegylated DNA (23mer DNA, sequence: 5'-GTC TTG CCG AAT TCC GCT GCA CT-3'; 14mer DNA, sequence: 5'-GTC TTG CCG AAT TC-3'), the protective group of the PEG linker was removed: The MMt-protective group of the DNA-PEG(8) linker conjugate bound to 1000 Å controlled pore glass (CPG) solid support (1 µmol, ca. 40 mg) was removed by addition of 3 % trichloroacetic acid in dry CH_2Cl_2 (3 x 200 µL) for 3 x 1 min. A yellow to orange color indicated successful removal of the protective group. The Fmoc-group of the DNA-PEG(4) linker conjugate bound to 1000 Å controlled pore glass (CPG) solid support (1 µmol, ca. 40 mg) was removed by addition of 20 % piperidine in dry DMF (0.4 mL). The reaction mixture was shaken for 5 min at room temperature. The CPG containing the deprotected DNA-PEG linker conjugate was washed three times with each 200 µL of 1 % TEA in MeCN, then DMF, MeOH, MeCN, and CH_2Cl_2. The pegylated DNA (1 µmol, ca. 40 mg) was coupled with pyrazolopyrimidine **53** (46.8 mg, 100 µmol, 100 eq.) to furnish DNA-pyrazolopyrimidine conjugate **58** according to the procedure for coupling of carboxylic acids to 5'-amino-linker modified DNA. For analysis, an aliquot of ca. 10 nmol of conjugate **58** was deprotected and cleaved from the CPG with 500 µL of AMA (AMA= aqueous ammonia (30 %)/ aqueous methylamine (40 %), 1:1, vol/vol) for 4 hours at room temperature. Then, 20 µL of 1 M Tris buffer (pH= 7.5) were added, the mixture was dried in a SpeedVac, re-dissolved in 100 µL of distilled water, and the product was analyzed by RP-HPLC (Gemini, 5u, C18, 110A column; 100*10.0 mm) with a gradient of aqueous triethylammonium acetate buffer (100 mM, pH= 8) and methanol (20 % – 70 % of methanol over 19 min).

5.3.2. Synthesis of model DNA-alkyne conjugates for evaluation of azide building blocks

Synthesis of model 14mer DNA-alkyne conjugate 59

The 14mer DNA (1 µmol, ca. 40 mg, sequence: 5'-GTC TTG CCG AAT TC-3') was coupled with pent-4-ynoic acid **59a** (9.8 mg, 100 µmol, 100 eq.) to furnish DNA conjugate **59** according to the procedure for coupling of carboxylic acids to 5'-amino-linker modified DNA. For analysis, an aliquot of ca. 10 nmol of conjugate **59** was deprotected and cleaved from the CPG with 500 µL of AMA (AMA= aqueous ammonia (30 %)/ aqueous methylamine (40 %), 1:1, vol/vol) for 4 hours at room temperature. Then, 20 µL of 1 M Tris buffer (pH= 7.5) were added, the mixture was dried in a SpeedVac, re-dissolved in 100 µL of distilled water, and the product was analyzed by RP-HPLC (Gemini, 5u, C18, 110A column; 100*10.0 mm) with a gradient of aqueous triethylammonium acetate buffer (100 mM, pH= 8) and methanol (20 % – 70 % of methanol over 19 min).

Synthesis of model DNA-glycine-naphtoic acid conjugate 60

The pegylated 23mer DNA (1 µmol, ca. 40 mg, sequence: 5'-GTC TTG CCG AAT TCC GCT TAC CG-3') was coupled with Fmoc-protected propargyl glycine **60a** (33.5 mg, 100 µmol, 100 eq.) to furnish DNA conjugate **60b** according to the procedure for coupling of carboxylic acids to 5'-amino-linker modified DNA. Then, unreacted amines were capped with acetic acid anhydride (a 1:1 mixture of THF/methylimidazole, 9:1, vol/vol, and THF/pyridine/acetic acid anhydride, 8:1:1, vol/vol was used), and the CPG was washed as described above. Prior coupling of the naphtoic acid **60c** to the pegylated DNA-glycine conjugate **60b**, the Fmoc-protective group of the conjugate bound to 1000 Å controlled pore glass (CPG) solid support (1 µmol, ca. 40 mg, sequence: 5'-GTC TTG CCG AAT TCC GCT TAC CG-3') was removed by addition of 20 % piperidine in dry DMF (0.4 mL). The reaction mixture was shaken for 5 min at room temperature. The CPG containing the deprotected DNA conjugate **60b** was washed three times with each 200 µL of 1 % TEA in MeCN, then DMF, MeOH, MeCN, and CH_2Cl_2. Then, the DNA-glycine conjugate **60b** (1 µmol, ca. 40 mg) was coupled with naphtoic acid **60c** (17.2 mg, 100 µmol, 100 eq.) to furnish DNA conjugate **60** according to the procedure for coupling of carboxylic acids to 5'-amino-linker modified DNA. For analysis, an aliquot of ca. 10 nmol of conjugate **60** was deprotected and cleaved from the CPG with 500 µL of AMA (AMA= aqueous ammonia (30 %)/ aqueous

methylamine (40 %), 1:1, vol/vol) for 4 hours at room temperature. Then, 20 µL of 1 M Tris buffer (pH= 7.5) were added, the mixture was dried in a SpeedVac, re-dissolved in 100 µL of distilled water, and the product was analyzed by RP-HPLC (Gemini, 5u, C18, 110A column; 100*10.0 mm) with a gradient of aqueous triethylammonium acetate buffer (100 mM, pH= 8) and methanol (20 % – 70 % of methanol over 19 min).

5.3.3. Coupling reactions of 94 carboxylic acids to the DNA-pyrazolopyrimidine conjugate

For library synthesis, sets of 20 carboxylic acids (see Table 16, building blocks ***a-cp***) were coupled to the DNA-pyrazolopyrimidine conjugate **58** (a total of 20 reactions was performed in parallel). For Fmoc-deprotection of DNA-pyrazolopyrimidine conjugate **58** (400 nmol, ca. 16 mg) bound to 1000 Å controlled pore glass (CPG) solid support, the conjugate was treated with 20 % piperidine in dry DMF (0.4 mL) for 5 min at room temperature. The solid support containing the Fmoc-deprotected conjugate **58** was filtered off and washed with each 3 x 200 µL of DMF, MeOH, MeCN, and CH_2Cl_2. Then, the batch of solid support with the DNA conjugate **58**, a set of 20 carboxylic acids (each 2 µmol per coupling reaction), and HATU as a coupling reagent were dried *in vacuo* for 15 min. Then, the batch of solid support containing the Fmoc-deprotected DNA conjugate **58** (16 mg) was split in 4 Eppendorf tubes (each 4 mg) on a balance, giving a total of 4 sub-batches. Each of these 4 sub-batches was suspended in 100 µL of dry DMF. These 4 suspensions were distributed to a total of 20 reaction vessels of a 96well plate, so that each reaction vessel contained ca. 20 nmol of a DNA conjugate **58** suspended in 20 µL of dry DMF. Then, each of the 20 carboxylic acids (2 µmol, 100 eq.) was dissolved in 20 µL of dry DMF. To these solutions were added each HATU (2 µmol, 100 eq.), dissolved in 20 µL of DMF (taken from a stock solution: 120 µmol, 76 mg in 2 mL of dry DMF), and DIPEA (0.85 µL, 5 µmol, 250 eq.) giving a total volume of ca. 60 µL. The 20 carboxylic acids were activated for 5 min with shaking. Then, activated carboxylic acids were added to the DNA-pyrazolopyrimidine conjugate **58**. The reaction mixtures were shaken at room temperature for 4 hours. The solid phase containing the amide coupling products was filtered off using a filter plate and washed subsequently with each 3 x 200 µL of DMF, MeOH, MeCN, and CH_2Cl_2, and dried *in vacuo* for 15 min. Then, the DNA conjugates **58*a*-58*cp*** were deprotected and cleaved from the CPG by treatment with 500 µL of AMA (AMA=

aqueous ammonia (30 %)/ aqueous methylamine (40 %)= 1:1, vol/vol) for 5 hours at room temperature. Samples were filtered directly from a filter plate into a 96well deep well plate. Then, 20 µL of 1 M Tris buffer (pH= 7.5) was added, the mixtures were dried in a SpeedVac, re-dissolved in 100 µL of distilled water, and all coupling products were purified by RP-HPLC (Gemini, 5u, C18, 110A column; 100*10.0 mm) with a gradient of aqueous triethylammonium acetate buffer (100 mM, pH= 8) and methanol (20 % – 70 % of methanol over 19 min). Fractions containing the product were collected, evaporated in a SpeedVac, co-evaporated with 3 x 200 µL of ethanol/distilled water (1:1) and analyzed by MALDI-TOF/TOF-MS analysis and by analytical HPLC to assert purity and identity of the conjugates. This procedure was repeated until all 94 carboxylic acids were coupled to DNA conjugate **58**.
All carboxylic acids ***a-cp*** were coupled to pegylated DNA-pyrazolopyrimidine conjugate **58** containing a PEG(8) linker serving as spacer between DNA and the pyrazolopyrimidine scaffold, except for carboxylic acids ***ag***, ***ai***, ***aj***, ***am***, ***an***, ***ap***, ***ap***, ***aq***, ***at***, ***av***, and ***ax*** that were coupled to the pegylated DNA conjugate **58** containing a PEG(4) linker.

Table 16. Yield, conversion rates and MALDI-TOF/TOF-MS data of compounds **58*a*-58*cp***.[a]

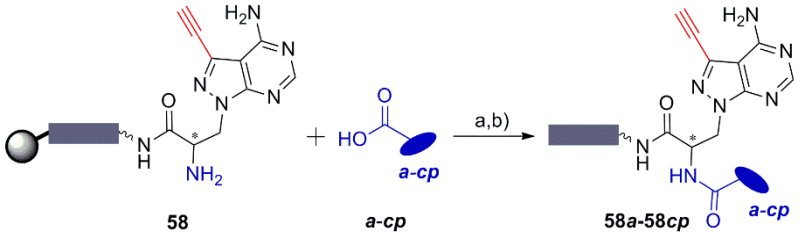

Conditions: a) HATU, DIPEA, DMF; b) AMA (aqueous ammonia (30 %)/ aqueous methylamine (40 %), 1:1, vol/vol), 30 min, room temperature.

No.	structure	yield [nmol][b]	conversion[c]	mass calc.	mass found[d]
a	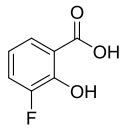	1.14	50	7935.4	7942.9
b	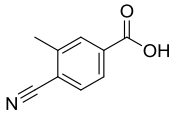	0.10	60	7940.5	7949.8
c	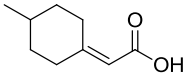	1.74	55	7933.5	7940.1
d	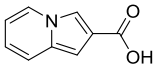	1.43	70	7940.5	7949.4
e	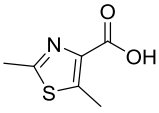	1.67	90	7936.5	7942.6
f	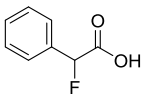	0.10	10	7933.5	7934.5
g	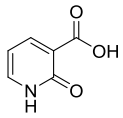	1.27	100	7918.4	7917.0
h	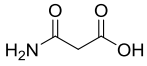	0.10	85	5145.6	5148.0
i	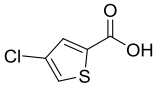	0.10	85	7941.9	7949.0
j	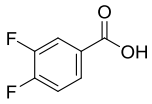	0.10	85	7937.4	7941.0
k	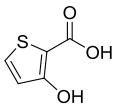	1.41	15	7923.4	7918.9
l	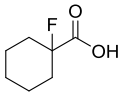	0.10	20	7925.5	7925.0

No.	structure	yield [nmol][b]	conversion[c]	mass calc.	mass found[d]
m	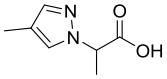	2.79	90	7933.5	7931.8
n	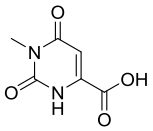	0.10	90	7949.4	7943.6
o	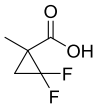	0.67	10	7915.4	7922.0
p	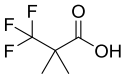	0.68	85	7935.4	7945.1
q	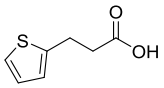	1.25	75	7935.5	7940.4
r	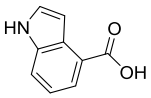	1.88	70	7940.5	7944.8
s	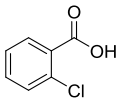	1.13	75	7935.9	7940.8
t	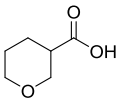	3.26	65	7909.5	7910.6
u	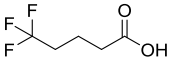	1.19	90	7935.4	7936.3
v	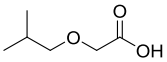	0.38	60	7911.5	7910.8
w	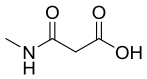	4.11	70	5159.6	5161.0
x	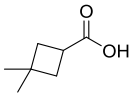	1.91	75	7907.5	7912.4
y	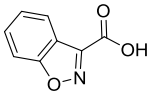	0.10	80	7942.5	7942.5
z	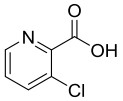	1.26	5	7936.9	7936.9
aa	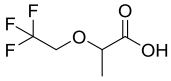	1.59	10	7951.4	7952.1

No.	structure	yield [nmol][b]	conversion[c]	mass calc.	mass found[d]
ab	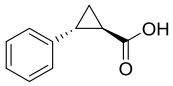	1.01	45	7941.5	7948.0
ac	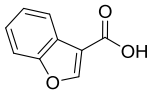	-	-	-	-
ad	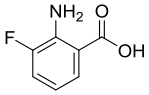	0.10	70	5199.7	5196.0
ae	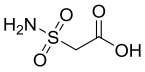	0.88	70	7918.5	7919.5
af	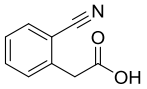	2.64	40	5203.7	5202.2
ag	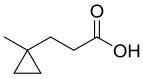	0.68	10	4994.5	4987.5
ah	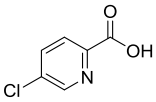	1.47	55	5200.1	5204.8
ai	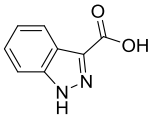	1.92	20	5028.5	5030.0
aj	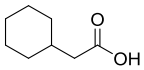	1.09	10	5008.5	5005.6
ak	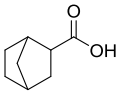	3.29	35	5182.7	5183.5
al	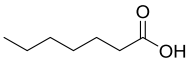	0.78	40	5172.7	5171.5
am		0.10	25	4968.4	4968.2
an	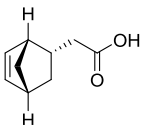	0.60	30	5018.5	5015.9
ao	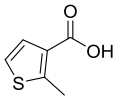	0.46	35	5008.5	5009.2
ap	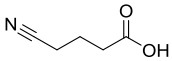	0.97	50	4979.4	4979.3

No.	structure	yield [nmol][b]	conversion[c]	mass calc.	mass found[d]
aq	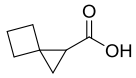	0.67	30	4992.5	4997.7
ar	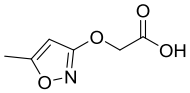	1.36	50	5199.6	5204.7
as	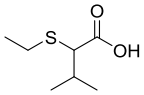	0.45	55	5204.8	5203.0
at	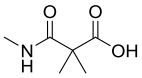	1.45	30	5011.5	5015.1
au	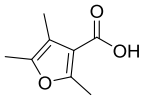	0.10	60	5196.7	5198.3
av	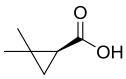	1.02	35	4980.5	4977.0
aw	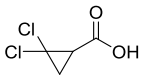	2.61	30	5197.5	5193.0
ax	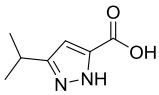	0.76	60	5020.5	5017.5
ay	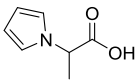	0.81	50	5181.7	5183.1
az	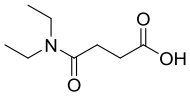	-	-	-	-
ba	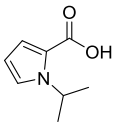	0.20	45	5195.8	5195.6
bb	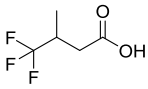	-	-	-	-
bc	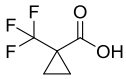	0.16	40	5196.6	5197.3
bd	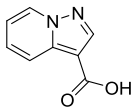	-	-	-	-
be	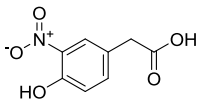	4.80	20	5239.7	5238.7

No.	structure	yield [nmol][b]	conversion[c]	mass calc.	mass found[d]
bf	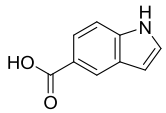	7.64	25	5203.7	5207.7
bg	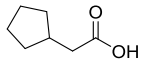	0.10	15	5170.7	5170.0
bh	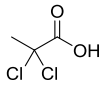	6.47	80	5185.5	5185.1
bi	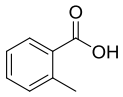	7.97	85	5178.7	5180.3
bj	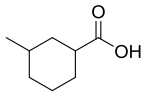	4.21	80	5184.7	5184.0
bk	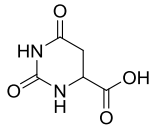	2.79	80	5200.6	5203.4
bl	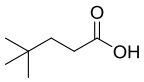	2.05	80	5172.7	5171.7
bm	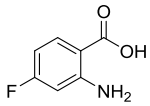	5.12	60	5197.7	5205.0
bn	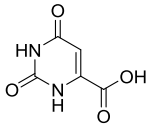	0.98	60	5198.6	5197.2
bo	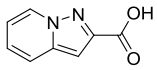	0.22	85	5204.7	5204.7
bp	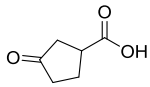	3.52	85	5170.7	5162.1
bq	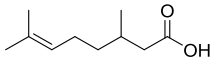	1.07	55	5212.8	5210.8
br	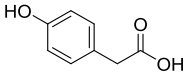	0.17	90	5194.7	5190.1
bs		5.99	80	5142.6	5144.9
bt	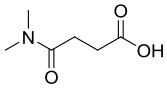	0.26	70	5187.8	5184.3

No.	structure	yield [nmol][b]	conversion[c]	mass calc.	mass found[d]
bu	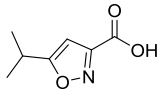	2.27	55	5197.7	5195.2
bv	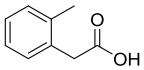	2.44	65	5192.7	5188.5
bw	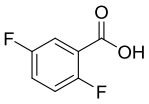	1.50	90	5200.6	5196.3
bx	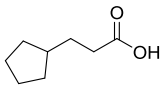	1.67	100	5184.7	5188.8
by	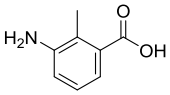	0.10	85	5193.7	5192.3
bz	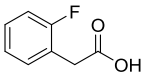	0.17	50	5196.7	5201.3
ca	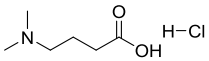	1.24	15	5210.2	5208.8
cb	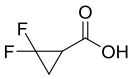	0.48	75	5164.6	5165.4
cc	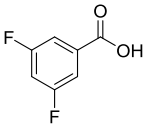	-	-	-	-
cd	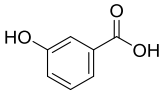	1.99	90	5180.6	5183.0
ce	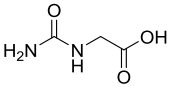	-	-	-	-
cf	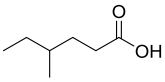	-	-	-	-
cg	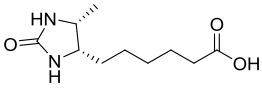	0.57	60	5258.7	5251.5
ch	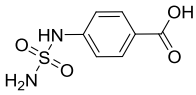	0.59	50	5256.8	5263.2
ci	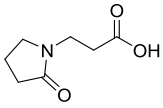	1.19	100	7947.5	7949.6

No.	structure	yield [nmol][b]	conversion[c]	mass calc.	mass found[d]
cj	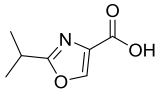	0.38	100	7945.5	7945.7
ck	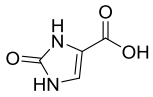	1.01	100	7907.4	7907.1
cl	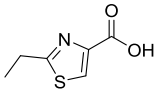	0.20	100	7936.5	7936.7
cm	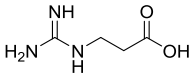	0.89	100	5173.7	5175.6
cn	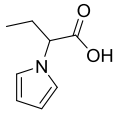	-	-	-	-
co	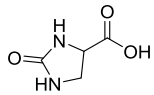	-	-	-	-
cp	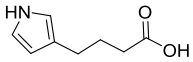	-	-	-	-

[a] **58*a*-58*g***, **58*i*-58*ab***, and **58*cp*-58*cr*** were coupled to the 23mer DNA, all other compounds were coupled to the 14mer DNA; [b] measured by Nanodrop; [c] conversion estimated based on the area under the curve of the product versus the educt in the HPLC-chromatograms, 100 %: no starting material detectable; [d] measured by MALDI-TOF/TOF-MS. Filled grey circle denotes solid support (controlled pore glass, CPG); wavy bond to DNA: 5'-(C6)-amino-PEG(4)/PEG(8) linker; bold bond: connection from the DNA oligonucleotide to the CPG.

5.3.4. Evaluation of halides for library synthesis

DEAE sepharose[57] (100 µL) was washed with 10 mM aq. NaAc buffer (2 × 350 µL) and water (2 × 350 µL). Then, 400 pmol of the DNA-alkyne conjugate **59** (sequence: 5'-GTC TTG CCG AAT TC-3') or **60** (sequence: 5'-GTC TTG CCG AAT TCC GCT TAC CG-3') was immobilized on DEAE anion exchange resin by incubation of an aqueous solution of the oligonucleotide conjugate (2 µL) with the resin for 15 min, followed by washing of the resin with 10 mM aq. NaAc buffer (2 × 350 µL), distilled water (2 × 350 µL), and MeOH/H_2O/DMF (2:2:1) mixture (2 × 350 µL). For the synthesis of the azide for *in situ*-CuAAC, 10 µmol of a halide ***1'-104'*** (Table 17) was dissolved in 800 µL of DMF in an Eppendorf tube, to this were added 100 µL of an aqueous Na-azide solution (123 µmol, 8 mg/100 µL) and 100 µL of TBAI in DMF (20 µmol, 7.5 mg/100 µL). Both Na-azide and TBAI solutions were prepared as stock solutions immediately before the substitution reaction. In order to generate the azides from halides, the reactions were shaken at room temperature for 8 hours. In case of aliphatic bromides and all chlorides, azide formation was performed at 70 °C for 4 hours. For parallel CuAAC, the DEAE sepharose carrying the oligonucleotide conjugates was suspended in 100 µL of DMF. Subsequently, 380 µL of H_2O/MeOH (1:1), the azide (1 µmol in 100 µL of DMF/H_2O (9:1), 2500 eq.), TBTA (0.026 mg in 20 µL of DMF, 0.05 µmol, 125 eq.), Na-ascorbate (0.01 mg in 10 µL of H_2O, 0.05 µmol, 125 eq.), and $CuSO_4{*}5H_2O$ (0.00125 mg in 10 µL of H_2O, 0.005 µmol, 12.5 eq.) were added to the suspension in this order. All solutions had been prepared as stock solutions immediately before the CuAAC reaction was started (TBTA: 2.9 mg in 2.2 mL of dry DMF; Na-ascorbate: 1.1 mg in 1.1 mL of distilled water; $CuSO_4{*}5H_2O$: 1.25 mg in 10 mL of distilled water). The reaction mixtures were shaken at 45 °C for overnight. Then, the DEAE sepharose was filtered over a 96well filter plate (20 µm), washed subsequently with each 3 x 200 µL of 1N aqueous EDTA, DMSO, distilled water, and 10 mM aq. NaAc buffer. After that, the oligonucleotide conjugates were eluted from DEAE sepharose into a receiver plate by shaking with 60 µL of 3 M NaAc buffer (pH= 4.75) for 30 minutes. The oligonucleotide conjugates were analyzed by MALDI-TOF/TOF-MS (Table 17).

Table 17. Evaluation of halides ***1'-104'***.

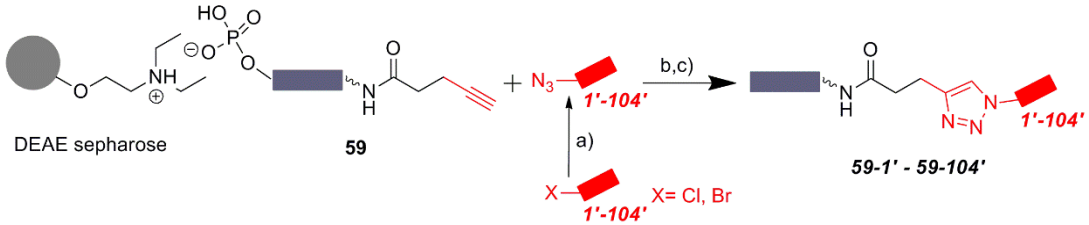

Conditions: a) NaN_3, TBAI, DMF; b) Cu(I), TBTA, Na-ascorbate, MeOH/H_2O/DMF (2:2:1), 45 °C, overnight; c) 3 M sodium acetate buffer (pH= 4.75), room temperature, 30 min.

No.	structure	halide	mass calc.	mass found[a]
1'	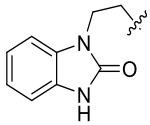	Cl	4692.1	4689.3
2'	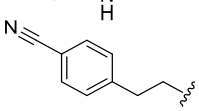	Br	4661.1	4669.0
3'	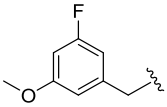	Br	4670.1	4669.0
4'	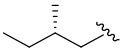	Br	4602.1	4600.0
5'	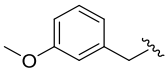	Br	4652.1	4653.0
6'	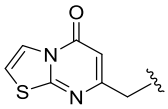	Cl	4696.1	-
7'	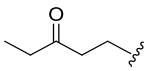	Cl	4616.0	4618.3
8'	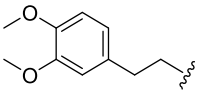	Br	4696.2	4693.0
9'	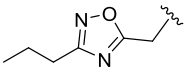	Cl	4656.1	4661.0
10' [b]	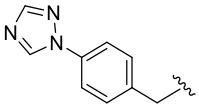	Br	4689.1	4698.0
11'	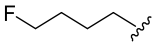	Br	4606.0	4610.0
12'	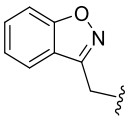	Br	4663.1	4664.0

No.	structure	halide	mass calc.	mass found[a]
13'	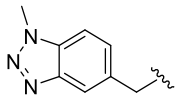	Br	4677.1	4672.1
14'	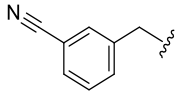	Br	4647.1	4653.0
15'	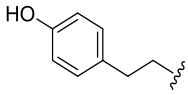	Br	4652.1	4656.7
16' [b]	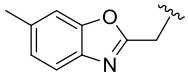	Cl	4677.1	4668.5
17'	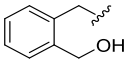	Br	4652.1	4651.3
18'	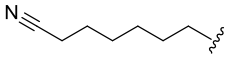	Br	4641.1	4650.0
19'	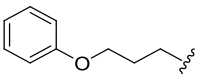	Br	4680.2	4682.5
20'	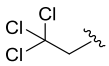	Cl	4663.4	4670.6
21'	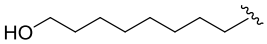	Br	4660.2	4663.0
22'		Br	4602.1	4603.5
23'	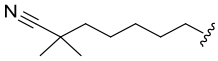	Br	4655.2	4648.0
24'	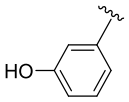	Cl	4652.1	4653.9
25'	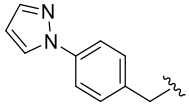	Br	4688.1	4693.6
26'	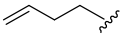	Br	4586.0	4583.1
27'	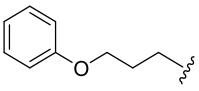	Br	4666.1	4654.3

No.	structure	halide	mass calc.	mass found[a]
28'	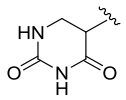	Br	4644.0	4647.6
29'	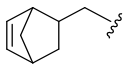	Cl	4638.1	4639.4
30'		Br	4588.0	4599.4
31'	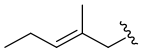	Br	4614.1	4619.3
32'	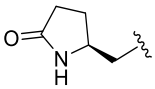	Br	4629.1	4629.9
33'	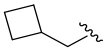	Br	4600.1	4581.6
34'	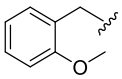	Cl	4651.8	4657.8
35'	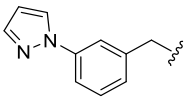	Cl	4688.1	4686.9
36'		Br	4616.1	4626.4
37'	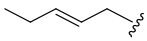	Br	4600.1	4600.2
38' [b]	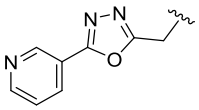	Cl	4691.1	4691.9
39'	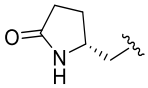	Br	4629.1	4637.4
40'	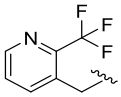	Cl	4691.1	4691.5
41'	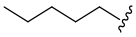	Br	4602.1	4602.8
42'	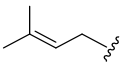	Br	4600.1	4599.8

No.	structure	halide	mass calc.	mass found[a]
43'	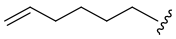	Br	4599.1	4600.4
44' [b]	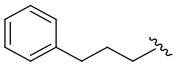	Cl	4650.1	4649.3
45'	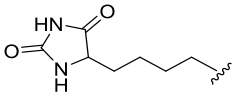	Br	4686.1	4679.0
46'	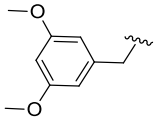	Br	4682.1	4683.1
47'	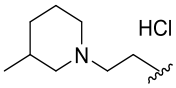	Cl	4693.6	4691.5
48'	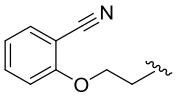	Br	4677.1	4675.2
49'	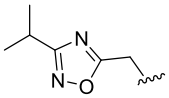	Cl	4656.1	4644.2
50'	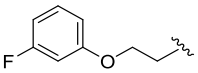	Br	4670.5	4670.5
51' [b]	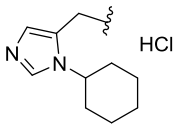	Cl	4731.0	4731.8
52'	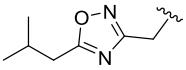	Cl	4670.1	4670.2
53' [b]	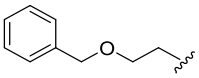	Cl	4710.6	4710.9
54'	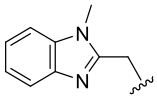	Br	4676.1	4676.9
55'	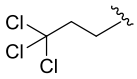	Br	4677.4	4677.1
56'	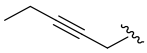	Br	4598.1	4598.1
57'	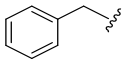	Br	4622.1	4622.4

No.	structure	halide	mass calc.	mass found[a]
58'	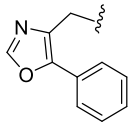	Br	4689.1	4689.1
59'	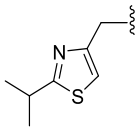	Cl	4671.2	4671.3
60'	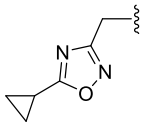	Cl	4654.1	4654.6
61'	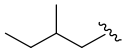	Br	4602.1	4602.4
62' [b]	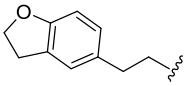	Br	4678.1	4672.0
63'	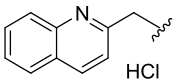	Cl	4673.1	4673.1
64'	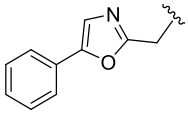	Cl	4689.1	4694.5
65'	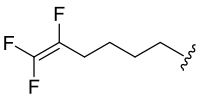	Br	4668.0	4667.8
66'	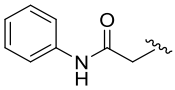	Br	4665.1	4666.2
67'	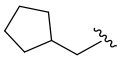	Br	4614.1	4626.7
68' [b]	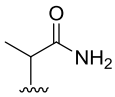	Br	4603.0	4602.6
69'	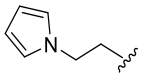	Br	4625.1	4625.1
70'	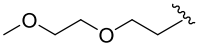	Br	4634.1	4622.8
71'	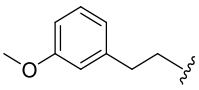	Br	4666.1	4666.5
72'	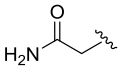	Br	4589.0	4585.2

No.	structure	halide	mass calc.	mass found[a]
73'	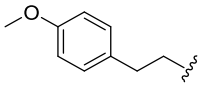	Cl	4666.1	4664.7
74'	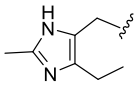	Cl	4654.1	4655.1
75' [b]	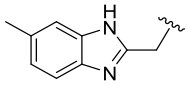	Cl	4676.1	4665.1
76' [b]		Br	4571.0	4571.1
77' [b]	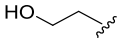	Br	4576.0	4574.1
78'	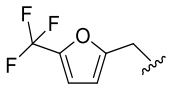	Br	4680.0	4680.2
79'	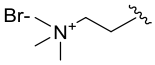	Br	4603.1	4592.1
80'	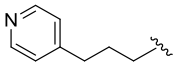	Cl	4651.1	4650.2
81'	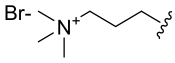	Br	4632.1	4630.5
82'	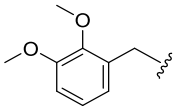	Cl	4682.1	4686.2
83'	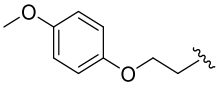	Br	4682.1	4683.3
84'	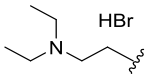	Br	4631.1	4637.1
85'	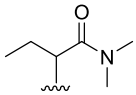	Br	4645.1	4646.1
86'	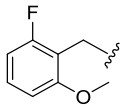	Br	4670.1	4671.0
87'	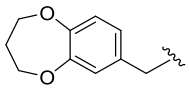	Cl	4694.1	-

No.	structure	halide	mass calc.	mass found[a]
88'	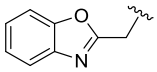	Cl	4663.0	4660.1
89'	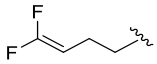	Br	4622.0	4613.2
90'	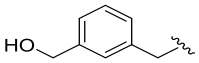	Br	4652.1	4655.2
91'	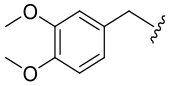	Cl	4682.1	4682.7
92'	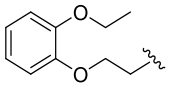	Br	4696.1	4698.2
93'	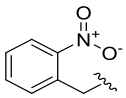	Br	4667.1	4670.3
94'	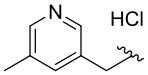	Cl	4637.1	4638.0
95'	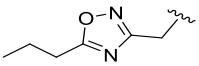	Cl	4656.1	4634.7
96'	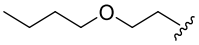	Cl	4632.1	4630.8
97'	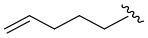	Br	4600.0	4609.3
98'	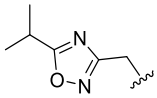	Cl	4656.1	4655.1
99'	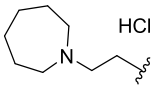	Cl	4657.1	4655.3
100'	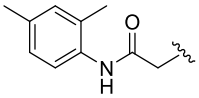	Br	4693.1	4665.0
101' [b]	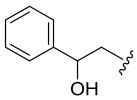	Br	4652.1	4658.0
102' [b]	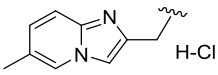	Cl	4676.1	4675.0

No.	structure	halide	mass calc.	mass found[a]
103'	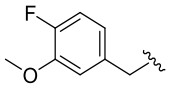	Br	4670.1	4665.4
104' [b]	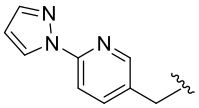	Cl	4689.1	4690.0

[a] measured by MALDI-TOF/TOF-MS; [b] incomplete conversion, more than 50 % conversion as estimated by MALDI-TOF/TOF-MS analysis.

5.3.5. Synthesis of the DNA-Encoded Library based on the pyrazolopyrimidine scaffold

DNA-small molecule conjugates were enzymatically encoded with T4-DNA ligase.[189] After that, DEAE sepharose (50 µL) was pipeted into 102 wells (102 x 50 µL) of a two 96well plates, washed with 10 mM aq. NaAc buffer (2 × 350 µL) and water (2 × 350 µL). Then, 20 pmol of pooled and encoded DNA small molecule conjugates **58*a*-58*cp*** (Table 16) was immobilized on DEAE anion exchange resin by incubation of an aqueous solution of the oligonucleotide conjugate (2 µL) with the resin for 15 min, followed by washing of the resin with 10 mM aq. NaAc buffer (2 × 350 µL), distilled water (2 × 350 µL), and MeOH/H_2O/DMF (2:2:1) mixture (2 × 350 µL). For the synthesis of the azide for *in situ*-CuAAC, 500 nmol of a halide ***1'-102'*** (Table 17) was dissolved in 40 µL of dry DMF in an Eppendorf tube, to this were added 5 µL of an aqueous Na-azide solution (61.5 µmol, 4 mg/5 µL, taken from a stock solution: 6273 µmol, 408 mg in 510 µL of distilled water) and 5 µL of TBAI in DMF (1 µmol, 0.37 mg/5 µL, taken from a stock solution: 102 µmol, 37.7 mg in 510 µL of dry DMF). Both Na-azide and TBAI solutions were prepared as stock solutions immediately before the substitution reaction. In order to generate the azide from halide, the reaction was shaken for 8 hours at room temeperature. In case of aliphatic bromides and all chlorides, azide formation was performed for 4 hours at 70 °C. For parallel CuAAC, the DEAE sepharose from each well carrying the DNA small molecule conjugates **58*a*-58*cp*** was suspended in 50 µL of dry DMF and transported each well into each glass vial. Subsequently, 190 µL of H_2O/MeOH (1:1), the azide (50 nmol in 5 µL of DMF/H_2O (9:1), 2500 eq.), TBTA (0.0013 mg in 1 µL of DMF, 2.5 nmol, 125 eq.), Na-ascorbate (0.0005 mg in 0.5 µL of H_2O, 2.5 nmol, 125 eq.), and $CuSO_4{*}5H_2O$ (0.0000625 mg in 0.5 µL of distilled water, 250 pmol, 12.5 eq.) were added to the suspension of DNA-small molecule conjugates in this order. All solutions had been prepared as stock solutions immediately before the CuAAC reaction was started (TBTA: 1.3 mg in 1 mL of dry DMF; Na-ascorbate: 5 mg in 5 mL of distilled water; $CuSO_4{*}5H_2O$: 1.25 mg in 10 mL of distilled water). The reaction mixtures were shaken in a glass well shaker at 45 °C for overnight. Then, the DEAE sepharose was transferred to a 96well filter plate, and washed subsequently with each 3 x 200 µL of DMF, 0.1 N aqueous EDTA to remove the copper-ion contaminants, MeOH/H_2O/DMF (2:2:1) mixture, water, and 10 mM aq. NaAc buffer. After that, the oligonucleotide conjugates were eluted from DEAE sepharose by shaking with 60 µL of 3 M

NaAc buffer (pH= 4.75) for 30 minutes and filtered directly from the filter plate into a 96well deep well plate. The products of the CuAAC were pooled and precipitated twice from ethanol at -80 °C.

5.3.6. Synthesis and characterization of the pyrazolopyrimidine scaffold

3-Iodo-1H-pyrazolo[3,4-d]pyrimidin-4-amine 55

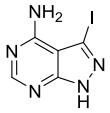

A solution of 3*H*-pyrazolo[3,4-d]pyrimidine-4-amine **54** (3.2 g, 23.68 mmol, 1.0 eq.) and *N*-iodo-succinimide (8 g, 35.5 mmol, 1.5 eq.) in DMF (26 mL) was stirred at 80 °C for 14 hours. The resulting product **55** precipitated from the solution. It was filtered off, rinsed with cold EtOH and dried *in vacuo* (4.7 g, 76 % yield). ^{1}H NMR (400 MHz, DMSO-d_6): δ 13.82 (s, 1H), 8.17 (s, 1H), 7.81 (br. s, 1H), 6.69 (br. s, 1H). ^{13}C-NMR (101 MHz, DMSO-d_6): δ 157.6, 156.1, 155.0, 102.5, 89.8. LC-MS (ESI) *m*/*z* Calcd. for [$C_5H_5IN_5$, M+H] $^{+}$: 261.96, found 262.02. Purity (HPLC): 97 %.

(*S*)-*tert*-Butyl 3-(4-amino-3-iodo-1*H*-pyrazolo[3,4-d]pyrimidin-1-yl)-2-((*tert*-butoxycarbonyl)amino)propanoate 56

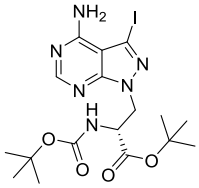

To a solution of **55** (350 mg, 1.3 mmol, 1.0 eq.) in dry THF (83 mL), triphenyl phosphine (703 mg, 2.7 mmol, 2.0 eq.), diisopropyldiazene-1,2-dicarboxylate (528 µL, 2.7 mmol, 2.0 eq.) and the protected (*S*)-serine (700 mg, 2.7 mmol, 2.0 eq.) were added. The reaction mixture was stirred under argon atmosphere at room temperature for 16 hours. The reaction was concentrated *in vacuo* and the product was purified by silica gel column chromatography (solvent system: hexanes/ ethyl acetate 60:40 to 20:80) to provide compound **56** (394 mg, 58 % yield). ^{1}H NMR (500 MHz, DMSO-d_6): δ 8.20 (s, 1H), 7.77 (br. s, 1H), 7.21 (d, ^{3}J= 8.1 Hz, 1H), 6.68 (br. s, 1H), 4.59 (d, ^{3}J= 6.9 Hz, 1H), 4.48 (d, ^{3}J= 6.9 Hz, 1H), 4.39 (q, ^{3}J= 7.3 Hz, 1H), 1.35 (s, 9H), 1.23 (s, 9H). ^{13}C-NMR (126 MHz, DMSO-d_6): δ 168.2, 158.1, 156.0, 155.4, 153.1, 100.1, 93.3, 82.5, 78.1, 53.3, 48.0, 28.1, 27.2. LC-MS (ESI) *m*/*z* Calcd. for [$C_{17}H_{26}IN_6O_4$, M+H] $^{+}$: 505.11, found 505.05; *m*/*z* Calcd. for [$C_{17}H_{25}IN_6NaO_4$, M+Na] $^{+}$: 527.09, found: 527.05. Purity (HPLC): 90 %.

(*S*)-*tert*-Butyl 3-(4-amino-3-((trimethylsilyl)ethynyl)-1*H*-pyrazolo[3,4-d]pyrimidin-1-yl)-2-((*tert*-butoxycarbonyl)amino)propanoate 57

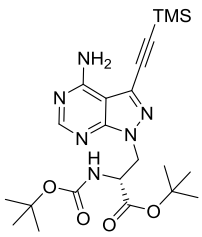

To a solution of compound **56** (394 mg, 0.78 mmol, 1.0 eq.) in dry DMF (10 mL), copper(I) iodide (30 mg, 0.15 mmol, 0.2 eq.), tetrakis(triphenylphosphine)palladium(0) (135 mg, 0.12 mmol, 0.15 eq.), triethylamine (436 µL, 3.12 mmol, 4.0 eq.) and trimethylsilylacetylene (2224 µL, 15.6 mmol, 20.0 eq.) were added. The reaction mixture was stirred under argon at room temperature for 18 hours. The reaction was concentrated *in vacuo* to a residue and the title compound was purified by silica gel column chromatography (solvent system: CH_2Cl_2/ MeOH 100:0 to 95:5) to provide the title compound **57** (285 mg, 77 % yield). ^{1}H NMR (500 MHz, DMSO-d$_6$): δ 8.24 (s, 1H), 7.78 (br. s, 1H), 7.19 (d, ^3J= 8.4 Hz, 1H), 6.28 (br. s, 1 H), 4.62 (d, ^3J= 6.1 Hz, 1H), 4.47 (d, ^3J= 7.7 Hz, 1H), 4.39 (q, ^3J= 7.4 Hz, 1H), 1.33 (s, 9H), 1.26 (s, 9H), 0.28 (s, 9H). ^{13}C-NMR (126 MHz, DMSO-d$_6$): δ 168.7, 157.6, 156.5, 154.9, 153.4, 128.3, 100.7, 81.0, 78.4, 53.4, 47.3, 28.0, 27.3, -0.5, signals for the ethinyl-carbons were not visible in the spectrum. LC-MS (ESI) *m*/*z* Calcd. for [$C_{22}H_{35}N_6O_4Si$, M+H] $^+$: 475.25, found 475.25; *m*/*z* Calcd. for [$C_{22}H_{34}N_6NaO_4Si$, M+Na] $^+$: 497.23, found: 497.25. Purity (HPLC): 98 %.

3-(4-Amino-3-ethynyl-1*H*-pyrazolo[3,4-d]pyrimidin-1-yl)-2-((*tert*-butoxycarbonyl)amino)propanoic acid 57a

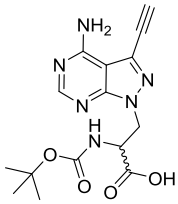

To a solution of compound **57** (270 mg, 0.56 mmol, 1.0 eq.) in MeOH (10 mL), potassium carbonate (102 mg, 0.72 mmol, 1.3 eq.) was added. The reaction mixture was stirred at room temperature for 24 hours. The consumption of starting material was monitored by TLC. Then, water (30 mL) was added and the solution was acidified to pH 6 with 1N aqueous HCl solution and the product was extracted with EtOAc (3 x 30 mL). The organic layers were combined, dried over anhydrous Na_2SO_4 and concentrated *in vacuo*. Purification by silica gel column chromatography (solvent system: CH_2Cl_2/ MeOH 80:20 to 50:50) yielded compound **57a** (140 mg, 71 % yield). LC-MS (ESI) *m*/*z* Calcd. for [$C_{15}H_{19}N_6O_4$, M+H] $^+$: 347.15, found 346.98. Purity (HPLC): 93 %.

2-Amino-3-(4-amino-3-ethynyl-1*H*-pyrazolo[3,4-d]pyrimidin-1-yl)propanoic acid 57b

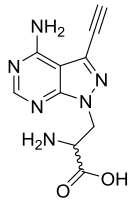

To a solution of compound **57a** (150 mg, 0.43 mmol, 1.0 eq.) in dry CH_2Cl_2 (8 mL), 1 mL of TFA was added. The reaction mixture was stirred at the room temperature for 20 hours. The consumption of the starting material was monitored by TLC. Then, the reaction mixture was evaporated *in vacuo* and co-evaporated with acetonitrile until TFA was completely removed. Compound **57b** (100 mg, 94 % yield) was used in the next step without further purification. LC-MS (ESI) *m*/*z* Calcd. for $[C_{10}H_{11}N_6O_2, M+H]^+$: 247.09, found 247.10. Purity (HPLC): 99 %.

2-((((9*H*-Fluoren-9-yl)methoxy)carbonyl)amino)-3-(4-amino-3-ethynyl-1*H*-pyrazolo[3,4-d]pyrimidin-1-yl)propanoic acid 53

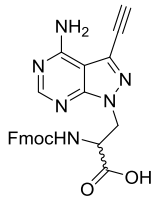

Compound **57b** (100 mg, 0.41 mmol, 1.0 eq.) was dissolved in water (1.4 mL) and sodium bicarbonate (68.2 mg, 0.81 mmol, 2.0 eq.) was added with stirring. The solution was cooled to 0 °C and *N*-(9-fluorenylmethoxycarbonyloxy)-succinimide (205 mg, 0.61 mmol, 1.5 eq.), pre-dissolved in 1,4-dioxane (1.4 mL), was added slowly. The reaction mixture was stirred at 0 °C for 1 hour and at room temperature for 20 hours. Then, water (20 mL) was added and the product was extracted with EtOAc (3 x 20 mL). The organic layers were combined and back extracted with sat. aqueous $NaHCO_3$ solution (60 mL). The aqueous solution was acidified to pH 1 with 10 % aq. HCl, and extracted with EtOAc (3 x 40 mL). The combined organic layers were dried over anhydrous $MgSO_4$ and concentrated *in vacuo*. The crude material was purified by column chromatography (solvent system: CH_2Cl_2/ MeOH 100:0 to 65:35) to provide **53** (135 mg, 71 % yield). ^{1}H NMR (500 MHz, DMSO-d_6): δ 8.17 (s, 1H), 7.86 (d, ^3J= 7.6 Hz, 2H), 7.54 (2 x d, ^3J= 7.6 Hz, and ^3J= 7.5 Hz, 2H), 7.39 (m, 2H), 7.28 (2 x d, ^3J= 7.9 Hz, 2H), 4.75-4.70 (m, 1H), 4.64-4.59 (s, 1H), 4.56-4.51 (m, 1H), 4.35-4.31 (m, 1H), 4.20-4.18 (m, 2H), 4.16-4.13 (m, 1H). ^{13}C-NMR (126 MHz, DMSO-d_6): δ 171.06, 156.6, 156.0, 155.2, 153.3, 143.8, 140.8, 127.8, 127.3, 125.9, 125.4, 125.3, 120.3, 101.0, 86.9, 74.9, 66.0, 53.4, 47.7, 46.6. LC-MS (ESI) *m*/*z* Calcd. for $[C_{25}H_{21}N_6O_4, M+H]^+$: 469.16, found 469.10. Purity (HPLC): 99 %. In the NMR spectrum of the title compound we observed two sets of signals that indicate racemization of the amino acid. Racemization of amino acids is reported to occur under basic conditions that we applied for the synthesis of compound **57a**.

5.4. Synthesis of the oligothymidine-initiated DNA-Encoded Library based on the pyrazol(in)e scaffold

5.4.1. Synthesis of the hexathymidine-alkyne conjugate

The pegylated hexT (1 µmol, ca. 36 mg) was coupled with *p*-ethynylbenzoic acid **133** (14.6 mg, 100 µmol, 100 eq.) to furnish **hexT-87** according to the procedure for coupling of carboxylic acids to 5'-amino-linker modified DNA. For analysis, an aliquot of ca. 10 nmol of conjugate **hexT-87** was deprotected and cleaved from the CPG with 500 µL of AMA (AMA= aqueous ammonia (30 %)/ aqueous methylamine (40 %), 1:1, vol/vol) for 30 min at room temperature. Then, 20 µL of 1 M Tris buffer (pH= 7.5) were added, the mixture was dried in a SpeedVac, re-dissolved in 100 µL of distilled water, and the product was analyzed by RP-HPLC (Gemini, 5u, C18, 110A column; 100*10.0 mm) with a gradient of aqueous triethylammonium acetate buffer (100 mM, pH= 8) and methanol (20 % – 70 % of methanol over 19 min).

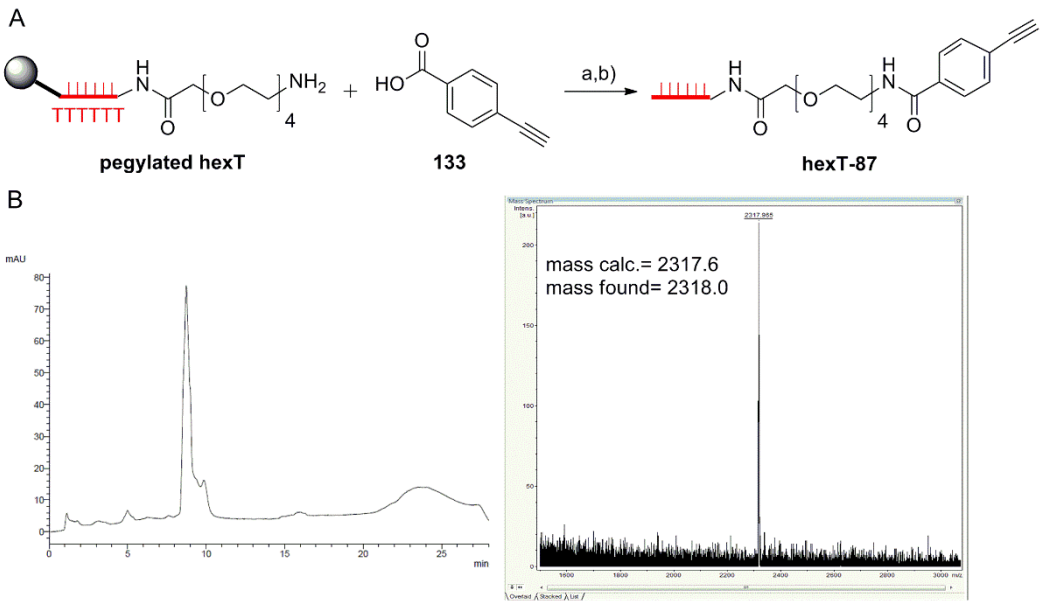

Figure 5.1. Synthesis of hexT-alkyne conjugate **hexT-87**. A) Reaction scheme of alkyne **hexT-87** formation. Reagents and conditions: a) HATU, DIPEA, dry DMF, room temperature, 4 hours; b) AMA (aqueous ammonia (30 %)/ aqueous methylamine (40 %)= 1:1, vol/vol), 30 min, room temperature. B) HPLC trace and MALDI-TOF/TOF-MS spectrum of **hexT-87**. Filled grey circle denotes solid support (controlled pore glass, CPG); wavy bond to hexT: 5'-(C6)-amino-linker; bold bond: connection from the hexT-oligonucleotide to the CPG.

5.4.2. Optimization of reaction conditions of the Au(I)-mediated annulation reaction

The solid support containing the hexathymidine-alkyne conjugate **hexT-87** (30 nmol, ca. 1.1 mg, the PEG linker is missing in this compound) was suspended in 30 µL of a solvent (Table 6). Then, hydrazide **88** and aldehyde **T**, each 30 µmol, dissolved in 30 µL of the same solvent (prepared as stock) were added to **hexT-87**. This was followed by an equimolar mixture of either catalyst ***A-C***/AgOTf or ***A-C***/$AgSbF_6$ at the amounts given in Table 6 which were suspended (***A-C***) or dissolved (AgOTf or $AgSbF_6$), respectively in 30 µL of the same solvent. The suspensions of the catalysts were prepared as stocks. Prior addition to **hexT-87** these were vortexed and pipetted up and down to add a homogeneous suspension. The reactions were shaken at the indicated temperatures overnight in Eppendorf tubes or in sealed 96well deep well plates. The reactions were neither run under protective gas nor were molecular sieves used. Then, the CPG was filtered off, washed with each 3 x 200 µL of 0.1 M EDTA, DMF, MeOH, MeCN, and CH_2Cl_2, and dried *in vacuo* for 15 min. The hexT conjugates were deprotected and cleaved from the CPG by treatment with 500 µL of AMA (AMA= aqueous ammonia (30 %)/ aqueous methylamine (40 %)= 1:1, vol/vol) for 30 minutes at room temperature. Samples were filtered directly from a filter plate into a 96well deep well plate. Then, 20 µL of 1 M Tris buffer (pH= 7.5) were added, the mixtures were dried in a SpeedVac, re-dissolved in 100 µL of distilled water, and all coupling products were purified by RP-HPLC (Gemini, 5u, C18, 110A column; 100*10.0 mm) with a gradient of aqueous triethylammonium acetate buffer (100 mM, pH= 8) and methanol (20 % – 70 % of methanol over 19 min). Fractions containing the product were collected, evaporated in a SpeedVac, co-evaporated with 3 x 200 µL of ethanol/distilled water (1:1) and analyzed by MALDI-TOF/TOF-MS analysis and by analytical HPLC.

5.4.3. Au(I)-mediated annulation reaction to hexathymidine-pyrazol(in)e conjugates

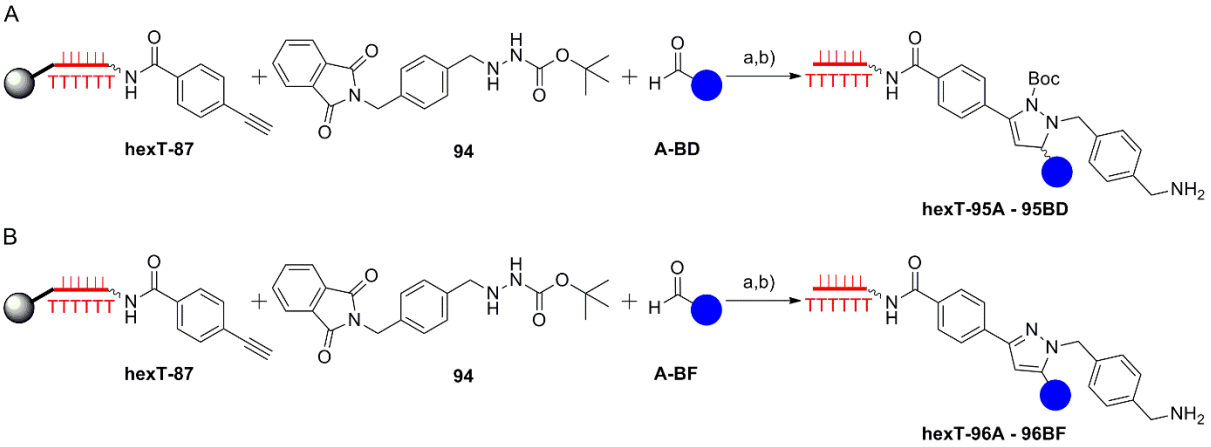

Figure 5.2. A) Synthesis of a pyrazoline library **hexT-95A - 95BD**; a) method **A** (Table 6b, entry 5) for aliphatic aldehydes; method **B** (Table 6c, entry 10) for aromatic aldehydes; b) AMA (aqueous ammonia (30 %)/ aqueous methylamine (40 %), 1:1, vol/vol), 30 min, room temperature; B) Synthesis of a pyrazole library **hexT-96A - 96BF**; c) method **C** (Table 6c, entry 11). Filled grey circle denotes solid support (controlled pore glass, CPG); wavy bond to hexT: 5'-(C6)-amino-PEG(4) linker; bold bond: connection from the hexT-oligonucleotide to the CPG.

Method A (Table 6b, entry 5): The solid support with the hexT conjugate **hexT-87**, aldehydes **A - BD** (Table 18), and hydrazide **94**, catalyst ***A*** (Fig. 3.15), and $AgSbF_6$ (each 12.5 µmol, 250 eq.) were dried *in vacuo* for 15 min. Then, a batch of solid support containing hexT conjugate **hexT-87** (18 mg, ca. 500 nmol) was suspended in 330 µL of dry MeCN. This suspension was distributed to a total of 10 reaction vessels of a 96well plate, so that each reaction vessel contained ca. 50 nmol of **hexT-87** suspended in 30 µL of dry MeCN. Then, 10 aldehydes from **A - BD** (50 µmol, 1000 eq.) each dissolved in 30 µL of dry MeCN were added to the split hexT conjugate **hexT-87**. To these suspensions were added hydrazide **94** (50 µmol, 1000 eq.) dissolved in 30 µL of dry MeCN (taken from a stock solution: 2750 µmol, 1048.9 mg in 1650 µL of dry MeCN) and the catalyst ***A***/$AgSbF_6$ (12.5 µmol, 250 eq.) suspended in 30 µL of dry MeCN (taken from a stock solution: 687.5 µmol, 604.5 mg of catalyst ***A*** and 236.1 mg of $AgSbF_6$ mixed in 1650 µL of dry MeCN) giving a total reaction volume of ca. 120 µL. The reaction mixtures were shaken at 50 °C overnight. The solid phase containing the pyrazolines **hexT-95A - 95BD** was filtered off on a filter plate and washed subsequently with each 3 x 200 µL of 0.1 M EDTA, DMF, MeOH, MeCN, and CH_2Cl_2, and

dried *in vacuo* for 15 min. Then, the hexT-pyrazoline conjugates **hexT-95A - 95BD** were deprotected and cleaved from the CPG with 500 µL of AMA (AMA= aqueous ammonia (30 %)/ aqueous methylamine (40 %)= 1:1, vol/vol) for 30 minutes at room temperature. The samples were filtered directly on a filter plate into a 96-deep well plate. Then, 20 µL of 1 M Tris buffer (pH= 7.5) were added, the mixtures were dried in a SpeedVac, re-dissolved in 100 µL of distilled water, and all coupling products were purified by RP-HPLC (Gemini, 5u, C18, 110A column; 100*10.0 mm) with a gradient of aqueous triethylammonium acetate buffer (100 mM, pH= 8) and methanol (20 % – 70 % of methanol over 19 min). Fractions containing the product were collected, evaporated in a SpeedVac, co-evaporated with 3 x 200 µL of ethanol/distilled water (1:1) and analyzed by MALDI-TOF/TOF-MS analysis and by analytical HPLC to assert purity and identity.

Method B (Table 6c, entry 10)**:** The solid support with the hexT conjugate **hexT-87**, aldehydes (Table 18) (each 50 µmol, 1000 eq.), hydrazide **94**, catalyst ***B*** (Fig. 3.15), and AgOTf were dried *in vacuo* for 15 min. Then, a batch of solid support containing hexT conjugate **hexT-87** (18 mg, ca. 500 nmol) was suspended in 330 µL of glacial acetic acid. This suspension was distributed to a total of 10 reaction vessels of a 96well plate, so that each reaction vessel contained ca. 50 nmol of a hexT conjugate **hexT-87** suspended in 30 µL of glacial acetic acid. Then, 10 aldehydes from **A - BD** (50 µmol, 1000 eq.) each dissolved in 30 µL of glacial acetic acid were added to the split hexT conjugate **hexT-87**. To these suspensions were added hydrazide **94** (50 µmol, 1000 eq.) dissolved in 30 µL of glacial acetic acid (taken from a stock solution: 2750 µmol, 1048.9 mg in 1650 µL of glacial acetic acid), and catalyst ***B***/AgOTf (12.5 µmol, 250 eq.) suspended in 30 µL of glacial acetic acid (taken from a stock solution: 687.5 µmol, 340.1 mg of catalyst ***B*** and 176.6 mg of AgOTf mixed in 1650 µL of glacial acetic acid) giving a total reaction volume of ca. 120 µL. The reaction mixtures were shaken at 50 °C overnight. The solid phase containing the pyrazolines **hexT-95A - 95BD** was filtered off on a filter plate and washed subsequently with each 3 x 200 µL of 0.1 M EDTA, DMF, MeOH, MeCN, and CH_2Cl_2, and dried *in vacuo* for 15 min. Then, the hexT-pyrazolines **hexT-95A - 95BD** were deprotected and cleaved from the CPG by treatment with 500 µL of AMA (AMA= aqueous ammonia (30 %)/ aqueous methylamine (40 %)= 1:1, vol/vol) for 30 minutes at room temperature. Samples were filtered directly from a filter plate into a 96-deep well plate. Then, 20 µL of 1 M Tris buffer (pH= 7.5) were added, the mixtures were dried in a SpeedVac, re-dissolved in 100 µL of distilled water, and all

coupling products were purified by RP-HPLC (Gemini, 5u, C18, 110A column; 100*10.0 mm) with a gradient of aqueous triethylammonium acetate buffer (100 mM, pH= 8) and methanol (20 % – 70 % of methanol over 19 min). Fractions containing the product were collected, evaporated in a SpeedVac, co-evaporated with 3 x 200 µL of ethanol/distilled water (1:1) and analyzed by MALDI-TOF/TOF-MS analysis and by analytical HPLC to assert purity and identity.

Method C (Table 6c, entry 11): as method **B**, reactions run at 60 °C.

Table 18. Yield and MALDI-TOF/TOF-MS data of compounds **hexT-95A - 95BD**.

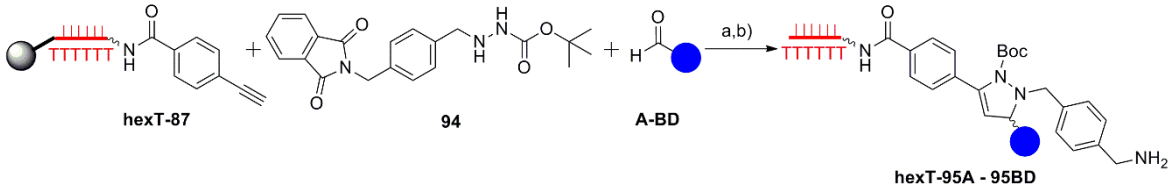

Conditions: a) method **A** (Table 6b, entry 5), b) AMA (aqueous ammonia (30 %)/ aqueous methylamine (40 %), 1:1, vol/vol), 30 min, room temperature.

No.	structure	yield [nmol][a]	mass calc.	mass found[b]
A	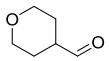	3.8	2665.1	2664.9[c]
C	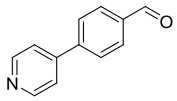	1.0	2734.2	2733.7[d]
E	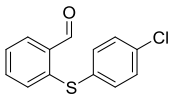	1.7	2799.7	2800.8[d]
F	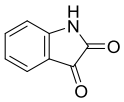	0.6	2698.1	2699.1[d]
I	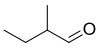	2.7	2637.1	2636.1[c]
J	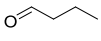	-	-	-
M	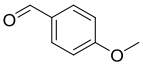	0.7	2687.1	2687.8[d]
N	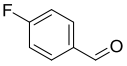	0.7	2675.1	2675.9[d]
T		4.9	2623.1	2623.7[c]
V	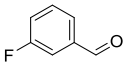	0.7	2675.1	2675.2[d]
W	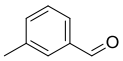	0.9	2671.1	2671.8[d]
AB	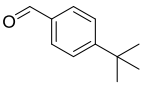	0.6	2713.2	2714.0[d]

No.	structure	yield [nmol][a]	mass calc.	mass found[b]
AD	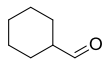	2.7	2663.1[c]	2663.5[c]
AE	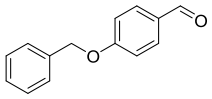	0.9	2763.2	2763.0[d]
AF	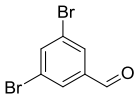	0.4	2814.9	2815.4[d]
AG	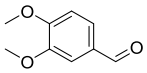	0.9	2717.1	2718.1[d]
AI	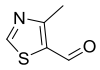	5.2	2678.1	2678.4[d]
AJ	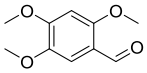	0.5	2747.2	2747.9[d]
AL	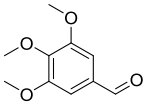	0.8	2747.2	2748.5[d]
AM	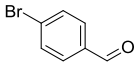	0.9	2736.0	2736.3[d]
AO		2.1	2651.1	2651.6[c]
BA	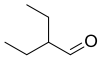	3.5	2651.1	2651.7[c]
BB		0.8	2621.0	2620.4[c]
BD		4.5	2649.1	2649.1[c]

[a] measured by Nanodrop; [b] measured by MALDI-TOF/TOF-MS; [c] synthesized according to the method **A** (Table 6); [d] synthesized according to the method **B** (Table 6). Filled grey circle denotes solid support (controlled pore glass, CPG); wavy bond to hexT: 5'-(C6)-amino-PEG(4) linker; bold bond: connection from the hexT-oligonucleotide to the CPG.

Table 19. Yield and MALDI-TOF/TOF-MS data of compounds **hexT-96A - 96BF**.

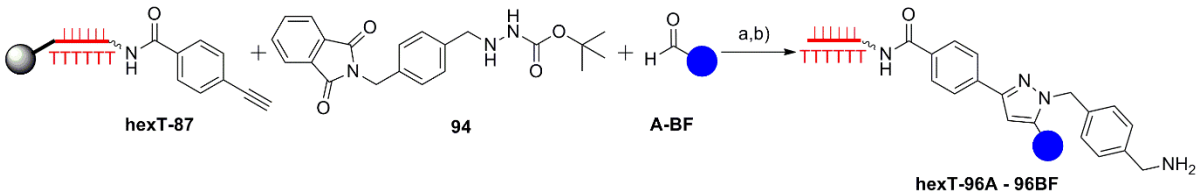

Conditions: a) method **C** (Table 6c, entry 11), b) AMA (aqueous ammonia (30 %)/ aqueous methylamine (40 %), 1:1, vol/vol), 30 min, room temperature.

No.	structure	yield [nmol][a]	mass calc.	mass found[b]
A	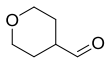	4.3	2563.0	2564.1
B	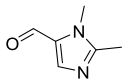	-	-	-
C	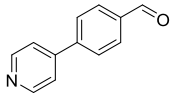	1.7	2632.0	2633.6
D	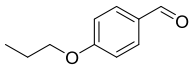	1.5	2613.0	2617.4
E	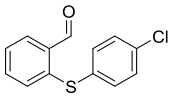	2.4	2697.5	2699.4
F[c]	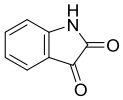	1.1	2598.0	2598.4
G	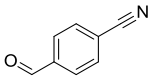	2.3	2580.0	2585.3
H	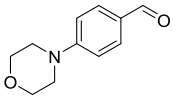	-	-	-
I		1.8	2535.0	2535.2
J	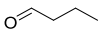	-	-	-
K	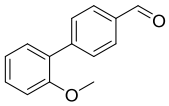	0.7	2661.1	2661.1
L	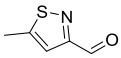	3.0	2576.0	2578.2

No.	structure	yield [nmol][a]	mass calc.	mass found[b]
M	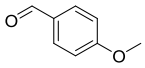	1.1	2585.0	2586.8
N	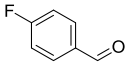	1.9	2573.0	2574.5
O	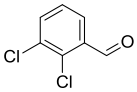	0.5	2623.8	2628.1
P	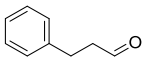	-	-	-
Q		-	-	-
R		-	-	-
S	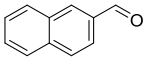	1.4	2605.0	2605.9
T		5.0	2520.9	2520.9
U	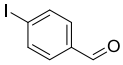	0.4	2680.8	2680.4
V	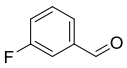	1.7	2573.0	2572.1
W	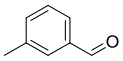	3.3	2569.0	2569.5
X	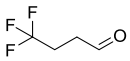	-	-	-
Y	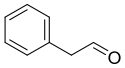	-	-	-
Z	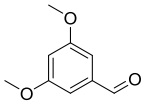	2.9	2615.0	2616.4
AA	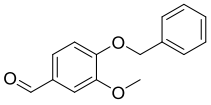	1.0	2691.1	2692.4

No.	structure	yield [nmol][a]	mass calc.	mass found[b]
AB	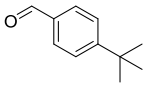	1.4	2611.0	2610.8
AC	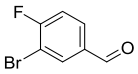	3.6	2651.8	2655.6
AD	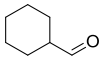	2.8	2561.0	2561.3
AE	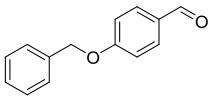	1.3	2661.1	2661.8
AF	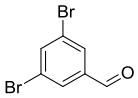	0.6	2712.7	2715.1
AG	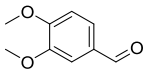	0.9	2615.0	2613.7
AH	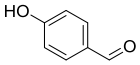	-	-	-
AI		7.0	2576.0	2578.1
AJ	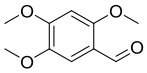	0.9	2645.0	2645.4
AK	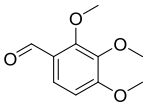	0.6	2645.0	2643.9
AL	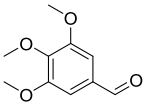	2.8	2645.0	2646.9
AM	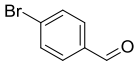	2.1	2633.8	2635.9
AN	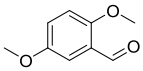	1.4	2615.0	2618.6
AO		2.1	2548.9	2552.7

No.	structure	yield [nmol][a]	mass calc.	mass found[b]
AP	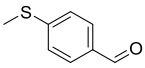	1.1	2601.0	2601.2
AQ	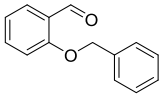	1.9	2661.1	2661.1
AR	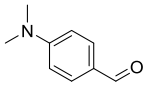	1.3	2598.0	2599.5
AS	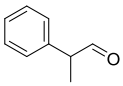	-	-	-
AT	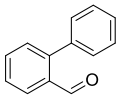	2.0	2631.0	2634.9
AU		4.5	2561.0	2561.5
AV	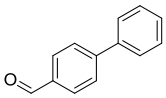	3.0	2631.0	2632.5
AW	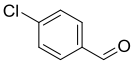	2.6	2589.4	2590.6
AX	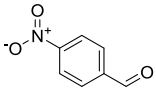	1.2	2600.0	2601.7
AY		1.3	2554.9	2554.2
AZ	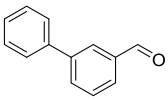	3.1	2631.0	2630.6
BA	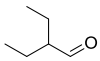	4.5	2549.0	2548.7
BB		1.1	2518.9	2518.7
BC	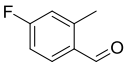	0.9	2587.0	2587.2

No.	structure	yield [nmol][a]	mass calc.	mass found[b]
BD		3.3	2547.0	2549.0
BE	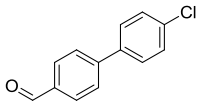	1.1	2665.5	2666.5
BF	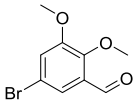	2.2	2693.9	2697.7

[a] measured by Nanodrop; [b] measured by MALDI-TOF/TOF-MS; [c] Boc-deprotected pyrazoline was obtained. Filled grey circle denotes solid support (controlled pore glass, CPG); wavy bond to hexT: 5'-(C6)-amino-PEG(4) linker; bold bond: connection from the hexT-oligonucleotide to the CPG.

5.4.4. HPLC chromatograms and MALDI-MS spectra of 20 representative library members

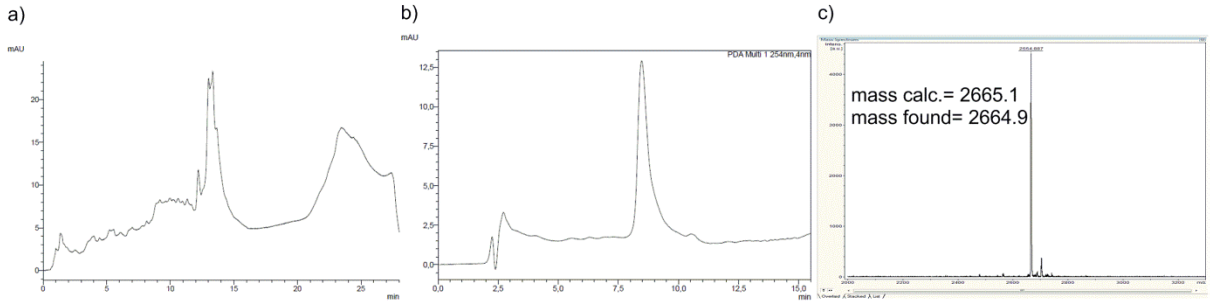

a) HPLC trace (preparative HPLC) of the crude hexT-pyrazoline conjugate **hexT-95A**. b) HPLC trace of the purified hexT-pyrazoline conjugate **hexT-95A**. c) MALDI-TOF/TOF-MS analysis of the purified hexT-pyrazoline conjugate **hexT-95A**.

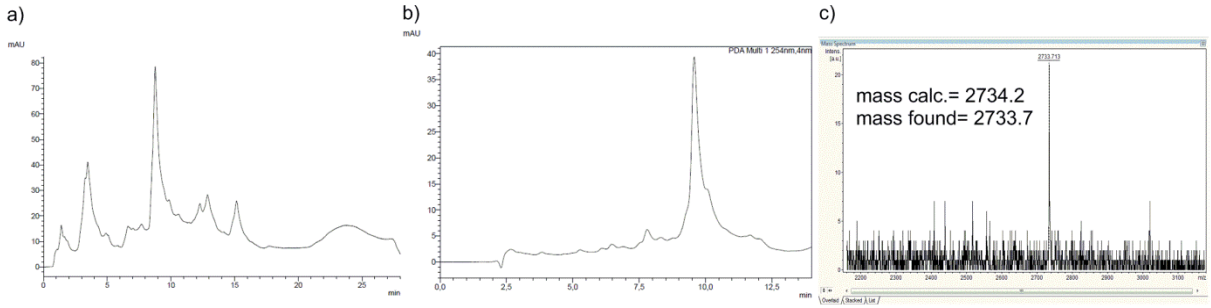

a) HPLC trace (preparative HPLC) of the crude hexT-pyrazoline conjugate **hexT-95C**. b) HPLC trace of the purified hexT-pyrazoline conjugate **hexT-95C**. c) MALDI-TOF/TOF-MS analysis of the purified hexT-pyrazoline conjugate **hexT-95C**.

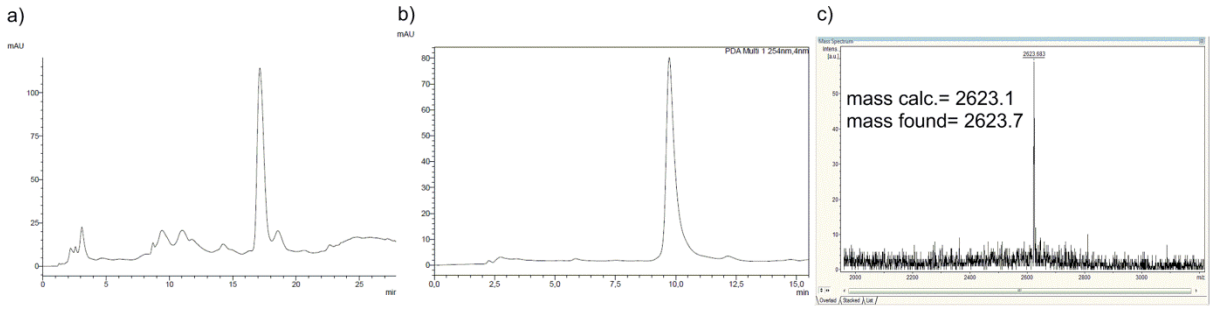

a) HPLC trace (preparative HPLC) of the crude hexT-pyrazoline conjugate **hexT-95T**. b) HPLC trace of the purified hexT-pyrazoline conjugate **hexT-95T**. c) MALDI-TOF/TOF-MS analysis of the purified hexT-pyrazoline conjugate **hexT-95T**.

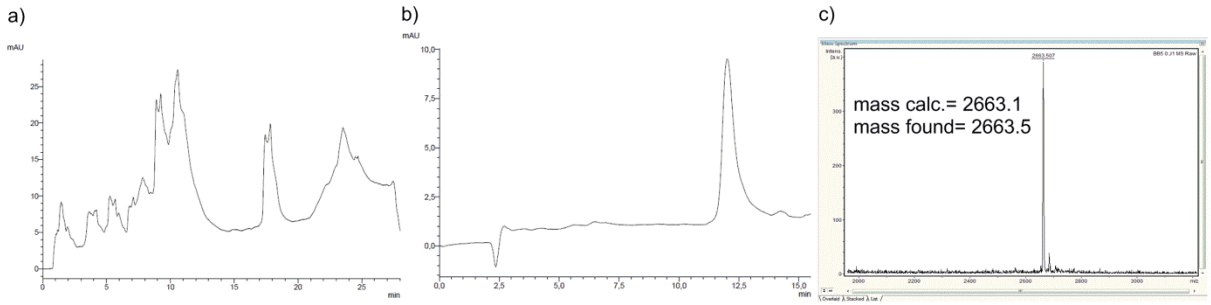

a) HPLC trace (preparative HPLC) of the crude hexT-pyrazoline conjugate **hexT-95AD**. b) HPLC trace of the purified hexT-pyrazoline conjugate **hexT-95AD**. c) MALDI-TOF/TOF-MS analysis of the purified hexT-pyrazoline conjugate **hexT-95AD**.

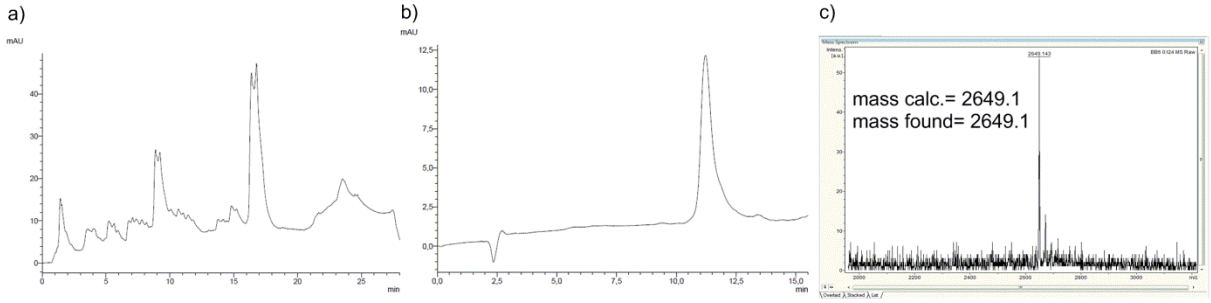

a) HPLC trace of the crude hexT-pyrazoline conjugate **hexT-95BD**. b) HPLC trace (preparative HPLC) of the purified hexT-pyrazoline conjugate **hexT-95BD**. c) MALDI-TOF/TOF-MS analysis of the purified hexT-pyrazoline conjugate **hexT-95BD**.

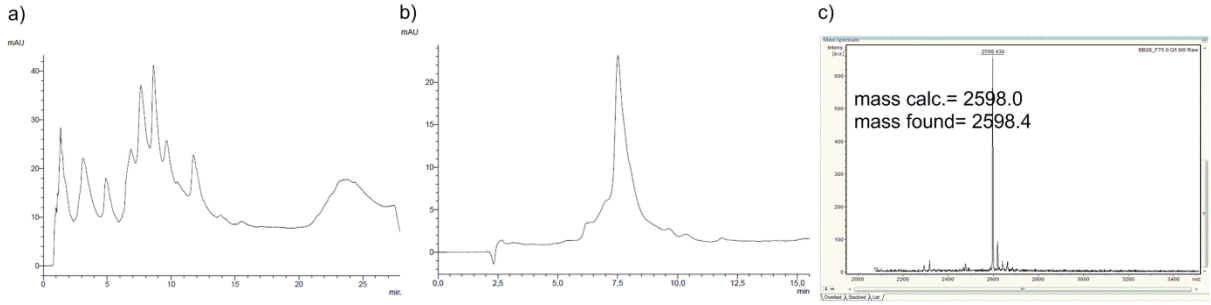

a) HPLC trace (preparative HPLC) of the crude hexT-pyrazoline conjugate **hexT-96F**. b) HPLC trace of the purified hexT-pyrazoline conjugate **hexT-96F**. c) MALDI-TOF/TOF-MS analysis of the purified hexT-pyrazoline conjugate **hexT-96F**.

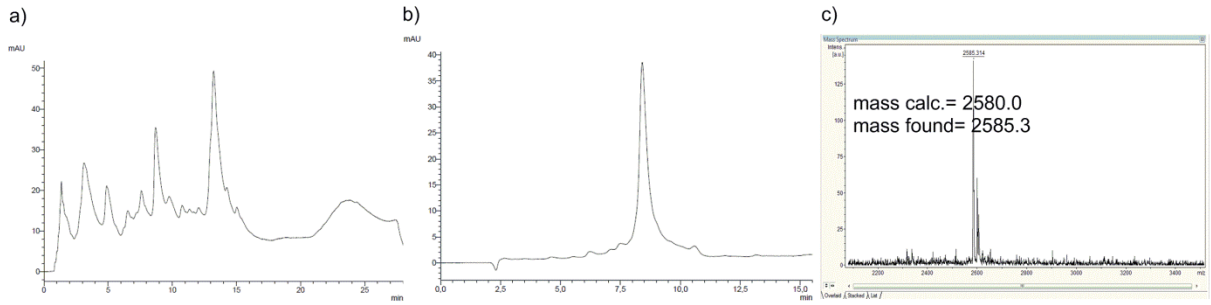

a) HPLC trace (preparative HPLC) of the crude hexT-pyrazole conjugate **hexT-96G**. b) HPLC trace of the purified hexT-pyrazole conjugate **hexT-96G**. c) MALDI-TOF/TOF-MS analysis of the purified hexT-pyrazole conjugate **hexT-96G**.

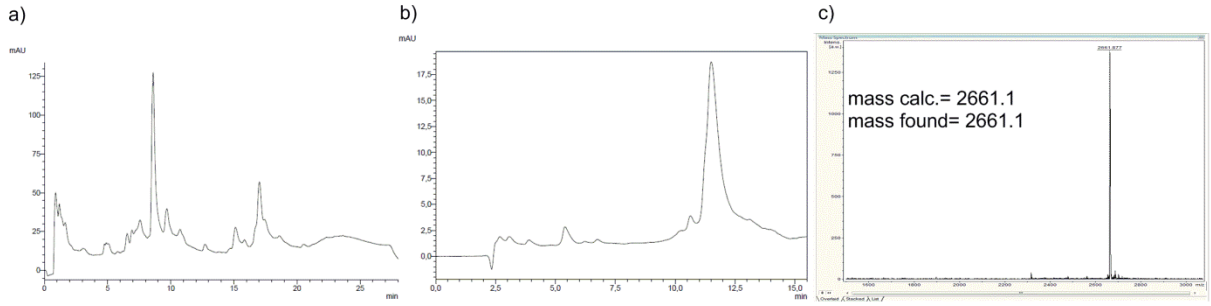

a) HPLC trace (preparative HPLC) of the crude hexT-pyrazole conjugate **hexT-96K**. b) HPLC trace of the purified hexT-pyrazole conjugate **hexT-96K**. c) MALDI-TOF/TOF-MS analysis of the purified hexT-pyrazole conjugate **hexT-96K**.

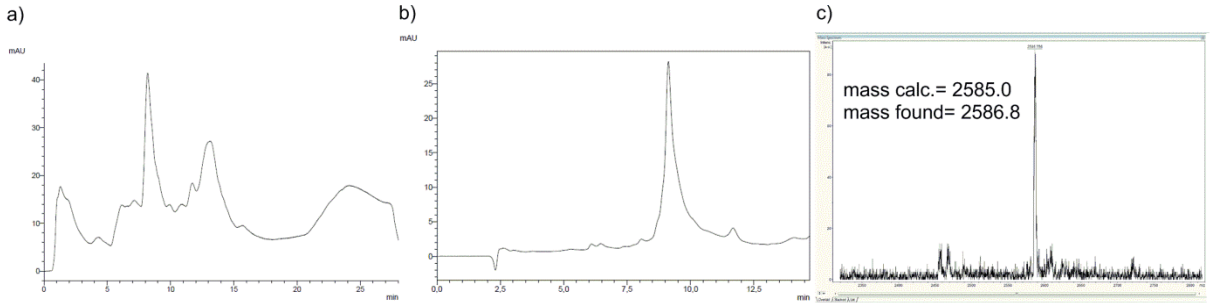

a) HPLC trace (preparative HPLC) of the crude hexT-pyrazole conjugate **hexT-96M**. b) HPLC trace of the purified hexT-pyrazole conjugate **hexT-96M**. c) MALDI-TOF/TOF-MS analysis of the purified hexT-pyrazole conjugate **hexT-96M**.

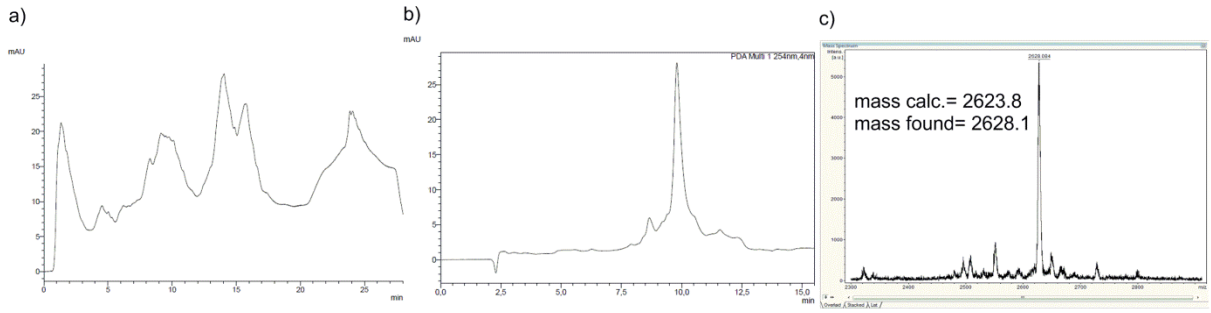

a) HPLC trace (preparative HPLC) of the crude hexT-pyrazole conjugate **hexT-96O**. b) HPLC trace of the purified hexT-pyrazole conjugate **hexT-96O**. c) MALDI-TOF/TOF-MS analysis of the purified hexT-pyrazole conjugate **hexT-96O**.

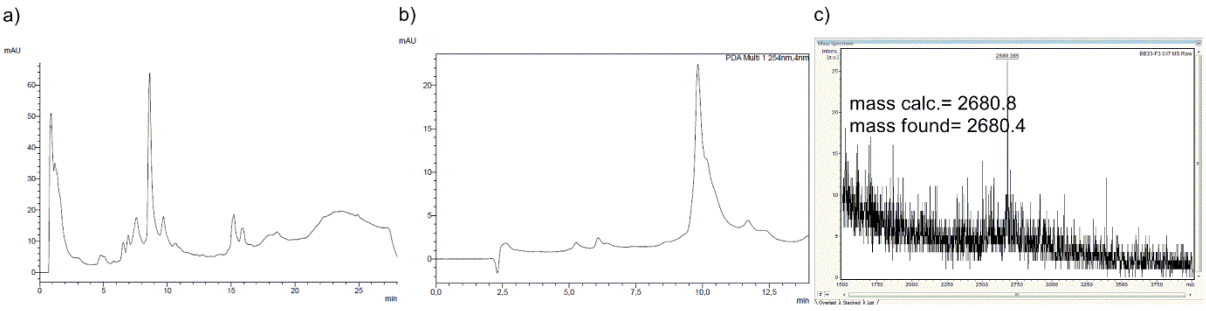

a) HPLC trace of (preparative HPLC) the crude hexT-pyrazole conjugate **hexT-96U**. b) HPLC trace of the purified hexT-pyrazole conjugate **hexT-96U**. c) MALDI-TOF/TOF-MS analysis of the purified hexT-pyrazole conjugate **hexT-96U**.

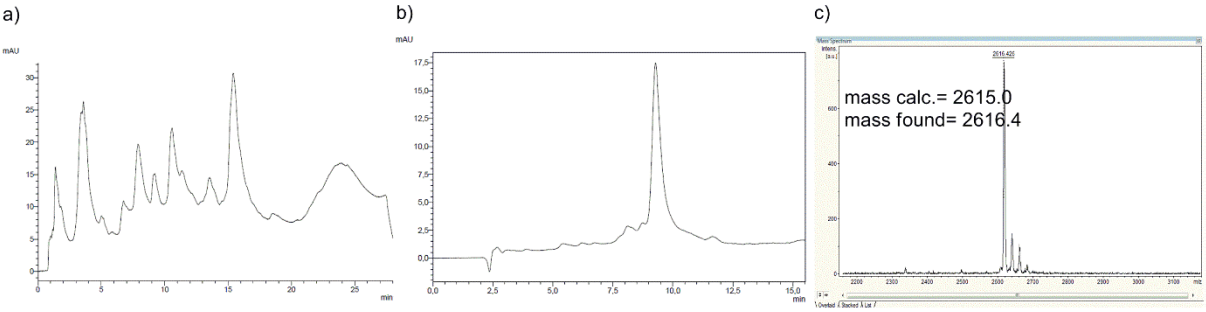

a) HPLC trace (preparative HPLC) of the crude hexT-pyrazole conjugate **hexT-96Z**. b) HPLC trace of the purified hexT-pyrazole conjugate **hexT-96Z**. c) MALDI-TOF/TOF-MS analysis of the purified hexT-pyrazole conjugate **hexT-96Z**.

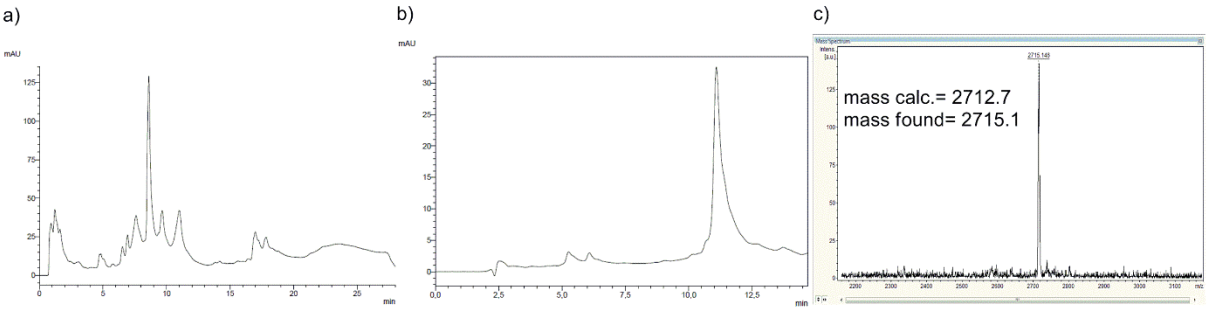

a) HPLC trace (preparative HPLC) of the crude hexT-pyrazole conjugate **hexT-96AF**. b) HPLC trace of the purified hexT-pyrazole conjugate **hexT-96AF**. c) MALDI-TOF/TOF-MS analysis of the purified hexT-pyrazole conjugate **hexT-96AF**.

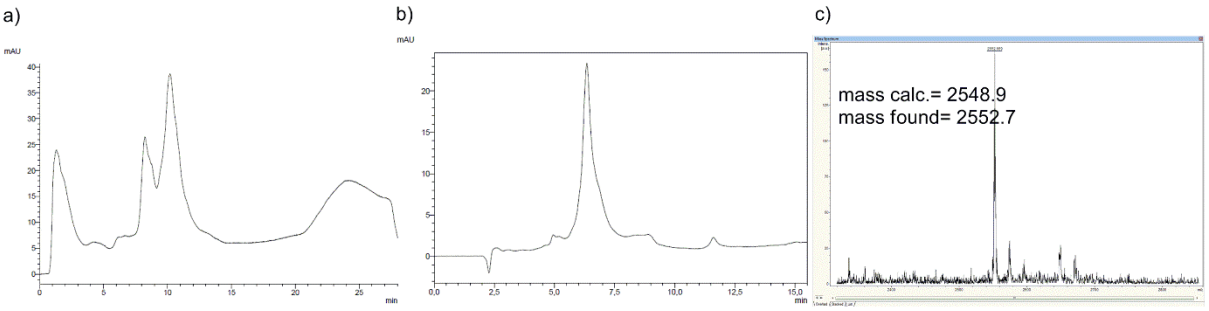

a) HPLC trace (preparative HPLC) of the crude hexT-pyrazole conjugate **hexT-96AO**. b) HPLC trace of the purified hexT-pyrazole conjugate **hexT-96AO**. c) MALDI-TOF/TOF-MS analysis of the purified hexT-pyrazole conjugate **hexT-96AO**.

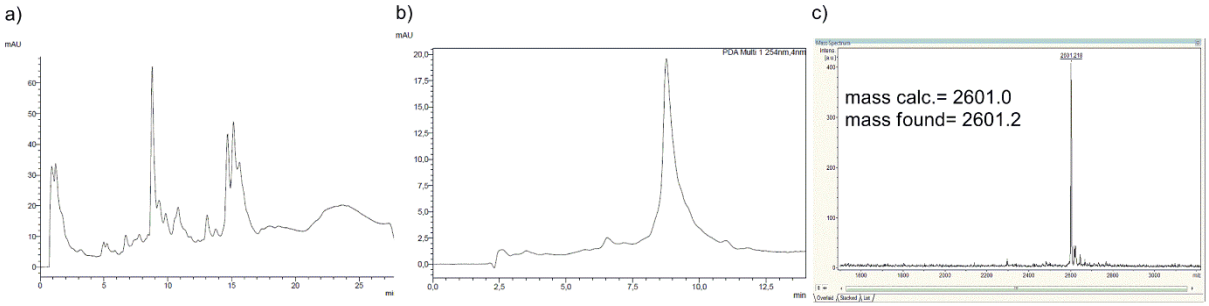

a) HPLC trace (preparative HPLC) of the crude hexT-pyrazole conjugate **hexT-96AP**. b) HPLC trace of the purified hexT-pyrazole conjugate **hexT-96AP**. c) MALDI-TOF/TOF-MS analysis of the purified hexT-pyrazole conjugate **hexT-96AP**.

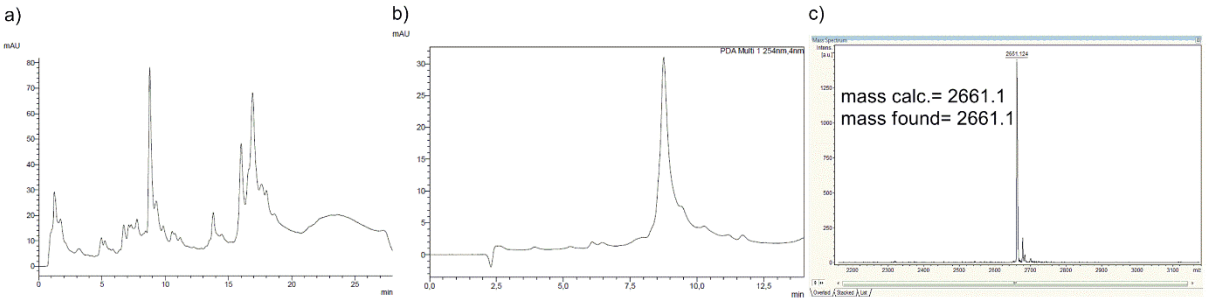

a) HPLC trace (preparative HPLC) of the crude hexT-pyrazole conjugate **hexT-96AQ**. b) HPLC trace of the purified hexT-pyrazole conjugate **hexT-96AQ**. c) MALDI-TOF/TOF-MS analysis of the purified hexT-pyrazole conjugate **hexT-96AQ**.

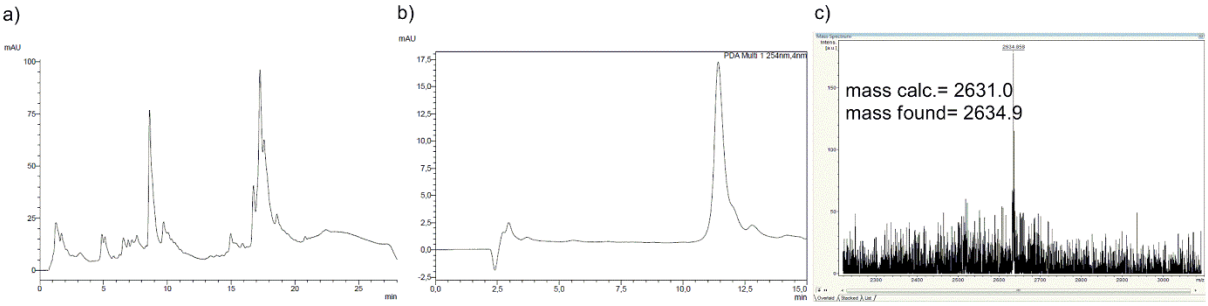

a) HPLC trace (preparative HPLC) of the crude hexT-pyrazole conjugate **hexT-96AT**. b) HPLC trace of the purified hexT-pyrazole conjugate **hexT-96AT**. c) MALDI-TOF/TOF-MS analysis of the purified hexT-pyrazole conjugate **hexT-96AT**.

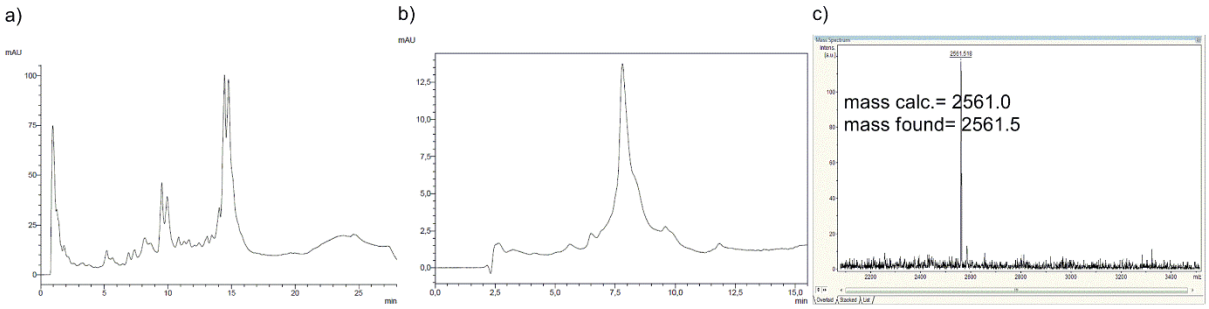

a) HPLC trace (preparative HPLC) of the crude hexT-pyrazole conjugate **hexT-96AU**. b) HPLC trace of the purified hexT-pyrazole conjugate **hexT-96AU**. c) MALDI-TOF/TOF-MS analysis of the purified hexT-pyrazole conjugate **hexT-96AU**.

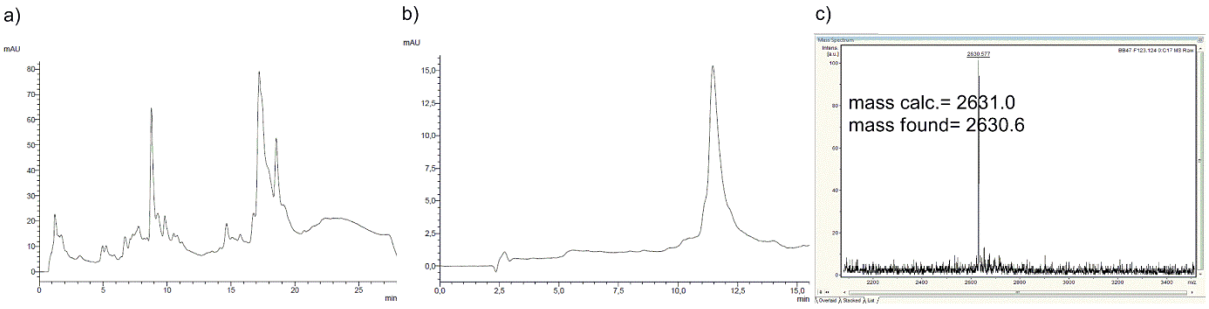

a) HPLC trace (preparative HPLC) of the crude hexT-pyrazole conjugate **hexT-96AZ**. b) HPLC trace of the purified hexT-pyrazole conjugate **hexT-96AZ**. c) MALDI-TOF/TOF-MS analysis of the purified hexT-pyrazole conjugate **hexT-96AZ**.

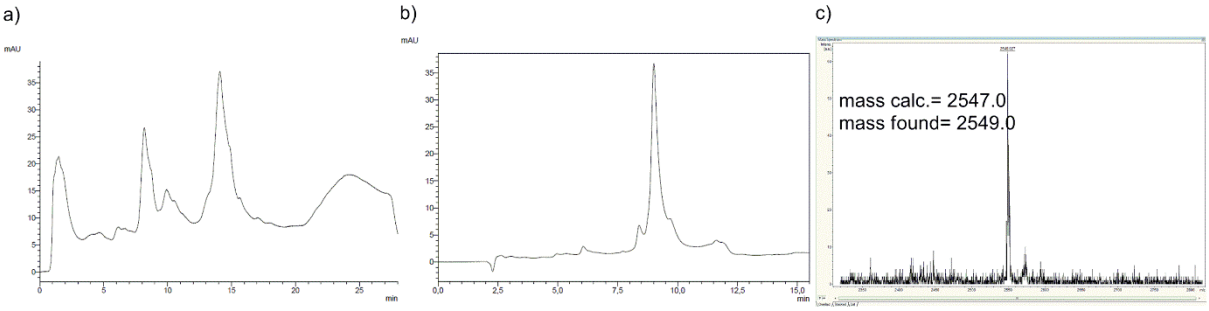

a) HPLC trace (preparative HPLC) of the crude hexT-pyrazole conjugate **hexT-96BD**. b) HPLC trace of the purified hexT-pyrazole conjugate **hexT-96BD**. c) MALDI-TOF/TOF-MS analysis of the purified hexT-pyrazole conjugate **hexT-96BD**.

5.4.5. HPLC chromatograms and MALDI-MS spectra of hexathymidine-pyrazolines - hydrazide scope

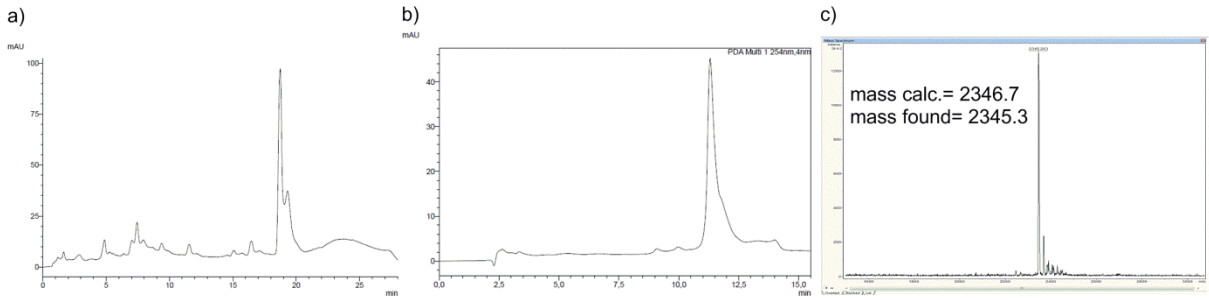

a) HPLC trace (preparative HPLC) of the crude hexT-pyrazoline conjugate **hexT-89T**. b) HPLC trace of the purified hexT-pyrazoline conjugate **hexT-89T**. c) MALDI-TOF/TOF-MS analysis of the purified hexT-pyrazoline conjugate **hexT-89T**.

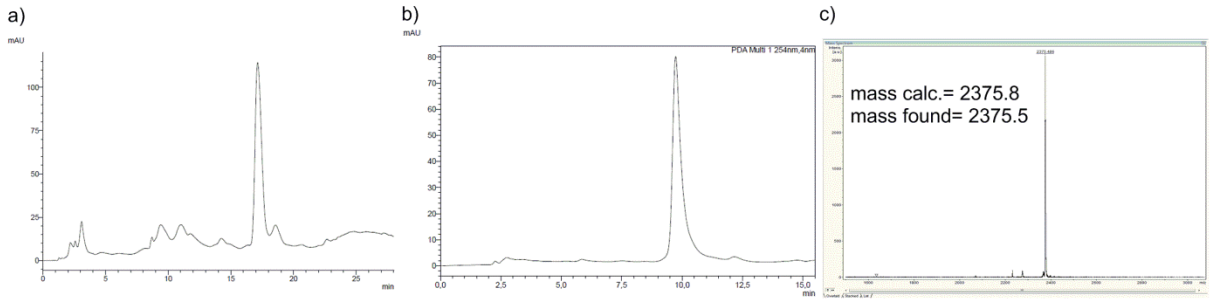

a) HPLC trace (preparative HPLC) of the crude hexT-pyrazoline conjugate **hexT-95T**. b) HPLC trace of the purified hexT-pyrazoline conjugate **hexT-95T**. c) MALDI-TOF/TOF-MS analysis of the purified hexT-pyrazoline conjugate **hexT-95T**.

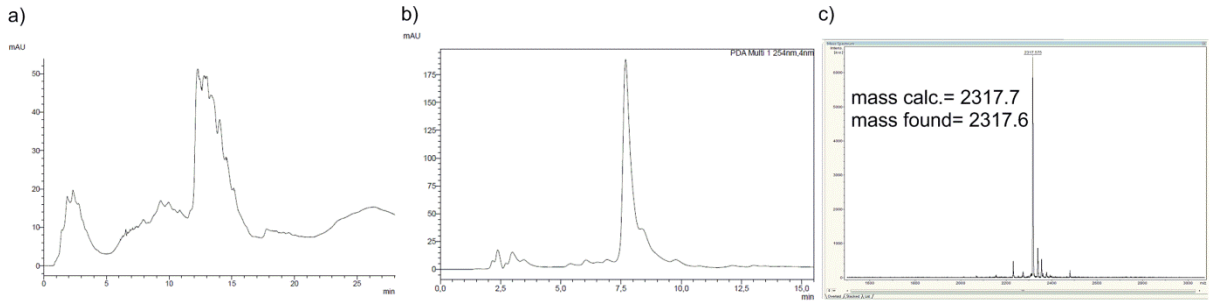

a) HPLC trace (preparative HPLC) of the crude hexT-pyrazoline conjugate **hexT-98T**. b) HPLC trace of the purified hexT-pyrazoline conjugate **hexT-98T**. c) MALDI-TOF/TOF-MS analysis of the purified hexT-pyrazoline conjugate **hexT-98T**.

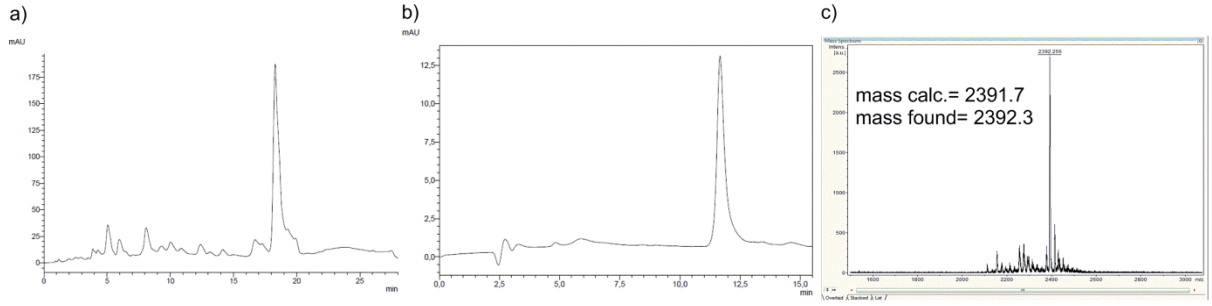

a) HPLC trace (preparative HPLC) of the crude hexT-pyrazoline conjugate **hexT-100T**. b) HPLC trace of the purified hexT-pyrazoline conjugate **hexT-100T**. c) MALDI-TOF/TOF-MS analysis of the purified hexT-pyrazoline conjugate **hexT-100T**.

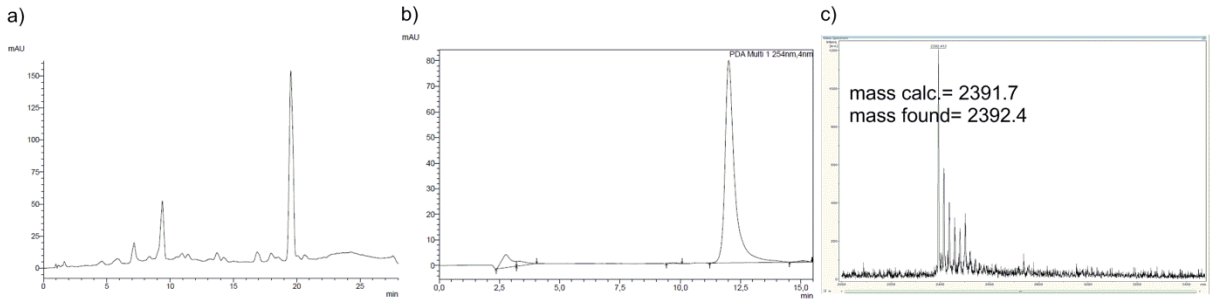

a) HPLC trace (preparative HPLC) of the crude hexT-pyrazoline conjugate **hexT-102T**. b) HPLC trace of the purified hexT-pyrazoline conjugate **hexT-102T**. c) MALDI-TOF/TOF-MS analysis of the purified hexT-pyrazoline conjugate **hexT-102T**.

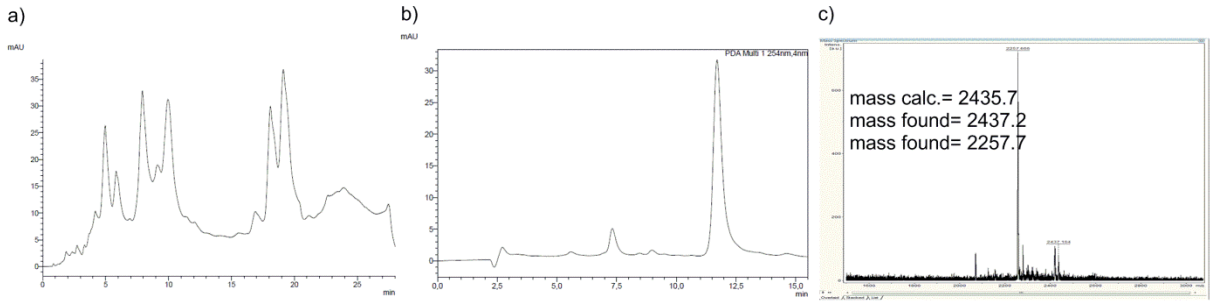

a) HPLC trace (preparative HPLC) of the crude hexT-pyrazoline conjugate **hexT-104T**. b) HPLC trace of the purified hexT-pyrazoline conjugate **hexT-104T**. c) MALDI-TOF/TOF-MS analysis of the purified hexT-pyrazoline conjugate **hexT-104T**.

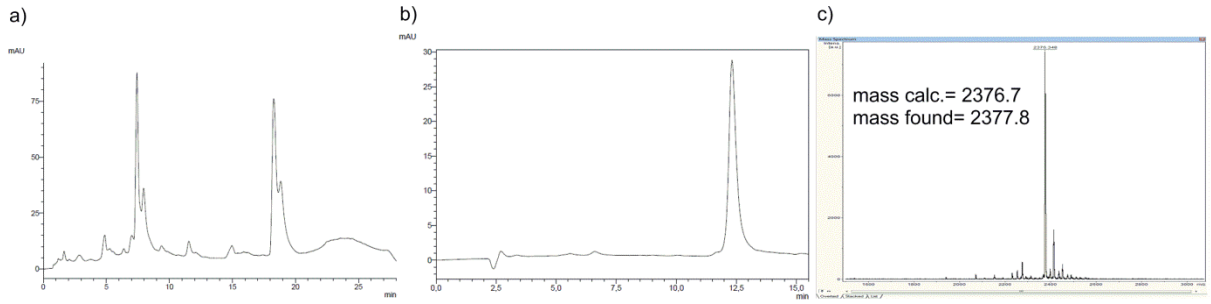

a) HPLC trace (preparative HPLC) of the crude hexT-pyrazoline conjugate **hexT-106T**. b) HPLC trace of the purified hexT-pyrazoline conjugate **hexT-106T**. c) MALDI-TOF/TOF-MS analysis of the purified hexT-pyrazoline conjugate **hexT-106T**.

5.4.6. Evaluation of carboxylic acids for library synthesis

DEAE sepharose[57] was pipetted on 96well filter plate (96 x 100 µL), washed with water (2 × 350 µL) and 10 mM aq. NaAc buffer (2 × 350 µL). Then, 500 pmol of the hexT-pyrazoline conjugate **hexT-95T**, **hexT-95-PEG(4)-T** or hexT-pyrazole conjugate **hexT-96T** was immobilized on DEAE anion exchange resin placed in each well position, by incubation of an aqueous solution of the oligonucleotide conjugate (2-20 µL) with the resin for 15 min, followed by washing of the resin with 10 mM aq. NaAc buffer (2 × 350 µL), distilled water (2 × 350 µL), and DMSO (2 × 350 µL). For activation of carboxylic acids, 25 µmol of each carboxylic acid (Table 20) was dissolved in 300 µL of dry DMSO in an Eppendorf tube, to this were added HOAt (2.5 µmol) dissolved in 50 µL of dry DMSO (taken from a stock solution: 275 µmol, 37.4 mg in 5.5 mL of dry DMSO) and EDC x HCl (25 µmol) dissolved in 50 µL of dry DMSO (taken from a stock solution: 2.75 mmol, 526.9 mg in 5.5 mL of dry DMSO). Activation mixtures were shaken at room temperature for 30 minutes. For parallel amide coupling, the DEAE sepharose carrying the hexT-pyrazoline conjugate **hexT-95T**, **hexT-95-PEG(4)-T** or hexT-pyrazole conjugate **hexT-96T** was suspended in 100 µL of dry DMSO and transferred from the 96well filter plate into a 96well deep well plate. After that, the activated carboxylic acids were added, and the reaction mixtures were shaken at room temperature overnight. Then, the DEAE sepharose was filtered over a 96 well filter plate (20 µm), washed subsequently with each 3 x 200 µL of DMSO, distilled water, and 10 mM aq. NaAc buffer. After that, the oligonucleotide conjugates were eluted from DEAE sepharose into a receiver plate by shaking with 60 µL of 3 M NaAc buffer (pH= 4.75) for 30 minutes. The oligonucleotide conjugates were analyzed by MALDI-MS.

Table 20. MALDI-TOF/TOF-MS data of hexT-pyrazol(in)e conjugates after amide coupling with carboxylic acids ***1-106***.

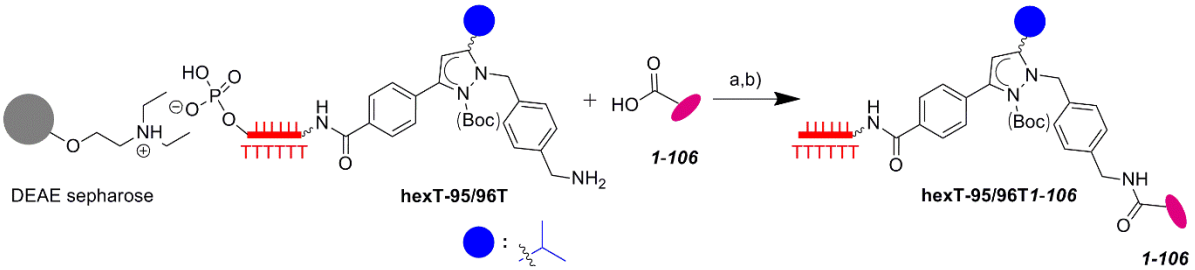

Conditions: a) HOAt, EDC × HCl, DMSO/ddH_2O (70/30), room temperature, overnight; b) 3 M sodium acetate buffer (pH= 4.75), room temperature, 30 min.

No.	structure	estimated conversion[a]	mass calc.	mass found[b]
1	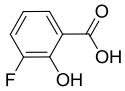	-	2513.9	starting material
2	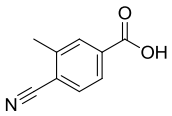	> 90 %	2518.9	2520.5
3	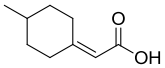	> 90 %	2512.0	2512.2
4	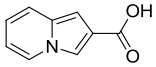	> 90 %	2416.8	2417.0[d]
5	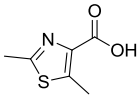	> 90 %	2515.0	2516.2
6	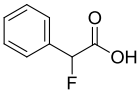	> 90 %	2511.9	2514.6
7	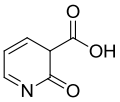	> 90 %	2496.9	2497.0
8	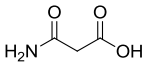	-	2460.9	starting material
9	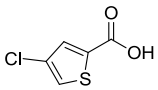	80 %	2520.3	2519.9
10	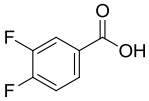	> 90 %	2515.3	2517.9
11	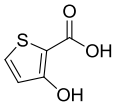	-	2501.3	starting material

No.	structure	estimated conversion[a]	mass calc.	mass found[b]
12	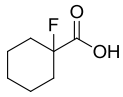	> 90 %	2503.4	2505.6
13	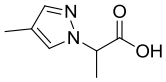	> 90 %	2511.4	2512.8
14	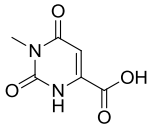	-	2527.8	starting material
15	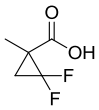	70 %	2493.3	2494.9
16	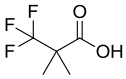	-	2513.9	starting material
17	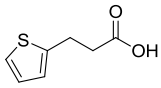	> 90 %	2514.0	2515.4
18	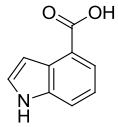	70 %	2518.9	2520.5
19	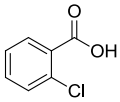	> 90 %	2514.0	2515.8
20	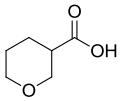	> 90 %	2487.9	2489.0
21	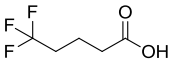	> 90 %	2513.9	2515.0
22	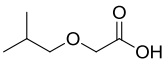	> 90 %	2489.8	2490.6
23	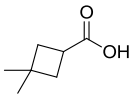	> 90 %	2485.9	2487.6
24	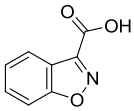	80 %	2520.9	2523.2
25	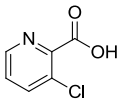	> 90 %	2515.3	2516.5
26	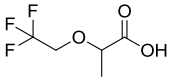	-	2529.9	starting material

No.	structure	estimated conversion[a]	mass calc.	mass found[b]
27	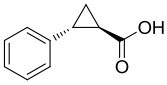	> 90 %	2519.9	2521.4
28	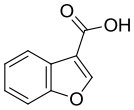	> 90 %	2764.2	2765.4[c]
29	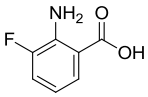	> 90 %	2757.2	2756.4[c]
30	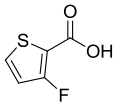	> 90 %	2401.8	2403.0[d]
31	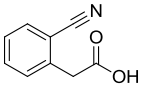	70 %	2416.8	2414.9[d]
32	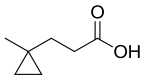	80 %	2733.2	2734.9[c]
33	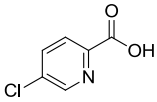	80 %	2413.2	2414.6[d]
34	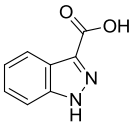	> 90 %	2417.8	2419.9[d]
35	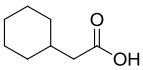	> 90 %	2500.0	2499.3
36	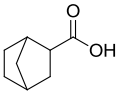	60 %	2497.9	2499.9
37	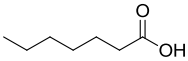	> 90 %	2735.2	2734.9[c]
38		> 90 %	2459.9	2461.6
39	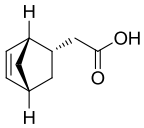	> 90 %	2757.3	2762.[c]
40	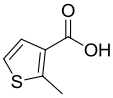	> 90 %	2500.0	2502.5
41	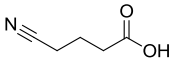	> 90 %	2718.2	2716.7[c]

No.	structure	estimated conversion[a]	mass calc.	mass found[b]
42	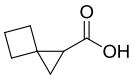	> 90 %	2731.2	2732.8[c]
43	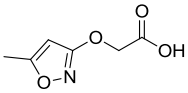	> 90 %	2762.1	2763.2[c]
44	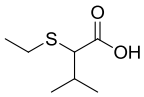	> 90 %	2417.9	2419.0[d]
45	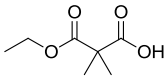	> 90 %	2415.8	2417.2[d]
46	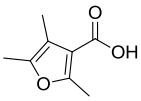	> 90 %	2759.2	2762.2[c]
47	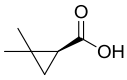	> 90 %	2369.7	2371.2[d]
48	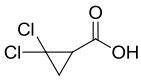	> 90 %	2410.6	2411.8[d]
49	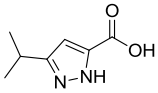	> 90 %	2409.8	2411.1[d]
50	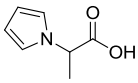	> 90 %	2496.9	2498.2
51	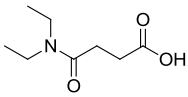	-	2428.8	starting material[d]
52	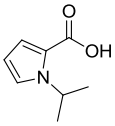	> 90 %	2510.9	2512.4
53	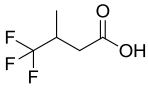	> 90 %	2513.9	2515.7
54	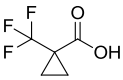	> 90 %	2511.8	2512.6
55	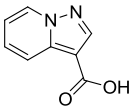	> 90 %	2519.9	2521.0
56	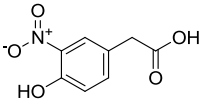	> 90 %	2802.2	2805.4[c]

No.	structure	estimated conversion[a]	mass calc.	mass found[b]
57	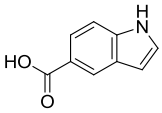	60 %	2518.9	2520.5
58	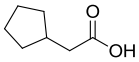	> 90 %	2485.9	2488.0
59	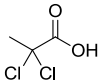	> 90 %	2500.7	2502.3
60	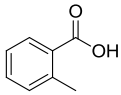	> 90 %	2493.9	2495.3
61	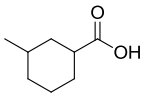	80 %	2499.9	2502.5
62	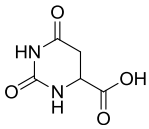	> 90 %	2515.9	2517.7
63	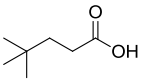	> 90 %	2487.9	2489.2
64	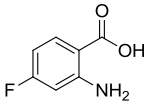	> 90 %	2512.9	2514.7
65	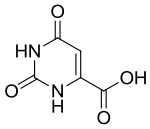	10 %	2513.9	2514.4
66	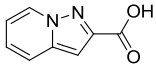	> 90 %	2519.9	2520.5
67	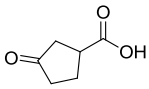	> 90 %	2485.9	2488.4
68	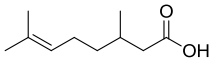	> 90 %	2528.0	2530.8
69	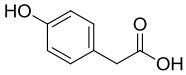	> 90 %	2509.9	2511.4
70		> 90 %	2457.9	2459.6
71	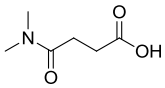	80 %	2502.9	2503.9

No.	structure	estimated conversion[a]	mass calc.	mass found[b]
72	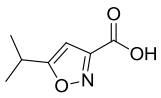	80 %	2512.9	2515.3
73	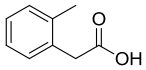	> 90 %	2507.9	2510.1
74	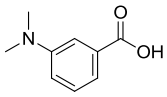	> 90 %	2522.9	2524.1
75	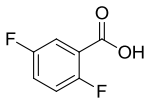	30 %	2515.9	2518.8
76	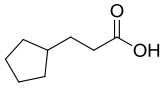	> 90 %	2500.0	2501.7
77	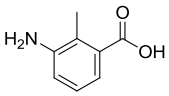	> 90 %	2406.8	2407.7[d]
78	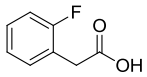	> 90 %	2511.9	2513.8
79	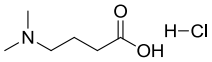	> 90 %	2488.9	2489.0
80	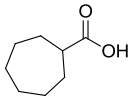	> 90 %	2500.0	2501.9
81	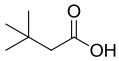	80 %	2473.9	2475.8
82	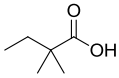	> 90 %	2371.8	2374.9[d]
83	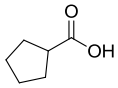	> 90 %	2471.9	2471.5
84	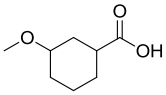	> 90 %	2413.8	2411.3[d]
85	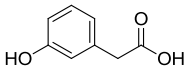	> 90 %	2407.8	2410.6[d]
86	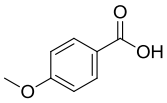	> 90 %	2407.8	2409.2[d]

No.	structure	estimated conversion[a]	mass calc.	mass found[b]
87	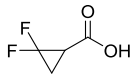	> 90 %	2377.7	2379.5[d]
88	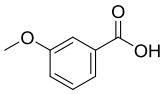	> 90 %	2509.9	2511.8
89	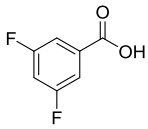	-	2413.7	starting material[d]
90	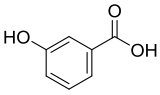	> 90 %	2495.9	2497.6
91	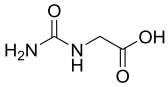	> 90 %	2373.7	2375.8[d]
92	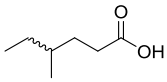	> 90 %	2487.9	2489.0
93	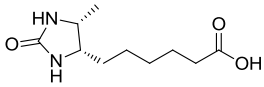	> 90 %	2821.3	2820.7[c]
94	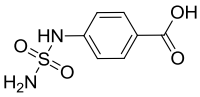	> 90 %	2574.0	2575.5
95	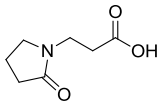	> 90 %	2514.9	2518.7
96	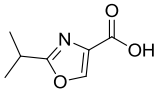	> 90 %	2512.9	2512.9
97	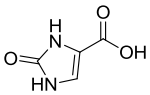	> 90 %	2485.8	2485.2
98	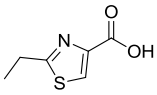	> 90 %	2514.9	2515.1
99	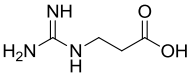	> 90 %	2488.9	2488.1
100	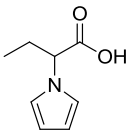	> 90 %	2510.9	2511.9
101	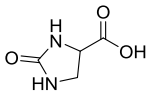	> 90 %	2487.8	2490.5

No.	structure	estimated conversion[a]	mass calc.	mass found[b]
102	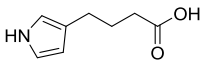	> 90 %	2510.9	2512.6
103	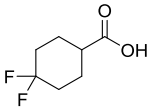	> 90 %	2521.9	2522.9
104	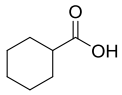	> 90 %	2485.9	2488.2
105	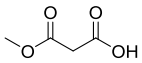	> 90 %	2475.8	2477.6
106	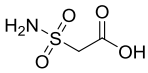	-	2496.9	starting material

[a] % conversion estimated based on the MALDI-TOF/TOF-MS data; [b] measured by MALDI-TOF/TOF-MS; [c] carboxylic acids coupled to the hexT-pyrazoline conjugate **hexT-95-PEG(4)-T** containing PEG(4) linker; [d] carboxylic acids coupled to the hexT-pyrazole conjugate **hexT-96T**.

5.4.6.1. MALDI-MS spectra of 20 representative amide coupling products

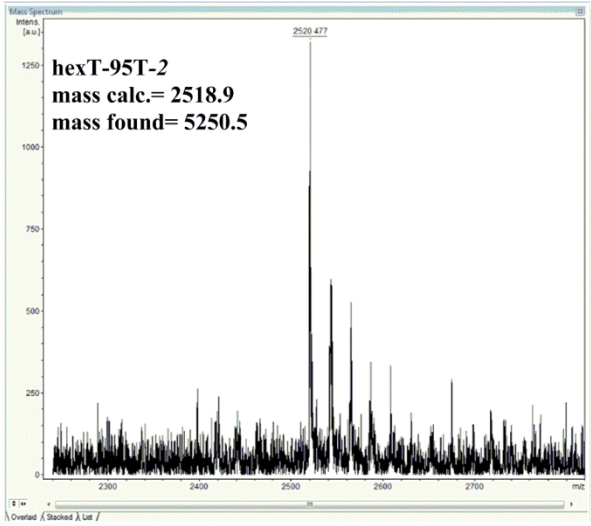

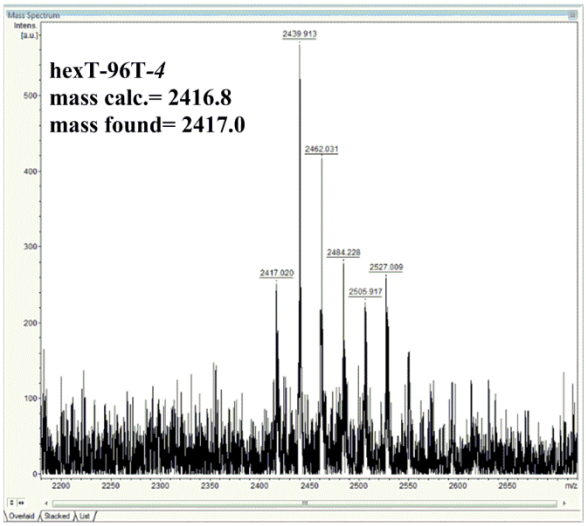

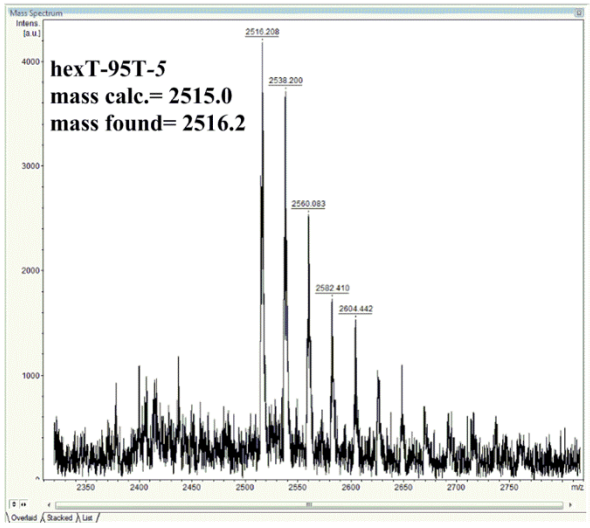

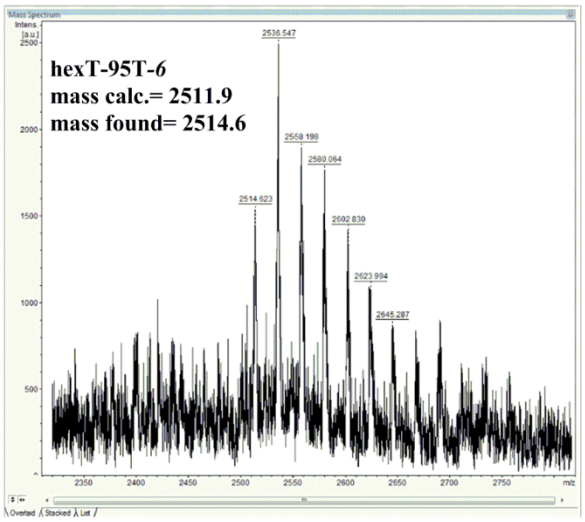

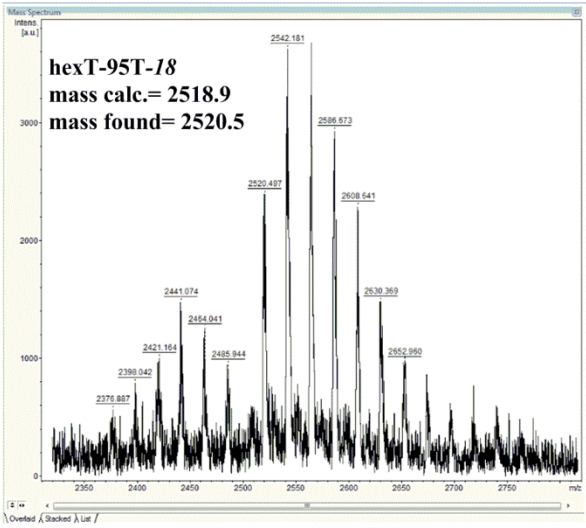

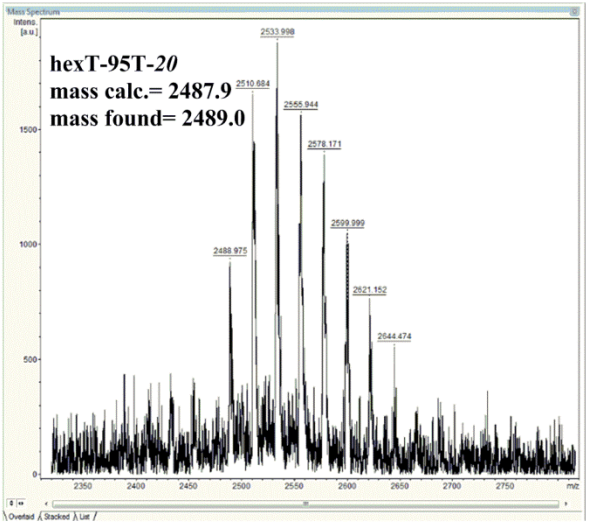

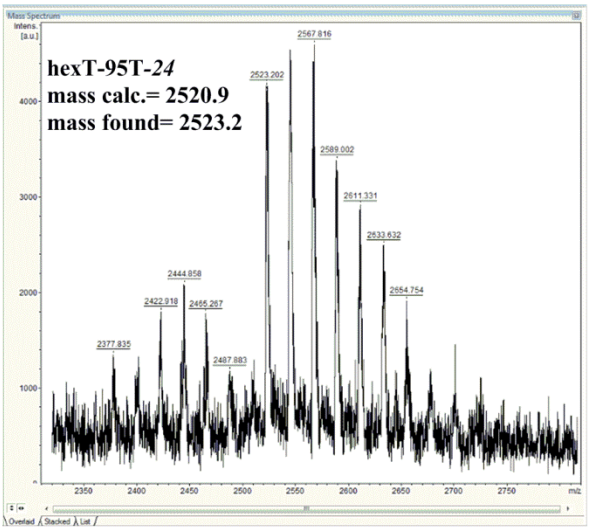
hexT-95T-*24*
mass calc.= 2520.9
mass found= 2523.2

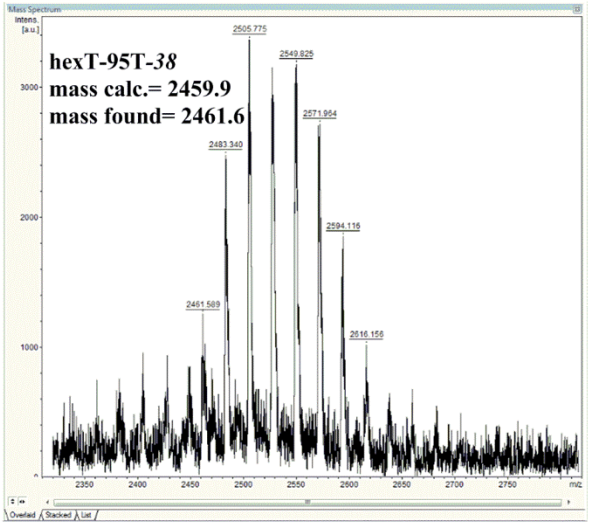
hexT-95T-*38*
mass calc.= 2459.9
mass found= 2461.6

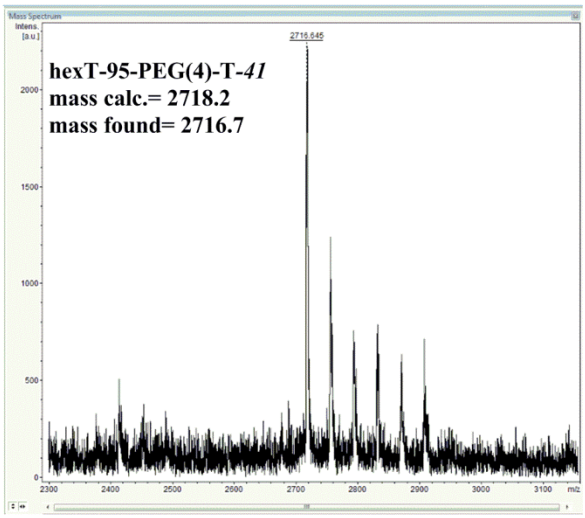
hexT-95-PEG(4)-T-*41*
mass calc.= 2718.2
mass found= 2716.7

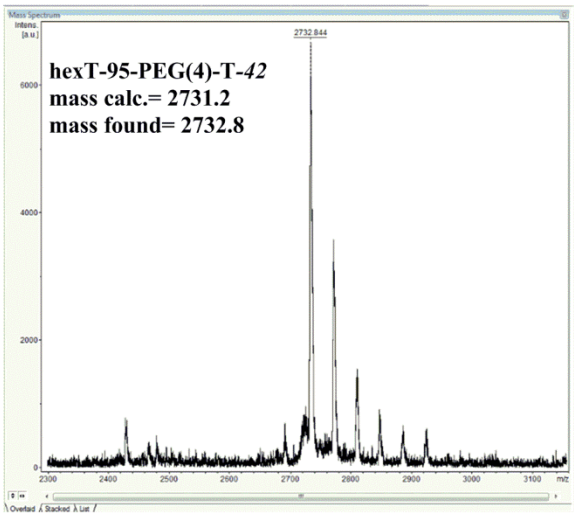
hexT-95-PEG(4)-T-*42*
mass calc.= 2731.2
mass found= 2732.8

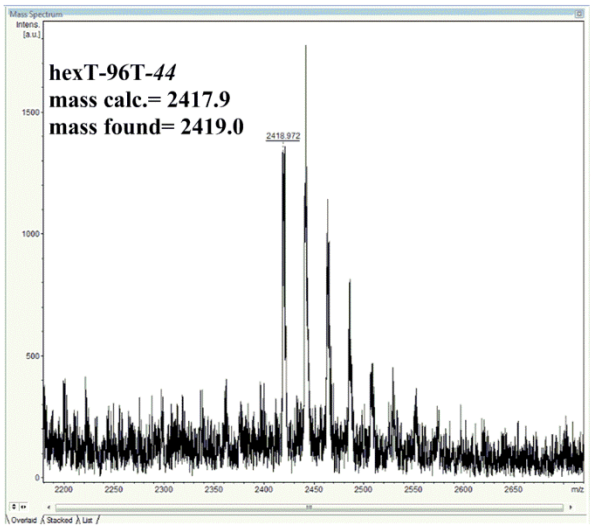
hexT-96T-*44*
mass calc.= 2417.9
mass found= 2419.0

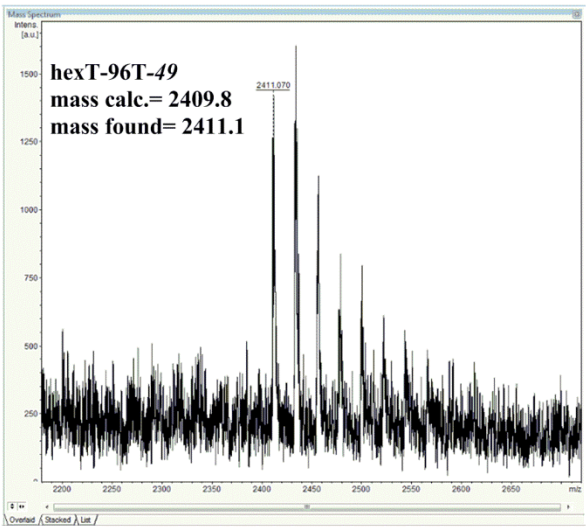
hexT-96T-*49*
mass calc.= 2409.8
mass found= 2411.1

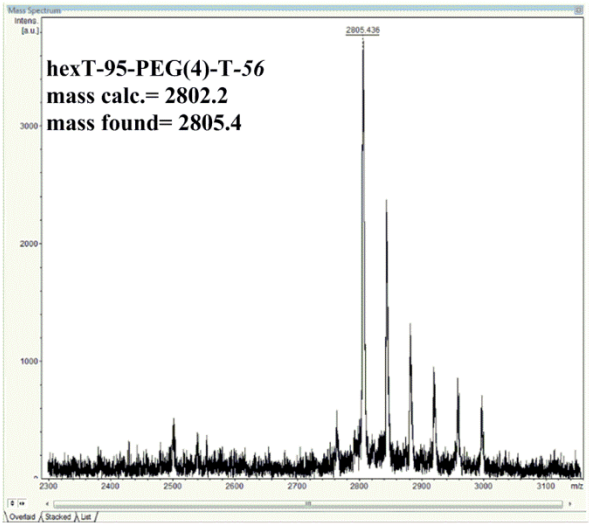
hexT-95-PEG(4)-T-*56*
mass calc.= 2802.2
mass found= 2805.4
2805.436

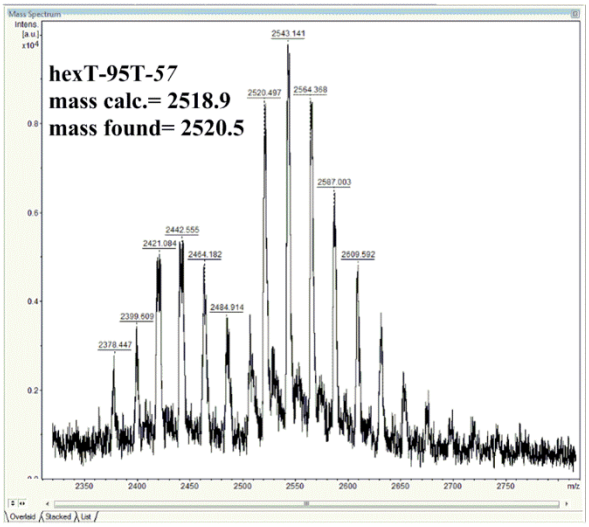
hexT-95T-*57*
mass calc.= 2518.9
mass found= 2520.5
2543.141
2520.497
2564.368
2587.003
2442.555
2421.084
2464.182
2609.592
2484.914
2399.609
2378.447

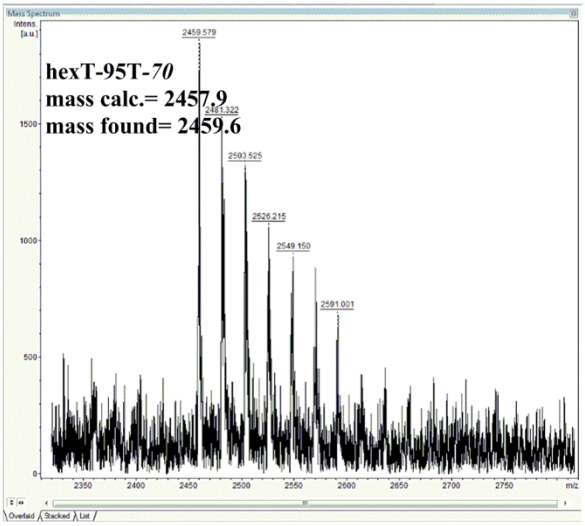
hexT-95T-*70*
mass calc.= 2457.9
mass found= 2459.6
2459.579
2481.322
2503.525
2526.215
2549.150
2591.001

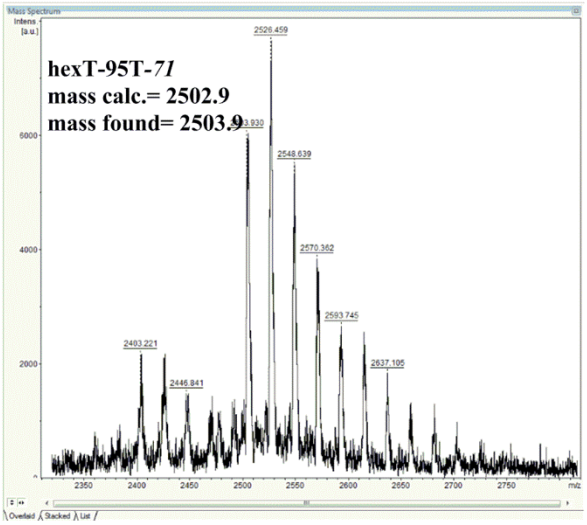
hexT-95T-*71*
mass calc.= 2502.9
mass found= 2503.9
2526.459
2548.639
2570.362
2593.745
2637.105
2403.221
2446.841

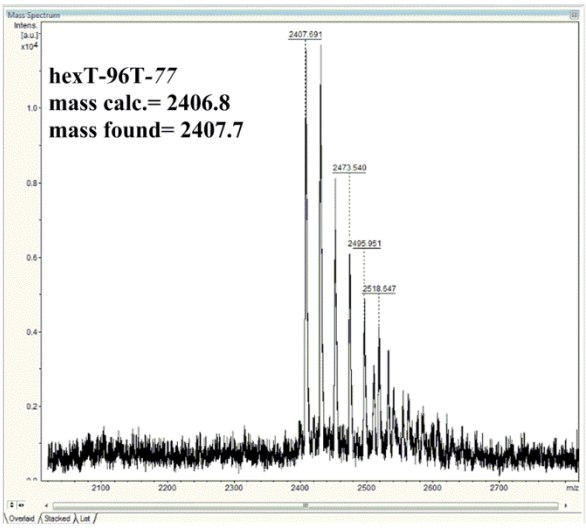
hexT-96T-*77*
mass calc.= 2406.8
mass found= 2407.7
2407.691
2473.540
2495.951
2518.647

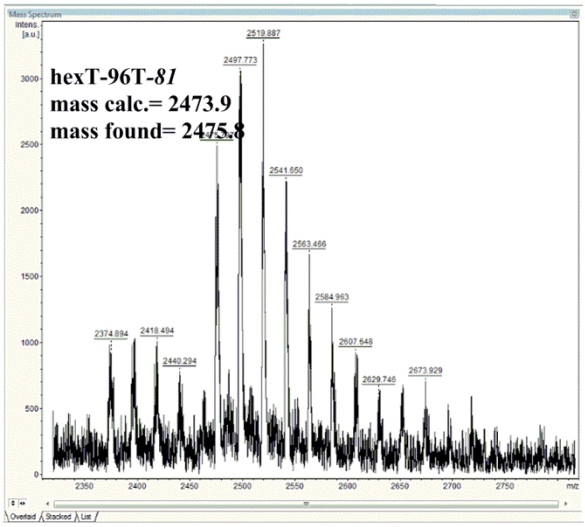
hexT-96T-*81*
mass calc.= 2473.9
mass found= 2475.8
2519.887
2497.773
2541.650
2563.466
2584.963
2607.648
2629.746
2673.929
2374.894
2418.494
2440.294

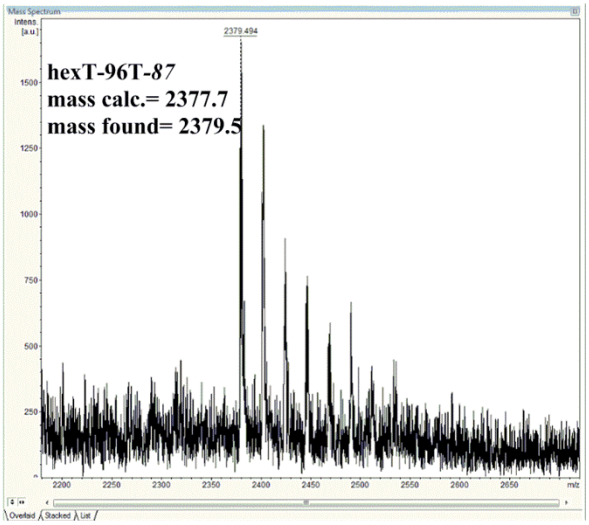
Mass Spectrum
Intens. [a.u.]
hexT-96T-*87*
mass calc.= 2377.7
mass found= 2379.5
2379.494
m/z
Overlaid
Stacked
List

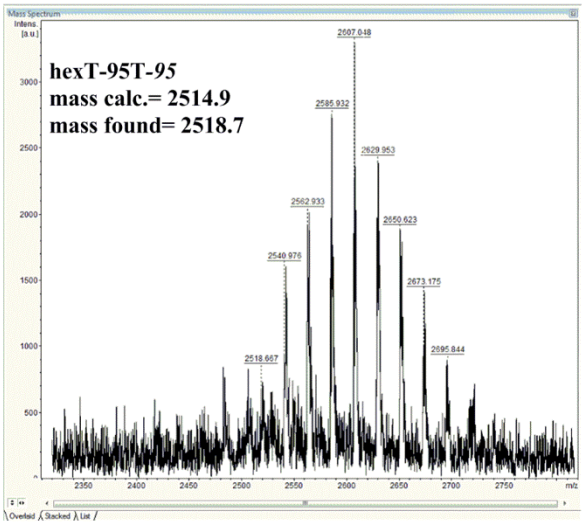
Mass Spectrum
Intens. [a.u.]
hexT-95T-*95*
mass calc.= 2514.9
mass found= 2518.7
2607.048
2585.932
2629.953
2562.933
2650.623
2540.976
2673.175
2518.667
2695.844
m/z
Overlaid
Stacked
List

5.4.7. Enzymatic encoding of hexathymidine conjugates: T4 ligation of duplex DNA sequences

5'-Phosphorylation of DNA oligonucleotides

20 µL phosphorylation reactions contained 14 µM (280 pmol) oligonucleotides, 10 units of PNK (T4 PNK, Thermo Fisher Scientific), 2 µL of 10 × PNK buffer A (500 mM Tris-HCl, 100 mM $MgCl_2$, 50 mM DTT, 1 mM spermidine, pH 7.6, 25 °C, Thermo Fisher Scientific), and 20 nmol of ATP (from a 10 mM aqueous solution of ATP, Thermo Fisher Scientific). The reactions were carried out at 37 °C for 30 minutes, and stopped by heat inactivation at 75 °C for 10 minutes.

Enzymatic ligation of double-stranded DNA

All DNA sequences are given in Tables 8 and 9. The indicated DNA oligonucleotides (Fig. 3.31) were annealed in a total reaction volume of 20 µL at 85 °C for 10 min and slowly cooled down to room temperature (25 °C). The ligation reactions contained 2 µM oligonucleotides (40 pmol of each oligonucleotide), 600 units of T4-DNA ligase, and 2 µL of 10 × T4-DNA ligase buffer (500 mM Tris-HCl, 100 mM $MgCl_2$, 50 mM DTT, 10 mM ATP, pH 7.6 at 25 °C). The ligations were carried out at 25 °C overnight, followed by heat inactivation at 75 °C for 10 minutes. Negative control reactions were performed in the same manner without addition of T4-DNA ligase.

Analysis of DNA ligations

Ligation reactions were analyzed by agarose gel electrophoresis (5.5 % agarose). Electrophoresis was carried out in TBE buffer (0.1 M Tris, 0.1 M H_3BO_3, 0.2 mM EDTA, pH= 8.3) at 150 V constant voltage for 75 minutes. DNA was stained with Midori Green Direct, and the GeneRuler Ultra Low Range DNA Ladder was used as reference.

Precipitation of DNA oligonucleotides

For precipitation of the DNA, EtOH was added to 70 % v/v. The precipitates were stored at -80 °C overnight, and centrifuged for 30 minutes (15000 rpm, 4 °C, centrifuge 5424 (Eppendorf AG, Hamburg)). The supernatant was removed, 70 % EtOH was added and the samples were stored at -80 °C for 1 hour. After centrifugation for 30 minutes (15000 rpm,

4 °C) the supernatant was removed and the DNA was dissolved in IDTE storage buffer (10 mM Tris, pH 7.5, 0.1 mM EDTA, IDT).

5.4.8. Synthesis and analysis of the pyrazol(in)e based oligothymidine-initiated DNA-Encoded Library (tiDEL)

5.4.8.1. Synthesis of the oligothymidine-initiated DNA-Encoded Library (tiDEL)

In total, 71 HPLC-purified hexT conjugates **hexT-95/96** (Tables 18, 19) depicted as oligonucleotide ***I*** in Figure 3.31 were placed in 96well plates and annealed with enzymatically phosphorylated oligonucleotides ***II/II´*** and ***III/III´*** at 85 °C for 10 min and slowly cooled down to room temperature (25 °C) (ligation scheme: Fig. 3.31, sequences: Tables 8, 9). The total reaction volume was 20 µL. This contained 40 pmol of each DNA oligonucleotide. Ligations were carried out at 25 °C for overnight and stopped by heat inactivation at 75 °C for 10 minutes. Control reactions were performed without T4-DNA ligase. To control the success of the ligation reactions an aliquot of 0.5 µL was taken from each reaction, pooled, and analyzed by agarose gel electrophoresis (Fig. 3.34A). All duplex DNA strands ***I-II-III/II´-III´*** corresponding to encoded hexT-conjugates **95A - 95BD** and **96A - 96BF** were pooled and precipitated. The pellet was dissolved in 540 µL of IDTE buffer and half of the total volume was distributed in 96 wells of a 96well plate in a way that each well position contained 20 pmol of pooled and encoded hexT-conjugates **95A - 95BD** and **96A - 96BF** (96 × 2.8 µL, duplex ***I-II-III/II´-III´*** in Figure 3.31). Then, the free 5'-end of the duplex DNA ***I-II-III/II´-III´*** and 96 oligonucleotides ***IV/IV´*** that contained the code for the carboxylic acid building block and the reverse primer sequence were phosphorylated with PNK**.** For ligation, the duplex DNA sequences ***I-II-III/II´-III´***, and ***IV/IV'*** (Fig. 3.31) were annealed at 85 °C for 10 minutes and slowly cooled down to room temperature. Control reactions were performed without T4-DNA ligase. After the ligation, the duplex DNA ***I-II-III-IV/II´-III´-IV´*** (83mer) encoded hexT conjugates **95A - 95BD**, **96A - 96BF** were transferred to a 96well filter plate containing DEAE anion exchange resin (96 x 80 µL) that was prepared as described above. In parallel, 96 carboxylic acids (Table 20) were activated as described above. For parallel amide coupling, the DEAE sepharose from each well carrying the pooled and encoded DNA small

molecule conjugates **hexT-95A - 95BD**, and **hexT-96A - 96BF** was suspended in 100 µL of dry DMSO and transported from the 96well filter plate into 96 glass vials. Amide coupling reactions were performed at room temperature for overnight. Then, the DEAE sepharose was transferred to a 96well filter plate, and washed subsequently with each 3 x 200 µL of DMSO, distilled water, and 10 mM aq. NaAc buffer. After that, the oligonucleotide conjugates were eluted from DEAE sepharose by shaking with 60 µL of 3 M NaAc buffer (pH= 4.75) for 30 minutes and filtered directly from the filter plate into a 96well deep well plate. The products of the amide coupling were pooled and precipitated twice as described above.

5.4.8.2. PCR amplification of the oligothymidine-initiated DNA-Encoded Library (tiDEL)

The final volume of each PCR reaction was 40 µL and contained 4 µL of 10 x PCR Rxn buffer, 1 µM of each primer, 3 mM of $MgCl_2$, 0.625 mM of each dNTP (dATP, dGTP, dTTP, and dCTP, corresponding to 2.5 mM of the mixture of dNTPs), and 10 µL of the template DNA. For amplification of the template DNA five units (1 µL) of Taq DNA polymerase were used. The PCR program started with predenaturation at 95 °C for one minute, followed by denaturation for 15 seconds at 95 °C, annealing for 15 seconds at 56 °C, and elongation for 30 seconds at 72 °C. After 25 cycles in total, the time for elongation was prolonged to seven minutes.

5.4.8.3. Affinity selection against streptavidin

Dynabeads® MyOne™ Streptavidin C1 (4 µL, 10 mg/mL) were transferred in an Eppendorf DNA LoBind microcentrifuge tube. Then, the magnetic beads were washed with 6 x 100 µL of PBS buffer (+0.01 % Tween®-20) in a following way: 100 µL of PBS buffer were added and the beads were resuspended by pipetting the slurry up and down, then the tube was placed on the magnetic rack until the beads stuck to the tube wall (30 s), and after aspiration supernatant was discarded. This procedure was repeated six times. At the end 10 µL of the PBS buffer were added to the beads, and the Eppendorf tube was shaking at non-magnetic rack at 4 °C for 30 minutes. After that the Eppendorf tube was placed on magnetic rack and after supernatant was discarded, the Eppendorf tube was removed from the magnetic-rack, and 100 µL of bead-blocking buffer (PBS buffer + 0.1 mg/mL BSA + 0.2 mg/mL herring

sperm DNA) were added. The tube was placed again on magnetic rack, and the supernatant was aspirated and discarded. The beads were washed again with 2 x 100 µL of the PBS buffer. Then, the Eppendorf tube was removed from the magnetic rack, and 49 µL of the PBS buffer and 1 µL of the tiDEL were added to the streptavidin beads. The tube was placed on non-magnetic rack and incubated with tiDEL at room temperature for 45 minutes while shaking on a platform shaker. After incubation with the tiDEL, the streptavidin beads were washed with 8 x 100 µL of washing buffer (PBS buffer + 0.1 mg/mL BSA). For elution of binding oligonucleotide-small molecule conjugates, 20 µL of distilled water were added to the beads, the tube was closed and heated at 80 °C for 5 minutes. Then the tube was opened, placed on the magnetic rack and the supernatant was collected into a new Eppendorf DNA LoBind microcentrifuge tube. This procedure was repeated two times, so that all together 40 µL of the eluate were obtained and finally stored at -20 °C.

A portion of the eluted DNA (10 µL out of 40 µL) was analyzed by agarose gel electrophoresis (5.5 % agarose) according to the protocol for analysis of ligation reactions, and another portion (10 µL out of 40 µL) was amplified by PCR (forward primer: 5'- GTA GAG CGT ACG TTA GGC AGG TCG GTG TGA ACG GAT TTG -3', backward primer: 5'- GTA GAG CGT ACG TTA GGC TGT AGA CCA TGT AGT TGA GGT CA-3'). The remaining 20 µL of the eluate were re-exposed to fresh streptavidin beads for a second selection round. The beads were washed and eluted as described above. After selection experiments, the coding DNA of the oligonucleotide-compound conjugates was amplified by PCR as described above. After PCR, corresponding samples were pooled and purified by Nucleospin® Gel and PCR Clean-Up Column and eluted with 20 µL of 5 mM Tris/HCl buffer, pH= 8.5.

5.4.9. Synthesis of reference molecules and intermediates

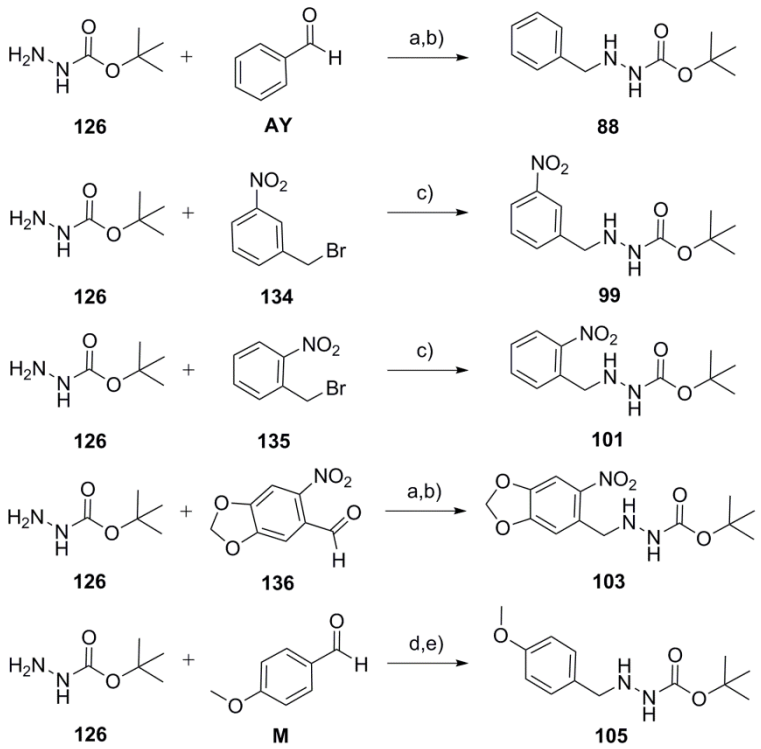

Figure 5.3. Synthesis of hydrazides **88**, **99**, **101**, **103**, and **105**. Reagents and conditions: a) dry THF, room temperature, 18 hours; b) dry THF (compound **88**) or dry MeOH (compound **103**), $NaBH_3CN$, room temperature, 18 hours; c) K_2CO_3, dry DMF, 90 °C, 30 min (compound **99**) or two hours (compound **101**); d) dry MeOH, 50 °C, 18 hours; e) 10 % Pd/C, room temperature, 1.5 h.

tert-Butyl-2-benzylidenehydrazine-1-carboxylate 137[218]

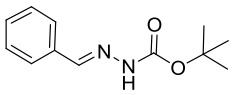

To a solution of *tert*-butyl carbazate **126** (1 g, 7.57 mmol, 1.0 eq.) in dry THF (10 mL) benzaldehyde **AY** was added (772 µL, 7.57 mmol, 1.0 eq.). The reaction mixture was stirred at room temperature for 18 hours. The reaction was concentrated *in vacuo* to a residue and the crude product was purified by column chromatography (solvent system: CH_2Cl_2/ ethyl acetate 100:0 to 90:10) to provide **137** (892 mg, 53 % yield). ^{1}H NMR (400 MHz, $CDCl_3$): δ 8.06 (s, 1H), 7.85 (br. s, 1H), 7.65-7.68 (m, 2H), 7.33-7.36 (m, 3H), 1.53 (s, 9H). ^{13}C NMR (100 MHz, $CDCl_3$): δ 153.0, 143.7, 134.0, 129.9, 128.7, 127.3, 81.6, 28.4. LC-MS (ESI) *m/z* Calcd. for $[C_{12}H_{17}N_2O_2, M+H]^+$: 221.13, found 221.20. Purity (HPLC): 90 %.

***tert*-Butyl 2-benzylhydrazine-1-carboxylate 88**[218]

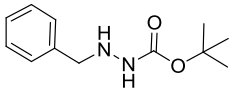

To a solution of *tert*-butyl-2-benzylidenehydrazine-1-carboxylate **137** (892 mg, 4.05 mmol, 1.0 eq.) dissolved in dry THF (9 mL), $NaBH_3CN$ (636.6 mg, 10.12 mmol, 2.5 eq.) was slowly added at 0 °C. Then acetic acid (6.07 mL, 106.1 mmol, 26.2 eq.) was added, and the reaction mixture was allowed to warm to room temperature, and to stir for 18 hours. Next day, an additional amount of $NaBH_3CN$ (636.6 mg, 10.12 mmol, 2.5 eq.) was added and the stirring was prolonged for one day. The crude product was extracted with ethyl acetate (3 x 30 mL). Organic layers were combined, washed with sat. aq. $NaHCO_3$ solution (100 mL) and brine (100 mL), dried over anhydrous $MgSO_4$ and concentrated *in vacuo*. The crude product obtained as white solid was dissolved in methanol (8 mL) and 1M NaOH solution (8 mL) and stirred at room temperature for 2 days. After that, methanol was removed under reduced pressure and extraction with ethyl acetate (3 x 30 mL) was performed. The combined organic layers were washed extensively with brine (3 x 100 mL), dried over anhydrous $MgSO_4$ and concentrated *in vacuo*. The crude product was purified by column chromatography (solvent system: CH_2Cl_2/ ethyl acetate 100:0 to 90:10) to provide **88** (567 mg, 62 % yield). ^{1}H NMR (500 MHz, $CDCl_3$): δ 7.32-7.37 (m, 4H), 7.28-7.30 (m, 1H), 6.17 (br. s, 1H), 4.19 (br. s, 1H), 3.99 (s, 2H), 1.46 (s, 9H). ^{13}C NMR (125 MHz, $CDCl_3$): δ 156.8, 137.8, 129.1, 128.6, 127.6, 80.6, 55.9, 28.5. LC-MS (ESI) *m*/*z* Calcd. for $[C_{12}H_{19}N_2O_2, M+H]^+$: 223.14, found 223.16. Purity (HPLC): 95 %.

***tert*-Butyl 2-(3-nitrobenzyl)hydrazinecarboxylate 99**

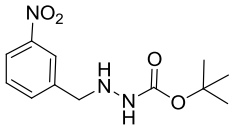

To a solution of 3-nitrobenzyl bromide **134** (100 mg, 0.46 mmol, 1.0 eq.) in dry DMF (2 mL), *tert*-butyl carbazate **126** (464.9 mg, 3.52 mmol, 7.6 eq.) and potassium carbonate (70.4 mg, 0.51 mmol, 1.1 eq.) were added. The reaction mixture was stirred at 90 °C for 30 minutes. After that, solvent was evaporated *in vacuo.* The crude product was extracted with diethyl ether (3 x 30 mL), combined organic layers were washed with brine (90 mL) and dried over anhydrous $MgSO_4$. The crude product was purified by column chromatography (solvent system: CH_2Cl_2/ ethyl acetate 100:0 to 75:25) to provide **99** (18 mg, 14 % yield). ^{1}H NMR (500 MHz, $CDCl_3$): δ 8.23 (s, 1H), 8.13 (dd, ^3J= 8.3 Hz and ^4J= 1.5 Hz, 1H), 7.68 (d, ^3J= 7.8 Hz, 1H), 7.5 (t, ^3J= 8.1 (x 2) Hz, 1H), 6.07 (br. s, 1H), 4.11 (s, 2H), 1.45 (s, 9H). ^{13}C NMR (125 MHz, $CDCl_3$): δ 157.4, 149.8, 140.3, 135.1, 129.5, 123.8, 122.6, 81.0, 55.0, 28.5. HRMS (ESI) *m*/*z* Calcd. for $[C_{12}H_{18}N_3O_4$,

M+H] $^{+}$: 268.1297, found 268.1293; *m/z* Calcd. for [$C_{12}H_{18}N_3NaO_4$, M+Na] $^{+}$: 290.1117, found: 290.1112. Purity (HPLC): 98 %.

tert-Butyl 2-(2-nitrobenzyl)hydrazinecarboxylate 101

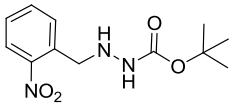

To a solution of 2-nitrobenzyl bromide **135** (300 mg, 1.39 mmol, 1.0 eq.) in dry DMF (2 mL), *tert*-butyl carbazate **126** (1394.8 mg, 10.55 mmol, 7.6 eq.) and potassium carbonate (211.3 mg, 1.53 mmol, 1.1 eq.) were added. The reaction mixture was stirred at 90 °C for 2 hours. After that, solvent was evaporated *in vacuo.* The crude product was extracted with diethyl ether (3 x 50 mL), combined organic layers were washed with brine (150 mL) and dried over anhydrous $MgSO_4$. The crude product was purified by column chromatography (solvent system: CH_2Cl_2/ ethyl acetate 100:0 to 75:25) to provide **101** (340 mg, 91 % yield). ^{1}H NMR (500 MHz, $CDCl_3$): δ 7.95 (d, ^{3}J= 7.95 Hz, 1H), 7.54-7.58 (m, 2H), 7.42-7.45 (m, 1H), 6.05 (br. s, 1H), 4.53 (br. s, 1H), 4.28 (s, 2H), 1.39 (s, 9H). ^{13}C NMR (125 MHz, $CDCl_3$): δ 156.8, 149.6, 133.3, 133.1, 131.9, 128.6, 125.0, 80.8, 53.4, 28.4. HRMS (ESI) *m/z* Calcd. for [$C_{12}H_{18}N_3O_4$, M+H] $^{+}$: 268.1297, found 268.1293; *m/z* Calcd. for [$C_{12}H_{18}N_3NaO_4$, M+Na] $^{+}$: 290.1117, found: 290.1112. Purity (HPLC): 99 %.

(_E_)-_tert_-Butyl 2-((6-nitrobenzo[d][1,3]dioxol-5-yl)methylene)hydrazinecarboxylate 138[229]

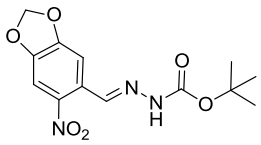

tert-Butyl 2-((6-nitrobenzo[d][1,3]dioxol-5-yl)methylene)hydrazine-1-carboxylate **138** was synthesized according to the procedure for synthesis of *tert*-butyl-2-benzylidenehydrazine-1-carboxylate **137** making use of *tert*-butyl carbazate **126** (1 g, 7.57 mmol, 1.0 eq.) and 6-nitro-benzo[d][1,3]dioxole-5-carbaldehyde **136** (1.476 g, 7.57 mmol, 1.0 eq.). Desired product **138** was obtained as a yellow solid (1.635 g, 70 % yield). ^{1}H NMR (500 MHz, $CDCl_3$): δ 8.44 (s, 1H), 8.25 (s, 1H), 7.63 (s, 1H), 7.50 (s, 1H), 6.14 (s, 2H), 1.53 (s, 9H) ppm. ^{13}C NMR (125 MHz, $CDCl_3$): δ 156.2, 152.3, 149.0, 144.4, 142.7, 126.5, 107.0, 105.3, 103.4, 82.1, 28.4 ppm. LC-MS (ESI) *m/z* Calcd. for [$C_{13}H_{15}N_3NaO_6$, M+Na]$^{+}$: 332.09, found 331.92. Purity (HPLC): 96 %.

***tert*-Butyl 2-((6-nitrobenzo[d][1,3]dioxol-5-yl)methyl)hydrazinecarboxylate 103**[229]

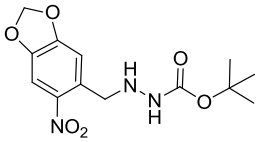

Compound **138** (1.03 g, 3.34 mmol, 1.0 eq.) was dissolved in methanol (21 mL) and $NaBH_3CN$ (1.05 g, 16.72 mmol, 5.0 eq.) was slowly added. Then one tip of a spoon of bromocresol green as indicator was added to turn the reaction mixture blue (pH > 5.4). To further acidify the solution, 1M pTsOH x H_2O solution in MeOH was added until the solution turned yellow (pH < 3.8). Then the reaction mixture was stirred at room temperature for 18 hours. The crude product was extracted with ethyl acetate (3 x 50 mL). Organic layers were combined, washed with sat. aq. $NaHCO_3$ solution (100 mL) and brine (100 mL), dried over anhydrous $MgSO_4$ and concentrated *in vacuo*. The crude product was purified by column chromatography (solvent system: CH_2Cl_2/ ethyl acetate 100:0 to 90:10) to provide **103** (747 mg, 72 % yield). ^{1}H NMR (500 MHz, $CDCl_3$): δ 7.51 (s, 1H), 7.01 (s, 1H), 6.10 (s, 2H), 6.08 (br. s, 1H), 4.56 (br. s, 1H), 4.19 (s, 2H), 1.41 (s, 9H). ^{13}C NMR (125 MHz, $CDCl_3$): δ 156.7, 151.8, 147.3, 143.3, 130.9, 110.5, 106.1, 103.0, 80.9, 53.8, 28.4. LC-MS (ESI) *m*/*z* Calcd. for $[C_{13}H_{17}N_3NaO_6, M+Na]^+$: 334.10, found 333.99. Purity (HPLC): 97 %.

***tert*-Butyl (E)-2-(4-methoxybenzylidene)hydrazine-1-carboxylate 139**[230]

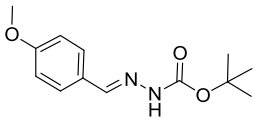

To a solution of *tert*-butyl carbazate **126** (2 g, 15.1 mmol, 1.0 eq.) in dry methanol (75 mL) anisaldehyde **M** was added (2.06 g, 15.1 mmol, 1.0 eq.). The reaction mixture was stirred at 50 °C for 18 hours. After that, the reaction was filtered, the precipitate was washed with pentane and dried *in vacuo* to provide **139** that was used in the next step without further purification (3.63 g, 96 % yield). ^{1}H NMR (300 MHz, $CDCl_3$): δ 8.05 (s, 1H), 7.80 (s, 1H), 7.61 (d, ^3J= 8.8 Hz, 2H), 6.88 (d, ^3J= 8.8 Hz, 2H), 3.81 (s, 3H), 1.53 (s, 9H). MS (ESI) *m*/*z* calcd. for $C_{13}H_{19}N_2O_2$: 251.14; found 251.21 $[M+H]^+$. Purity (HPLC): 97 %. The analytical data are consistent with the literature values.

tert-Butyl 2-(4-methoxybenzyl)hydrazine-1-carboxylate 105[230]

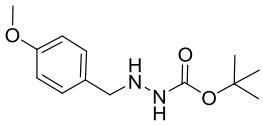

To a solution of *tert*-butyl-2-benzylidenehydrazine-1-carboxylate **139** (2.0 g, 7.99 mmol, 1.0 eq.) dissolved in dry methanol (40 mL) was 10 % Pd/C (0.01 eq.) added. The reaction mixture was stirred at room temperature under argon atmosphere for 1.5 hour. Then, the reaction mixture was filtered over Celite pad and concentrated *in vacuo*. The crude product was dissolved in hot ethanol and placed for crystallization at -2 °C for overnight to provide **105** (1.16 g, 58 % yield). ^{1}H NMR (300 MHz, $CDCl_3$): δ 7.30 (d, ^{3}J= 8.4 Hz, 2H), 6.88 (d, ^{3}J= 8.8 Hz, 2H), 6.25 (br. s, 1H), 3.96 (s, 2H), 3.81 (s, 3H), 3.33 (br. s, 1H), 1.47 (s, 9H). LC-MS (ESI) *m/z* Calcd. for [$C_{13}H_{21}N_2O_3$, M+H] $^{+}$: 253.16, found 253.25. Purity (HPLC): 97 %. The analytical data are consistent with the literature values.[230]

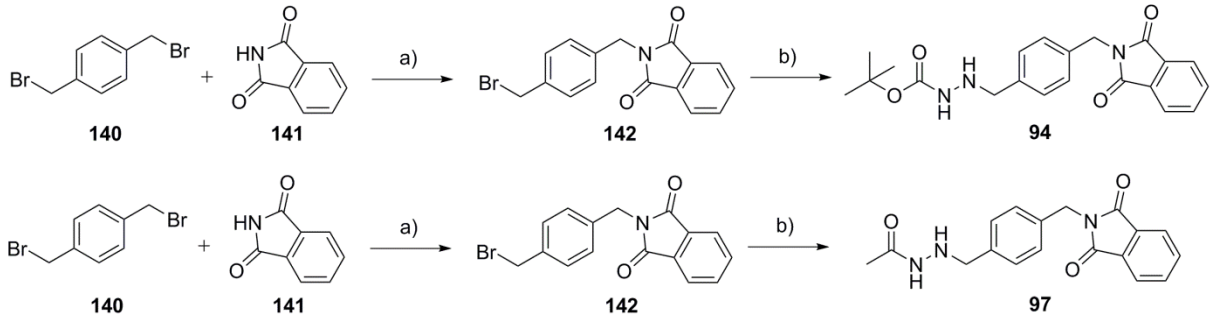

Figure 5.4. Synthesis of the hydrazides **94** and **97**. Reagents and conditions: a) K_2CO_3 in MeCN, room temperature, 18 hours; b) *tert*-butyl carbazate (**126**) or acetohydrazide (**143**), K_2CO_3, dry CH_2Cl_2, room temperature, 18 hours.

2-(4-(Bromomethyl)benzyl)isoindoline-1,3-dione 142[231]

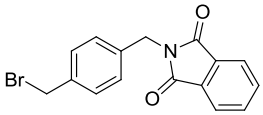

To a solution of phthalimide **141** (1.0 g, 6.8 mmol, 1.0 eq.) in dry acetonitrile (60 mL), 1,4-bis(bromomethyl)benzene **140** (1794 mg, 6.8 mmol, 1.0 eq.), 18-crown-6 (26.9 mg, 1.0 mmol, 0.15 eq.) and potassium carbonate (3.8 g, 27 mmol, 4.0 eq.) were added. The reaction mixture was stirred under argon atmosphere at room temperature for 18 hours. After that, ethyl acetate (200 mL) was added and the reaction mixture was filtered over filter paper. The filtrate was concentrated *in vacuo* and the crude product was purified by column chromatography (solvent system: hexanes/ CH_2Cl_2 100:0 to 90:10) to provide **142** (1.4 g, 63 % yield). ^{1}H NMR (500 MHz, $CDCl_3$): δ 7.83-7.85 (m, 2H), 7.70-7.72 (m, 2H), 7.41 (d, ^{3}J= 8.2 Hz, 2H), 7.34 (d, ^{3}J= 8.2 Hz, 2H), 4.85 (s, 2H), 4.44 (s, 2H). ^{13}C NMR (125 MHz, $CDCl_3$): δ 168.1, 137.5, 136.7,

134.2, 132.1, 129.5, 129.2, 123.5, 41.3, 33.2. LC-MS (ESI) *m/z* Calcd. for [$C_{16}H_{13}BrNO_2$, M+H]$^+$: 330.01, found 330.05. Purity (HPLC): 99 %.

tert-Butyl 2-(4-((1,3-dioxoisoindolin-2-yl)methyl)benzyl)hydrazinecarboxylate 94

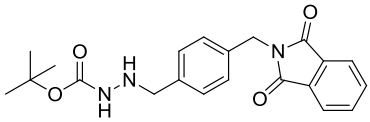

To a solution of **142** (500 mg, 1.51 mmol, 1.0 eq.) in dry CH_2Cl_2 (12 mL), *tert*-butyl carbazate **126** (1521 g, 11.51 mmol, 7.6 eq.) and potassium carbonate (229.4 mg, 1.66 mmol, 1.1 eq.) were added. The reaction mixture was stirred under argon atmosphere at room temperature for 18 hours. After that, ethyl acetate (100 mL) was added and the reaction mixture was filtered over filter paper. The filtrate was concentrated *in vacuo* and the crude product was purified by column chromatography (solvent system: hexanes/ ethyl acetate 100:0 to 75:25) to provide **94** (481 mg, 84 % yield). mp 144-147 °C; ^{1}H NMR (500 MHz, $CDCl_3$): δ 7.83-7.85 (m, 2H), 7.68-7.72 (m, 2H), 7.40 (d, ^3J= 7.9 Hz, 2H), 7.29 (d, ^3J= 7.95 Hz, 2H), 6.01 (br. s, 1H), 4.83 (s, 2H), 4.12 (br. s, 1H), 3.94 (s, 2H), 1.43 (s, 9H). ^{13}C NMR (125 MHz, $CDCl_3$): δ 168.18, 156.79, 135.67, 134.14, 132.20, 129.63, 129.43, 128.90, 123.49, 80.67, 55.45, 41.43, 28.46. HRMS (ESI) *m/z* Calcd. for [$C_{21}H_{24}N_3O_4$, M+H]$^+$: 382.1767, found 382.1761; *m/z* Calcd. for [$C_{21}H_{24}N_3NaO_4$, M+Na] $^+$: 404.1586, found: 404.1579. Purity (HPLC): 95 %.

_N_'-(4-((1,3-Dioxoisoindolin-2-yl)methyl)benzyl)acetohydrazide 97

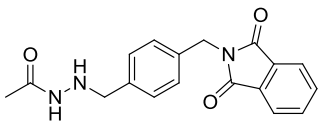

To a solution of **142** (500 mg, 1.51 mmol, 1.0 eq.) in dry CH_2Cl_2 (12 mL), acetohydrazide **143** (852.6 mg, 11.51 mmol, 7.6 eq.) and potassium carbonate (229.4 mg, 1.5 mmol, 1.1 eq.) were added. The reaction mixture was stirred under argon atmosphere at room temperature for 18 hours. After that, ethyl acetate (100 mL) was added and the reaction mixture was filtered over filter paper. The filtrate was concentrated *in vacuo* and the crude product was purified by column chromatography (solvent system: ethyl acetate/ MeOH 100:0 to 95:05) to provide **97** (150 mg, 31 % yield). mp 136-138 °C; ^{1}H NMR (500 MHz, $CDCl_3$): δ 7.83-7.85 (m, 2H), 7.70-7.72 (m, 2H), 7.39 (d, ^3J= 7.8 Hz, 2H), 7.29 (d, ^3J= 7.95 Hz, 2H), 6.98 (br. s, 1H), 4.83 (s, 2H), 4.88 (br. s, 1H), 3.92 (s, 2H), 1.89 (s, 3H). ^{13}C NMR (125 MHz, $CDCl_3$): δ 168.2, 137.5, 135.8, 134.2, 129.3, 128.8, 123.5, 123.2, 55.4, 41.4, 21.3. LC-MS (ESI) *m/z* Calcd. for [$C_{18}H_{18}N_3O_3$, M+H] $^+$: 324.13, found 323.97. Purity (HPLC): 98 %.

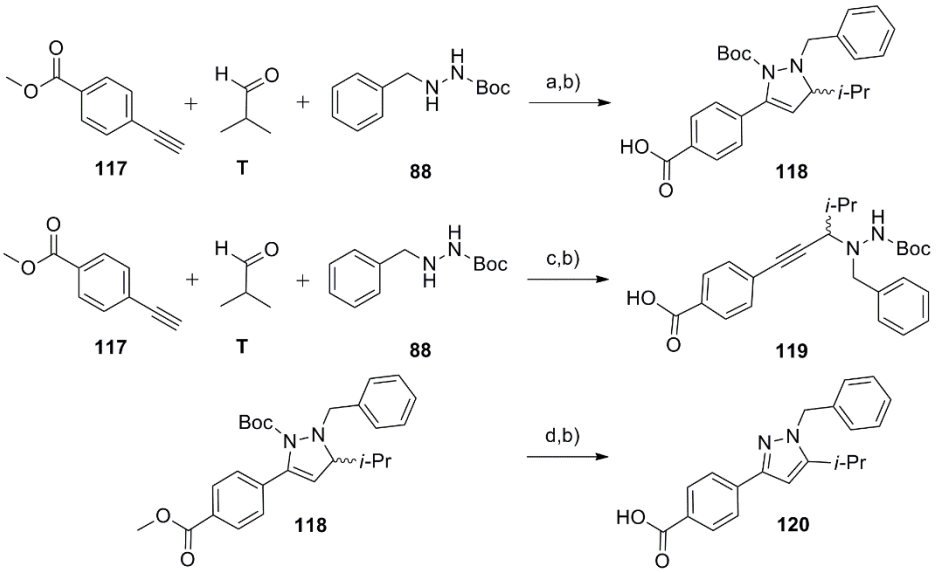

Figure 5.5. Synthesis of reference molecules **PL-C**, **PH-C**, and **P-C**. Reagents and conditions: a) Au(I)/Ag(I), toluene, 50 °C, 16 hours; b) NaOH in MeOH/ H_2O, room temperature, 16 hours; c) AgOTf, dry toluene, 50 °C, 4 hours; d) DDQ, CH_2Cl_2, room temperature, 3 hours.

tert-Butyl 2-benzyl-3-isopropyl-5-(4-(methoxycarbonyl)phenyl)-2,3-dihydro-1*H*-pyrazole -1-carboxylate 145[207]

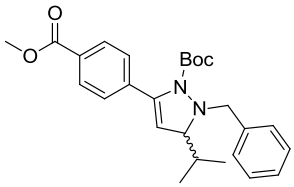

To a solution of methyl 4-ethynylbenzoate **144** (120.0 mg, 0.75 mmol, 1.2 eq.), *tert*-butyl 2-benzylhydrazine-1-carboxylate **88** (138.6 mg, 0.62 mmol, 1.0 eq.) and isobutyraldehyde **T** (68.4 µL, 0.75 mmol, 1.2 eq.) in dry toluene (2.7 mL), chloro(triphenylphosphine)gold(I) (PPh_3AuCl, 15.4 mg, 0.03 mmol, 0.05 eq.) and silver trifluoromethanesulfonate (AgOTf, 8.0 mg, 0.03 mmol, 0.05 eq.) were added. The reaction mixture was stirred at 50 °C for 16 hours argon atmosphere. After that, it was filtered over celite pad and concentrated *in vacuo*. The crude product was purified by column chromatography (solvent system: hexanes/ ethyl acetate 100:0 to 90:10) to provide **145** (262 mg, 96 % yield). mp 84-88 °C; ^{1}H NMR (400 MHz, $CDCl_3$): δ 8.00 (d, ^3J= 8.8 Hz, 2H), 7.45-7.50 (m, 4H), 7.27-7.35 (m, 3H), 5.58 (d, ^3J= 2.9 Hz, 1H), 4.08 (d, ^2J= -12.2 Hz, 1H), 3.92 (s, 3H), 3.75 (d, ^2J= -12.2 Hz, 1H), 3.30 (dd, ^3J= 6.1 Hz and ^3J= 3.2 Hz, 1H), 1.47-1.57 (m, 1H), 1.24 (s, 9H), 0.79 (d, ^3J= 6.8 Hz, 3H), 0.76 (d, ^3J= 6.8 Hz, 3H). ^{13}C NMR (100 MHz, $CDCl_3$): δ 167.0, 154.9, 141.9, 138.0, 137.0, 130.6, 129.5, 129.4, 128.1, 127.5, 126.9, 113.0, 81.0, 74.1, 63.0, 52.2, 32.9, 28.0, 18.5, 18.3. HRMS (ESI) *m*/*z* Calcd. for [$C_{26}H_{33}N_2O_4$, M+H]$^+$: 437.2440, found 437.2433; *m*/*z* Calcd. for [$C_{26}H_{32}N_2NaO_4$, M+Na] $^+$: 459.2260, found: 459.2250. Purity (HPLC): 98 %.

4-(1-Benzyl-2-(*tert*-butoxycarbonyl)-5-isopropyl-2,5-dihydro-1*H*-pyrazol-3-yl)benzoic acid PL-C

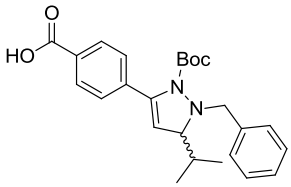

To a solution of **145** (200 mg, 0.37 mmol, 1.0 eq.) in dry MeOH (3.8 mL), 2 M aqueous NaOH (3.8 mL) was added. The reaction mixture was stirred at room temperature for 16 hours. After that, MeOH was evaporated *in vacuo* and reaction mixture was extracted with CH_2Cl_2 (3 x 5 mL). The combined organic layers were dried over anhydrous $MgSO_4$, concentrated *in vacuo* and purified by column chromatography (solvent system: CH_2Cl_2/ MeOH 100:0 to 95:5) to provide the compound **PL-C** (67.7 mg, 43 % yield). mp 107-109 °C; ^{1}H NMR (400 MHz, $CDCl_3$): δ 8.01-8.08 (m, 2H), 7.34-7.43 (m, 4H), 7.21-7.31 (m, 3H), 5.44 (br. s, 1H), 4.04 (d, ^2J= -11.7 Hz, 1H), 3.67 (d, ^2J= -12.2 Hz, 1H), 3.21 (br. s, 1H), 1.41-1.48 (m, 1H), 1.20 (s, 9H), 0.73 (d, ^3J= 6.8 Hz, 3H), 0.69 (d, ^3J= 6.8 Hz, 3H). ^{13}C NMR (100 MHz, $CDCl_3$): δ 169.9, 154.8, 142.1, 139.5, 137.0, 130.6, 129.9, 129.9, 128.09, 127.5, 126.6, 104.6, 80.9, 73.8, 62.9, 32.8, 28.0, 18.4, 18.3. HRMS (ESI) *m*/*z* Calcd. for [$C_{25}H_{31}N_2O_4$, M+H] $^+$: 423.2284, found: 423.2276. Purity (HPLC): 98 %.

***tert*-Butyl 2-benzyl-2-(1-(4-(methoxycarbonyl)phenyl)-4-methylpent-1-yn-3yl)hydrazine-carboxylate 146**[207]

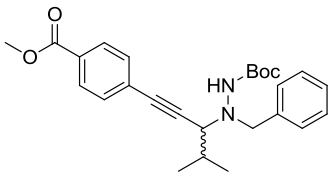

To a solution of methyl 4-ethynylbenzoate **144** (100.0 mg, 0.62 mmol, 1.2 eq.), *tert*-butyl 2-benzylhydrazine-1-carboxylate **88** (115.6 mg, 0.52 mmol, 1.0 eq.) and isobutyraldehyde **T** (57.0 µL, 0.62 mmol, 1.2 eq.) in dry toluene (2.6 mL), silver trifluoromethanesulfonate (AgOTf, 2.7 mg, 0.01 mmol, 0.02 eq.) was added. The reaction mixture was stirred at 50 °C for 4 hours under argon atmosphere. After that, it was filtered over celite pad and concentrated *in vacuo*. The crude product was purified by column chromatography (solvent system: hexanes/ ethyl acetate 100:0 to 90:10) to provide **146** (62 mg, 27 % yield). ^{1}H NMR (500 MHz, $CDCl_3$): δ 8.02 (d, ^3J= 8.2 Hz, 2H), 7.54 (d, ^3J= 7.9 Hz, 2H), 7.39-7.50 (m, 2H), 7.27-7.34 (m, 3H), 3.93 (s, 3H), 3.25 (br. s, 1H), 1.86-1.93 (m, 1H), 1.39 (s, 9H), 1.13 (d, ^3J= 6.4 Hz, 3H), 1.05 (d, ^3J= 6.7 Hz, 3H). ^{13}C NMR (125 MHz, $CDCl_3$): δ 166.6, 166.4, 132.6, 131.9, 129.7, 129.7, 128.3, 127.7, 126.2, 100.0, 82.5**,** 82.0, 63.8, 52.5, 52.4, 31.2, 28.3, 20.3, 20.2. HRMS (ESI) *m*/*z* Calcd. for [$C_{26}H_{33}N_2O_4$, M+H] $^+$: 437.2440, found 437.2434; *m*/*z* Calcd. for [$C_{26}H_{32}N_2NaO_4$, M+Na] $^+$: 459.2260, found: 459.2252. Purity (HPLC): 95 %.

4-(3-(2-(*tert*-Butoxycarbonyl)-1-(2-nitrobenzyl)hydrazinyl)-4-methylpent-1-yn-1-yl) benzoic acid PH-C

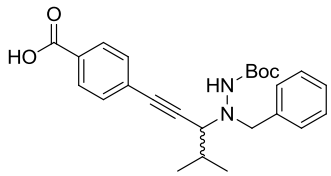

To a solution of **146** (37 mg, 0.08 mmol, 1.0 eq.) in dry MeOH (0.8 mL), 2 M aqueous NaOH (0.8 mL) was added. The reaction mixture was stirred at room temperature for 16 hours. After that, MeOH was evaporated *in vacuo* and reaction mixture was extracted with CH_2Cl_2 (3 x 5 mL). The combined organic layers were dried over anhydrous $MgSO_4$, concentrated *in vacuo* and purified by column chromatography (solvent system: CH_2Cl_2/ MeOH 100:0 to 95:5) to provide the compound **PH-C** (23.6 mg, 66 % yield). ^{1}H NMR (400 MHz, $CDCl_3$): δ 7.65-7.74 (m, 2H), 7.47 (d, ^3J= 6.8 Hz, 2H), 7.28-7.43 (m, 5H), 4.00-4.04 (m, 1H), 3.91-3.98 (m, 1H), 3.16-3.25 (m, 1H), 1.83-1.93 (m, 1H), 1.39 (s, 9H), 1.14 (d, ^3J= 6.4 Hz, 3H), 1.05 (d, ^3J= 6.7 Hz, 3H). ^{13}C NMR (100 MHz, $CDCl_3$): δ 169.0, 166.8, 132.4, 131.9, 131.8, 130.0, 129.8, 128.3, 127.6, 100.1, 82.4, 81.4, 65.0, 55.7, 31.5, 28.3, 20.3. HRMS (ESI) *m*/*z* Calcd. for [$C_{25}H_{31}N_2O_4$, M+H] $^+$: 423.2284, found: 423.2276. Purity (HPLC): 99 %.

Methyl 4-(1-benzyl-5-isopropyl-1H-pyrazol-3-yl)benzoate 147

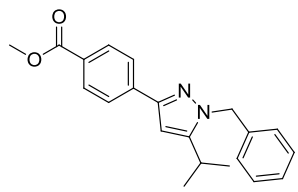

To a solution of pyrazoline **145** (150.0 mg, 0.34 mmol, 1.0 eq.) in dry dichloromethane (1.6 mL), 2,3-dichloro-5,6-dicyano-1,4-benzoquinone (DDQ, 115.8 mg, 0.51 mmol, 1.5 eq.) was added. The reaction mixture was stirred at room temperature for 3 hours. After that, reaction was quenched by addition of sat. aq. $NaHCO_3$ solution (0.7 mL). Then, the reaction mixture was extracted with CH_2Cl_2 (3 x 5 mL). The combined organic layers were dried over anhydrous $MgSO_4$, concentrated *in vacuo* and purified by column chromatography (solvent system: hexanes/ ethyl acetate 100:0 to 80:20) to provide **147** (109 mg, 95 % yield). mp 92-94 °C; ^{1}H NMR (500 MHz, $CDCl_3$): δ 7.98 (d, ^3J= 8.2 Hz, 2H), 7.82 (d, ^3J= 8.2 Hz, 2H), 7.22-7.25 (m, 2H), 7.17-7.19 (m, 1H), 7.03 (d, ^3J= 7.6 Hz, 2H), 6.41 (s, 1H), 5.32 (s, 2H), 3.85 (s, 3H), 2.77-2.85 (m, 1H), 1.12 (d, ^3J= 6.7 Hz, 6H). ^{13}C NMR (125 MHz, $CDCl_3$): δ 167.3, 151.6, 149.4, 138.3, 137.4, 130.1, 128.8, 127.7, 126.6, 125.4, 100.5, 53.2, 51.2, 25.7, 23.0, 18.8, 18.5. HRMS (ESI) *m*/*z* Calcd. for [$C_{21}H_{23}N_2O_2$, M+H] $^+$: 335.1760, found: 335.1753. Purity (HPLC): 99 %.

4-(1-Benzyl-5-isopropyl-1H-pyrazol-3-yl)benzoic acid P-C

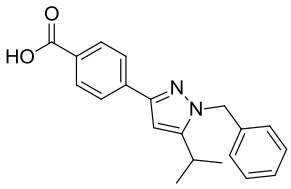

To a solution of pyrazole **147** (80 mg, 0.24 mmol, 1.0 eq.) in dry MeOH (2.5 mL), 2 M aqueous NaOH (2.5 mL) was added. The reaction mixture was stirred at room temperature for 16 hours. After that, MeOH was evaporated *in vacuo* and reaction mixture was extracted with CH_2Cl_2 (3 x 5 mL). The combined organic layers were dried over anhydrous $MgSO_4$, concentrated *in vacuo* and purified by column chromatography (solvent system: CH_2Cl_2/ MeOH 100:0 to 95:5) to provide the compound **P-C** (54.5 mg, 71 % yield). mp 167-169 °C; ^{1}H NMR (500 MHz, $CDCl_3$): δ 8.07 (d, ^3J= 8.2 Hz, 2H), 7.86 (d, ^3J= 8.2 Hz, 2H), 7.24-7.17 (m, 3H), 7.05 (d, ^3J= 7.6 Hz, 2H), 6.43 (s, 1H), 5.35 (s, 2H), 2.78-2.86 (m, 1H), 1.13 (d, ^3J= 7.0 Hz, 6H). ^{13}C NMR (125 MHz, $CDCl_3$): δ 171.8, 155.3, 150.3, 141.9, 138.6, 133.5, 132.6, 132.5, 130.1, 128.7, 128.5, 126.8, 124.6, 114.4, 81.4, 76.6, 59.7, 33.0, 27.9, 18.8, 18.5. HRMS (ESI) *m*/*z* Calcd. for $[C_{20}H_{21}N_2O_2, M+H]^+$: 321.1603, found: 321.1618. Purity (HPLC): 99 %.

5.5. Synthesis of hexathymidine-6-oxa-1,2-diazaspiro-[4.4]nona-ne conjugates by Au(I)-mediated [3+2]-cycloaddition

5.5.1. Synthesis of DNA-aldehyde, -hydrazide, and -alkynol conjugates

5.5.1.1. Synthesis of DNA-aldehyde conjugates

The hexT/C/TC/A/G/ACT/ACGT (1 µmol each) was coupled with 2-(4-formylphenoxy)acetic acid **148** (18.0 mg, 100 µmol, 100 eq.) to furnish **hexT/C/TC/A/G/ACT/ACGT-115** conjugates according to the procedure for coupling of carboxylic acids to 5'-amino-linker modified DNA. For analysis, an aliquot of ca. 10 nmol of each conjugate **hexT/C/TC/A/G/ACT/ACGT-115** was deprotected and cleaved from the CPG with 500 µL of AMA (AMA= aqueous ammonia (30 %)/ aqueous methylamine (40 %), 1:1, vol/vol) for 30 min (hexT/C/TC) or for 4 hours (hexA/G/ACT/ACGT) at room temperature. Then, 20 µL of 1 M Tris buffer (pH= 7.5) were added, the mixture was dried in a SpeedVac, and re-dissolved in 100 µL of distilled water. After purification products were analyzed by analytical RP-HPLC (Gemini, 5u, C18, 110A column; 100*4.6 mm) with a gradient of aqueous triethylammonium acetate buffer (10 mM, pH= 8) and methanol (30 % – 90 % of methanol over 15 min).

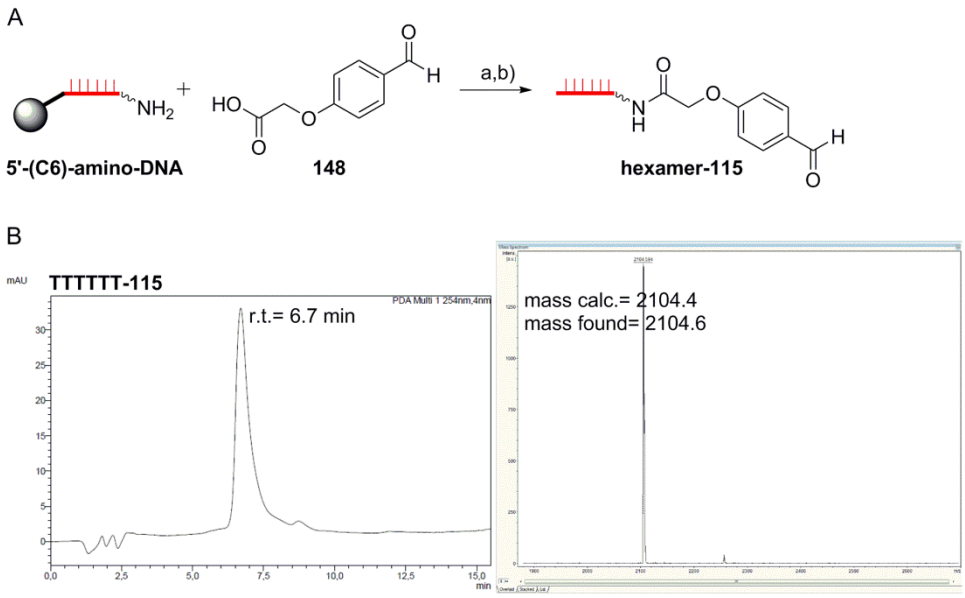

C

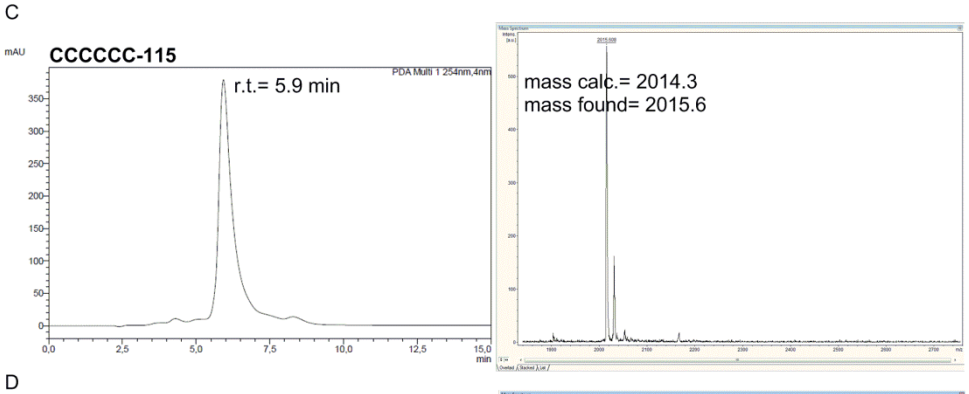
mAU
CCCCCC-115
PDA Multi 1 254nm,4nm
r.t.= 5.9 min
min
mass calc.= 2014.3
mass found= 2015.6

D

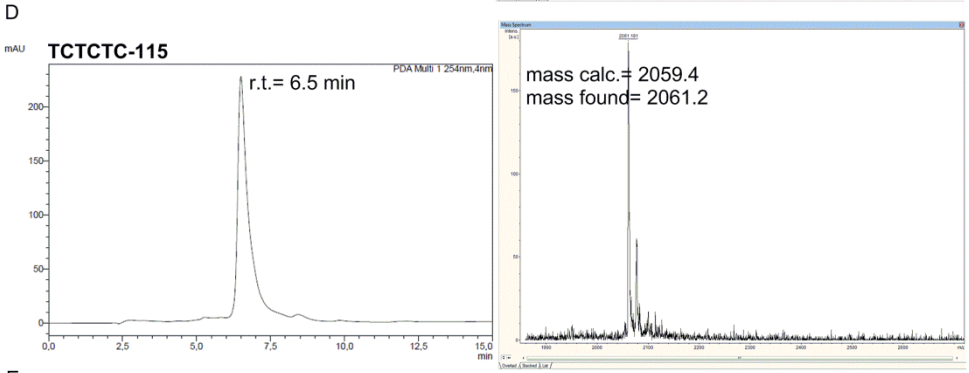
mAU
TCTCTC-115
PDA Multi 1 254nm,4nm
r.t.= 6.5 min
min
mass calc.= 2059.4
mass found= 2061.2

E

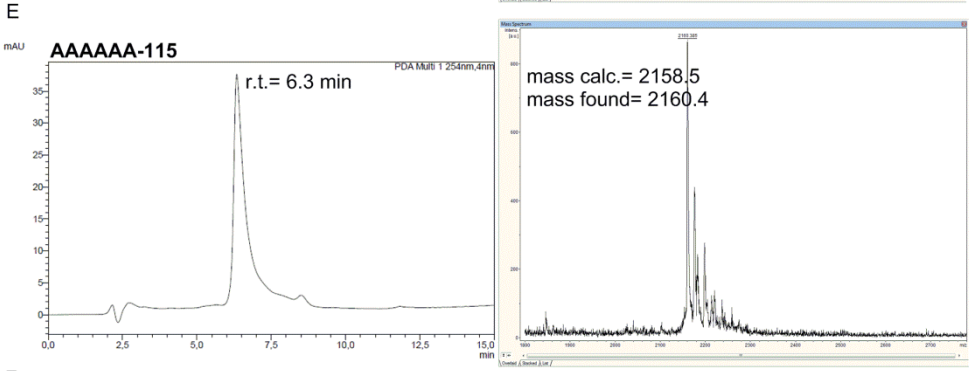
mAU
AAAAAA-115
PDA Multi 1 254nm,4nm
r.t.= 6.3 min
min
mass calc.= 2158.5
mass found= 2160.4

F

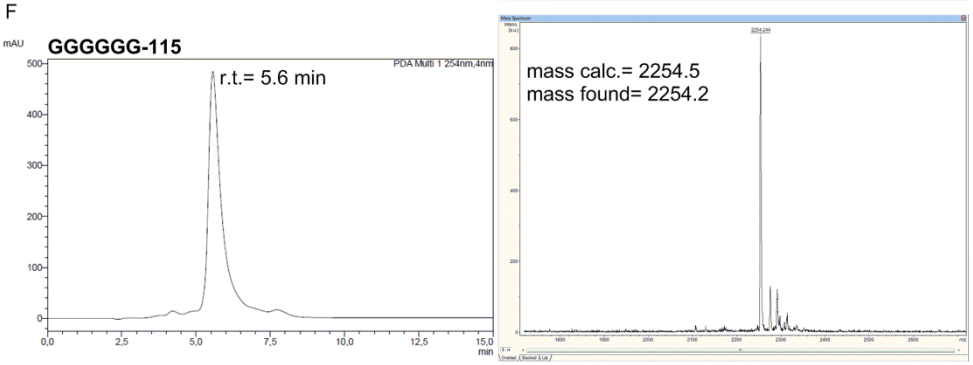
mAU
GGGGGG-115
PDA Multi 1 254nm,4nm
r.t.= 5.6 min
min
mass calc.= 2254.5
mass found= 2254.2

G

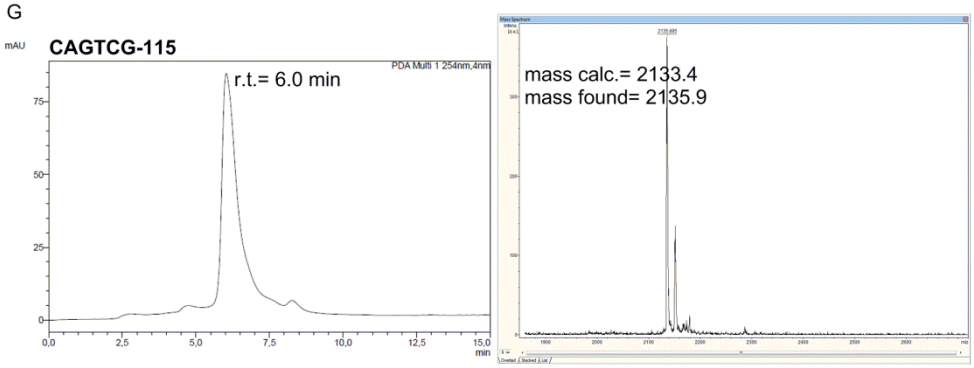
mAU
CAGTCG-115
PDA Multi 1 254nm,4nm
r.t.= 6.0 min
min
mass calc.= 2133.4
mass found= 2135.9

Figure 5.6. Synthesis of DNA-aldehyde conjugates **hexamer-115**. A) Synthesis scheme. Reagents and conditions: a) HATU, DIPEA, dry DMF, room temperature, 4 hours; b) AMA (aqueous ammonia (30 %)/ aqueous methylamine (40 %), 1:1, vol/vol), 30 min (for hexT/C/TC) or 4 hours (for hexA/G/ACT/ACGT), room temperature (aliquot); B) HPLC trace and MALDI-TOF/TOF-MS spectrum of the purified conjugate **hexT-115**; C) HPLC trace and MALDI-TOF/TOF-MS spectrum of the purified conjugate **hexC-115**; D) HPLC trace and MALDI-TOF/TOF-MS spectrum of the purified conjugate **hexTC-115**; E) HPLC trace and MALDI-TOF/TOF-MS spectrum of the purified conjugate **hexA-115**; F) HPLC trace and MALDI-TOF/TOF-MS spectrum of the purified conjugate **hexG-115**; G) HPLC trace and MALDI-TOF/TOF-MS spectrum of the purified conjugate **hexACGT-115**. Filled grey circle denotes solid support (controlled pore glass, CPG); wavy bond to DNA: 5'-(C6)-amino-linker; bold bond: connection from the DNA oligonucleotide to the CPG.

5.5.1.2. Synthesis of hexathymidine-hydrazide conjugate

Solution of compound **126** (25.6 mg, 200 mM) in 960 µL of 300 mM MOPS buffer and 20 µL of dry DMF was added to sodium cyanoborohydride (12.2 mg, 200 mM), followed by addition of glacial acetic acid (11.2 µL, 200 mM). The whole mixture was added to the CPG-bound conjugate **hexT-115** (300 nmol, ca. 11 mg) and the reaction mixture was shaken at 37 °C overnight. Then, the CPG containing the DNA conjugate **hexT-119** was filtered over a filter column, and washed as described above. For analysis, an aliquot of ca. 10 nmol of the DNA conjugate **hexT-119** was deprotected and cleaved from the CPG by treatment with 500 µL of AMA (AMA= aqueous ammonia (30 %)/ aqueous methylamine (40 %), 1:1, vol/vol) for 30 min at room temperature. To this solution 20 µL of 1 M Tris buffer (pH= 7.5) were added, the mixture was dried in a SpeedVac, re-dissolved in 100 µL of distilled water, and the product was purified/analyzed by RP-HPLC (Gemini, 5u, C18, 110A column; 50*10.0 mm) with a gradient of aqueous triethylammonium acetate buffer (100 mM, pH= 8) and methanol (20 % – 80 % of methanol over 18 min).

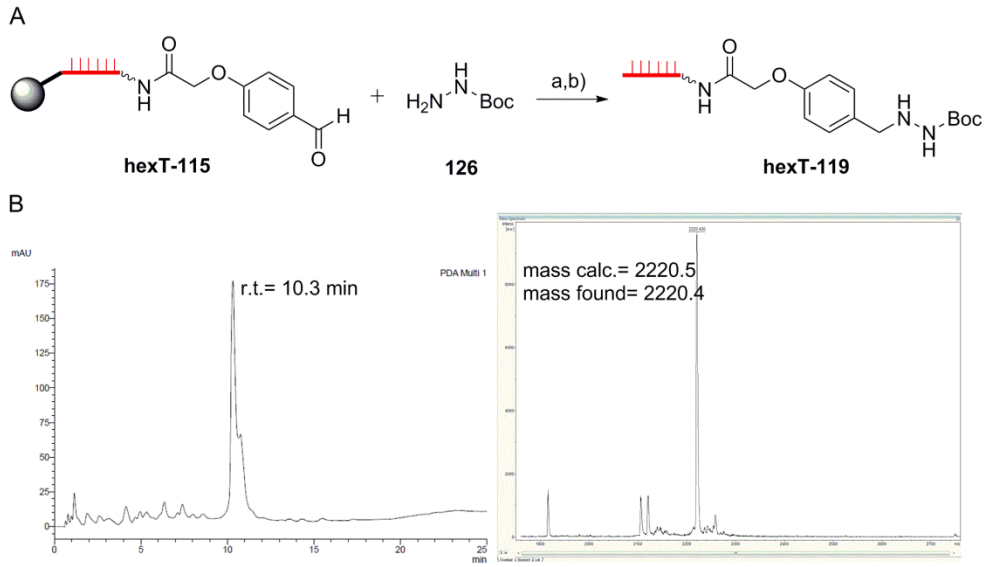

Figure 5.7. Synthesis of hexT-hydrazide conjugate **hexT-119**. A) Synthesis scheme for compound **hexT-119**. Reagents and conditions: a) $NaBH_3CN$, glacial AcOH, 37 °C, overnight; b) AMA (aqueous ammonia (30 %)/ aqueous methylamine (40 %), 1:1, vol/vol), 30 min, room temperature (aliquot); B) HPLC trace of the crude and MALDI-TOF/TOF-MS spectrum of the purified conjugate **hexT-119**. Filled grey circle denotes solid support (controlled pore glass, CPG); wavy bond to hexT: 5'-(C6)-amino-linker; bold bond: connection from the hexT-oligonucleotide to the CPG.

5.5.1.3. Synthesis of hexathymidine-alkynol conjugate

The hexT (1 µmol, ca. 36 mg) was coupled with 4-(5-((*tert*-butyldimethylsilyl)oxy)pent-1-yn-1-yl)benzoic acid **149** (31.8 mg, 100 µmol, 100 eq.) to furnish **hexT-150** conjugate according to the procedure for coupling of carboxylic acids to 5'-amino-linker modified DNA. Then, the TBMS-group of the CPG-bound conjugate **hexT-150** was removed by incubation with 200 µL of 1 M TBAF solution in THF at room temperature for 30 seconds, and then washed as described above. The procedure was repeated three times to yield **hexT-127**. For analysis, an aliquot of ca. 10 nmol of conjugates **hexT-127** and **hexT-150** was deprotected and cleaved from the CPG with 500 µL of AMA (AMA= aqueous ammonia (30 %)/ aqueous methylamine (40 %), 1:1, vol/vol) for 30 min at room temperature. Then, 20 µL of 1 M Tris buffer (pH= 7.5) were added, the mixture was dried in a SpeedVac, and re-dissolved in 100 µL of distilled water. After purification products were analyzed by analytical RP-HPLC (Gemini, 5u, C18, 110A column; 100*4.6 mm) with a gradient of aqueous triethylammonium acetate buffer (10 mM, pH= 8) and methanol (30 % – 90 % of methanol over 15 min).

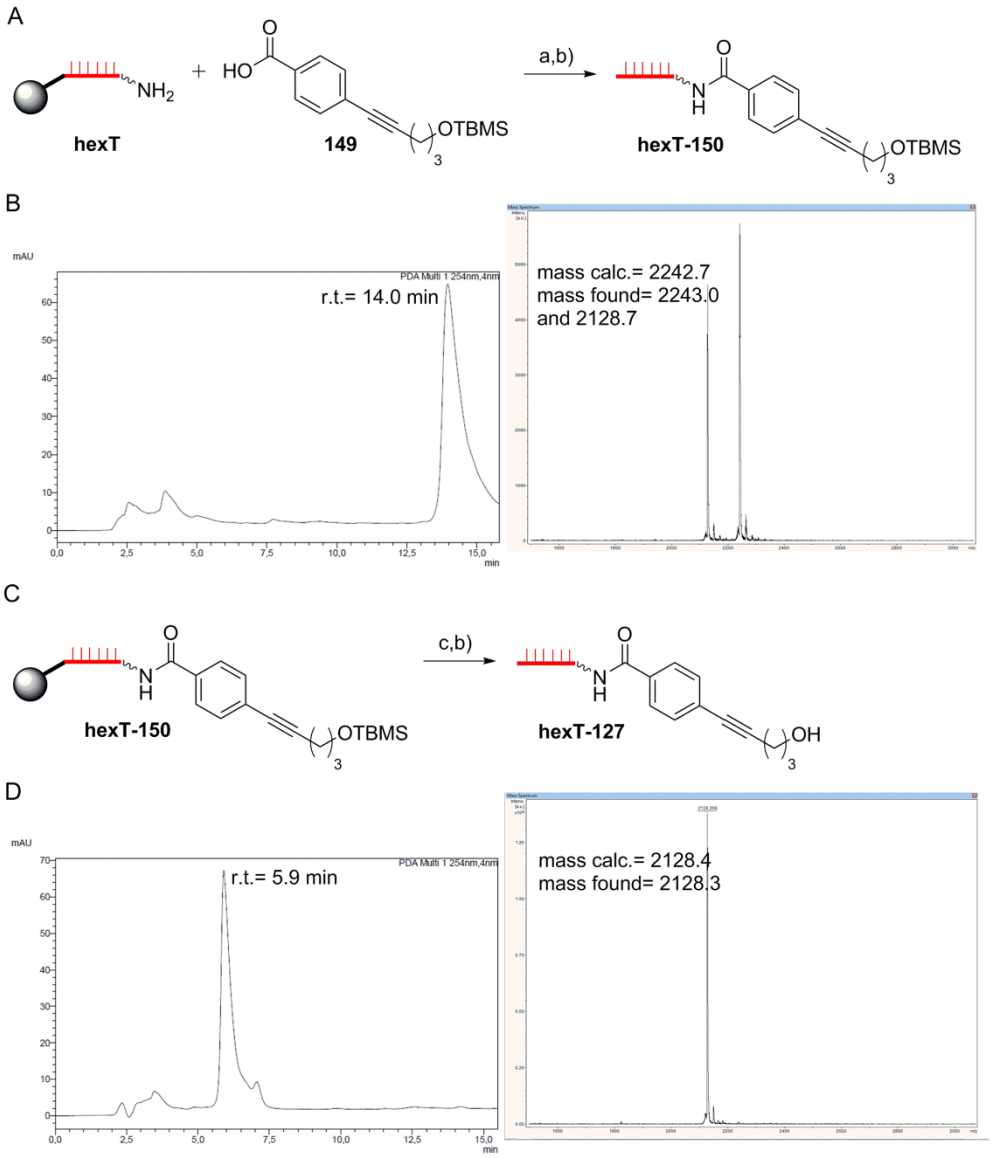

Figure 5.8. Synthesis of hexT-alkynol conjugates **hexT-127** and **hexT-150**. A) Synthesis scheme for compound **hexT-150**. Reagents and conditions: a) HATU, DIPEA, dry DMF, room temperature, 4 hours; b) AMA (aqueous ammonia (30 %)/ aqueous methylamine (40 %), 1:1, vol/vol), 30 min, room temperature (aliquot); B) HPLC trace and MALDI-TOF/TOF-MS spectrum of the purified conjugate **hexT-150**; loss of *tert*-butyldimethylsilyl group upon irradiation in the mass spectrometer was observed; C) synthesis scheme for compound **hexT-127**. Reagents and conditions: c) 1 M TBAF solution in THF; b) AMA (aqueous ammonia (30 %)/ aqueous methylamine (40 %), 1:1, vol/vol), 30 min, room temperature (aliquot); D) HPLC trace and MALDI-TOF/TOF-MS spectrum of the purified conjugate **hexT-127**. Filled grey circle denotes solid support (controlled pore glass, CPG); wavy bond to hexT: 5'-(C6)-amino-linker; bold bond: connection from the hexT-oligonucleotide to the CPG.

5.5.2. Optimization of reaction conditions of the Au(I)-mediated [3+2]-cycloaddition

An aldehyde component as connectivity between hexT and spirocycle

The solid support containing the hexathymidine-aldehyde conjugate **hexT-115** (30 nmol, ca. 1.1 mg) was suspended in 15 µL of a solvent (see Table 10). Then, *tert*-butyl 2-benzylhydrazinecarboxylate **88** and pent-4-yn-1-ol **107a**, at the amounts given in Table 10, dissolved in 15 µL of the same solvent (prepared as stock) were added to **hexT-115**. This was followed by an equimolar mixture of catalyst ***A***/$AgSbF_6$ at the amounts given in Table 10 which was suspended (***A***) or dissolved ($AgSbF_6$), respectively in 15 µL of the same solvent. The suspension of the catalyst was prepared as stock. Prior addition to **hexT-115** it was vortexed and pipetted up and down to add a homogeneous suspension. The reactions were shaken at room temperature overnight in Eppendorf tubes under normal atmosphere. Then, the CPG was filtered off, washed with each 3 x 200 µL of 0.1 M EDTA, DMF, MeOH, MeCN, and CH_2Cl_2, and dried *in vacuo* for 15 min. The hexT conjugates were deprotected and cleaved from the CPG by treatment with 500 µL of AMA for 30 minutes at room temperature. Then, 20 µL of 1 M Tris buffer (pH= 7.5) were added, the mixtures were dried in a SpeedVac, re-dissolved in 100 µL of distilled water, and all products were purified by RP-HPLC (Gemini, 5u, C18, 110A column; 100*10.0 mm or 50*10.0 mm) with a gradient of aqueous triethylammonium acetate buffer (100 mM, pH= 8) and methanol (20 % – 70 % of methanol over 19 min (for 100*10.0 mm column), or 20 % – 80 % of methanol over 18 min (for 50*10.0 mm column)). Fractions containing the product were collected, evaporated in a SpeedVac, co-evaporated with 3 x 200 µL of ethanol/distilled water (1:1) and analyzed by MALDI-TOF/TOF-MS analysis and by analytical HPLC to assert purity and identity.

A hydrazide component as connectivity between hexT and spirocycle

The solid support containing the hexathymidine-hydrazide conjugate **hexT-119** (30 nmol, ca. 1.1 mg) was suspended in 15 µL of a solvent (see Table 12). Then, aldehyde **AY** and pent-4-yn-1-ol **107a**, at the amounts given in Table 12, dissolved in 15 µL of the same solvent (prepared as stock) were added to **hexT-119**. This was followed by an equimolar mixture of catalyst ***A***/$AgSbF_6$ at the amounts given in Table 12 which was suspended (***A***) or dissolved ($AgSbF_6$), respectively in 15 µL of the same solvent. The suspension of the catalyst was prepared as stock. Prior addition to **hexT-119** it was vortexed and pipetted up and down to

add a homogeneous suspension. The reactions were shaken at room temperature overnight in Eppendorf tubes under normal atmosphere. Then, the CPG was filtered off, washed with each 3 x 200 µL of 0.1 M EDTA, DMF, MeOH, MeCN, and CH_2Cl_2, and dried *in vacuo* for 15 min. The hexT conjugates were deprotected and cleaved from the CPG by treatment with 500 µL of AMA for 30 minutes at room temperature. Then, 20 µL of 1 M Tris buffer (pH= 7.5) were added, the mixtures were dried in a SpeedVac, re-dissolved in 100 µL of distilled water, and all products were purified by RP-HPLC (Gemini, 5u, C18, 110A column; 50*10.0 mm) with a gradient of aqueous triethylammonium acetate buffer (100 mM, pH= 8) and methanol 20 % – 80 % of methanol over 18 min. Fractions containing the product were collected, evaporated in a SpeedVac, co-evaporated with 3 x 200 µL of ethanol/distilled water (1:1) and analyzed by MALDI-TOF/TOF-MS analysis and by analytical HPLC to assert purity and identity.

An alkynol component as connectivity between hexT and spirocycle

The solid support containing the hexathymidine-alkynol conjugate **hexT-127** (30 nmol, ca. 1.1 mg) was suspended in 30 µL of a solvent (see Table 14). Then, aldehyde **AY** (30 µmol, 1000 eq.) and *tert*-butyl 2-(4-methoxybenzyl)hydrazine-1-carboxylate **105** (30 µmol, 1000 eq.), at the amounts given in Table 14, dissolved in 30 µL of the same solvent (prepared as stock) were added to **hexT-127**. This was followed by an equimolar mixture of catalyst ***A***/$AgSbF_6$ (7.5 µmol, 250 eq.) at the amounts given in Table 14 which was suspended (***A***) or dissolved ($AgSbF_6$), respectively in 30 µL of the same solvent. The suspension of the catalyst was prepared as stock. Prior addition to **hexT-127** it was vortexed and pipetted up and down to add a homogeneous suspension. The reactions were shaken at the indicated temperatures overnight in Eppendorf tubes. The reactions were run in a presence of drying agents or without (see Table 14). Then, the CPG was filtered off, washed with each 3 x 200 µL of 0.1 M EDTA, DMF, MeOH, MeCN, and CH_2Cl_2, and dried *in vacuo* for 15 min. The hexT conjugates were deprotected and cleaved from the CPG by treatment with 500 µL of AMA for 30 minutes at room temperature. Then, 20 µL of 1 M Tris buffer (pH= 7.5) were added, the mixtures were dried in a SpeedVac, re-dissolved in 100 µL of distilled water, and all products were purified by RP-HPLC (Gemini, 5u, C18, 110A column; 50*10.0 mm) with a gradient of aqueous triethylammonium acetate buffer (100 mM, pH= 8) and methanol 20 % – 80 % of methanol over 18 min. Fractions containing the product were collected, evaporated in a

SpeedVac, co-evaporated with 3 x 200 µL of ethanol/distilled water (1:1) and analyzed by MALDI-TOF/TOF-MS analysis and by analytical HPLC to assert purity and identity.

5.5.3. Au(I)-mediated [3+2]-cycloaddition to DNA-6-oxa-1,2-diazaspiro[4.4]nonane conjugates

The solid support containing the one of the components **DNA-115** or **hexT-119** (30 nmol, ca. 1.1 mg) was suspended in 15 µL of THF. Then, for synthesis of 6-oxa-1,2-diazaspiro[4.4]nonane conjugates **DNA-116**: hydrazide (15 µmol, 500 eq.) and alkynol (30 µmol, 1000 eq.) dissolved in 15 µL of THF (prepared as stock) were added to **DNA-115**. For synthesis of 6-oxa-1,2-diazaspiro[4.4]nonane conjugates **hexT-120**: aldehyde (30 µmol, 1000 eq.) and alkynol (30 µmol, 1000 eq.) dissolved in 15 µL of THF (prepared as stock) were added to **hexT-119**. In both cases, this was followed by addition of an equimolar mixture of catalyst ***A***/$AgSbF_6$ (7.5 µmol, 250 eq.) which was suspended (***A***) or dissolved ($AgSbF_6$), respectively in 15 µL of THF. The suspension of the catalyst was prepared as stock. Prior addition to **DNA-115** or **hexT-119** this was vortexed and pipetted up and down to add a homogeneous suspension. The reactions were shaken at room temperature for 20 hours in Eppendorf tubes. The reactions were not run under protective gas, neither drying agents were used. Then, the CPG was filtered off, washed with each 3 x 200 µL of 0.1 M EDTA, DMF, MeOH, MeCN, and CH_2Cl_2, and dried *in vacuo* for 15 min. The hexamer conjugates were deprotected and cleaved from the CPG by treatment with 500 µL of AMA for 30 minutes (hexT/hexC/hexTC) or for 4 hours (hexA/hexG/hexACT/hexACGT) at room temperature. Then, 20 µL of 1 M Tris buffer (pH= 7.5) were added, the mixtures were dried in a SpeedVac, re-dissolved in 100 µL of distilled water, and all products were purified by RP-HPLC (Gemini, 5u, C18, 110A column; 50*10.0 mm) with a gradient of aqueous triethylammonium acetate buffer (100 mM, pH= 8) and methanol (20 % – 80 % of methanol over 18 min). Fractions containing the product were collected, evaporated in a SpeedVac, co-evaporated with 3 x 200 µL of ethanol/distilled water (1:1) and analyzed by MALDI-TOF/TOF-MS analysis and by analytical HPLC to assert purity and identity.

5.5.4. HPLC chromatograms and MALDI-MS spectra of hexathymidine-6-oxa-1,2-diazaspiro[4.4]nonane conjugates - reactant scope

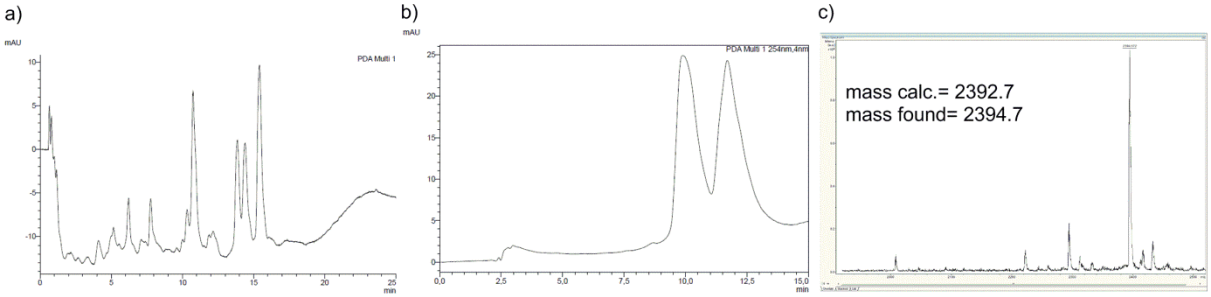

a) HPLC trace (preparative HPLC) of the crude spirocycle conjugate **hexT-120a**. b) HPLC trace of the purified spirocycle conjugate **hexT-120a**. c) MALDI-TOF/TOF-MS analysis of the purified spirocycle conjugate **hexT-120a**.

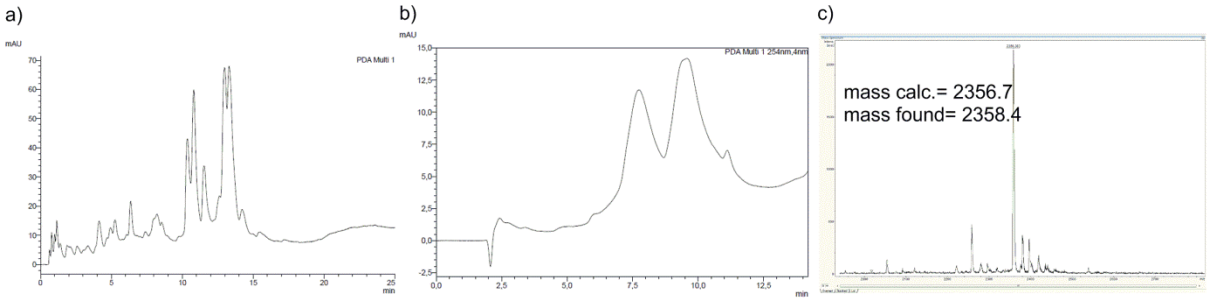

a) HPLC trace (preparative HPLC) of the crude spirocycle conjugate **hexT-120d**. b) HPLC trace of the purified spirocycle conjugate **hexT-120d**. c) MALDI-TOF/TOF-MS analysis of the purified spirocycle conjugate **hexT-120d**.

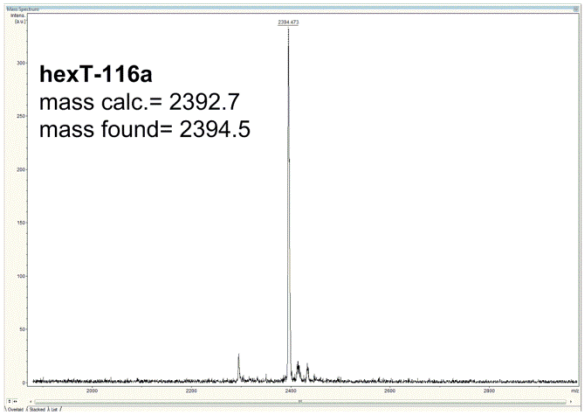

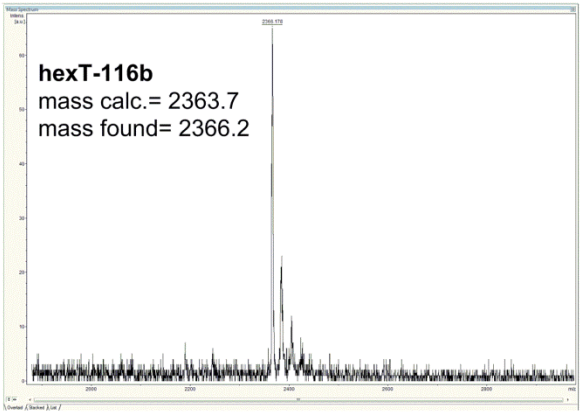

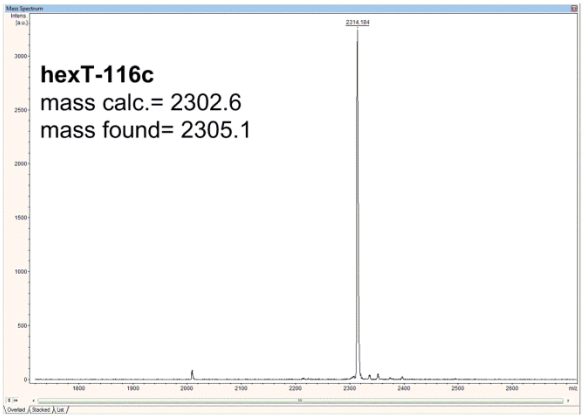
hexT-116c
mass calc.= 2302.6
mass found= 2305.1

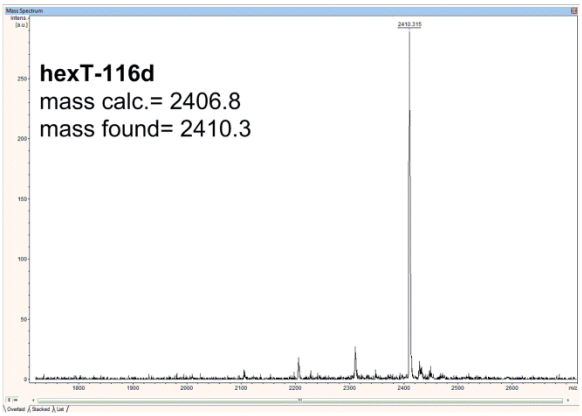
hexT-116d
mass calc.= 2406.8
mass found= 2410.3

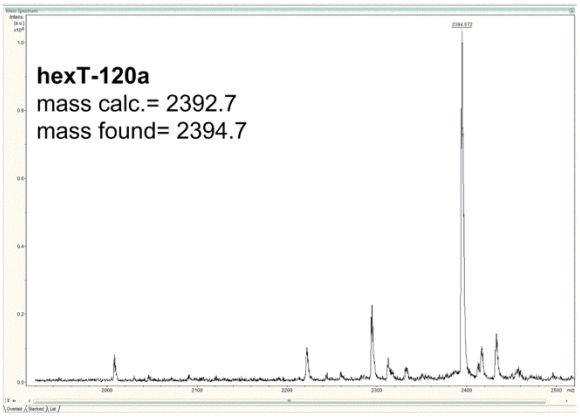
hexT-120a
mass calc.= 2392.7
mass found= 2394.7

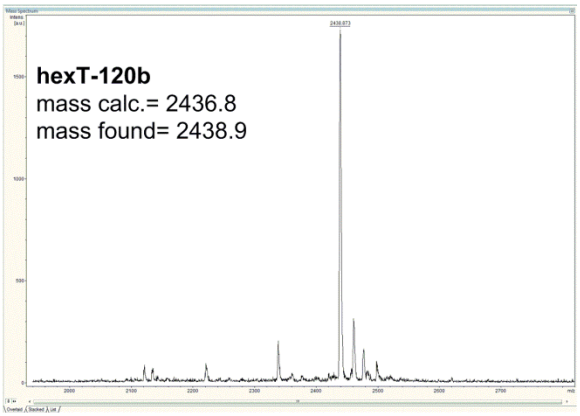
hexT-120b
mass calc.= 2436.8
mass found= 2438.9

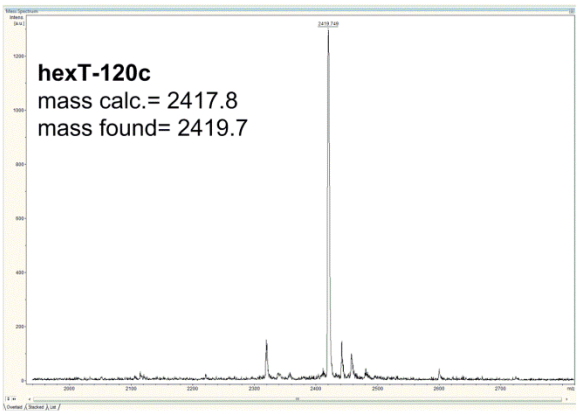
hexT-120c
mass calc.= 2417.8
mass found= 2419.7

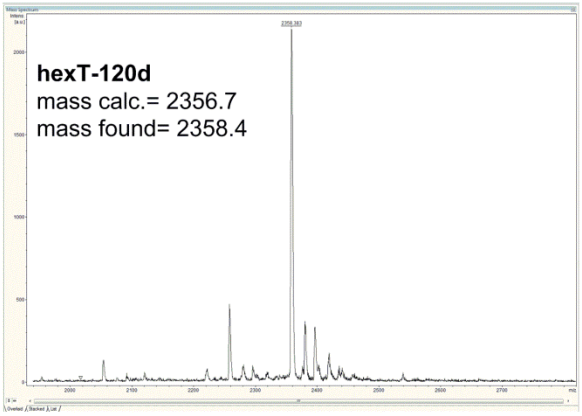
hexT-120d
mass calc.= 2356.7
mass found= 2358.4

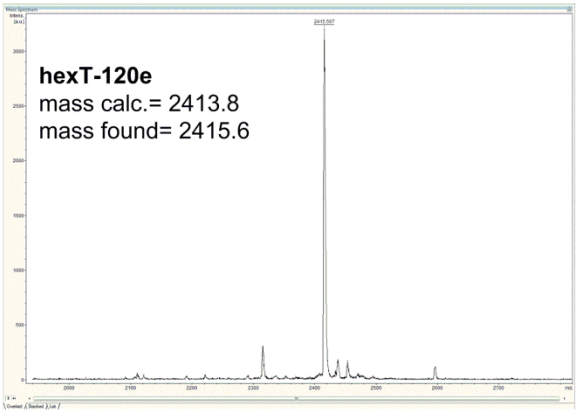
hexT-120e
mass calc.= 2413.8
mass found= 2415.6

5.5.5. MALDI-MS spectra of DNA-6-oxa-1,2-diazaspiro[4.4]nonane conjugates - sequence scope

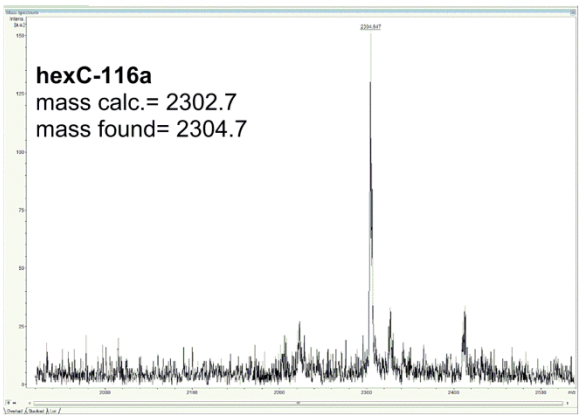

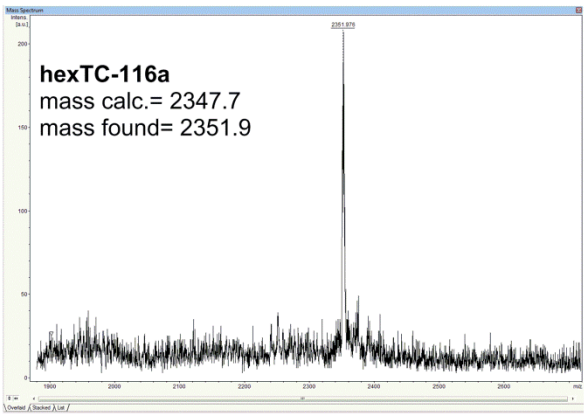

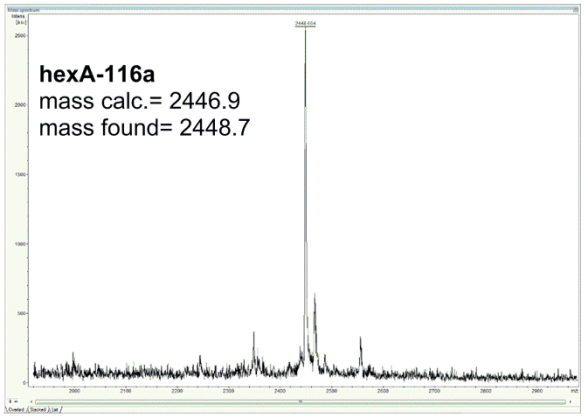

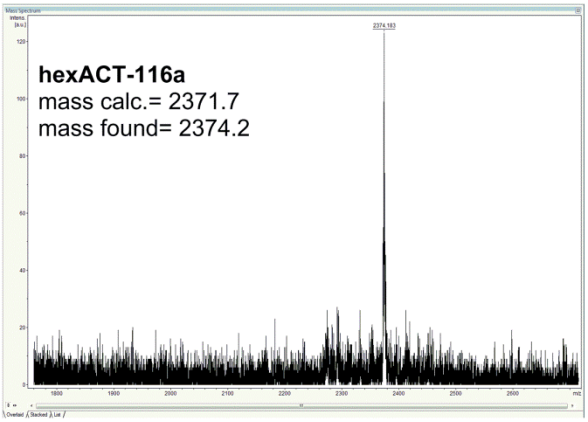

5.5.6. Synthesis of hexapyrimidine-pyrazoline and -ß-carboline conjugates

Synthesis of hexTC-alkyne conjugate hexTC-87 and hexTC-tryptophane conjugate hexTC-131

The hexTC (250 nmol, ca. 9 mg) was coupled either with *p*-ethynylbenzoic acid **133** (3.7 mg, 25 µmol, 100 eq.) to furnish **hexTC-87**, or with Fmoc-L-tryptophane **151** (10.7 mg, 25 µmol, 100 eq.) to furnish **hexTC-131**, according to the procedure for coupling of carboxylic acids to 5'-amino-linker modified DNA. For analysis, an aliquot of ca. 10 nmol of each conjugate **hexTC-87** and **hexTC-131** was deprotected and cleaved from the CPG with 500 µL of AMA (AMA= aqueous ammonia (30 %)/ aqueous methylamine (40 %), 1:1, vol/vol) for 30 min at room temperature. Then, 20 µL of 1 M Tris buffer (pH= 7.5) were added, the mixtures were dried in a SpeedVac, re-dissolved in 100 µL of distilled water, and the conjugates were purified by RP-HPLC (Gemini, 5u, C18, 110A column; 50*10.0 mm) with a gradient of aqueous triethylammonium acetate buffer (100 mM, pH= 8) and methanol (20 % – 80 % of methanol over 18 min). Fractions containing the product were collected, evaporated in a SpeedVac, co-evaporated with 3 x 200 µL of ethanol/distilled water (1:1) and analyzed by MALDI-TOF/TOF-MS analysis, and by analytical HPLC.

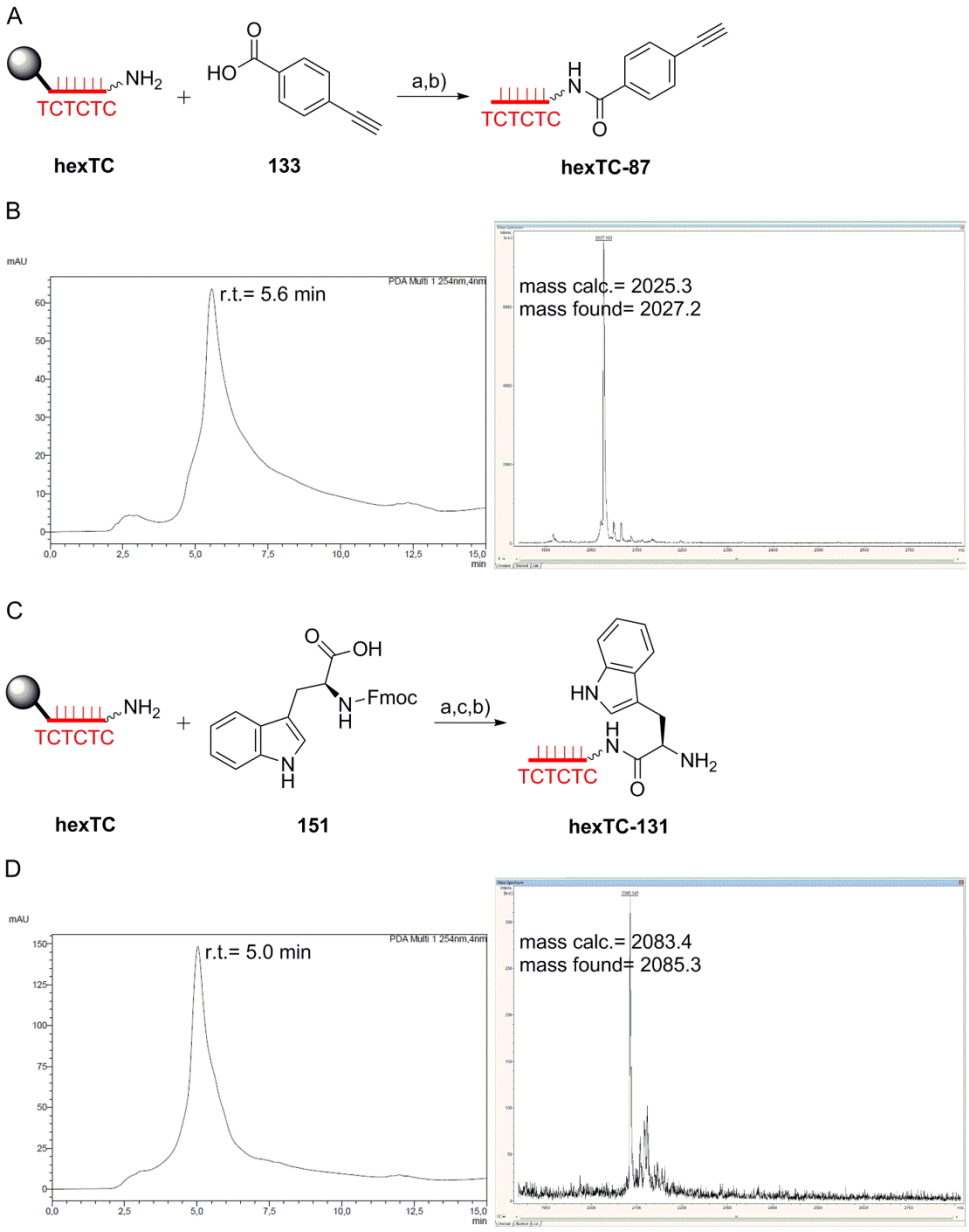

Figure 5.9. Synthesis of hexTC-alkyne conjugate **hexTC-87** and hexTC-tryptophane conjugate **hexTC-131**. A) Synthesis scheme for conjugate **hexTC-87**. Reagents and conditions: a) HATU, DIPEA, dry DMF, room temperature, 4 hours; b) AMA (aqueous ammonia (30 %)/ aqueous methylamine (40 %), 1:1, vol/vol), 30 min, room temperature (aliquot); B) HPLC trace and MALDI-TOF/TOF-MS spectrum of the purified conjugate **hexTC-87**; C) synthesis scheme for compound **hexTC-131**. Reagents and conditions: a) HATU, DIPEA, dry DMF, room temperature, 4 hours; b) AMA (aqueous ammonia (30 %)/ aqueous methylamine (40 %), 1:1, vol/vol), 30 min, room temperature (aliquot); c) 20 % piperidine in dry DMF; D) HPLC trace and MALDI-TOF/TOF-MS spectrum of the purified conjugate **hexTC-131**. Filled grey circle denotes solid support (controlled pore glass, CPG); wavy bond to hexTC: 5'-(C6)-amino-linker; bold bond: connection from the hexTC oligonucleotide to the CPG.

Synthesis of hexTC-pyrazoline conjugate hexTC-89 by Au(I)-mediated annulation reaction

The pyrazoline **hexTC-89** was synthesized according to the **method A** (Table 6) for synthesis of hexT-pyrazolines (Chapter 5.4.3), making use of **hexTC-87** (50 nmol, ca. 1.8 mg), hydrazide **88** (11.1 mg, 50 µmol, 1000 eq.), isobutyraldehyde **T** (4.56 µL, 50 µmol, 1000 eq.), and catalyst ***A***/$AgSbF_6$ (11 mg of ***A***, 4.3 mg of $AgSbF_6$, 12.5 µmol, 250 eq.).

Synthesis of hexTC-β-carboline conjugate hexTC-132 by Pictet-Spengler reaction

The solid support bearing conjugate **hexTC-131** (30 nmol, ca. 1.1 mg) was dried *in vacuo* for 15 min. Solution of 2 % TFA in dry CH_2Cl_2 was prepared. Then, benzaldehyde **AY** (3.06 µL, 30 µmol, 1000 eq.) dissolved in 45 µL of 2 % TFA/ CH_2Cl_2 solution was added to the CPG containing conjugate **hexTC-131**. The reaction mixture was shaken at room temperature overnight. Then, the CPG was filtered off, washed with each 3 x 200 µL of DMF, MeOH, MeCN, and CH_2Cl_2, and dried *in vacuo* for 15 min. The β-carboline **hexTC-132** was deprotected and cleaved from the CPG by treatment with 500 µL of AMA (AMA= aqueous ammonia (30 %)/ aqueous methylamine (40 %)= 1:1, vol/vol) for 30 minutes at room temperature. Then, 20 µL of 1 M Tris buffer (pH= 7.5) were added, the mixture was dried in a SpeedVac, re-dissolved in 100 µL of distilled water, and the product was purified by RP-HPLC (Gemini, 5u, C18, 110A column; 50*10.0 mm) with a gradient of aqueous triethylammonium acetate buffer (100 mM, pH= 8) and methanol (20 % – 80 % of methanol over 18 min). Fractions containing the product were collected, evaporated in a SpeedVac, co-evaporated with 3 x 200 µL of ethanol/distilled water (1:1) and analyzed by MALDI-TOF/TOF-MS analysis, and by analytical HPLC.

5.5.7. Synthesis of small molecule intermediates

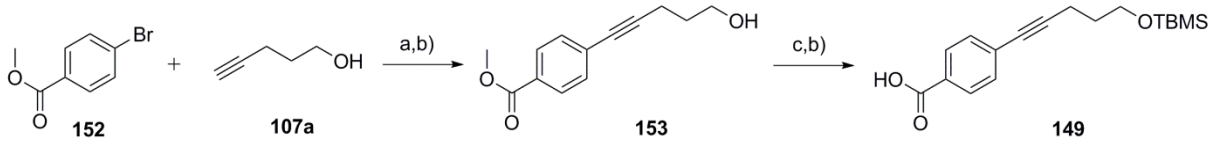

Figure 5.10. Synthesis of alkynol **149**. Reagents and conditions: a) $Pd(PPh_3)_2Cl_2$, CuI, TEA, 90 °C, 18 hours; b) BMS-Cl, imidazole, dry CH_2Cl_2, room temperature, 18 hours; c) dry THF/ MeOH (1/1), room temperature, 6 hours.

Methyl 4-(5-hydroxypent-1-yn-1-yl)benzoate 153[232]

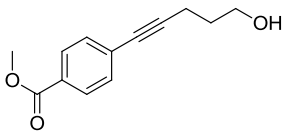

To a suspension of methyl 4-bromo-benzoate **152** (1 g, 4.65 mmol, 1.0 eq.) in TEA (9.3 mL), bis(triphenylphosphine)palladium(II) dichloride (164.6 mg, 0.23 mmol, 0.05 eq.) and copper(I) iodide (59.8 mg, 0.35 mmol, 0.075 eq.) were added. The suspension was flushed with argon for 5 minutes before the pent-4-yn-1-ol **107a** (432.7 µL, 4.65 mmol, 1.0 eq.) was added. The reaction mixture was stirred at 90 °C for 18 hours. After that, the reaction mixture was concentrated *in vacuo*. The resulting crude was filtered over Celite pad with a layer of silica on the top, and eluted with petroleum ether. Then, the solvent was evaporated *in vacuo* and the crude product was purified by column chromatography (solvent system: hexanes/ ethyl acetate 100:0 to 50:50) to provide **153** (540 mg, 53 % yield). ^{1}H-NMR (500 MHz, $CDCl_3$): δ 7.91 (d, ^3J=8.5 Hz, 2H), 7.40 (d, ^3J=8.3 Hz, 2H), 3.87 (s, 3H), 3.77 (t, ^3J=6.1 Hz, 2H), 2.52 (t, ^3J=7.0 Hz, 2H), 2.36 (br s, 1H), 1.81-1.86 (quint, ^3J=6.6 Hz, 2H); ^{13}C-NMR (125 MHz, $CDCl_3$): δ 166.8, 131.5, 129.4, 128.7, 93.0, 80.5, 77.2, 61.5, 52.3, 31.3, 16.1. LC-MS (ESI) *m/z* Calcd. for $[C_{13}H_{15}O_3, M+H]^+$: 219.1, found 219.17. Purity (HPLC): 95 %.

Methyl 4-(5-((*tert*-butyldimethylsilyl)oxy)pent-1-yn-1-yl)benzoate 154[233]

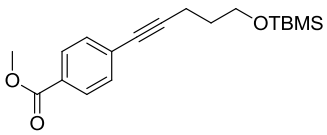

To a solution of methyl 4-(5-hydroxypent-1-yn-1-yl)benzoate **153** (200 mg, 0.92 mmol, 1.0 eq.) in dry CH_2Cl_2 (1.5 mL), imidazole (156.0 mg, 2.29 mmol, 2.5 eq.) was added, and subsequently *tert*-butyldimethylsilyl chloride (151.9 mg, 1.01 mmol, 1.1 eq.) under argon atmosphere at 0 °C over 1 minute while stirring. The reaction mixture was allowed to warm to room temperature and to stir for 18 hours. Then, water was added to the reaction mixture, and the crude product was extracted with CH_2Cl_2 (3 x 20 mL). The combined organic layers were dried over

anhydrous $MgSO_4$. Then, solvent was evaporated *in vacuo* and the crude product was purified by column chromatography (solvent system: hexanes/ ethyl acetate 100:0 to 50:50) to provide **154** (229 mg, 75 % yield). ^{1}H-NMR (500 MHz, $CDCl_3$): δ 7.96 (d, ^3J=8.1 Hz, 2H), 7.44 (d, ^3J=8.1 Hz, 2H), 3.92 (s, 3H), 3.76 (t, ^3J=6.1 Hz, 2H), 2.53 (t, ^3J=7.1 Hz, 2H), 1.79-1.85 (quint, ^3J=6.5 Hz, 2H), 0.92 (s, 9H), 0.08 (s, 6H); ^{13}C-NMR (125 MHz, $CDCl_3$): δ 168.8, 131.6, 129.5, 128.9, 93.6, 80.3, 61.7, 60.6, 52.3, 31.7, 18.5, 16.0, 14.3, -5.2. LC-MS (ESI) *m*/*z* Calcd. for [$C_{19}H_{29}O_3Si$, M+H] $^+$: 332.19, found 333.51. Purity (HPLC): 97 %.

4-(5-((*tert*-Butyldimethylsilyl)oxy)pent-1-yn-1-yl)benzoic acid 149

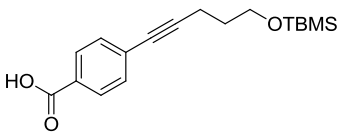

To a solution of methyl 4-(5-((*tert*-butyldimethylsilyl)oxy)pent-1-yn-1-yl)benzoate **154** (219 mg, 658.6 mmol, 1.0 eq.) in 10 mL of THF/ MeOH mixture (1:1), aq. 1.6 M NaOH solution (10 mL) was added, and the reaction mixture was stirred at room temperature for 6 hours. After that, water (20 mL) was added and reaction mixture was acidified with aq. 2 M HCl solution to pH= 1. Then, crude mixture was extracted with ethyl acetate (3 x 20 mL), combined organic layers were washed with brine (20 mL), and dried over anhydrous $MgSO_4$. Then, solvent was evaporated *in vacuo* and the crude product was purified by column chromatography (solvent system: hexanes/ ethyl acetate 100:0 to 50:50) to provide **149** (144 mg, 69 % yield). ^{1}H-NMR (500 MHz, $CDCl_3$): δ 8.03 (d, ^3J=8.3 Hz, 2H), 7.47 (d, ^3J=8.2 Hz, 2H), 3.76 (t, ^3J=6.1 Hz, 2H), 2.53 (t, ^3J=7.2, 2H), 1.80-1.85 (quint, ^3J=6.5 Hz, 2H), 0.91 (s, 9H), 0.08 (s, 6H); ^{13}C-NMR (125 MHz, $CDCl_3$): δ 171.8, 131.7, 130.2, 129.9, 128.1, 94.2, 80.3, 61.7, 31.6, 26.1, 18.5, 16.1, -5.2. LC-MS (ESI) *m*/*z* Calcd. for [$C_{19}H_{30}O_3Si$, M+H] $^+$: 319.17, found 319.20. Purity (HPLC): 97 %.

6. Literature

[1] S. L. Schreiber, J. D. Kotz, M. Li, J. Aube, C. P. Austin, J. C. Reed, H. Rosen, E. L. White, L. A. Sklar, C. W. Lindsley, B. R. Alexander, J. A. Bittker, P. A. Clemons, A. de Souza, M. A. Foley, M. Palmer, A. F. Shamji, M. J. Wawer, O. McManus, M. Wu, B. Zou, H. Yu, J. E. Golden, F. J. Schoenen, A. Simeonov, A. Jadhav, M. R. Jackson, A. B. Pinkerton, T. D. Chung, P. R. Griffin, B. F. Cravatt, P. S. Hodder, W. R. Roush, E. Roberts, D. H. Chung, C. B. Jonsson, J. W. Noah, W. E. Severson, S. Ananthan, B. Edwards, T. I. Oprea, P. J. Conn, C. R. Hopkins, M. R. Wood, S. R. Stauffer, K. A. Emmitte, N. I. H. M. L. P. Team, *Cell* **2015**, *161*, 1252-1265.

[2] T. I. Oprea, A. Tropsha, J. L. Faulon, M. D. Rintoul, *Nat Chem Biol* **2007**, *3*, 447-450.

[3] E. S. Lander, L. M. Linton, B. Birren, C. Nusbaum, M. C. Zody, J. Baldwin, K. Devon, K. Dewar, M. Doyle, W. FitzHugh, R. Funke, D. Gage, K. Harris, A. Heaford, J. Howland, L. Kann, J. Lehoczky, R. LeVine, P. McEwan, K. McKernan, J. Meldrim, J. P. Mesirov, C. Miranda, W. Morris, J. Naylor, C. Raymond, M. Rosetti, R. Santos, A. Sheridan, C. Sougnez, Y. Stange-Thomann, N. Stojanovic, A. Subramanian, D. Wyman, J. Rogers, J. Sulston, R. Ainscough, S. Beck, D. Bentley, J. Burton, C. Clee, N. Carter, A. Coulson, R. Deadman, P. Deloukas, A. Dunham, I. Dunham, R. Durbin, L. French, D. Grafham, S. Gregory, T. Hubbard, S. Humphray, A. Hunt, M. Jones, C. Lloyd, A. McMurray, L. Matthews, S. Mercer, S. Milne, J. C. Mullikin, A. Mungall, R. Plumb, M. Ross, R. Shownkeen, S. Sims, R. H. Waterston, R. K. Wilson, L. W. Hillier, J. D. McPherson, M. A. Marra, E. R. Mardis, L. A. Fulton, A. T. Chinwalla, K. H. Pepin, W. R. Gish, S. L. Chissoe, M. C. Wendl, K. D. Delehaunty, T. L. Miner, A. Delehaunty, J. B. Kramer, L. L. Cook, R. S. Fulton, D. L. Johnson, P. J. Minx, S. W. Clifton, T. Hawkins, E. Branscomb, P. Predki, P. Richardson, S. Wenning, T. Slezak, N. Doggett, J. F. Cheng, A. Olsen, S. Lucas, C. Elkin, E. Uberbacher, M. Frazier, et al., *Nature* **2001**, *409*, 860-921.

[4] J. McCafferty, A. D. Griffiths, G. Winter, D. J. Chiswell, *Nature* **1990**, *348*, 552-554.

[5] A. S. Kang, C. F. Barbas, K. D. Janda, S. J. Benkovic, R. A. Lerner, *Proc Natl Acad Sci U S A* **1991**, *88*, 4363-4366.

[6] E. T. Boder, K. D. Wittrup, *Nat Biotechnol* **1997**, *15*, 553-557.

[7] D. S. Wilson, A. D. Keefe, J. W. Szostak, *Proc Natl Acad Sci U S A* **2001**, *98*, 3750-3755.

[8] J. Hanes, A. Pluckthun, *Proc Natl Acad Sci U S A* **1997**, *94*, 4937-4942.

[9] A. D. Ellington, J. W. Szostak, *Nature* **1990**, *346*, 818-822.

[10] C. Tuerk, L. Gold, *Science* **1990**, *249*, 505-510.

[11] R. M. Franzini, D. Neri, J. Scheuermann, *Acc Chem Res* **2014**, *47*, 1247-1255.

[12] R. E. Kleiner, C. E. Dumelin, D. R. Liu, *Chem Soc Rev* **2011**, *40*, 5707-5717.

[13] S. Brenner, R. A. Lerner, *Proc Natl Acad Sci U S A* **1992**, *89*, 5381-5383.

[14] R. M. Franzini, C. Randolph, *J Med Chem* **2016**, *59*, 6629-6644.

[15] H. Salamon, M. Klika Škopić, K. Jung, O. Bugain, A. Brunschweiger, *ACS Chem Biol* **2016**, *11*, 296-307.

[16] H. F. Deng, H. O'Keefe, C. P. Davie, K. E. Lind, R. A. Acharya, G. J. Franklin, J. Larkin, R. Matico, M. Neeb, M. M. Thompson, T. Lohr, J. W. Gross, P. A. Centrella, G. K. O'Donovan, K. L. Bedard, K. van Vloten, S. Mataruse, S. R. Skinner, S. L. Belyanskaya, T. Y. Carpenter, T. W. Shearer, M. A. Clark, J. W. Cuozzo, C. C. Arico-Muendel, B. A. Morgan, *J Med Chem* **2012**, *55*, 7061-7079.

[17] L. Mannocci, Y. X. Zhang, J. Scheuermann, M. Leimbacher, G. De Bellis, E. Rizzi, C. Dumelin, S. Melkko, D. Neri, *P Natl Acad Sci USA* **2008**, *105*, 17670-17675.

[18] M. A. Clark, R. A. Acharya, C. C. Arico-Muendel, S. L. Belyanskaya, D. R. Benjamin, N. R. Carlson, P. A. Centrella, C. H. Chiu, S. P. Creaser, J. W. Cuozzo, C. P. Davie, Y. Ding, G. J. Franklin, K. D. Franzen, M. L. Gefter, S. P. Hale, N. J. V. Hansen, D. I. Israel, J. W. Jiang, M. J. Kavarana, M. S. Kelley, C. S. Kollmann, F. Li, K. Lind, S. Mataruse, P. F. Medeiros, J. A. Messer, P. Myers, H. O'Keefe, M. C. Oliff, C. E. Rise, A. L. Satz, S. R. Skinner, J. L. Svendsen, L. J. Tang, K. van Vloten, R. W. Wagner, G. Yao, B. G. Zhao, B. A. Morgan, *Nature Chemical Biology* **2009**, *5*, 647-654.

[19] A. Litovchick, C. E. Dumelin, S. Habeshian, D. Gikunju, M. A. Guie, P. Centrella, Y. Zhang, E. A. Sigel, J. W. Cuozzo, A. D. Keefe, M. A. Clark, *Sci Rep-Uk* **2015**, *5*.

[20] A. D. Keefe, M. A. Clark, C. D. Hupp, A. Litovchick, Y. Zhang, *Curr Opin Chem Biol* **2015**, *26*, 80-88.

[21] X. Y. Li, D. R. Liu, *Angew Chem Int Edit* **2004**, *43*, 4848-4870.

[22] B. N. Tse, T. M. Snyder, Y. H. Shen, D. R. Liu, *J Am Chem Soc* **2008**, *130*, 15611-15626.

[23] Y. Z. Li, P. Zhao, M. D. Zhang, X. Y. Zhao, X. Y. Li, *J Am Chem Soc* **2013**, *135*, 17727-17730.

[24] M. H. Hansen, P. Blakskjaer, L. K. Petersen, T. H. Hansen, J. W. Hojfeldt, K. V. Gothelf, N. J. V. Hansen, *J Am Chem Soc* **2009**, *131*, 1322-1327.

[25] S. Melkko, J. Scheuermann, C. E. Dumelin, D. Neri, *Nature Biotechnology* **2004**, *22*, 568-574.

[26] M. M. Kemp, M. Weiwer, A. N. Koehler, *Bioorgan Med Chem* **2012**, *20*, 1979-1989.

[27] M. A. Clark, *Curr Opin Chem Biol* **2010**, *14*, 396-403.

[28] R. M. Franzini, T. Ekblad, N. Zhong, M. Wichert, W. Decurtins, A. Nauer, M. Zimmermann, F. Samain, J. Scheuermann, P. J. Brown, J. Hall, S. Graslund, H. Schuler, D. Neri, *Angew Chem Int Edit* **2015**, *54*, 3927-3931.

[29] S. Melkko, L. Mannocci, C. E. Dumelin, A. Villa, R. Sommavilla, Y. X. Zhang, M. G. Grutter, N. Keller, L. Jermutus, R. H. Jackson, J. Scheuermann, D. Neri, *ChemMedChem* **2010**, *5*, 584-590.

[30] J. S. Disch, G. Evindar, C. H. Chiu, C. A. Blum, H. Dai, L. Jin, E. Schuman, K. E. Lind, S. L. Belyanskaya, J. H. Deng, F. Coppo, L. Aquilani, T. L. Graybill, J. W. Cuozzo, S. Lavu, C. Mao, G. P. Vlasuk, R. B. Perni, *J Med Chem* **2013**, *56*, 3666-3679.

[31] F. Buller, M. Steiner, K. Frey, D. Mircsof, J. Scheuermann, M. Kalisch, P. Buhlmann, C. T. Supuran, D. Neri, *ACS Chem Biol* **2011**, *6*, 336-344.

[32] A. L. Satz, *ACS Chem Biol* **2015**, *10*, 2237-2245.

[33] G. Gentile, G. Merlo, A. Pozzan, G. Bernasconi, B. Bax, P. Bamborough, A. Bridges, P. Carter, M. Neu, G. Yao, C. Brough, G. Cutler, A. Coffin, S. Belyanskaya, *Bioorg Med Chem Lett* **2012**, *22*, 1989-1994.

[34] H. F. Yang, P. F. Medeiros, K. Raha, P. Elkins, K. E. Lind, R. Lehr, N. D. Adams, J. L. Burgess, S. J. Schmidt, S. D. Knight, K. R. Auger, M. D. Schaber, G. J. Franklin, Y. Ding, J. L. DeLorey, P. A. Centrella, S. Mataruse, S. R. Skinner, M. A. Clark, J. W. Cuozzo, G. Evindar, *Acs Med Chem Lett* **2015**, *6*, 531-536.

[35] R. E. Kleiner, C. E. Dumelin, G. C. Tiu, K. Sakurai, D. R. Liu, *J Am Chem Soc* **2010**, *132*, 11779-11791.

[36] G. Georghiou, R. E. Kleiner, M. Pulkoski-Gross, D. R. Liu, M. A. Seeliger, *Nature Chemical Biology* **2012**, *8*, 366-374.

[37] C. A. Lipinski, F. Lombardo, B. W. Dominy, P. J. Feeney, *Adv Drug Deliver Rev* **2001**, *46*, 3-26.

[38] F. Samain, T. Ekblad, G. Mikutis, N. Zhong, M. Zimmermann, A. Nauer, D. Bajic, W. Decurtins, J. Scheuermann, P. J. Brown, J. Hall, S. Graslund, H. Schuler, D. Neri, R. M. Franzinit, *J Med Chem* **2015**, *58*, 5143-5149.

[39] H. F. Deng, J. Y. Zhou, F. S. Sundersingh, J. Summerfield, D. Somers, J. A. Messer, A. L. Satz, N. Ancellin, C. C. Arico-Muendel, K. L. Bedard, A. Beljean, S. L. Belyanskaya, R. Bingham, S. E. Smith, E. Boursier, P. Carter, P. A. Centrella, M. A.

Clark, C. W. Chung, C. P. Davie, J. L. Delorey, Y. Ding, G. J. Franklin, L. C. Grady, K. Herry, C. Hobbs, C. S. Kollmann, B. A. Morgan, L. J. Kaushansky, Q. Zhou, *Acs Med Chem Lett* **2015**, *6*, 919-924.

[40] Y. Ding, H. O'Keefe, J. L. DeLorey, D. I. Israebt, J. A. Messer, C. H. Chiu, S. R. Skinner, R. E. Matico, M. F. Murray-Thompson, F. Li, M. A. Clark, J. W. Cuozzo, C. Arico-Muendel, B. A. Morgan, *Acs Med Chem Lett* **2015**, *6*, 888-893.

[41] K. T. Reema, J. J. McAtee, S. Belyanskaya, M. Brandt, G. D. Brown, M. H. Costell, Y. Ding, J. W. Dodson, S. H. Eisennagel, R. E. Fries, J. W. Gross, M. R. Harpel, D. A. Holt, D. I. Israel, L. J. Jolivette, D. Krosky, H. Li, Q. N. Lu, T. Mandichak, T. Roethke, C. G. Schnackenberg, B. Schwartz, L. M. Shewchuk, W. S. Xie, D. J. Behm, S. A. Douglas, A. L. Shaw, J. P. Marino, *Bioorg Med Chem Lett* **2013**, *23*, 3584-3588.

[42] P. L. Podolin, B. J. Bolognese, J. F. Foley, E. Long, B. Peck, S. Umbrecht, X. J. Zhang, P. Zhu, B. Schwartz, W. S. Xie, C. Quinn, H. W. Qi, S. Sweitzer, S. Chen, M. Galop, Y. Ding, S. L. Belyanskaya, D. I. Israel, B. A. Morgan, D. J. Behm, J. P. Marino, E. Kurali, M. S. Barnette, R. J. Mayer, C. L. Booth-Genthe, J. F. Callahan, *Prostag Oth Lipid M* **2013**, *104*, 25-31.

[43] D. J. Payne, M. N. Gwynn, D. J. Holmes, D. L. Pompliano, *Nat Rev Drug Discov* **2007**, *6*, 29-40.

[44] C. Arico-Muendel, Z. R. Zhu, H. Dickson, D. Parks, J. Keicher, J. H. Deng, L. Aquilani, F. Coppo, T. Graybill, K. Lind, A. Peat, M. Thomson, *Antimicrob Agents Ch* **2015**, *59*, 3450-3459.

[45] M. Leimbacher, Y. X. Zhang, L. Mannocci, M. Stravs, T. Geppert, J. Scheuermann, G. Schneider, D. Neri, *Chem-Eur J* **2012**, *18*, 7729-7737.

[46] F. Buller, Y. X. Zhang, J. Scheuermann, J. Schafer, P. Buhlmann, D. Neri, *Chem Biol* **2009**, *16*, 1075-1086.

[47] C. S. Kollmann, X. P. Bai, C. H. Tsai, H. F. Yang, K. E. Lind, S. R. Skinner, Z. R. Zhu, D. I. Israel, J. W. Cuozzo, B. A. Morgan, K. Yuki, C. Xie, T. A. Springer, M. Shimaoka, G. Evindar, *Bioorg Med Chem* **2014**, *22*, 2353-2365.

[48] B. A. Seigal, W. H. Connors, A. Fraley, R. M. Borzilleri, P. H. Carter, S. L. Emanuel, J. Fargnoli, K. Kim, M. Lei, J. G. Naglich, M. E. Pokross, S. L. Posy, H. Shen, N. Surti, R. Talbott, Y. Zhang, N. K. Terrett, *J Med Chem* **2015**, *58*, 2855-2861.

[49] P. A. Harris, B. W. King, D. Bandyopadhyay, S. B. Berger, N. Campobasso, C. A. Capriotti, J. A. Cox, L. Dare, X. Y. Dong, J. N. Finger, L. C. Grady, S. J. Hoffmann, J. U. Jeong, J. Kang, V. Kasparcova, A. S. Lakdawala, R. Lehr, D. E. McNulty, R.

Nagilla, M. T. Ouellette, C. S. Pao, A. R. Rendina, M. C. Schaeffer, J. D. Summerfield, B. A. Swift, R. D. Totoritis, P. Ward, A. M. Zhang, D. H. Zhang, R. W. Marquis, J. Bertin, P. J. Gough, *J Med Chem* **2016**, *59*, 2163-2178.

[50] P. A. Harris, S. B. Berger, J. U. Jeong, R. Nagilla, D. Bandyopadhyay, N. Campobasso, C. A. Capriotti, J. A. Cox, L. Dare, X. Y. Dong, P. M. Eidam, J. N. Finger, S. J. Hoffman, J. Kang, V. Kasparcova, B. W. King, R. Lehr, Y. F. Lan, L. K. Leister, J. D. Lich, T. T. MacDonald, N. A. Miller, M. T. Ouellette, C. S. Pao, A. Rahman, M. A. Reilly, A. R. Rendina, E. J. Rivera, M. C. Schaeffer, C. A. Sehon, R. R. Singhaus, H. H. Sun, B. A. Swift, R. D. Totoritis, A. Vossenkamper, P. Ward, D. D. Wisnoski, D. H. Zhang, R. W. Marquis, P. J. Gough, J. Bertin, *J Med Chem* **2017**, *60*, 1247-1261.

[51] J. W. Cuozzo, P. A. Centrella, D. Gikunju, S. Habeshian, C. D. Hupp, A. D. Keefe, E. A. Sigel, H. H. Soutter, H. A. Thomson, Y. Zhang, M. A. Clark, *Chembiochem* **2017**, *18*, 864-871.

[52] A. I. Chan, L. M. McGregor, T. Jain, D. R. Liu, *J Am Chem Soc* **2017**, *139*, 10192-10195.

[53] L. M. McGregor, T. Jain, D. R. Liu, *J Am Chem Soc* **2014**, *136*, 3264-3270.

[54] C. C. Arico-Muendel, *MedChemComm* **2016**, *7*, 1898-1909.

[55] M. L. Malone, B. M. Paegel, *ACS Comb Sci* **2016**, *18*, 182-187.

[56] A. L. Satz, J. P. Cai, Y. Chen, R. Goodnow, F. Gruber, A. Kowalczyk, A. Petersen, G. Naderi-Oboodi, L. Orzechowski, Q. Strebel, *Bioconjugate Chem* **2015**, *26*, 1623-1632.

[57] D. R. Halpin, J. A. Lee, S. J. Wrenn, P. B. Harbury, *Plos Biol* **2004**, *2*, 1031-1038.

[58] K-C. Luk, A. L. Satz (2014) *A Handbook for DNA-Encoded Chemistry: DNA-compatible chemistry*, 1st ed., Wiley, Hoboken.

[59] Y. Y. Chen, A. S. Kamlet, J. B. Steinman, D. R. Liu, *Nat Chem* **2011**, *3*, 146-153.

[60] Z. J. Gartner, B. N. Tse, R. Grubina, J. B. Doyon, T. M. Snyder, D. R. Liu, *Science* **2004**, *305*, 1601-1605.

[61] X. Y. Li, Z. J. Gartner, B. N. Tse, D. R. Liu, *J Am Chem Soc* **2004**, *126*, 5090-5092.

[62] L. J. Fan, C. P. Davie, *Chembiochem* **2017**, *18*, 843-847.

[63] Y. Z. Li, E. Gabriele, F. Samain, N. Favalli, F. Sladojevich, J. Scheuermann, D. Neri, *Acs Comb Sci* **2016**, *18*, 438-443.

[64] S. J. Wrenn, R. M. Weisinger, D. R. Halpin, P. B. Harbury, *J Am Chem Soc* **2007**, *129*, 13137-13143.

[65] Z. J. Gartner, D. R. Liu, *J Am Chem Soc* **2001**, *123*, 6961-6963.

[66] C. Cao, P. Zhao, Z. Li, Z. T. Chen, Y. Y. Huang, Y. Bai, X. Y. Li, *Chem Commun* **2014**, *50*, 10997-10999.

[67] Y. Ding, J. L. DeLorey, M. A. Clark, *Bioconjugate Chem* **2016**, *27*, 2597-2600.

[68] M. M. Rozenman, D. R. Liu, *Chembiochem* **2006**, *7*, 253-256.

[69] Z. J. Gartner, M. W. Kanan, D. R. Liu, *Angew Chem Int Edit* **2002**, *41*, 1796-1800.

[70] M. W. Kanan, M. M. Rozenman, K. Sakurai, T. M. Snyder, D. R. Liu, *Nature* **2004**, *431*, 545-549.

[71] X. J. Lu, S. E. Roberts, G. J. Franklin, C. P. Davie, *MedChemComm* **2017**, *8*, 1614-1617.

[72] X. J. Lu, L. J. Fan, C. B. Phelps, C. P. Davie, C. P. Donahue, *Bioconjugate Chem* **2017**, *28*, 1625-1629.

[73] A. Omumi, D. G. Beach, M. Baker, W. Gabryelski, R. A. Manderville, *J Am Chem Soc* **2011**, *133*, 42-50.

[74] Y. Ding, M. A. Clark, *Acs Comb Sci* **2015**, *17*, 1-4.

[75] X. H. Chen, A. Roloff, O. Seitz, *Angew Chem Int Edit* **2012**, *51*, 4479-4483.

[76] F. Buller, L. Mannocci, Y. X. Zhang, C. E. Dumelin, J. Scheuermann, D. Neri, *Bioorg Med Chem Lett* **2008**, *18*, 5926-5931.

[77] X. Tian, G. S. Basarab, N. Selmi, T. Kogej, Y. Zhang, M. Clark, R. A. Goodnow, *MedChemComm* **2016**, *7*, 1316-1322.

[78] E. R. Wood, R. Bledsoe, J. Chai, P. Daka, H. F. Deng, Y. Ding, S. Harris-Gurley, L. H. Kryn, E. Nartey, J. Nichols, R. T. Nolte, N. Prabhu, C. Rise, T. Sheahan, J. B. Shotwell, D. Smith, V. Tai, J. D. Taylor, G. Tomberlin, L. P. Wang, B. Wisely, S. Y. You, B. Xia, H. Dickson, *J Biol Chem* **2015**, *290*, 19681-19696.

[79] P. Blakskjaer, T. Heitner, N. J. V. Hansen, *Curr Opin Chem Biol* **2015**, *26*, 62-71.

[80] (a) B. E. Evans, K. E. Rittle, M. G. Bock, R. M. Dipardo, R. M. Freidinger, W. L. Whitter, G. F. Lundell, D. F. Veber, P. S. Anderson, R. S. L. Chang, V. J. Lotti, D. J. Cerino, T. B. Chen, P. J. Kling, K. A. Kunkel, J. P. Springer, J. Hirshfield, *J Med Chem* **1988**, *31*, 2235-2246; (b) M. E. Welsch, S. A. Snyder, B. R. Stockwell, *Curr Opin Chem Biol* **2010**, *14*, 347-361.

[81] E. J. Brown, M. W. Albers, T. B. Shin, K. Ichikawa, C. T. Keith, W. S. Lane, S. L. Schreiber, *Nature* **1994**, *369*, 756-758.

[82] E. Jacinto, M. N. Hall, *Nat Rev Mol Cell Biol* **2003**, *4*, 117-126.

[83] N. Hay, N. Sonenberg, *Genes Dev* **2004**, *18*, 1926-1945.

[84] M. K. Holz, J. Blenis, *J Biol Chem* **2005**, *280*, 26089-26093.

[85] X. M. Ma, J. Blenis, *Nat Rev Mol Cell Biol* **2009**, *10*, 307-318.

[86] J. B. Easton, P. J. Houghton, *Oncogene* **2006**, *25*, 6436-6446.

[87] C. A. Sparks, D. A. Guertin, *Oncogene* **2010**, *29*, 3733-3744.

[88] S. Schenone, M. Radi, F. Musumeci, C. Brullo, M. Botta, *Chem Rev* **2014**, *114*, 7189-7238.

[89] A. Carracedo, J. Baselga, P. P. Pandolfi, *Cell Cycle* **2008**, *7*, 3805-3809.

[90] K. J. Curran, J. C. Verheijen, J. Kaplan, D. J. Richard, L. Toral-Barza, I. Hollander, J. Lucas, S. Ayral-Kaloustian, K. Yu, A. Zask, *Bioorg Med Chem Lett* **2010**, *20*, 1440-1444.

[91] P. Liu, H. Cheng, T. M. Roberts, J. J. Zhao, *Nat Rev Drug Discov* **2009**, *8*, 627-644.

[92] S. M. Maira, C. Voliva, C. Garcia-Echeverria, *Expert Opin Ther Tar* **2008**, *12*, 223-238.

[93] M. G. Bursavich. P. W. Nowak, D. Malwitz, S. Lombardi, A. M. Gilbert, N. Zhang, S.m Ayral-Kaloustian, J. T. Anderson, N. Brooijmans, US Patent 20100015141, 2010.

[94] D. M. Goldstein, T. Gabriel, *Curr Top Med Chem* **2005**, *5*, 1017-1029.

[95] A. R. Clark, J. L. Dean, *Open Rheumatol J* **2012**, *6*, 209-219.

[96] I. Aligas, S. Gradl, J. Gunzner, S. Mathieu, J. Rudolph, Z. Wem, S. M. Wenglowsky, WO Patent 2011025947, 2011.

[97] S. Mathieu, S. N. Gradl, L. Ren, Z. Wen, I. Aliagas, J. Gunzner-Toste, W. Lee, R. Pulk, G. Zhao, B. Alicke, J. W. Boggs, A. J. Buckmelter, E. F. Choo, V. Dinkel, S. L. Gloor, S. E. Gould, J. D. Hansen, G. Hastings, G. Hatzivassiliou, E. R. Laird, D. Moreno, Y. Ran, W. C. Voegtli, S. Wenglowsky, J. Grina, J. Rudolph, *J Med Chem* **2012**, *55*, 2869-2881.

[98] J. Das, R. V. Moquin, S. Pitt, R. Zhang, D. R. Shen, K. W. McIntyre, K. Gillooly, A. M. Doweyko, J. S. Sack, H. Zhang, S. E. Kiefer, K. Kish, M. McKinnon, J. C. Barrish, J. H. Dodd, G. L. Schieven, K. Leftheris, *Bioorg Med Chem Lett* **2008**, *18*, 2652-2657.

[99] R. S. Jope, G. V. Johnson, *Trends Biochem Sci* **2004**, *29*, 95-102.

[100] F. Kawakami, M. Suzuki, N. Shimada, G. Kagiya, E. Ohta, K. Tamura, H. Maruyama, T. Ichikawa, *FEBS J* **2011**, *278*, 4895-4904.

[101] J. O. Ban, J. H. Oh, S. M. Son, D. Won, H. S. Song, S. B. Han, D. C. Moon, K. W. Kang, M. J. Song, J. T. Hong, *Cancer Biol Ther* **2011**, *12*, 288-296.

[102] A. J. Peat, D. Garrido, J. A. Boucheron, S. L. Schweiker, S. H. Dickerson, J. R. Wilson, T. Y. Wang, S. A. Thomson, *Bioorg Med Chem Lett* **2004**, *14*, 2127-2130.

[103] D. O. Morgan, *Nature* **1995**, *374*, 131-134.

[104] C. J. Sherr, *Science* **1996**, *274*, 1672-1677.

[105] S. Bahceci, B. Chan, D. S. Chan, J. Chen, T. P. Forsyth, M. Franzini, V. Jammalamadaka, J. W. Jeong, L. R. Jones, R. M. Kelley, WO Patent 2010003133, 2010.

[106] M. A. Lemmon, J. Schlessinger, *Cell* **2010**, *141*, 1117-1134.

[107] S. R. Hubbard, J. H. Till, *Annu Rev Biochem* **2000**, *69*, 373-398.

[108] A. Ullrich, J. Schlessinger, *Cell* **1990**, *61*, 203-212.

[109] N. E. Hynes, H. A. Lane, *Nat Rev Cancer* **2005**, *5*, 341-354.

[110] R. Ducray, P. Ballard, B. C. Barlaam, M. D. Hickinson, J. G. Kettle, D. J. Ogilvie, C. B. Trigwell, *Bioorg Med Chem Lett* **2008**, *18*, 959-962.

[111] E. Foulstone, S. Prince, O. Zaccheo, J. L. Burns, J. Harper, C. Jacobs, D. Church, A. B. Hassan, *J Pathol* **2005**, *205*, 145-153.

[112] G. Pandini, F. Frasca, R. Mineo, L. Sciacca, R. Vigneri, A. Belfiore, *J Biol Chem* **2002**, *277*, 39684-39695.

[113] R. D. Hubbard, N. Y. Bamaung, F. Palazzo, Q. Zhang, P. Kovar, D. J. Osterling, X. Hu, J. L. Wilsbacher, E. F. Johnson, J. Bouska, J. Wang, R. L. Bell, S. K. Davidsen, G. S. Sheppard, *Bioorg Med Chem Lett* **2007**, *17*, 5406-5409.

[114] W. N. Pappano, P. M. Jung, J. A. Meulbroek, Y. C. Wang, R. D. Hubbard, Q. Zhang, M. M. Grudzien, N. B. Soni, E. F. Johnson, G. S. Sheppard, C. Donawho, F. G. Buchanan, S. K. Davidsen, R. L. Bell, J. Wang, *BMC Cancer* **2009**, *9*, 314.

[115] R. B. Irby, T. J. Yeatman, *Oncogene* **2000**, *19*, 5636-5642.

[116] R. Roskoski, Jr., *Biochem Biophys Res Commun* **2004**, *324*, 1155-1164.

[117] J. H. Hanke, J. P. Gardner, R. L. Dow, P. S. Changelian, W. H. Brissette, E. J. Weringer, B. A. Pollok, P. A. Connelly, *J Biol Chem* **1996**, *271*, 695-701.

[118] (a) V. G. Brunton, M. C. Frame, *Curr Opin Pharmacol* **2008**, *8*, 427-432; (b) S. Schenone, F. Manetti, M. Botta, *Curr Pharm Des* **2007**, *13*, 2118-2128.

[119] C. Tintori, A. L. Fallacara, M. Radi, C. Zamperini, E. Dreassi, E. Crespan, G. Maga, S. Schenone, F. Musumeci, C. Brullo, A. Richters, F. Gasparrini, A. Angelucci, C. Festuccia, S. Delle Monache, D. Rauh, M. Botta, *J Med Chem* **2015**, *58*, 347-361.

[120] S. Grant, P. Dent, *Clin Cancer Res* **2004**, *10*, 2205-2207.

[121] (a) J. B. Bolen, N. Rosen, M. A. Israel, *Proc Natl Acad Sci U S A* **1985**, *82*, 7275-7279; (b) J. O'Shaughnessy, V. Deseau, S. Amini, N. Rosen, J. B. Bolen, *Oncogene Res* **1987**, *2*, 1-18; (c) C. Bjelfman, F. Hedborg, I. Johansson, M. Nordenskjold, S. Pahlman, *Cancer Res* **1990**, *50*, 6908-6914; (d) T. Matsunaga, H. Takahashi, N.

Ohnuma, M. Tanabe, H. Yoshida, J. Iwai, H. Shirasawa, B. Simizu, *Cancer Res* **1991**, *51*, 3148-3152; (e) D. Finlay, K. Vuori, *Cancer Res* **2007**, *67*, 11704-11711.

[122] (a) T. Matsunaga, H. Shirasawa, M. Tanabe, N. Ohnuma, H. Takahashi, B. Simizu, *Cancer Res* **1993**, *53*, 3179-3185; (b) T. Matsunaga, H. Shirasawa, M. Tanabe, N. Ohnuma, K. Kawamura, T. Etoh, H. Takahashi, B. Simizu, *Int J Cancer* **1994**, *58*, 793-798.

[123] N. Isakov, B. Biesinger, *Eur J Biochem* **2000**, *267*, 3413-3421.

[124] A. Burchat, D. W. Borhani, D. J. Calderwood, G. C. Hirst, B. Li, R. F. Stachlewitz, *Bioorg Med Chem Lett* **2006**, *16*, 118-122.

[125] R. W. Hendriks, S. Yuvaraj, L. P. Kil, *Nat Rev Cancer* **2014**, *14*, 219-232.

[126] L. A. Honigberg, A. M. Smith, M. Sirisawad, E. Verner, D. Loury, B. Chang, S. Li, Z. Pan, D. H. Thamm, R. A. Miller, J. J. Buggy, *Proc Natl Acad Sci U S A* **2010**, *107*, 13075-13080.

[127] J. A. Dubovsky, K. A. Beckwith, G. Natarajan, J. A. Woyach, S. Jaglowski, Y. Zhong, J. D. Hessler, T. M. Liu, B. Y. Chang, K. M. Larkin, M. R. Stefanovski, D. L. Chappell, F. W. Frissora, L. L. Smith, K. A. Smucker, J. M. Flynn, J. A. Jones, L. A. Andritsos, K. Maddocks, A. M. Lehman, R. Furman, J. Sharman, A. Mishra, M. A. Caligiuri, A. R. Satoskar, J. J. Buggy, N. Muthusamy, A. J. Johnson, J. C. Byrd, *Blood* **2013**, *122*, 2539-2549.

[128] I. Alkorta, J. Elguero, *J Chil Chem Soc* **2015**, *60*, 2966-2970.

[129] H. Yoshimura, S. Sekine, H. Adachi, Y. Uematsu, A. Mitani, N. Futaki, N. Shimizu, *Protein Expres Purif* **2011**, *80*, 41-46.

[130] B. Yao, J. Xu, R. C. Harris, M. Z. Zhang, *Am J Physiol-Renal* **2008**, *294*, F433-F439.

[131] H. Haruna, T. Shimizu, Y. Ohtsuka, Y. Yarita, T. Fujii, T. Kudo, Y. Yamashiro, *Pediatr Int* **2008**, *50*, 1-6.

[132] S. Yoshida, M. Ujiki, X. Z. Ding, C. Pelham, M. S. Talamonti, R. H. Bell, W. Denham, T. E. Adrian, *Mol Cancer* **2005**, *4*.

[133] K. G. Peri, P. Hardy, D. Y. Li, D. R. Varma, S. Chemtob, *J Biol Chem* **1995**, *270*, 24615-24620.

[134] A. L. F. Sampaio, J. Dalli, V. Brancaleone, F. D'Acquisto, M. Perretti, C. Wheatley, *Mediat Inflamm* **2013**.

[135] R. Calvello, M. A. Panaro, M. L. Carbone, A. Cianciulli, M. G. Perrone, P. Vitale, P. Malerba, A. Scilimati, *Pharmacol Res* **2012**, *65*, 137-148.

[136] A. Ostojic, R. Vrhovac, S. Verstovsek, *Future Oncol* **2011**, *7*, 1035-1043.

[137] K. Yamaoka, P. Saharinen, M. Pesu, V. E. T. Holt, O. Silvennoinen, J. J. O'Shea, *Genome Biol* **2004**, *5*.

[138] P. Wu, T. E. Nielsen, M. H. Clausen, *Trends Pharmacol Sci* **2015**, *36*, 422-439.

[139] C. G. M. Wilson, M. R. Arkin, *Curr Top Microbiol* **2011**, *348*, 25-59.

[140] (a) A. C. Braisted, J. D. Oslob, W. L. Delano, J. Hyde, R. S. McDowell, N. Waal, C. Yu, M. R. Arkin, B. C. Raimundo, *J Am Chem Soc* **2003**, *125*, 3714-3715; (b) B. C. Raimundo, J. D. Oslob, A. C. Braisted, J. Hyde, R. S. McDowell, M. Randal, N. D. Waal, J. Wilkinson, C. H. Yu, M. R. Arkin, *J Med Chem* **2004**, *47*, 3111-3130; (c) C. D. Thanos, W. L. DeLano, J. A. Wells, *P Natl Acad Sci USA* **2006**, *103*, 15422-15427.

[141] M. I. Rosatti, M. T. Beconi, M. Cordoba, *Biocell* **2004**, *28*, 311-316.

[142] W. Tian, G. Q. Han, J. Zhu, J. J. Qi, Q. Q. Chen, J. T. Zhao, C. H. Zheng, L. Zhang, Y. J. Zhou, J. G. Lv, *Bioorg Med Chem Lett* **2013**, *23*, 4177-4184.

[143] L. H. Jones, G. Allan, R. Corbau, D. S. Middleton, C. E. Mowbray, S. D. Newman, C. Phillips, R. Webster, M. Westby, *Chem Biol Drug Des* **2011**, *77*, 393-397.

[144] R. Corbau, J. Mori, C. Phillips, L. Fishburn, A. Martin, C. Mowbray, W. Panton, C. Smith-Burchnell, A. Thornberry, H. Ringrose, T. Knochel, S. Irving, M. Westby, A. Wood, M. Perros, *Antimicrob Agents Ch* **2010**, *54*, 4451-4463.

[145] L. H. Jones, G. Allan, O. Barba, C. Burt, R. Corbau, T. Dupont, T. Knochel, S. Irving, D. S. Middleton, C. E. Mowbray, M. Perros, H. Ringrose, N. A. Swain, R. Webster, M. Westby, C. Phillips, *J Med Chem* **2009**, *52*, 1219-1223.

[146] P. W. Hinds, *Cancer Cell* **2003**, *3*, 305-307.

[147] G. Castanedo, K. Clark, S. M. Wang, V. Tsui, M. L. Wong, J. Nicholas, D. Wickramasinghe, J. C. Marsters, D. Sutherlin, *Bioorg Med Chem Lett* **2006**, *16*, 1716-1720.

[148] J. Sun, X. H. Lv, H. Y. Qiu, Y. T. Wang, Q. R. Du, D. D. Li, Y. H. Yang, H. L. Zhu, *Eur J Med Chem* **2013**, *68*, 1-9.

[149] P. G. Wyatt, A. J. Woodhead, V. Berdini, J. A. Boulstridge, M. G. Carr, D. M. Cross, D. J. Davis, L. A. Devine, T. R. Early, R. E. Feltell, E. J. Lewis, R. L. McMenamin, E. F. Navarro, M. A. O'Brien, M. O'Reilly, M. Reule, G. Saxty, L. C. A. Seavers, D. M. Smith, M. S. Squires, G. Trewartha, M. T. Walker, A. J. A. Woolford, *J Med Chem* **2008**, *51*, 4986-4999.

[150] P. Pevarello, M. G. Brasca, R. Amici, P. Orsini, G. Traquandi, L. Corti, C. Piutti, P. Sansonna, M. Villa, B. S. Pierce, M. Pulici, P. Giordano, K. Martina, E. L. Fritzen, R. A. Nugent, E. Casale, A. Cameron, M. Ciomei, F. Roletto, A. Isacchi, G. Fogliatto, E.

Pesenti, W. Pastori, A. Marsiglio, K. L. Leach, P. M. Clare, F. Fiorentini, M. Varasi, A. Vulpetti, M. A. Warpehoski, *J Med Chem* **2004**, *47*, 3367-3380.

[151] R. Hoshino, Y. Chatani, T. Yamori, T. Tsuruo, H. Oka, O. Yoshida, Y. Shimada, S. Ari-i, H. Wada, J. Fujimoto, M. Kohno, *Oncogene* **1999**, *18*, 813-822.

[152] N. X. Li, D. Batt, M. Warmuth, *Curr Opin Invest Dr* **2007**, *8*, 452-456.

[153] B. J. Newhouse, J. D. Hansen, J. Grina, M. Welch, G. Topalov, N. Littman, M. Callejo, M. Martinson, S. Galbraith, E. R. Laird, B. J. Brandhuber, G. Vigers, T. Morales, R. Woessner, N. Randolph, J. Lyssikatos, A. Olivero, *Bioorg Med Chem Lett* **2011**, *21*, 3488-3492.

[154] (a) E. F. Choo, J. P. Driscoll, J. Feng, B. Liederer, E. Plise, N. Randolph, Y. Shin, S. Wong, Y. Ran, *Xenobiotica* **2009**, *39*, 700-709; (b) R. T. Coutts, R. Dawe, G. W. Dawson, S. H. Kovach, *Drug Metab Dispos* **1976**, *4*, 35-39; (c) S. Heberling, U. Girreser, S. Wolf, B. Clement, *Biochem Pharmacol* **2006**, *71*, 354-365.

[155] P. Alexiou, K. Pegklidou, M. Chatzopoulou, I. Nicolaou, V. J. Demopoulos, *Curr Med Chem* **2009**, *16*, 734-752.

[156] F. Giacco, M. Brownlee, *Circ Res* **2010**, *107*, 1058-1070.

[157] S. K. Srivastava, K. V. Ramana, A. Bhatnagar, *Endocr Rev* **2005**, *26*, 380-392.

[158] U. C. S. Yadav, K. V. Ramana, S. K. Srivastava, *Chem-Biol Interact* **2011**, *191*, 339-345.

[159] R. Tammali, S. K. Srivastava, K. V. Ramana, *Curr Cancer Drug Tar* **2011**, *11*, 560-571.

[160] U. C. S. Yadav, S. K. Srivastava, K. V. Ramana, *Curr Mol Med* **2010**, *10*, 540-549.

[161] N. Papastavrou, M. Chatzopoulou, K. Pegklidou, I. Nicolaou, *Bioorgan Med Chem* **2013**, *21*, 4951-4957.

[162] (a) S. E. Sweeney, *Nat Rev Rheumatol* **2009**, *5*, 475-477; (b) J. Saklatvala, *Curr Opin Pharmacol* **2004**, *4*, 372-377; (c) S. Kumar, J. Boehm, J. C. Lee, *Nat Rev Drug Discov* **2003**, *2*, 717-726; (d) G. Wagner, S. Laufer, *Med Res Rev* **2006**, *26*, 1-62; (e) J. Westra, P. C. Limburg, *Mini-Rev Med Chem* **2006**, *6*, 867-874.

[163] J. Das, R. V. Moquin, A. J. Dyckman, T. L. Li, S. Pitt, R. Zhang, D. R. Shen, K. W. McIntyre, K. Gillooly, A. M. Doweyko, J. A. Newitt, J. S. Sack, H. J. Zhang, S. E. Kiefer, K. Kish, M. McKinnon, J. C. Barrish, J. H. Dodd, G. L. Schieven, K. Leftheris, *Bioorg Med Chem Lett* **2010**, *20*, 6886-6889.

[164] J. Das, R. V. Moquin, S. Pitt, R. Zhang, D. R. Shen, K. W. McIntyre, K. Gillooly, A. M. Doweyko, J. S. Sack, H. J. Zhang, S. E. Kiefer, K. Kish, M. McKinnon, J. C. Barrish, J. H. Dodd, G. L. Schieven, K. Leftheris, *Bioorg Med Chem Lett* **2008**, *18*, 2652-2657.

[165] G. S. Hassan, S. M. Abou-Seri, G. Kamel, M. M. Ali, *Eur J Med Chem* **2014**, *76*, 482-493.

[166] J. H. M. Lange, H. K. A. C. Coolen, H. H. van Stuivenberg, J. A. R. Dijksman, A. H. J. Herremans, E. Ronken, H. G. Keizer, K. Tipker, A. C. McCreary, W. Veerman, H. C. Wals, B. Stork, P. C. Verveer, A. P. den Hartog, N. M. J. de Jong, T. J. P. Adolfs, J. Hoogendoorn, C. G. Kruse, *J Med Chem* **2004**, *47*, 627-643.

[167] J. Adam, P. Cowley, *Expert Opin Ther Pat* **2002**, *12*, 1475-1489.

[168] R. G. Pertwee, *Addict Biol* **2000**, *5*, 37-46.

[169] R. Gomez, M. Navarro, B. Ferrer, J. M. Trigo, A. Bilbao, I. Del Arco, A. Cippitelli, F. Nava, D. Piomelli, F. R. de Fonseca, *J Neurosci* **2002**, *22*, 9612-9617.

[170] W. Hall, *Drug Alcohol Rev* **1998**, *17*, 433-444.

[171] B. L. Hungund, B. S. Basavarajappa, C. Vadasz, G. Kunos, F. R. de Fonseca, G. Colombo, S. Serra, L. Parsons, G. F. Koob, *Alcohol Clin Exp Res* **2002**, *26*, 565-574.

[172] R. G. Pertwee, *Gut* **2001**, *48*, 859-867.

[173] S. L. Davies, J. S. Silvestre, X. Guitart, *Drug Future* **2005**, *30*, 479-495.

[174] M. V. King, C. A. Marsden, K. C. F. Fone, *Trends Pharmacol Sci* **2008**, *29*, 482-492.

[175] D. E. Nichols, C. D. Nichols, *Chem Rev* **2008**, *108*, 1614-1641.

[176] F. J. Monsma, Y. Shen, R. P. Ward, M. W. Hamblin, D. R. Sibley, *Mol Pharmacol* **1993**, *43*, 320-327.

[177] M. Ruat, E. Traiffort, J. M. Arrang, J. Tardivellacombe, J. Diaz, R. Leurs, J. C. Schwartz, *Biochem Bioph Res Co* **1993**, *193*, 268-276.

[178] A. van Loevezijn, J. Venhorst, W. I. I. Bakker, C. G. de Korte, W. de Looff, S. Verhoog, J. W. van Wees, M. van Hoeve, R. P. V. de Woestijne, M. A. W. van der Neut, A. J. M. Borst, M. J. P. van Dongen, N. M. W. J. de Bruin, H. G. Keizer, C. G. Kruse, *J Med Chem* **2011**, *54*, 7030-7054.

[179] K. Kalinsky, F. G. Holuska, *Expert Rev Anticanc* **2007**, *7*, 715-724.

[180] A. S. Dhillon, S. Hagan, O. Rath, W. Kolch, *Oncogene* **2007**, *26*, 3279-3290.

[181] Y. S. Yang, Q. S. Li, S. Sun, Y. B. Zhang, X. L. Wang, F. Zhang, J. F. Tang, H. L. Zhu, *Bioorgan Med Chem* **2012**, *20*, 6048-6058.

[182] Y. Luo, S. Zhang, K. M. Qiu, Z. J. Liu, Y. S. Yang, J. Fu, W. Q. Zhong, H. L. Zhu, *Bioorg Med Chem Lett* **2013**, *23*, 1091-1095.

[183] J. P. Johnston, *Biochem Pharmacol* **1968**, *17*, 1285-&.

[184] M. Yamada, H. Yasuhara, *Neurotoxicology* **2004**, *25*, 215-221.

[185] P. Riederer, M. B. H. Youdim, *J Neurochem* **1986**, *46*, 1359-1365.

[186] H. H. Fernandez, J. J. Chen, *Pharmacotherapy* **2007**, *27*, 174s-185s.

[187] V. N. Badavath, I. Baysal, G. Ucar, B. N. Sinha, V. Jayaprakash, *Acs Med Chem Lett* **2016**, *7*, 56-61.

[188] R. Fioravanti, N. Desideri, M. Biava, L. P. Monaco, L. Grammatica, M. Yanez, *Bioorg Med Chem Lett* **2013**, *23*, 5128-5130.

[189] M. Klika Škopić, O. Bugain, K. Jung, S. Onstein, S. Brandherm, T. Kalliokoski, A. Brunschweiger, *MedChemComm* **2016**, *7*, 1957-1965.

[190] (a) I. Schwope, C. F. Bleczinski, C. Richert, *J Org Chem* **1999**, *64*, 4749-4761; (b) R. M. Franzini, F. Samain, M. Abd Elrahman, G. Mikutis, A. Nauer, M. Zimmermann, J. Scheuermann, J. Hall, D. Neri, *Bioconjug Chem* **2014**, *25*, 1453-1461.

[191] T. Kalliokoski, *ACS Comb Sci* **2015**, *17*, 600-607.

[192] A. Brunschweiger, L. F. Gebert, M. Lucic, U. Pradere, H. Jahns, C. Berk, J. Hunziker, J. Hall, *Chem Commun (Camb)* **2016**, *52*, 156-159.

[193] J. Baell, M. A. Walters, *Nature* **2014**, *513*, 481-483.

[194] R. D. Gorham, Jr., V. Nunez, J. H. Lin, S. H. Rooijakkers, V. I. Vullev, D. Morikis, *J Med Chem* **2015**, *58*, 9535-9545.

[195] W. H. Sauer, M. K. Schwarz, *J Chem Inf Comput Sci* **2003**, *43*, 987-1003.

[196] N. C. Firth, N. Brown, J. Blagg, *J Chem Inf Model* **2012**, *52*, 2516-2525.

[197] C. N. Tetzlaff, I. Schwope, C. F. Bleczinski, J. A. Steinberg, C. Richert, *Tetrahedron Lett* **1998**, *39*, 4215-4218.

[198] L. H. Yuen, R. M. Franzini, *Bioconjugate Chem* **2017**, *28*, 1076-1083.

[199] A. B. MacConnell, P. J. McEnaney, V. J. Cavett, B. M. Paegel, *ACS Comb Sci* **2015**, *17*, 518-534.

[200] B. Lippert, *Coordinative Bond Formation Between Metal Ions and Nucleic Acid Bases, in Nucleic Acid-Metal Ion Interactions*, (ed N. V. Hud), Royal Society of Chemistry, 2009.

[201] B. Lippert, *Alterations of Nucleobase pK_a Values upon Metal Coordination: Origins and Consequences, in Progress in Inorganic Chemistry, Volume 54* (ed K. D. Karlin), John Wiley & Sons, Inc., Hoboken, New York, 1996.

[202] B. Lippert, P. J. S. Miguel, *Accounts Chem Res* **2016**, *49*, 1537-1545.

[203] R. B. Martin, *Platinum Complexes: Hydrolysis and Binding to N(7) and N(1) of Purines, in Cisplatin: Chemistry and Biochemistry of a Leading Anticancer Drug* (ed B. Lippert), Verlag Helvetica Chimica Acta, Zürich, 1999.

[204] S. Kanvah, J. Joseph, G. B. Schuster, R. N. Barnett, C. L. Cleveland, U. Landman, *Accounts Chem Res* **2010**, *43*, 280-287.

[205] A. Kotschy, G. Timári, *Heterocycles from Transition Metal Catalysis: Formation and Functionalization*, Springer, Dordrecht, 2009.

[206] H. C. Shen, T. H. Graham, *Drug Discov Today Technol* **2013**, *10*, e3-14.

[207] Y. Suzuki, S. Naoe, S. Oishi, N. Fujii, H. Ohno, *Org Lett* **2012**, *14*, 326-329.

[208] J. Liu, *Phys Chem Chem Phys* **2012**, *14*, 10485-10496.

[209] A. Brunschweiger, N. Krause, A. Antonchick, M. Klika Škopić, H. Salamon, O. Bugain, K. Jung, B. Wagner, WO 2017108741 A1, 2017.

[210] M. Klika Škopić, H. Salamon, O. Bugain, K. Jung, A. Gohla, L. J. Doetsch, D. Dos Santos, A. Bhat, B. Wagner, A. Brunschweiger, *Chem Sci* **2017**, *8*, 3356-3361.

[211] M. Klika Škopić, S. Willems, J. Schieven, B. Wagner, A. Brunschweiger, *Org Biomol Chem* **2017**, DOI: 10.1039/C7OB02347B.

[212] R. Martin, M. Rodriguez Rivero, S. L. Buchwald, *Angew Chem Int Ed Engl* **2006**, *45*, 7079-7082.

[213] G. Xu, C. Zhu, W. Gu, J. Li, J. Sun, *Angew Chem Int Ed Engl* **2015**, *54*, 883-887.

[214] T. Hashimoto, Y. Takiguchi, K. Maruoka, *J Am Chem Soc* **2013**, *135*, 11473-11476.

[215] Y. Suzuki, S. Naoe, S. Oishi, N. Fujii, H. Ohno, *Org Lett* **2012**, *14*, 326-329.

[216] A. Domling, W. Wang, K. Wang, *Chem Rev* **2012**, *112*, 3083-3135.

[217] A. Zhdanko, M. E. Maier, *Angew Chem Int Ed Engl* **2014**, *53*, 7760-7764.

[218] B. Wagner, W. Hiller, H. Ohno, N. Krause, *Org Biomol Chem* **2016**, *14*, 1579-1583.

[219] R. E. Ebule, D. Malhotra, G. B. Hammond, B. Xu, *Adv Synth Catal* **2016**, *358*, 1478-1481.

[220] A. Zhdanko, M. E. Maier, *Acs Catal* **2015**, *5*, 5994-6004.

[221] B. Ranieri, I. Escofet, A. M. Echavarren, *Org Biomol Chem* **2015**, *13*, 7103-7118.

[222] M. Q. Jia, M. Bandini, *Acs Catal* **2015**, *5*, 1638-1652.

[223] A. Zhdanko, M. E. Maier, *Chem-Eur J* **2014**, *20*, 1918-1930.

[224] A. Zhdanko, M. E. Maier, *Angew Chem Int Edit* **2014**, *53*, 7760-7764.

[225] (a) N. Ben Hamadi, M. Msaddek, *Cr Chim* **2011**, *14*, 997-1001; (b) K. Khosravi, *Res Chem Intermediat* **2015**, *41*, 5253-5260; (c) G. S. Ananthnag, A. Adhikari, M. S.

Balakrishna, *Catal Commun* **2014**, *43*, 240-243; (d) N. Nakamichi, Y. Kawashita, M. Hayashi, *Org Lett* **2002**, *4*, 3955-3957.

[226] W. Decurtins, M. Wichert, R. M. Franzini, F. Buller, M. A. Stravs, Y. X. Zhang, D. Neri, J. Scheuermann, *Nat Protoc* **2016**, *11*, 764-780.

[227] M. Satake, K. Ofuji, H. Naoki, K. J. James, A. Furey, T. McMahon, J. Silke, T. Yasumoto, *J Am Chem Soc* **1998**, *120*, 9967-9968.

[228] The reference molecule **SP-C** for 6-oxa-1,2-diazaspiro[4.4]nonane was synthesized by Justin Schieven, from working group of Prof. Krause, TU Dortmund.

[229] E. Wieczerzak, J. Kozlowska, L. Lankiewicz, Z. Grzonka, *Pol J Chem* **2002**, *76*, 1693-1697.

[230] T. P. Burkholder, J. R. Clayton, L. Ma, *US010152181* (*A1*), **2010**.

[231] M. S. Gibson, R. W. Bradshaw, *Angew Chem Int Edit* **1968**, *7*, 919-930.

[232] E. C. Taylor, P. M. Harrington, *J Org Chem*, **1990**, *55*, 3222-3227.

[233] L. Cleary, H. Yoo, K. J. Shea, *Org Lett*, **2011**, *13*, 1781-1783.

Abbreviations

AcOH	acetic acid
AMA	aqueous ammonia (30 %)/ aqueous methylamine (40 %), 1:1, vol/vol)
AgOTf	silver trifluoromethanesulfonate
$AgSbF_6$	silver hexafluoroantimonate
ATP	adenosine triphosphate
aq.	aqueous
bp	base pair
CPG	controlled pore glass
Cs_2CO_3	caesium carbonate
CsOH	caesium hydroxide
CuAAC	copper(I)-catalyzed alkyne-azide cycloaddition
CuBr	copper(I) bromide
CuI	copper(I) iodide
$Cu(OAc)_2$	copper(II) acetate
$CuSO_4$* $5H_2O$	copper(II) sulfate pentahydrate
DBU	2,3,4,6,7,8,9,10-octahydropyrimido[1,2-*a*]azepine
DDQ	2,3-dichloro-5,6-dicyano-1,4-benzoquinone
DEAE	diethylaminoethanol
DEL	DNA-Encoded Library
DIPEA	*N*,*N*-diisopropylethylamine
DMA	*N*,*N*-dimethylacetamide
DMF	dimethylformamide

DMSO	dimethyl sulfoxide
DMT-MM	4-(4,6-dimethoxy-1,3,5-triazin-2-yl)-4-methylmorpholinium chloride
DNA	deoxyribonucleic acid
DTT	dithiothreitol
EDC	*N*-(3-dimethylaminopropyl)-*N′*-ethylcarbodiimide
EDTA	ethylenediaminetetraacetic acid
eq.	equivalent
EtOH	ethanol
Fmoc	fluorenylmethyloxycarbonyl
HATU	*N*-[(dimethylamino)-1*H*-1,2,3-triazolo-[4,5-*b*]pyridin-1-ylmethylene]-*N*-methylmethanaminium hexafluorophosphate *N*-oxide
hexT	hexathymidine oligonucleotide adapter
HOAt	1-hydroxy-7-azabenzotriazole
HPLC	High Performance Liquid Chromatography
H_3BO_3	boric acid
KOH	potassium hydroxide
LC-MS	Liquid Chromatography - Mass Spectrometry
MALDI-TOF/TOF-MS	Matrix Assisted Laser Desorption/Ionization-Time of Flight/ Time of Flight-Mass Spectrometry
MeCN	acetonitrile
$MeNH_2$	methylamine
MeOH	methanol
$MgCl_2$	magnesium chloride
MOPS	3-morpholinopropane-1-sulfonic acid
MMt	monomethoxytrityl

mRNA	messenger ribonucleic acid
$NaBH_4$	sodium borohydride
$NaBH_3CN$	sodium cyanoborohydride
NaCl	sodium chloride
NaOAc	sodium acetate
NaOH	sodium hydroxide
$NaIO_4$	sodium periodate
NaN_3	sodium azide
Na_2PdCl_4	sodium tetrachloropalladate(II)
NH_3	ammonia
NMR	Nuclear Magnetic Resonance
PBS	phosphate buffered saline
PCR	Polymerase Chain Reaction
PEG	polyethylene glycol
$Pd(OAc)_2$	palladium(II) acetate
$Pd(PPh_3)_4$	tetrakis(triphenyl- phosphine)palladium(0)
PNK	polynucleotide kinase
RP-HPLC	Reversed-Phase High-Performance Liquid Chromatography
rt	room temperature
r.t.	retention time
$Ru(bpy)_3Cl_2$	ruthenium-tris(2,2'-bipyridyl) dichloride
SELEX	systematic evolution of ligands by exponential enrichment
TAPS	3-{[1,3-dihydroxy-2-(hydroxymethyl)propan-2-yl]amino}propane-1-sulfonic acid
TPPTS	trisodium 3-bis(3-sulfonatophenyl)phosphanylbenzenesulfonate

TBAI	tetra-n-butylammonium bromide
TBTA	1-(1-benzyltriazol-4-yl)-*N*,*N*-bis[(1-benzyltriazol-4-yl)methyl]methanamine
t-BuOH	*tert*-butanol
t-BuXPhos Pd G1	*t*-butyl[2-(di-*tert*-butylphosphino)-2′,4′,6′-triisopropyl-1,1′-biphenyl][2-(2-aminoethyl)phenyl)] palladium (II) chloride
TFA	trifluoroacetic acid
THF	tetrahydrofuran
TiDEC	Thymidine-initiated DNA-Encoded Chemistry
tiDEL	oligothymidine-initiated DNA-Encoded Library
TPPTS	triphenylphosphine-3,3′,3″-trisulfonic acid trisodium salt
Tris	2-amino-2-(hydroxymethyl)propane-1,3-diol
$Zr(DS)_4$	zirconium tetrakis(dodecyl sulfate)
1,3-DC	1,3-dipolar cycloaddition

Acknowledgements

First of all, I would like to thank to Prof. Dr. Daniel Rauh for giving me an opportunity to pursue my doctoral studies in his working group, and for his support to our research.

My immense thank goes to Dr. Andreas Brunschweiger for great project he gave me and for his expert quidance throughout my research. Thank you for numerous discussions, helpful thoughts, great ideas, and motivation. Also, thank you for your patience (especially in a last few days), and for answering all of my questions. Thank you for everything!

I would like to thank to Prof. Dr. Herbert Waldmann for accepting to be one the examiners of my PhD thesis and for being a part of my thesis advisory comittee. I am especially grateful for his critical review of my work and my scientific progress during my TAC group meetings.

I would like to thank to Dr. Andrey P. Antonchick for being a part of my thesis advisory committee and for his constructive feedback on my research.

I would like to thank to Prof. Dr. Norbert Krause for his nice chemistry that served as an inspiration for part of my work. I am particularly thankful to his former student Dr. Bernd Wagner, and his current PhD student Justin Schieven on helpful discussions.

I would like to thank for membership in International Max Planck Research School (IMPRS) in Chemical and Molecular Biology. Especially, I would like to thank to IMPRS coordinators Christa Hornemann and Dr. Lucia Sironi for always being ready to answer my questions.

I would like to thank the Christiane Nüsslein-Volhard - Bayer Foundation for funding me during my PhD studies (03.2015. – 08.2016.).

I would like to thank to Tuomo Kalliokoski from the Lead-Discovery Center GmbH, Dortmund, for chemoinformatic analysis of the pyrazolopyrimidine DNA-Encoded Library (DEL).

I would like to thank to group members: Olivia Bugain, Kathrin Jung, and Hazem Salamon, and remarkably to my students: Anne Gohla, Denise dos Santos, and Suzanne Willems. Girls, you are simply great! Thank you for everything!

My thank also goes to colleague Steven Smith that helped me formatting the thesis.

I am very thankful to my parents, and to my brothers and sisters for their huge support, especially during my studying days. Mother, thank you for all your sacrifices you did for me, and for always being on my side. Dear dad, you left your imprint deep in my being. I know you would be very proud of me.

Finally, I would like to thank to the best husband ever (my husband) Bojan for his enormous patience, support, and his understanding. Also huge thanks goes to our daughter Aleksandra for having a lot of patience with her bussy mother. I love you.

Želim se zahvaliti obitelji Škopić (Srijeđanima) na njihovoj podršci, posebno tijekom mog boravka u Zagrebu. Također, hvala ide Škopićima u Nijmegenu na njihovoj gostoljubivosti na početku mog boravka u Europi, posebno hvala Sretku na svakodnevnoj vožnji iz Nijmegena u Dortmund i nazad u svrhu pronalaska mog stana.

Ogromna hvala ide mojim najdražim Klikama, mojim roditeljima Blanki i Slavku, te braći i sestrama (starosnim redom): Saši, Marini, Ani i Josipu, na tome što su uvijek bili uz mene i uvijek me podržavali na mome putu, a posebno tijekom mojih studentskih dana. Draga mama tebi ogromna hvala za sva žrtvovanja radi mene, na tome što si uvijek bila na mojoj strani i što si me učila što je ispravno. Ti si najbolja mama na svijetu! Dragi tata, svoj si trag ostavio duboko u meni. Jednog dana ću ti opet sve ispričati. Znam da bi bio ponosan na mene.

I na kraju, najveća hvala ide najboljem suprugu, mom Bojanu. Dušo moja draga, hvala ti na beskrajnoj strpljivosti i razumijevanju, a posebno u posljednjih nekoliko mjeseci. Sve je puno lakše kada si ti uz mene. Znam da nije uvijek lako i zato puno ti hvala na svemu! Zajedno s tobom, velika hvala ide i mojoj najdražoj djevojčici Aleksandri. Volim vas puno!

Curriculum Vitae

Personal Details:

Name: Klika Škopić, Mateja

Date of birth: 01.03.1987.

Place of birth: Pakrac, Croatia

Nationality: Croatian

Education and work experience:

11.2013. - 12.2017.	Doctoral student at the Faculty of Chemistry and Chemical Biology, Technical University of Dortmund. PhD thesis: "*Development of Synthesis Methodology for DNA-Encoded Libraries*", scientific guidance: Dr. Andreas Brunschweiger, supervisor: Prof. Dr. Daniel Rauh.
10.2009. - 09.2011.	Graduate student at the Faculty of Chemical Engineering and Technology, course: Applied Chemistry, module: Applied Organic Chemistry, University of Zagreb. Graduate thesis: "*Synthesis of pyrimidine nucleozide mimetics as potential cytostatic agents*"; supervisor : Prof. Dr. Silvana Raić-Malić.
09.2010. - 02.2011.	Stayed at the Faculty of Technology in Novi Sad in Serbia, under the European exchange program Erasmus Mundus ECW-BASILEUS.
10.2005. - 07.2009.	Undergraduate student at the Faculty of Chemical Engineering and Technology, course: Applied Chemistry, University of Zagreb. Bachelor thesis: "*New precursors for ^{18}F radiolabeling*"; supervisor: Prof. Dr. Silvana Raić-Malić.
2006. - 2007.	Suspension of student rights for maternity leave.

Work experience:

02.2013. - 09.2013. Associate scientist - medicinal chemist in Laboratory of synthetic and medicinal chemistry, Department of Chemistry, Fidelta Ltd., Zagreb, Croatia.

10.2011. - 12.2012. Associate scientist - medicinal chemist in Laboratory of synthetic and medicinal chemistry, Department of Chemistry, Galapagos research center Ltd., Zagreb, Croatia.

Awards:

2010. Dean's Award for notable student research work, Faculty of Chemical Engineering and Technology, University of Zagreb, Croatia.

2016. Lecture award at 7th Junges Chemie Symposium Ruhr 2016, Dortmund.

Scholarships:

Since 08.2015. member of the International Max Planck Research School (IMPRS) in Chemical and Molecular Biology, Dortmund.

03.2015. - 08.2016. Christiane Nüsslein-Volhard - Bayer Foundation.

Eidesstattliche Versicherung (Affidavit)

Klika Škopić, Mateja
Name, Vorname
(Surname, first name)

173660
Matrikel-Nr.
(Enrolment number)

Belehrung: Wer vorsätzlich gegen eine die Täuschung über Prü- fungsleistungen betreffende Regelung einer Hochschul- prüfungsordnung verstößt, handelt ordnungswidrig. Die Ordnungswidrigkeit kann mit einer Geldbuße von bis zu 50.000,00 € geahndet werden. Zuständige Verwaltungs- behörde für die Verfolgung und Ahndung von Ordnungs- widrigkeiten ist der Kanzler/die Kanzlerin der Techni- schen Universität Dortmund. Im Falle eines mehrfachen oder sonstigen schwerwiegenden Täuschungsversu- ches kann der Prüfling zudem exmatrikuliert werden, § 63 Abs. 5 Hochschulgesetz NRW. Die Abgabe einer falschen Versicherung an Eides statt ist strafbar. Wer vorsätzlich eine falsche Versicherung an Eides statt abgibt, kann mit einer Freiheitsstrafe bis zu drei Jahren oder mit Geldstrafe bestraft werden, § 156 StGB. Die fahrlässige Abgabe einer falschen Versicherung an Eides statt kann mit einer Freiheitsstrafe bis zu einem Jahr oder Geldstrafe bestraft werden, § 161 StGB. Die oben stehende Belehrung habe ich zur Kenntnis genommen.	Official notification: Any person who intentionally breaches any regulation of university examination regulations relating to deception in examination performance is acting improperly. This offence can be punished with a fine of up to EUR 50,000.00. The competent administrative authority for the pursuit and prosecution of offences of this type is the chancellor of the TU Dortmund University. In the case of multiple or other serious attempts at deception, the candidate can also be unenrolled, Section 63, paragraph 5 of the Universities Act of North Rhine-Westphalia. The submission of a false affidavit is punishable. Any person who intentionally submits a false affidavit can be punished with a prison sentence of up to three years or a fine, Section 156 of the Criminal Code. The negligent submission of a false affidavit can be punished with a prison sentence of up to one year or a fine, Section 161 of the Criminal Code. I have taken note of the above official notification.
Ich versichere hiermit an Eides statt, dass ich die vorlie- gende Dissertation mit dem Titel selbstständig und ohne unzulässige fremde Hilfe angefertigt habe. Ich habe keine anderen als die angegebenen Quellen und Hilfs- mittel benutzt sowie wörtliche und sinngemäße Zitate kenntlich gemacht. Die Arbeit hat in gegenwärtiger oder in einer anderen Fassung weder der TU Dortmund noch einer anderen Hochschule im Zusammenhang mit einer staatlichen oder akademischen Prüfung vorgelegen	I hereby swear that I have completed the present dissertation independently and without inadmissible external support. I have not used any sources or tools other than those indicated and have identified literal and analogous quotations. The thesis in its current version or another version has not been presented to the TU Dortmund University or another university in connection with a state or academic examination.*

Ort, Datum
(Place, date)

Unterschrift
(Signature)

Titel der Dissertation:
(Title of the thesis):

Development of Synthesis Methodology for DNA-Encoded Libraries

*Please be aware that solely the German version of the affidavit ("Eidesstattliche Versicherung") for the PhD thesis is the official and legally binding version.

Ort, Datum
(Place, date)

Unterschrift
(Signature)